Synthesis of Novel Chiral Bipyrimidine Diphosphine and Aminoalcohol Ligands and their Application in Asymmetric Catalysis

A Thesis

Forwarded to

Department of Applied Biology and Chemical Technology

For the Degree of Doctor of Philosophy

At The Hong Kong Polytechnic University

By Chen Gang

July 2003

Declaration

I hereby declare that this thesis summarize my own research work carried out since my registration at the Hong Kong Polytechnic University for the degree of Doctor of Philosophy in April, 1999, and that, to the best of my knowledge and belief, it produces no material previously published or written nor material which has been accepted for the award of any other degree or diploma, excepted where due acknowledgement has been made in the text.

(Signed)

Chen Gang

March, 2003

ACKNOWLEDGEMENTS

I would like to express my most heartfelt thanks to my supervisor Prof. Albert S. C. Chan for his valuable advice, encouragement and discussion throughout the course of my work. Under his supervision, I got a precious training on how to accomplish research work, how to overcome problems and how to be a potential scientist. His supervision is a great treasure to me because he showed me the correct way to think about a project and to do research work. Only with his guidance I can overcome the problems in my research work and my study can turn to be rewarding finally. This experience is surely much helpful for my future.

I wish to give my special thanks to my co-supervisor, Dr. Chiu-Wing Yip, for his valuable guidance and comments on this thesis.

I am very grateful to all colleagues and friends in our laboratory for their kind help. They are Dr. Wenhao Hu, Dr. Xinshu Li, Dr. Jing Wu, Prof. Zhongyuan Zhou, Dr. Rongwei Guo, Dr. Terry Au-Yeung, Dr. Waihim Kwok, Dr. Guoshu Chen, Dr. Yueming Li, Dr. Lijin Xu, Mr. Kimhung Lam, Mr Puierh Tong, Dr. Lailai Wong, Dr. Liqing Qiu, Ms. Xia Jia, Dr. Alex, Miss Alison Lam, Dr. Liang Liang, Dr. Dongsheng Liu, Mr. S. S. Chan, Dr. Rongliang Lou, Dr. Tianhu Li, Dr. Qiaohong Huang, Dr. Jianying Qi, Dr. Jian Chen, Dr. Ming Yan, Dr. Gui Lu, Dr. Lingyu Huang and Dr. Hua Chen.

I am obliged to all staff, especially the technical service crew, of the Department of Applied Biology and Chemical Technology for their technical supports.

Finally, I would like to acknowledge the Research Committee of The Hong Kong Polytechnic University for the award of a studentship and the conference attendance grant. I also greatly thank the Hong Kong Polytechnic University ASD Fund (Project ERB03) and UGC Areas of Excellence Scheme in Hong Kong for financial support.

Chen Gang

March, 2003

Abstract of the thesis entitled "Synthesis of Novel Chiral Bipyrimidine Diphosphine and Aminoalcohol Ligands and their Application in Asymmetric Catalysis"

Submitted by Chen Gang

For the degree of Doctor of Philosophy

At The Hong Kong Polytechnic University in July, 2003

Palladium-catalyzed asymmetric allylic alkylation (**AAA**) is one of the most powerful tools for the sterically controlled introduction of carbon-carbon and carbon-heteroatom bond formation. In this thesis work, a novel chiral atropisomeric diphosphine ligand, 5,5′-bis(diphenylphosphino)-1,1′,3,3′-tetramethyl-4,4′-bipyrimidine-2,2′,6,6′-(1*H*,1′*H*,3*H*,3′*H*)-tetrone (PM-Phos) was developed, whose palladium complex exhibited good to excellent enantioselectivity in catalytic asymmetric allylic alkylation.

PM-Phos is the first bipyrimidine-type diphosphine ligand. The synthetic highlight includes an interesting "halogen-dance" reaction, a crucially modified Ullmann coupling procedure and an unexpected methyl group rearrangement. With the palladium-catalyzed allylic alkylation of 1,3-diphenyl-2-propenyl acetate with malonates as a model reaction, the asymmetric induction properties of PM-Phos was preliminarily tested. In this reaction, the optimal nucleophile was dimethyl malonate, the optimal solvent was CH_2Cl_2 and the optimal base was NaOAc. The catalytic activity of the PM-Phos palladium complex was excellent especially at room

temperature. The enantioselectivity was fair at room temperature, but good at 0^{o}C and almost excellent at a lower temperature (up to 95% ee at -40 ^{o}C).

Another part of this thesis work is the synthesis of novel chiral amino alcohol ligands. With L-valine as starting material, new amino alcohol ligands with two stereogenic centers, i.e., 1*R*-[2′-(6′-methoxynaphthyl)]-2*S*-amino-3-methylbutan-1-ol (**4-6a**) and 1*R*-[2′-(6′-methoxynaphthyl)]-2*S*-pyrrolidinyl-3-methylbutan-1-ol (**4-8**), were synthesized. The enantioselective borane reduction of acetophenone catalyzed by the amino alcohols **4-6a** provided high ee's (up to 97%). The enantioselective diethylzinc addition to aldehydes catalyzed by the N,N-cycloalkylated amino alcohol **4-8** also afforded the corresponding chiral secondary alcohols with good to excellent ee's (up to 98%).

The third part of this thesis work is based on chiral ruthenium-complex catalysts recycled by ion exchangers and their application in asymmetric hydrogenation. The ruthenium complex of P-Phos was an excellent catalyst for the asymmetric hydrogenation of β-ketoesters. After the reaction, the catalyst was separated easily by a column packed with silica gel-based ion exchanger and was used in the subsequent recycling runs of the reaction with a slight loss of enantioselectivity and activity. This result indicates that the special nitrogen-containing feature of P-Phos favors the stability and recyclability of its ruthenium complex catalyst in asymmetric hydrogenation.

ABBREVIATIONS

Ar	aryl
BICP	bis(diphenylphosphino)-dicyclopentane
BINAP	2, 2′-bis(diphenylphosphino)-1,1′-binaphthyl
BINAPO	2,2′-bis(diphenylphospinyl)-1,1′-binaphthyl
BINOL	1,1′-bi-2-naphthol (or 2,2′-dihydroxy-1,1′-binaphthyl)
BIPHEP	2,2′-bis(diphenylphosphino)-1,1′-biphenyl
Bn	benzyl
BPPM	N-(terbutoxycarbonyl)-4-(diphenylphosphino)-2-[(diphenylphosphino)methyl]pyrrolidine
BSA	N,O-bis(trimethylsilyl)acetamide
Bu or n-Bu	normal (primary) butyl
t-Bu	*ter*t-butyl
Chiraphos	2,3-bis(diphenylphosphino)butane
COD	1,5-cyclooctadiene
Cp	cyclopentadienyl
DAIB	3-*exo*-(dimethylamino)isoborneol
DBTA	dibenzoyl-L-tartaric acid
de	diasteromeric excess
Deguphos	1-substituted 3,4-bis(diphenylphosphino)pyrrolidine
dehydronaproxen	2-(6′-methoxy-2′-naphthyl)propenoic acid
DIOP	2,3-*O*-isopropylidene-2,3-dihydroxy-1,4-bis(diphenylphosphino)butane
DIPAMP	1,2-bis[(*o*-methoxyphenyl)phenylphosphino]-1,1′-biphenyl
DMF	dimethylformamide
DuPHOS	substituted 1,2-bis(phospholano)benzene
L-DOPA	L-3-(3,4-dihydroxyphenyl)analine

ee	enantiomeric excess
GC	gas chromatography
J	coupling constant (in NMR)
LDA	lithium diisopropylamide
MeO-BIPHEP	2,2′-bis(diphenylphosphino)-6,6′-dimethoxy-1,1′-biphenyl
h (or hr)	hour
HPLC	high-performance liquid chromatography
HRMS	high-resolution mass spectrometry
Me	Methyl
MS	mass spectrometry
m/z	mass-to-charge ratio (in mass spectrometry)
naproxen	2-(6′-methoxy-2′-naphthyl)propanoic acid
NMR	nuclear magnetic resonance
PHANEPHOS	4,12-bis(diphenylphosphino)-[2,2]-paracyclophane
Ph	Phenyl
P-Phos	2,2′,6,6′-tetramethoxy-4,4′-bis(diphenylphosphino)-3,3′-bipyridine
PM-Phos	5,5′-Bis(diphenylphosphino)-1,1′,3,3′-tetramethyl-4,4′-bipyrimidine-2,2′,6,6′-(1*H*, 1′*H*, 3*H*, 3′*H*)-tetrone
rt	room temperature
S/C	substrate to catalyst ratio
SEGHOS	4,4′-bi-1,3-benzodioxole-5,5′-diyl-bis(diphenylphosphine)
SpirOP	1,6-bis-(diphenylphosphinoxy)spiro-[4,4]-norane
TangPhos	1,1′-di-*tert*-butyl-[2,2′]-diphospholanyl
THF	tetrahydrofuran
[α]	special optical rotation

Key Compounds and Structures

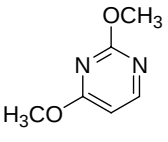

2-1

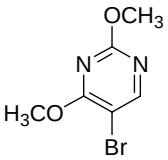

2-2

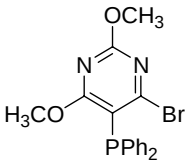

2-3

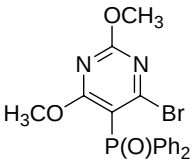

2-4

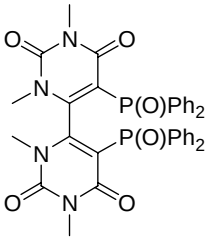

2-5

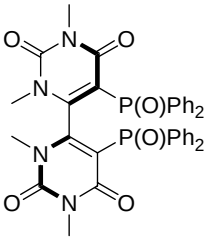

(*R*)-2-6

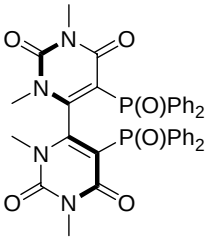

(*S*)-2-6

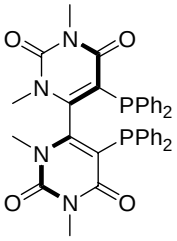

(*R*)-2-7

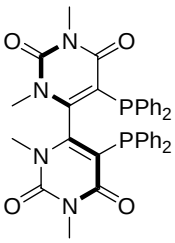

(*S*)-2-7

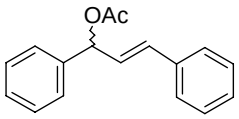

3-1

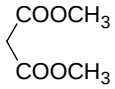

3-2

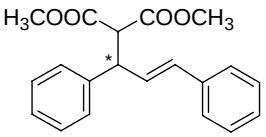

3-3

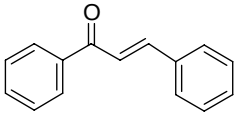

3-4

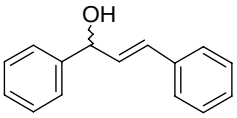

3-5

3-6

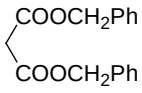

3-7

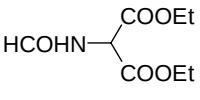

3-8

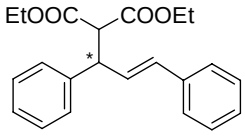

3-9

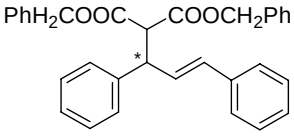

3-10

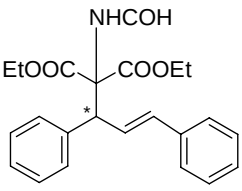

3-11

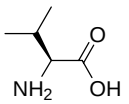

4-1

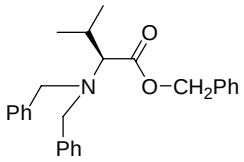

4-2

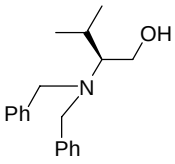

4-3

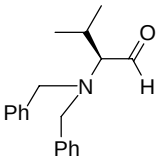

4-4

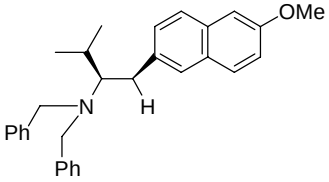

4-5a

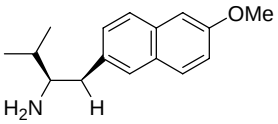

4-6a

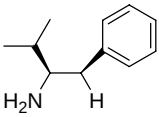

4-6c

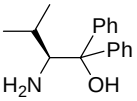

4-7

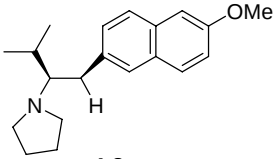

4-8

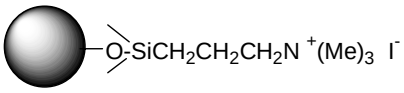

5-1

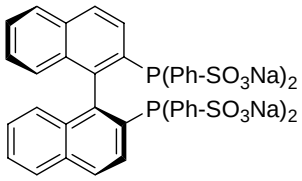

(*S*)-**5-2**

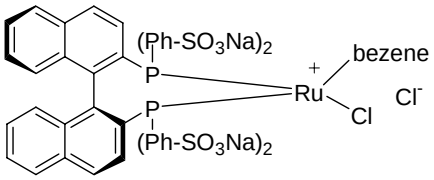

(*S*)-**5-3**

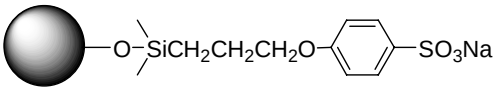

5-4

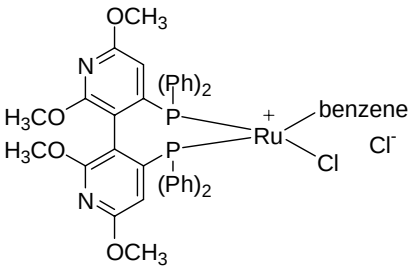

(*S*)-**5-5**

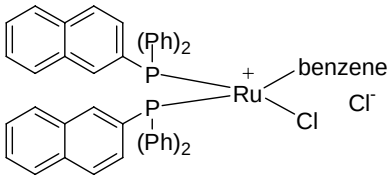

(*S*)-**5-6**

Contents

Chapter 1
Asymmetric Catalysis and Asymmetric Palladium-Catalyzed Allylic Alkylations

1.1. Principles of Asymmetric Catalysis [1, 2, 3]

1.1.1 Chirality and Asymmetric Synthesis

Molecular chirality is a principal element in nature that plays a key role in life and in scientific research. A wide range of biological and physical functions is generated through precise molecular recognition that requires matching of chirality. Biological systems, in most cases, recognized the members of a pair of enantiomers as different substances, and the two enantiomers will elicit different responses. Thus, one enantiomer may act as a very effective therapeutic drug whereas the opposite enantiomer may be highly toxic. So it has been shown for many pharmaceuticals that only one enantiomer contains all of the desired activity, and the other is not. Therefore, the preparation of enantiomerically pure compounds plays a critical role in the development of pharmaceuticals, agrochemicals, flavors, fragrances and other biologically active materials.

It is the responsibility of synthetic chemists to provide highly efficient and reliable methods for the synthesis of desired compounds in an enantiomerically pure state, which is 100% enantiomeric excess.

So far, several ways have been developed to obtain optically pure organic compounds which are listed in the following:

1. Isolation from nature.
2. Fermentation.
3. Resolution methods including chemical resolution, chiral chromatography, kinetic resolution and so on.
4. Asymmetric transformation.
5. Asymmetric synthesis.

Among the above stated methods, asymmetric synthesis is the most feasible, accessible and potential technique. The importance and practicality of asymmetric synthesis as a tool to obtain enantiomerically pure or enriched compounds has been fully acknowledged by chemists in synthetic organic chemistry, medicinal chemistry, agricultural chemistry, natural products chemistry, pharmaceutical industries, and agricultural industries. This prominence is due to the explosive development of newer and more efficient methods created by the efforts of many scientists during the past 30 years.

Asymmetric synthesis is especially defined as the reactions in which a prochiral (non-chiral or achiral) substrate is converted to a chiral unit with enantiomeric excess under chiral inducing agents (including chiral reagents, chiral auxiliaries and chiral catalysts). If a chiral catalyst is used, the reaction can be called asymmetric catalytic reaction, in which, the little amount asymmetric catalyst usually coordinates with the substrate or reagent to form an active and stereoselective intermediate firstly and give a chiral product finally and then catalyst is released for next catalytic recycle.

1.1.2. Asymmetric Catalysis

Among various asymmetric reactions, the most desirable and the most challenging is catalytic asymmetric synthesis since one chiral catalyst can create millions of chiral product molecules, just as enzymes do in biological systems. So, catalytic asymmetric synthesis has significant economic advantages over stoichiometric asymmetric synthesis in industrial scale production of enantiomerically pure compounds. However, until the early 1970's, the resolution of racemates was the most usual method in preparation of chiral compounds. Catalytic asymmetric synthesis of chiral compounds was still a dream. The advances in this area turned chemists dreams into reality. One major breakthrough in this pursuit came from the incorporation of chiral ligangds in transition metal catalysts. The Monsanto L-dopa process was successfully commercialized in mid-70's based on the asymmetric hydrogenation of prochiral olefin. This technology has become an industrial flagship in asymmetric catalysis since its successful commercialization in the mid 1970's**(Scheme 1-1).**

So far, a large number of catalytic asymmetric reactions have been developed. These reactions can be classified into some principle categories as the follows:

1. Asymmetric hydrogenation.
2. Asymmetric isomerization.
3. Asymmetric cyclopropanation.
4. Asymmetric oxidation including epoxidation and dihydroxylation.

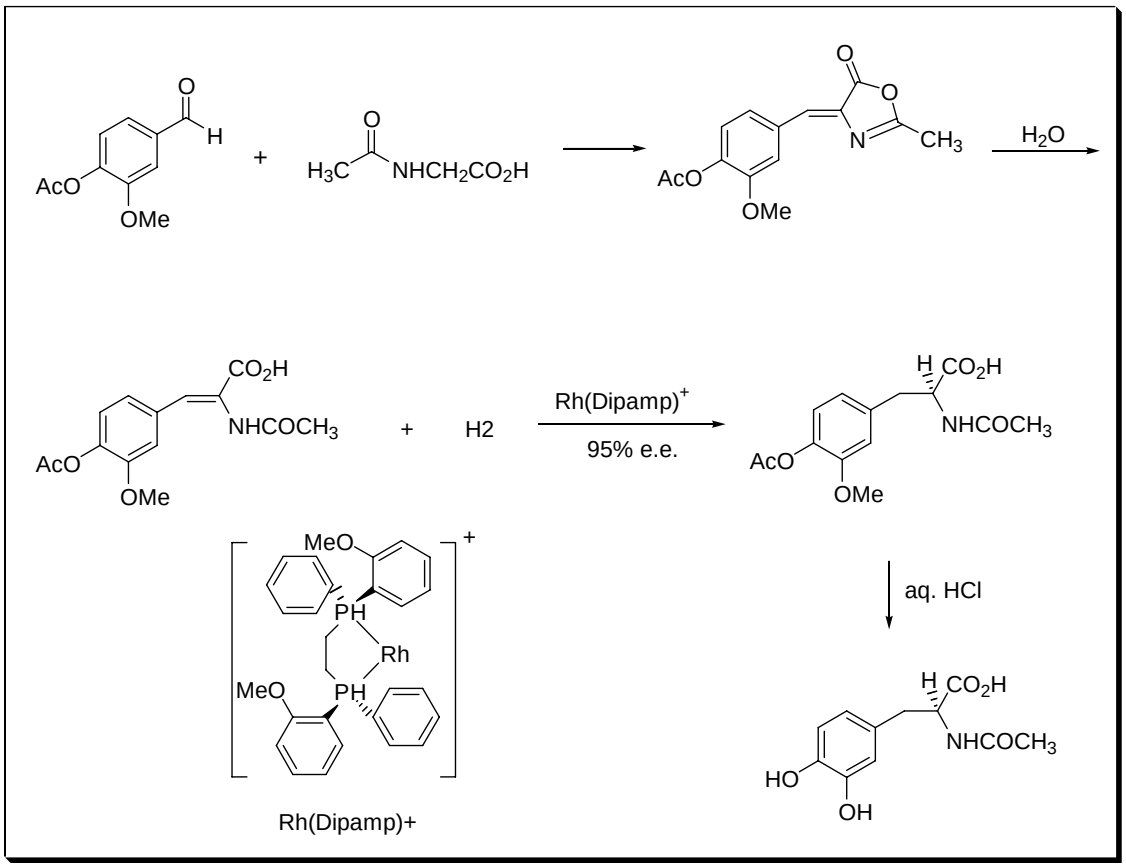

Scheme 1-1. The Monsando L-Dopa process

5. Asymmetric carbonylation.

6. Asymmetric hydrosilylation.

7. Asymmetric C-C bond forming reactions such as **Allylic Allylation**, Grinard cross-coupling and Aldol reactions.

8. Asymmetric phase transfer reaction.

9. Other Asymmetric reactions.

Among the significant achievements in basic research: (i) asymmetric hydrogenation of α-acetaminoacrylate, a ground-breaking work by Knowles *et al.*; (ii) the Sharpless epoxidation by Sharpless *et al.*; and (iii) the second-generation

asymmetric hydrogenation processes developed by Noyori *et al*. deserve particular attention because of the tremendous impact that these processes have made in synthetic organic chemistry. In fact, a number of catalytic asymmetric reactions, including the “Takasago Process” (asymmetric isomerization), the “Sumitomo Process” (asymmetric cyclopropanation), and the “Arco Process” (asymmetric Sharpless epoxidation) have been commercialized in 1980s. These Processes supplement the epoch-making “Monsanto Process”. Extensive research on new and effective catalytic asymmetric reactions will surely continue beyond the year 2000, and catalytic asymmetric processes promoted by man-made chiral catalysts will become mainstream chemical technology in the 21st century.

1.1.3. Asymmetric Catalysts

Usually, the most effective asymmetric catalysts are coordinated complexes of transition metals and chiral ligands, and due to this kind of special composition, the complexes can show not only effective catalytic activity, but also high enantioselectivity. The usually used chiral ligands for preparing asymmetric catalysts can also been classified into several main categories such as phospine ligand, amino alcohol ligand, diamine ligand, phosphine amine ligand and so on. Among these ligands, chiral phosphine ligands take a very important part among which the most famous is BINAP.

1.1.4. The General mechanism of Asymmetric Catalysis

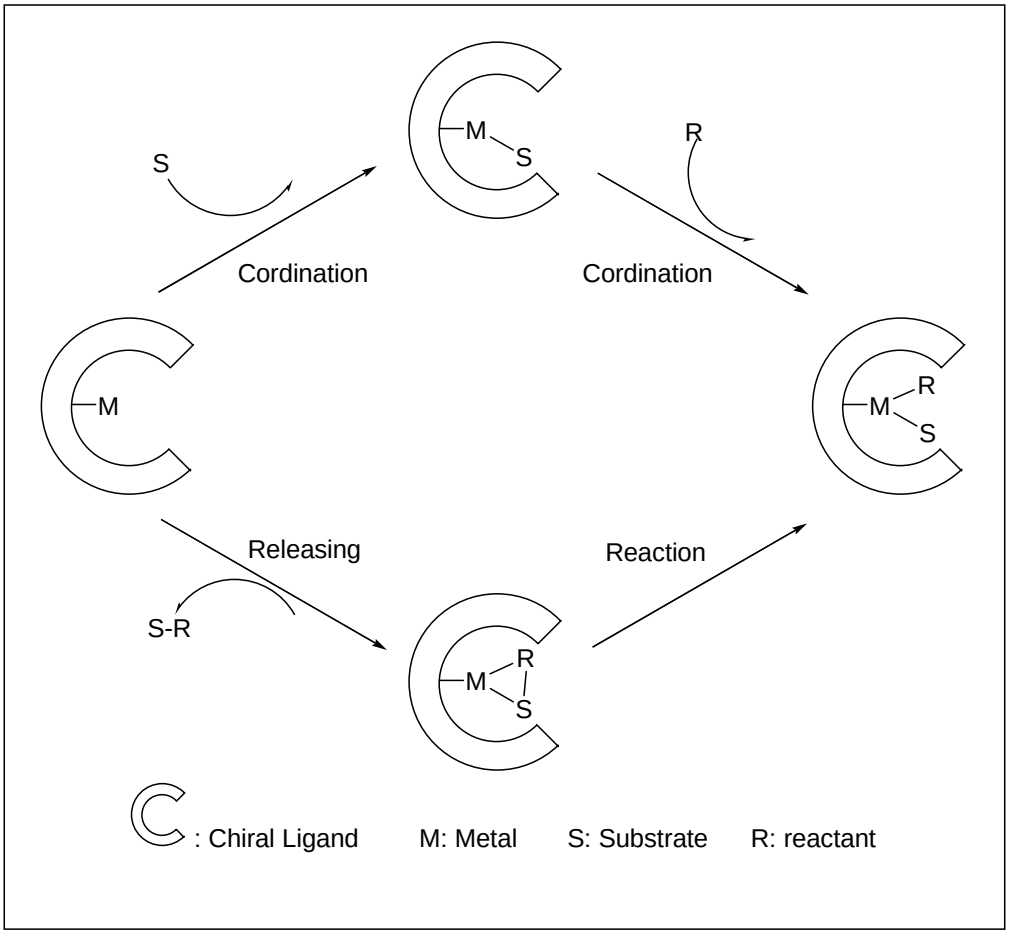

Scheme 1-2

The general mechanism of asymmetric catalysis is outlined above (**Scheme 1-2**). In most cases, a complex of chiral ligand and transition metal forms the asymmetric catalyst which provides chiral induction to the reaction. The function of the central transition metal is to activate the reaction and hence provide the catalytic activity, while the chiral ligand is responsible for providing an asymmetric environment for the reaction. At the first step of a usual catalytic cycle, the substrate coordinates with the central metal of the catalyst, and then the reactant coordinates with the metal too or

reacts with the activated substrate directly, and finally the product forms in the chiral environment and is released from the catalyst. That's the overall general process for what happens in asymmetric catalytic reaction.

1.2. Asymmetric Allylic Alkylations (AAA) [4]

1.2.1. Introduction

Efficient and reliable amplification of chirality has borne its greatest fruit with transition metal-catalyzed reactions since enantiocontrol may often be imposed by replacing an achiral or chiral racemic ligand with one that is chiral and scalemic. While the most thoroughly developed enantioselective transition metal-catalyzed reactions are those involving transfer of oxygen (epoxidation and dihydroxylation) [5,6] and molecular hydrogen,[7] the area of enantioselective transition metal-catalyzed allylic alkylations which may involve C-C as well as C-X (X = H or heteroatom) bond formation.[8-13] has attracted much research attention in recent years. The synthetic utility of transition metal-catalyzed allylic alkylations has been soundly demonstrated since its introduction nearly three decades ago.[14-25] Allylic reactions usually refer to processes which result in nucleophilic displacements on allylic substrates (**Scheme 1-3**).

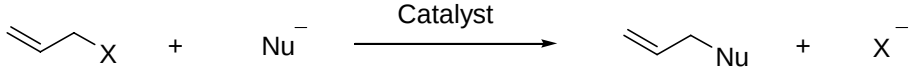

Scheme 1-3.

Such reactions have been recorded with a broad range of metal complexes including those derived from nickel, palladium, platinum, rhodium, iron, ruthenium, molybdenum, and tungsten, among which palladium is the most effective. Virtually, all of the efforts to date in asymmetrization of the reactions have focused on palladium-catalyzed reactions

Bringing asymmetric induction to such reactions represents an important new dimension to their use in synthesis. There are two general classes of reactions of the type represented in **Scheme 1-3** which differ in the nature of the nucleophile. "Hard" nucleophiles, defined as those derived from conjugate acids whose pK_a > 25, normally effect such reactions by attachment of the nucleophile to the metal followed by reductive elimination as depicted in **Scheme 1-4**. This process has not been extensively developed in the achiral version. The lack of such development probably stems, in part, from its duplication of organocopper chemistry. On the other the hand, the reaction with "soft" nucleophiles, defined as those derived from conjugate acids whose pK_a < 25, normally follows a different course as outlined in **Scheme 1-5**. Intrinsic to this pathway is the fact that bond breaking and making events occur outside the coordination sphere of the metal, i.e., on the face of the π-allyl unit opposite the transition metal and its attendant ligands. Thus, the leaving group and the nucleophile are segregated from the chiral environment of the ligand by the π-allyl moiety.

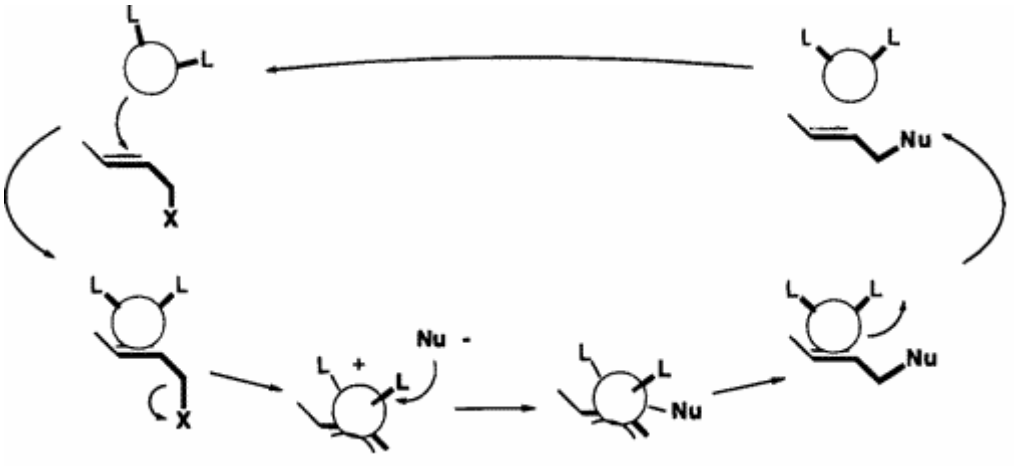

Scheme 1-4. Allylic Alkylation with Hard Nucleophiles

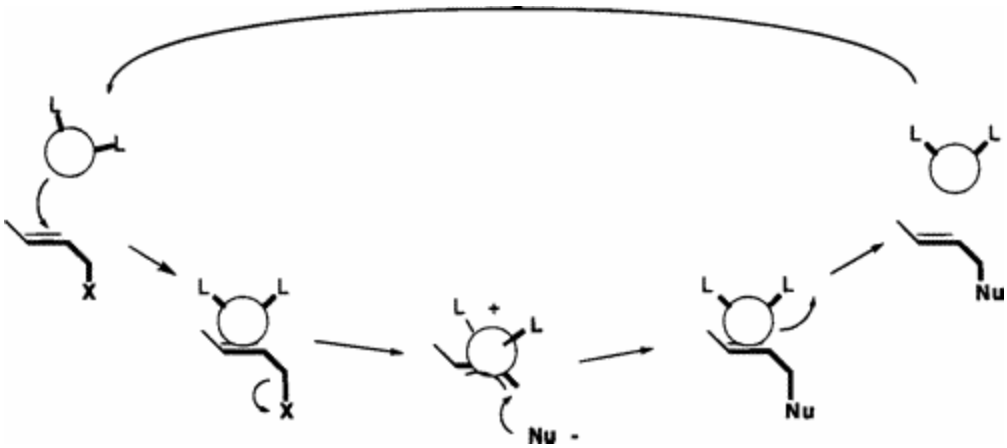

Scheme 1-5. Allylic Alkylation with Soft Nucleophiles

The first example of an enantioselective palladium-catalyzed allylic substitution reaction with a stabilized nucleophile was reported in 1977 by Barry Trost.[26] Since this beginning, much work has been done to harness the asymmetric potential of allylic alkylations, but only recently have these reactions developed into processes where high enantioselectivities may be realized with a wide range of substrates in a predictable fashion. The lag time in this development may stem from the

stereochemical requirements that the chiral ligands must somehow reach across the plane of the allyl fragment to transfer their chirality to the event responsible for the enantiodiscrimination.

1.2.2. The General Mechanism and Catalytic Cycle of Asymmetric Allylic Alkylation

The mechanism of metal-catalyzed alllylic alkylation is generally believed to involve the four fundamental steps illustrated in **Scheme 1-6**.[27-30].The key feature of the catalytic cycle is the intermediacy of (π-allyl)metal compex. Its generation and subsequent reaction represent, respectively, the bond-breaking and –making events in which the source of chiral induction can be derived. Depending on the structure of the substrate, every step provides an opportunity for enantioselection, except for decomplexation, which occurs after bond formation. Because the rates of these catalytic steps are delicately balanced, both the rate-limiting step and the selectivity-determining step may vary depending on the reaction conditions.

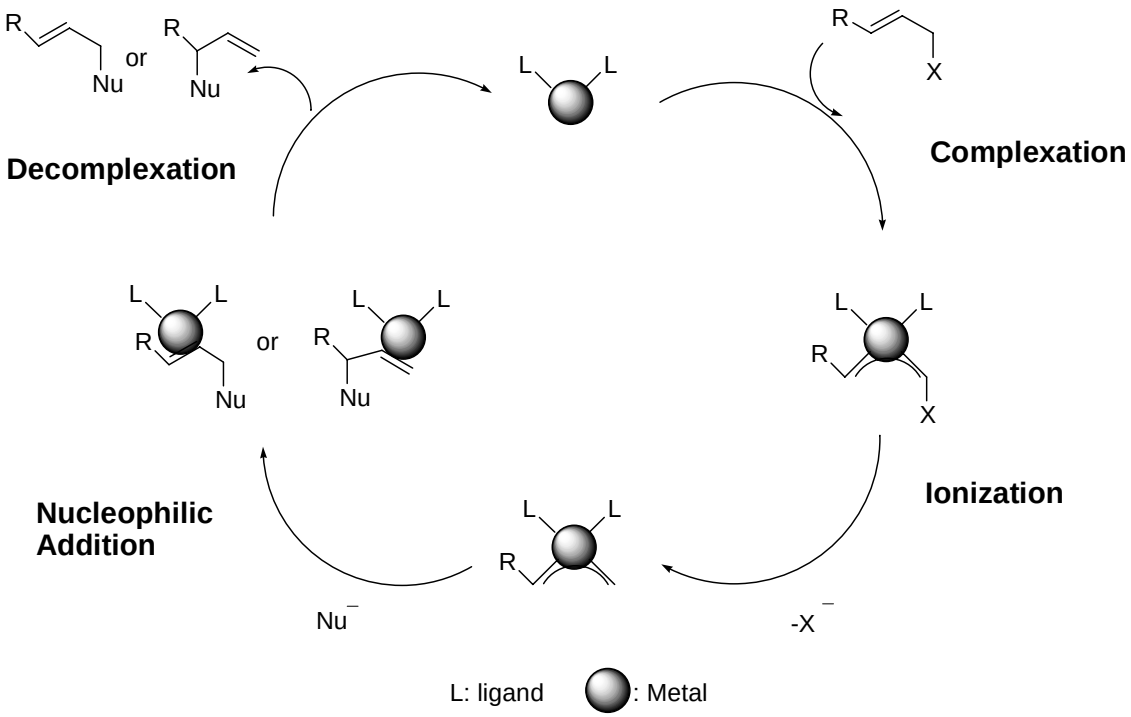

Scheme 1-6. Catalytic cycle of transition metal catalyzed allylic alkylation.

Although ionization usually proceeds with inversion of stereochemistry regardless of the nucleophile, the addition of a nucleophile involves two pathways in which the nature of the nucleopile leads to different stereochemical consequences (**Scheme 1-7**). The "soft" (stabilized) nucleophiles, defined as those derived from conjugate acids whose pK_a < 25, usually add to the ally ligand from the side opposite to the metal, giving rise to product with overall retention of stereochemistry.[31-33] On the other hand, with "hard" (unstabilized) nucleophiles (pK_a > 25), the addition normally occurs via transmetallation where the nucleophile attacks the metal center of the π-allyl intermediate and the resultant adduct collapses to product by reductive elimination,

resulting in inversion of stereochemistry.[34-40] Exceptions to these generalities have been claimed.

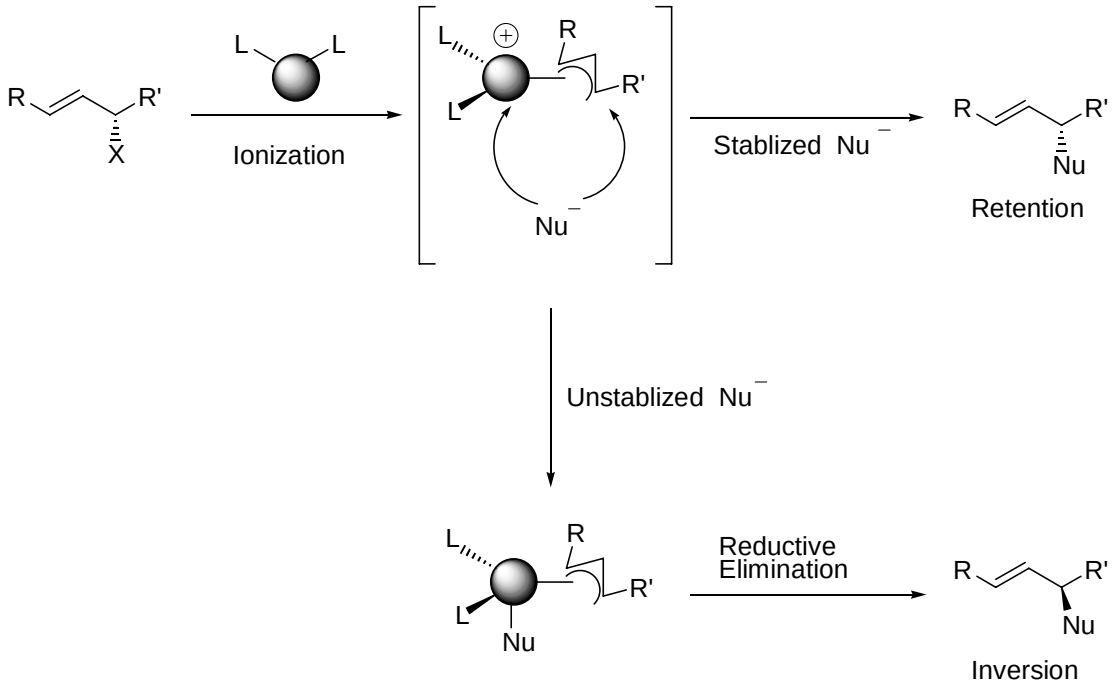

Scheme 1-7. Addition of stabilized and unstabilized nucleophiles.

In the alkylation with most commonly used stabilized nucleophiles, one quite obvious problem associated with this process is the physical separation between the chiral ligand and the reaction site. Both bond-breaking and –forming occur on the π-allyl face opposite the metal and its attendant ligand. Thus, efficient transfer of the chirality over the ally barrier is a key to a successful strategy for asymmetric allylic alkylation.

1.2.3. Chiral Induction and Opportunities for Enantiodiscrimination

For a process to provide 100% enantiomeric excess in 100% yield, the enantiodetermining step must involve the distinction between enantiotopic groups or

faces. All popular enantioselective transition metal-catalyzed reactions involve additions to π systems. In contrast, allylic alkylations involve displacements at sp^3 centers. The ability to convert racemic starting material into optically pure material in such an event-completely, without the waste of a kinetic resolution-presently is almost unique to transition metal-catalyzed allylic alkylations, the exception being those processes involving a dynamic kinetic resolution such as in the hydrogenation of substituted β-keto esters. The general catalytic cycle for transition metal-catalyzed allylic alkylations by stabilized nucleophiles is composed of five primary steps (**Scheme 1-6**). These steps are (a) metal-olefin complexation, (b) ionization, (c) enantioface discrimination of the π-allyl complex, (d) nucleophilic attack at enantiotopic termini, and (e) enantioface discrimination in the nucleophile. Decomplexation of the metal from the olefinic product cannot change the stereochemistry of the product.

A unique feature of the transition-metal-catalyzed allylic alkylation is its ability to convert starting materials of various symmetry types, such as racemic, meso- and achiral compounds, into optically pure material. Strategies to effect such transformations derive from recognition of the stereochemical courses in each step of the catalytic cycle and analysis of symmetry elements in the substrate or intermediate. **Figure 1-1** summarizes the potential sources of enantiodiscrimination in transition metal-catalyzed allylic alkylations in these steps.

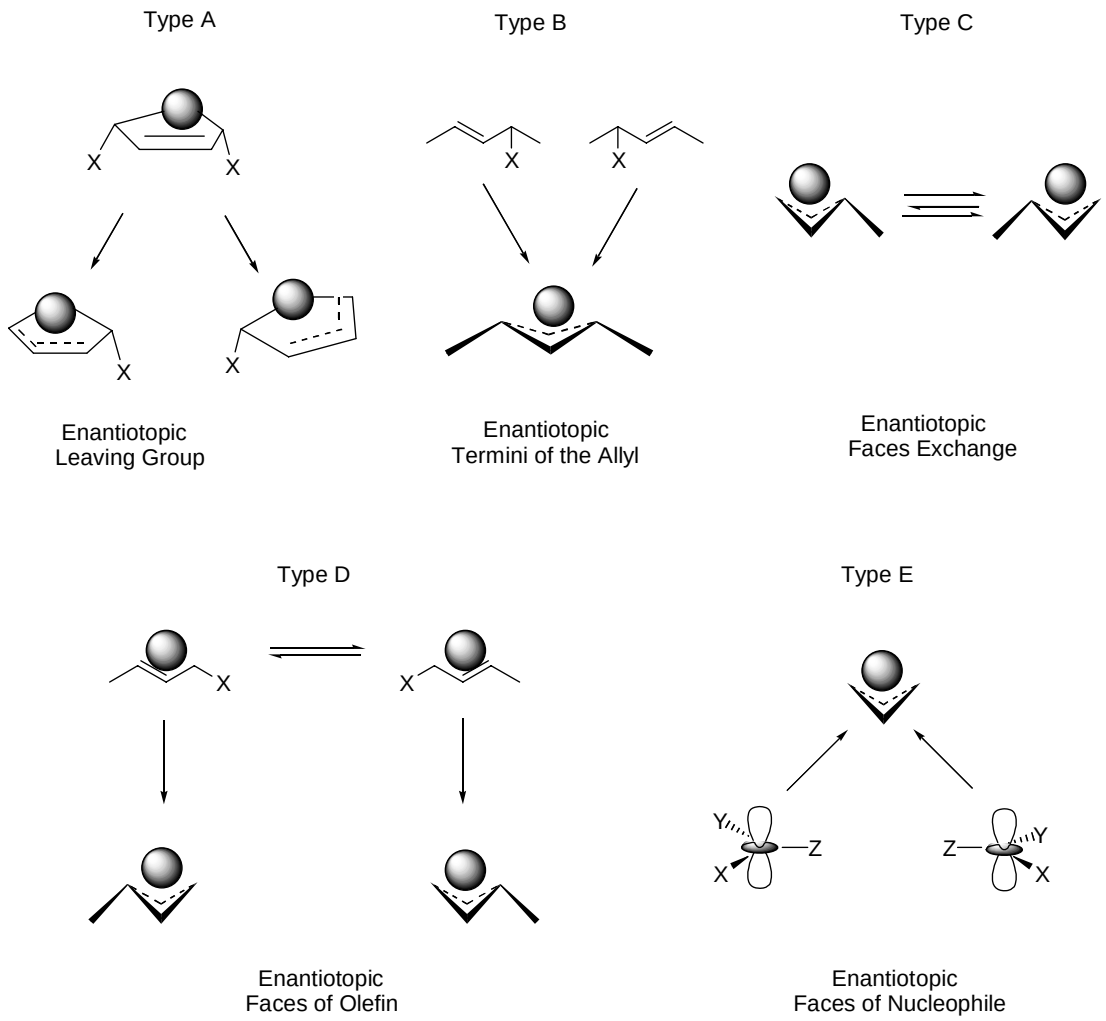

Figure 1-1. Sources of enantiodiscrimination in transition metal-catalyzed allylic alkylations.

The first strategy involves discrimination between enantiotopic leaving groups (Type A). In the second approach, two enantiomers of a racemic substrate converge into a metal π-allyl complex wherin preferential attack of the nucleophile at one of either allylic termini leads to asymmetric induction, a process that may be referred to as a dynamic kinetic enantioselective transformation (Type B). The third requires differentiation between two enantiotopic transition states in the nucleophilic addition to rapidly interconverting enantiomericπ–allyl intermediates, also a dynamic kinetic

enantioselective transformation (Type C). Alternatively, an enantiomeric intermediate is generated from enantiofacial complexation of an alkene (Type D). When the nucleophile is a prochiral compound of a rapidly equilibrating racemic mixture, asymmetric induction can be also possible at the nucleophile (Type E).

1.2.4. Chiral Ligands

The problem in metal-catalyzes allylic alkylation has naturally led to design of chiral catalysts in such a way that asymmetry is effectively transmitted to the reaction event occurring distal to the ligand. As depicted in **Figure 1-2**, Three concepts have been proposed:

1) Attaching a functional techer to the ligand to induce interaction with an incoming nucleophile .[41-42]

2) Imposing electronic desymmetrization on the donor atoms of the ligand whereby defferent bond lengths a and b promote differential reactivity at each allylic terminus.[43]

3) Providing the substrate with chiral space, which may derive, for example, by a propeller-like arry of aryl groups whose chirality is induced by a conformational bias of edge-face interactions which, in turn, ultimately originates from primary

stereogenic centers.[44] In all of these cases, non-C_2 symmetric as well as symmetric ligands may be envisioned.

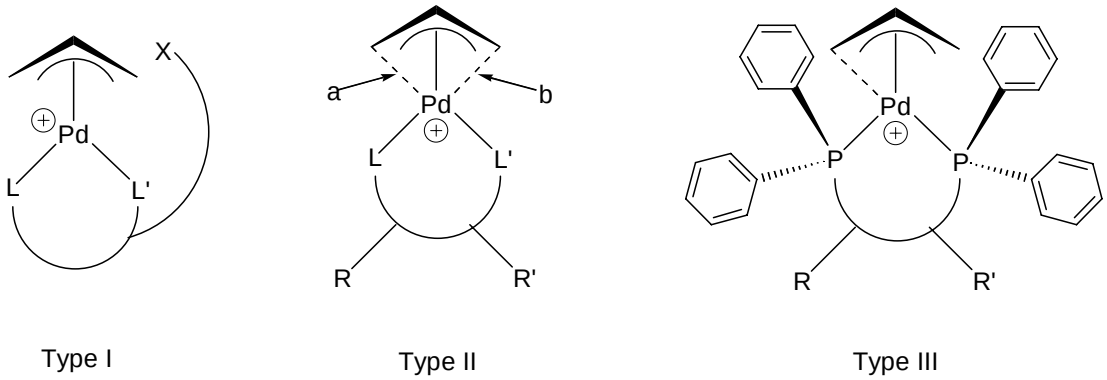

Figure 1-2. Concepts used in ligand design.

As many endeavors in transition metal catalysis, the design, synthesis and screening of chiral ligands have played a pivotal role in the development of the asymmetric allylic alkylation reaction. A series of C_2-symmetry diphospines such as DiPAMP, chiraphos, DIOP, and BINAP, which gave high enantioselectivities in asymmetric hydrogenations, were used in early work. However, these "borrowed ligands" exhibited only modest performance in this area. Soon after, many new ligands have been developed by modifying these relatively simple structured ligands. Virtually all of the elements constituting a chiral ligand such as the type of symmetry, donor atoms, node of denticity (e.g., mono- vs. bidentation), and combination of these have been explored. Consequently, impressive progress has been made in the design of ligands, which are primarily for AAA.

Figure 1-3 to **Figure 1-6** show a selection of some ligands that have been successfully used in the palladium-catalyzed AAA reaction. They are classified into

four categories: 1) chiral phosphines, 2) dinitrogen ligands, 3) P,N-chelate ligands, and 4) mixed chelated ligands.

The chirality at the phosphorus atom such as in DiPAMP, which was originally thought a necessary element, is not required to achieve high enantioselectivity. Neither is C_2-symmetry of the ligand although it provides a simple way of reducing the number of possible transition states by a factor of two 50. A growing number of new ligands, which lack C_2-symmetry, have given successful results in many different reactions. In addition, it has been shown that high enantioselectivities can also be obtained from the use of several monophosphines. Another notable feature of the ligand morphology is the diverse source of the ligand chirality. Starting from the point chirality of phosphorous and carbon atoms, various types of stereogenicity such as axial and planar chirality and combination of these have been utilized.

Although most of the early studies focused on the use of phosphine ligands, recently, nitrogen ligands have been used in enantioselective allylic alkylations with increasing frequency. Both sp^2 (imine) and sp^3 (amine) hybridized nitrogens have

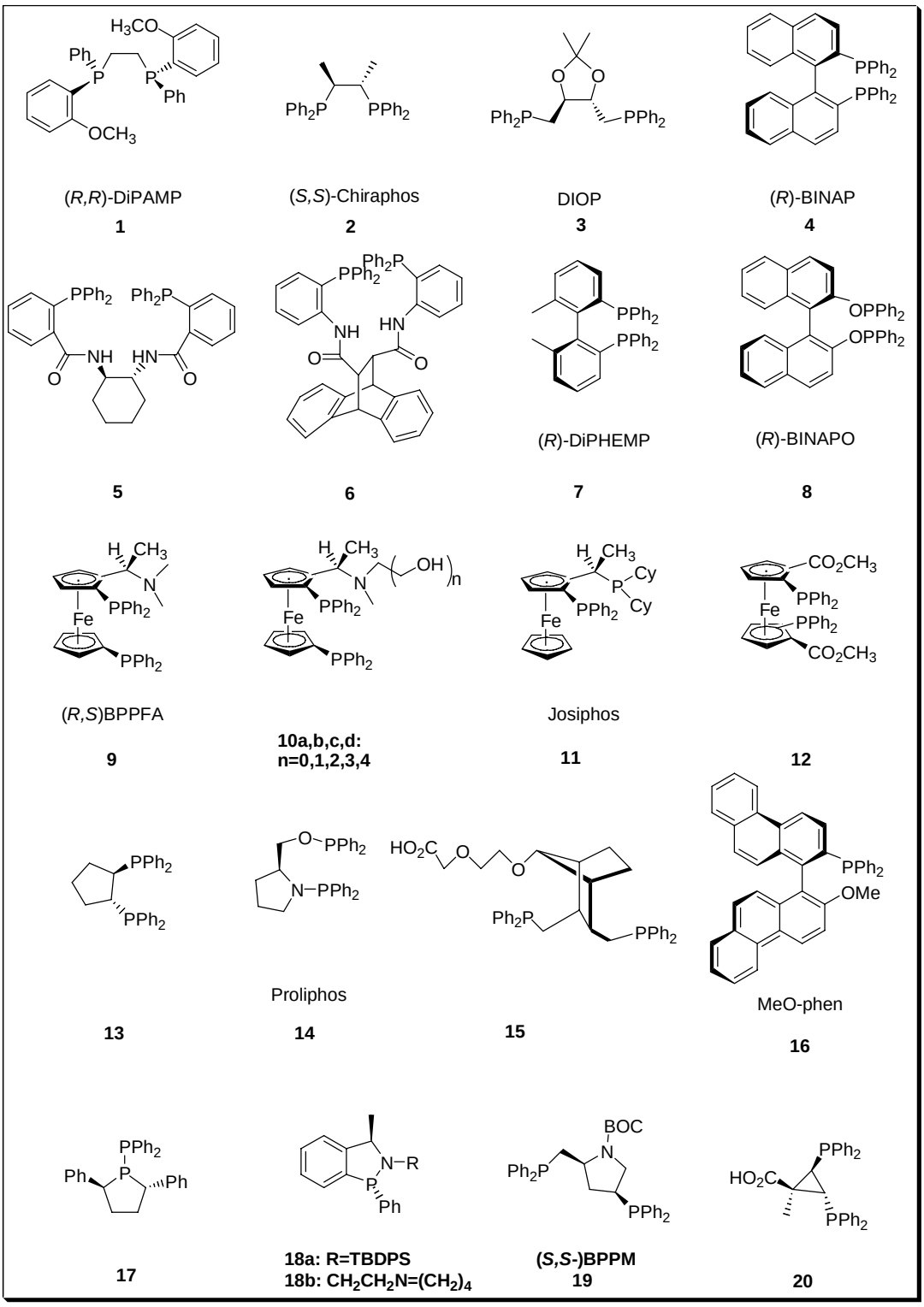

Figure 1-3. Some chiral ligands based on phosphorus for AAA

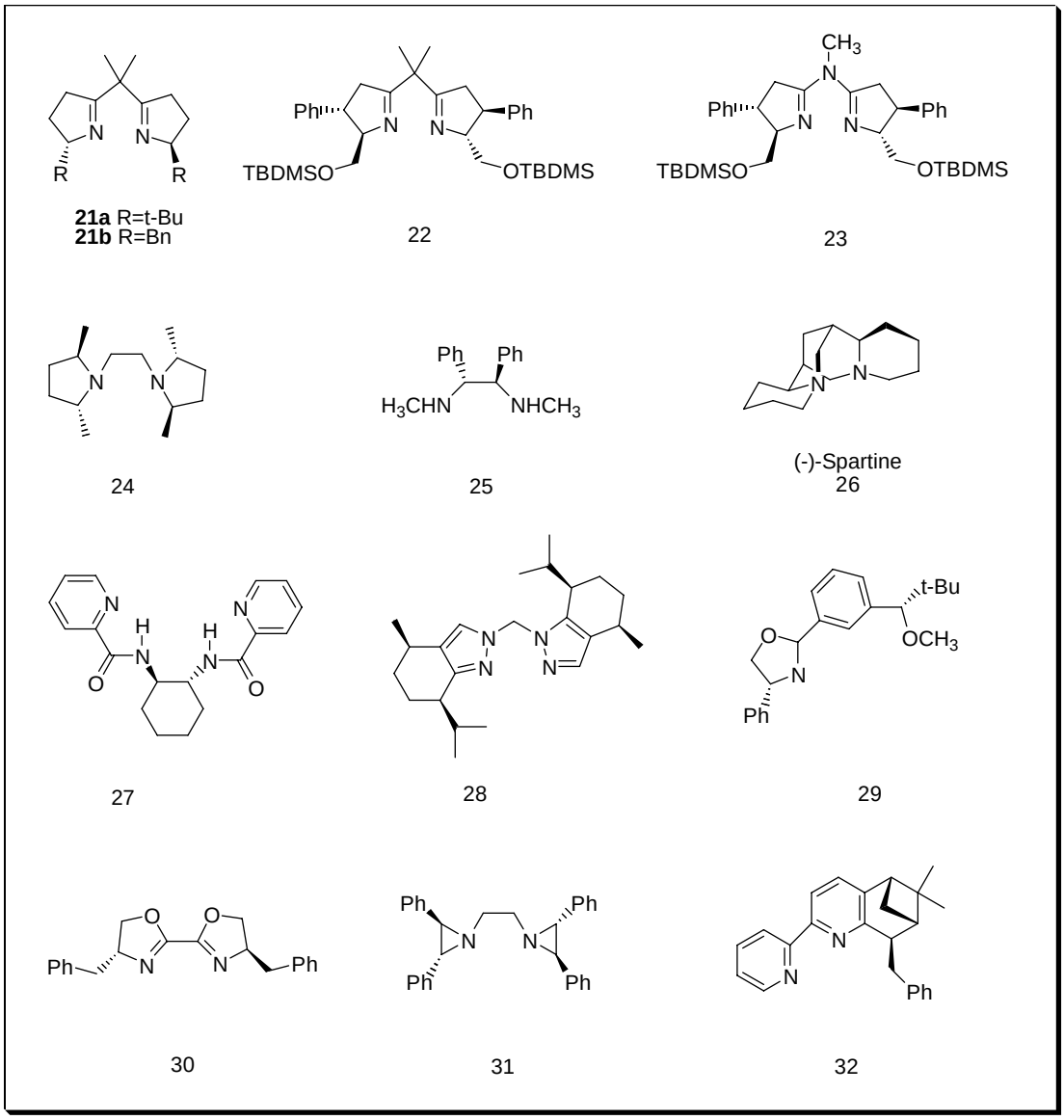

Figure 1-4. Some Chiral dinitrogen ligands for AAA

been proved effective as donor atoms. As shown through the examples, a remarkably high level of enantioselectivity has been recorded with the dinitrogen ligands listed in **Figure 1-4**. However, up to the present, such strong donor-type ligands have exhibited limited scope in the catalytic processes.

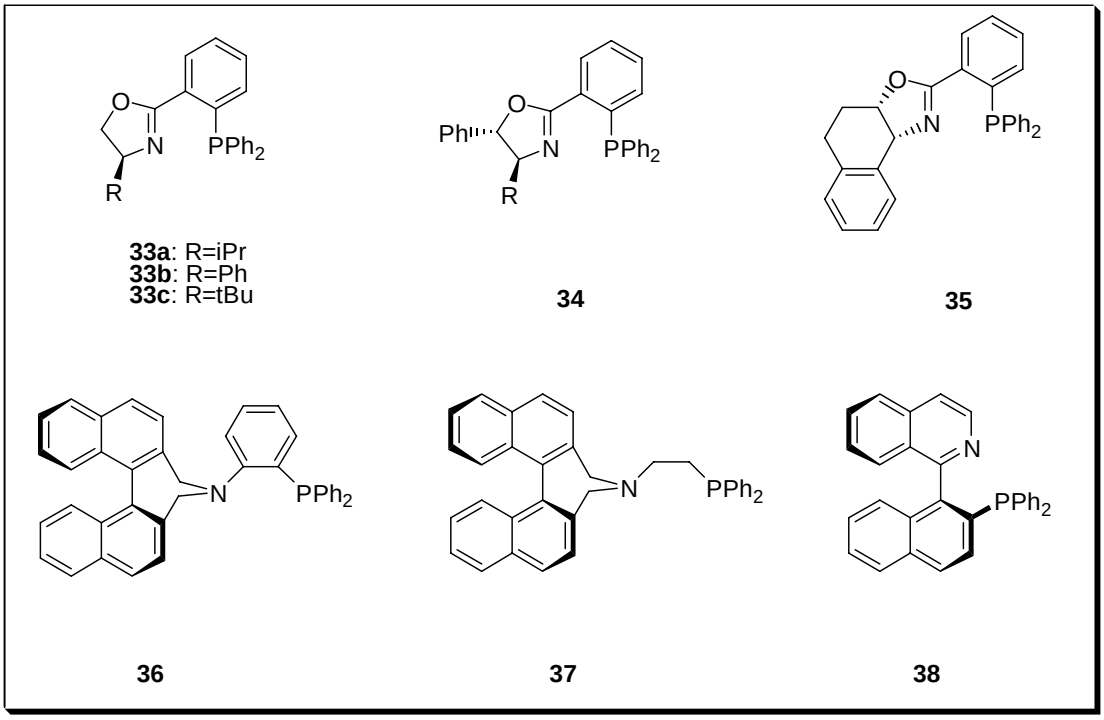

Figure 1-5. Some Chiral P,N-chelate ligands for AAA

The distinct electronic (i.e., electronic desymmetrization) and steric properties of different donor atoms influence the reactivity of allyl substrates through the metal. Much interest has recently been drawn to this type of ligand, resulting in the synthesis of a variety of ligands involving metal coordination by both N and P as illustrated in **Figure1-5**. Bidentate ligands with different ligating atoms such as phosphinooxazolines can lead to high enantioselectivity. It is thought that the oxazoline moiety provides the source of asymmetry and the phosphorus atom enhances reactivity. The stereochemical outcome is most consistent with the mechanism involving nucleophilic addition trans to the phosphorus atom as supported by X-ray and NMR studies.

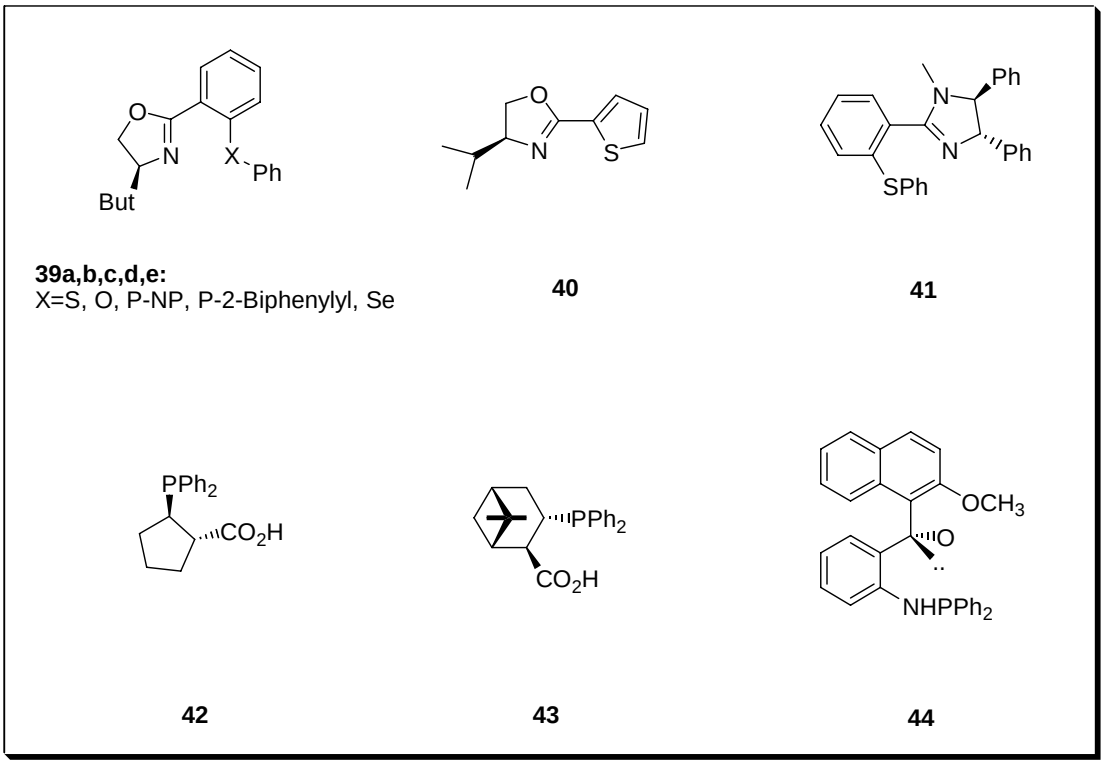

Figure 1-6. Some chiral ligands with mixed donor atoms for AAA

Variations on this theme have led to the design of mixed chelate-type ligands as shown in **Figure 1-6**. Bidentate ligands derived from various combinations of phosphorus, nitrogen, oxygen, sulphur, and selenium are able to provide high enantioselectivity. Similar to the P,N-chelate ligands, the origin of enantioselectivity has been proposed to be the preferential nucleophilic attack trans to the better π-acceptor. However, the poor binding ability of some donor atoms raises doubts as to the bidentate binding of these ligands. Therefore, the results obtained with these ligands should be interpreted with caution.

1.3. Palladium-Catalyzed Allylic Allylations with Stabilized Nucleophiles

Palladium-catalyzed allylic alkylations can be classified into two categories which use stabilized nucleophiles or unstabilized nucleophiles respectively. The later has not been extensively developed into asymmetric reactions. So we'll focus on the reactions with stabilized nucleophiles.

Palladium-catalyzed allylic alkylation can also be classified by the sources of enantiodiscrimination or the drives of chiral induction into the following categories.

- AAA induced by enantioselective ionization.
- AAA induced by desymmetrization of meso-π-allyl complexes.
- AAA induced by enantioselection involving enantioface exchange.
- Enantioselective alkylation of prochiral nucleophiles.

We'll focus to illustrate the AAA induced by desymmetrization of meso-π-allyl complexes as much as possible because it has been studied much intensively and usually acts as the first model reaction to test the catalytic properties of a newly synthesized chiral ligand.

Desymmetrization of Meso-π-Allyl Complexes:

1. Alkylation of 1,3-Diarylallyl Substrates with Carbon Nucleophiles

The 1,3-diphenylallyl system was introduced as a test substrate to contrast with the 1,1,3-triphenylallyl system in order to probe the importance of different mechanisms for asymmetric induction.[45] Early results with BINAP and BINAPO were encouraging (**Scheme 1-7**). Subsequently, this substrate has become the "standard" to compare different chiral ligands. The sensitivity of this system to the reaction conditions becomes evident from the significant difference in ee which is observed when different Pd(0) sources are used (**Scheme1-7**).[46]

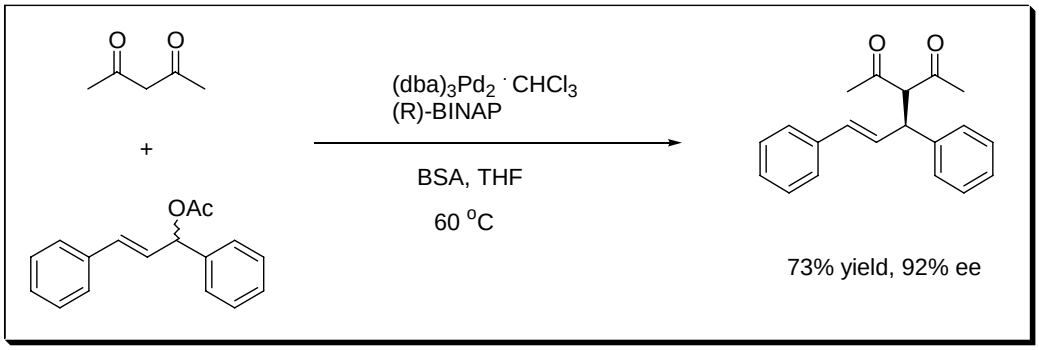

Scheme 1-7

Since the nucleophile is directly involved in the enantiodiscriminating step, its structure is expected to affect the ee. In terms of structure, both the constitution (i.e., malonate, 1,3-diketone, disulfone, etc.) and the nature of the ion pair play roles. Thus, the ee shows a dependence on how the nucleophile is generated. While the sodium salts are frequently employed, the potential for aggregate formation obfuscates the true nature of the nucleophile. For example, alkylation of **45** with dimethyl sodiomalonate using ligand **38** gives the alkylation product in 67% ee in THF and

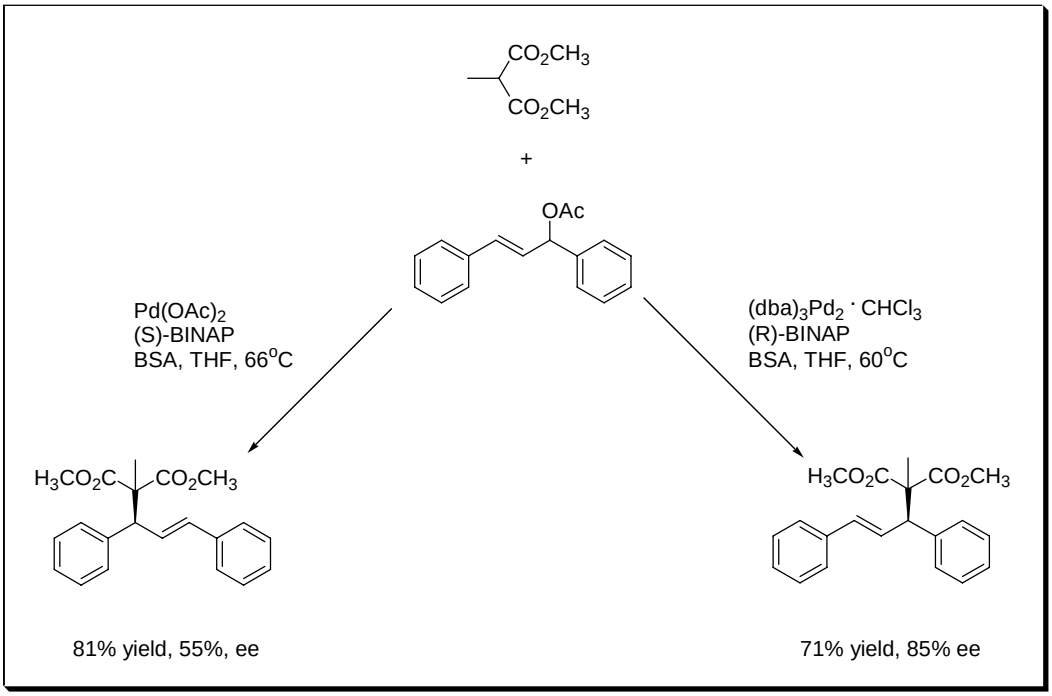

Scheme 1-8

78% ee in acetonitrile; but using the sodium salt with 15-crown-5 in acetonitrile increases it to 95%.[47] Thus, changing the nature of the ion pair has a significant effect on ee. In many cases, the best ee's are obtained by use of *N*,*O*-bis(trimethylsilyl)acetamide (BSA), sometimes in the presence of added acetate ion.[45] Reactions performed with ligand **28** reveal an effect of halide ion under these conditions with the ee increasing from 51% with iodide and 67% with bromide to 83% with chloride.[48]

Table 1-1 summarizes the enantioselectivities obtained in the alkylation of the diphenylallyl system with stabilized nucleophiles using various different ligand

designs (**Scheme 1-9**). The enantioselectivities are the best reported in the reference given (whether optimized or not).

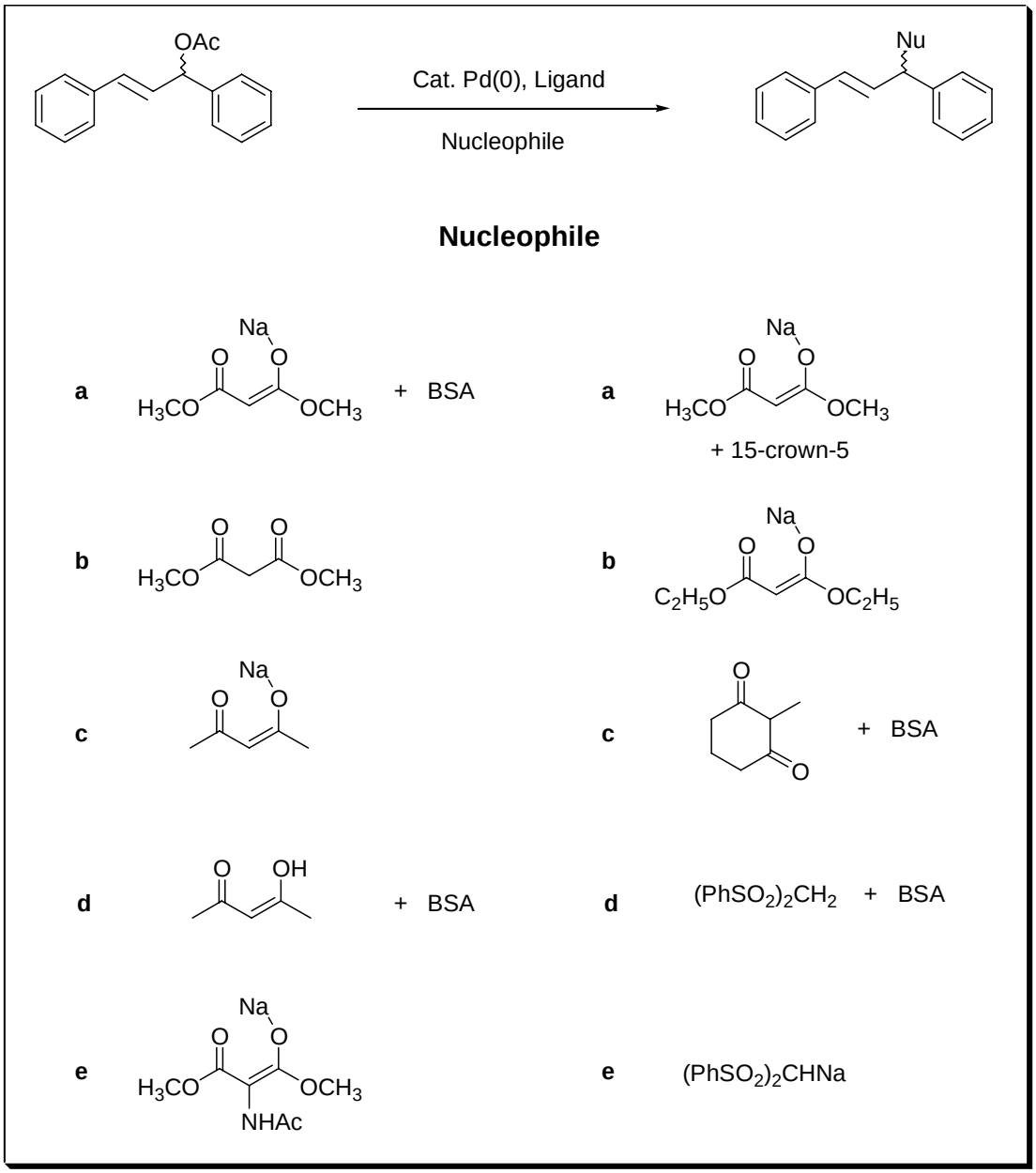

Scheme 1-9

Table 1-1. Allylic Alkylation of 1,3-Diphenylprop-2-enyl Acetate with Carbon Nucleophiles

entry	ligand	Nu[a]	Pd source	% yield	% ee	Ref.
1	**38**	a[a-d]	$[C_3H_5Pd]BF_4$	nd	<79	47
2	**36**	a	$[Pd(OAc)_2]$	95	96	49
3	**26**	a[b]	$[C_3H_5Pd]PF_6$	81	95	50,51
4	**2**	a	$[C_3H_5PdCl]_2$	86	90	52
5	isosparteine	a[b]	$[C_3H_5Pd]PF_6$	87	82	50,51
6	**40**	a	$[C_3H_5PdCl]_2$	89	81	53
7	**15**	a	$[(dba)_3{\cdot}CHCl]_3$	60	49	54
8	**10b**	a	$[C_3H_5PdCl]_2$	40	92	55
9	**10c**	a	$[C_3H_5PdCl]_2$	85	96	56
10	(*S*)-(-)-BINAP	a	$[C_3H_5PdCl]_2$	80	34	57
11	PROLIPHOS	a[c]	$[C_3H_5Pd]BF_4$	99	30	58,59
12	**31**	b	$[C_3H_5PdCl]_2$	89	99	60
13	**33b**	b[b]	$[C_3H_5PdCl]_2$	99	99	61,62
14	**33a**	b[b]	$[C_3H_5PdCl]_2$	98	98	61,62,63
15	**22**	b	$[C_3H_5PdCl]_2$	97	97	64
16	**39aa**	b[c]	$[C_3H_5PdCl]_2$	92	96	65,66
17	**37**	b[c]	$[C_3H_5PdCl]_2$	96	96	67
18	**23**	b[c]	$[C_3H_5PdCl]_2$	97	95	68
19	**25**	b	$[(dba)_2Pd]$	83	95	69
20	**39e**	b	$[C_3H_5PdCl]_2$	50-84	95	63
21	**11**	b[c]	$[C_3H_5PdOTf]$		93	70,71
22	**39bb**	b[c]	$[C_3H_5PdCl]_2$	100	92	66
23	**18aa**	b[c]	$[C_3H_5PdCl]_2$	56	92	72
24	**24**	b[d]	$[C_3H_5PdCl]_2$	98	91	73
25	(*S*)-(-)-BINAP	b[c]	$[C_3H_5PdCl]_2$	85	90	47
26	**21b**	b[c]	$[C_3H_5PdCl]_2$	97	88	64
27	**34**	b[c]	$[C_3H_5PdCl]_2$	85	85	61

28	**28**	b[c]	$[C_3H_5Pd]PF_6$	70	84	48
29	**8a**	b	$[(dba)_3Pd_2{\cdot}CHCl]_3$	88	79	46
30	**38**	b[c]	$[C_3H_5Pd]BF_4$	nd	79	47
31	**39c**	b[c]	$[C_3H_5PdCl]_2$	98	78	63
32	**30**	a	$[C_3H_5PdCl]_2$	86	77	64
33	**18b**	b[c]	$[C_3H_5PdCl]_2$	86	60	72
34	**10b**	c	$[C_3H_5PdCl]_2$	97	90	55
35	**2**	a	$[C_3H_5Pd]ClO_4$	96	22	74
36	**3**	c	$[C_3H_5PdCl]_2$	88	0	55
37	**33bb**	d[c]	$[C_3H_5PdCl]_2$	98	97	61
38	(*S*)-(-)-BINAP	d	$[(dba)_3Pd_2{\cdot}CHCl_3]$	73	92	46
39	(*S*)-(-)-BINAP	e	$[C_3H_5PdCl]_2$	92	95	57
40	**2**	e	$[C_3H_5PdCl]_2$	98	91	57
41	(*S*,*R*)-BPPFA	e	$[C_3H_5PdCl]_2$	79	52	57
43	**33b**	f	$[C_3H_5PdCl]_2$	98	97	61
44	**20**	g	$[Pd(OAc)_2]$	68	85	75
45	(*S*)-(-)-BINAP	h	$[(dba)_3Pd_2{\cdot}CHCl_3]$	46	66	46
46	**33a**	i	$[C_3H_5PdCl]_2$	87	88	76
47	**33a**	j[b]	$[C_3H_5PdCl]_2$	78	93	65

[a] In THF (for a-j, see eq 26).[b] In DMF.[c] In CH_2Cl_2.[d] In CH_3CN.[e] In CD_2Cl_2.

Table 1-1 reveals that a wide variety of bidentate ligands ranging from bisphosphines to aminophosphines to bisamines are capable of inducing high ee in this case. One notable feature of the diphenylallyl system is the prominence of ligands which lack C_2 symmetry.[50,48] The enantiomeric excess obtained for ligand **28** (entry 28) was more than twice as high as either of the closely related two C_2 symmetrical isomers.[48] The most extensive and general advances for acyclic substrates bearing

bulky substituents have come with the development and study of (phosphinoaryl)oxazoline ligands (entries 13, 14, and 31).[61] These ligands give diarylallyl adducts with high enantioselectivities in excellent yields. A wide range of (phosphinoaryl)oxazolines may be easily prepared in two steps from readily available chiral amino alcohols **(Scheme 1-10**). The highest enantioselectivities seem to come from **33a** (R = *i*-Pr) and **33c** (R = *t*-Bu).

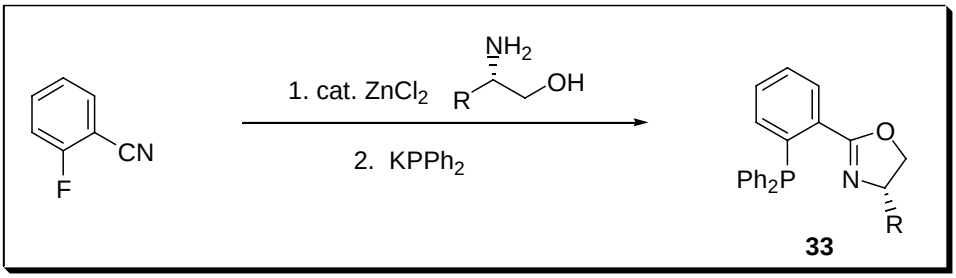

Scheme 1-10

Oxazoline ligands (entries 13, 14, and 26) do not exchange enantiofaces during the reaction. Alkylation of optically pure (*R*)-**46** with dimethyl malonate and BSA

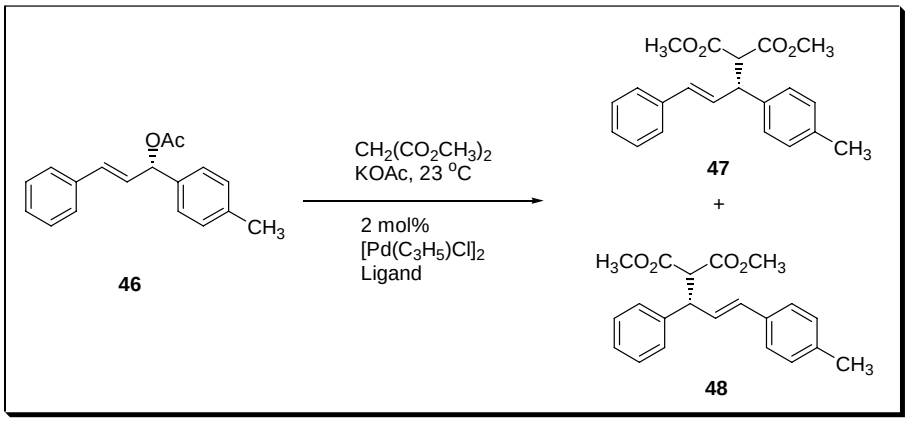

Scheme 1-11

using triphenylphosphine afforded only the regioisomers (*R*)-**47** and (*S*)-**48** in close to a 1:1 ratio with each in enantiomerically pure form (**Scheme 1-11**).

Ligands **21b**, (+)-*ent*-**33b**, and **33b** afforded (*R*)-**47** and (*S*)-**48** in 93:7, 99:1, and 1:99 ratios, respectively. Again, these regioisomers were enantiomerically pure. This strongly suggests a double inversion mechanism without enantioface exchange. This example illustrates the ability of the ligand to dictate regiochemistry, albeit in a relatively unbiased case. The prospect for such chiral ligands to control regioselectivity is potentially an exciting solution to a long-standing issue in allylic alkylation.

The many early attempts to use ligands such as BINAP and DIOP in these reactions met with disappointing results. However, entries 10, 25, 37, 38, 39, and 44 demonstrate the importance of reaction conditions in achieving good enantioselectivities. In this case, (*S*)-BINAP can give enantiomeric excesses as low as 34% with dimethyl sodiomalonate in THF or as high as 90% with dimethyl malonate/BSA in dichloromethane. The use of sodiomalonates does not preclude good ee's; if the sodium salt of 2-acetamidomalonate is used, then BINAP provides the desired alkylation product with 94% ee.[57] The factors responsible for the good enantioselectivities available with 2-acetamidomalonate may extend beyond simple steric interactions since dimethyl malonate and 2-acetamidomalonate afford products of opposite configuration. The lesson here is a simple one. Reaction conditions can

and should be optimized for each new ligand/substrate/nucleophile combination in order to assess ligand efficacy.

2. Other Reactions featured with Desymmetrization of Meso-π-Allyl Complexes:

With the mechanism of desymmetrization of Meso-π-Allyl Complexes, there are still other types of asymmetric allylic alkylation reactions, such as:

- Alkylation of 1,3-Diarylallyl Substrates with Heteroatom Nucleophiles;
- Alkylation of Acyclic 1,3-Dialkylallyl Substrates;
- .Alkylation of Cyclic Allylic Substrates.

However, we mainly focused on the alkylation of 1,3-diarylallyl substrates with carbon nucleophiles to preliminarily test the catalytic properties of our ligands.

1.4. Summary

In the past two decades great strides have been made in developing the palladium-catalyzed allylic alkylations. Various approaches have led to better understanding of the reaction, and good enantioselectivities have been obtained. Many reactions have been developed and have reached a level where they can emulate other well-developed asymmetric catalytic methods. Compared to asymmetric hydrogenation and oxygenation, allylic alkylations have two special and very useful features which are:

- Asymmetric allylic alkylation can form many different bond to carbon, such as C-C, C-N and C-O in high stereoselective fasion.

- Their mechanisms are more complicated. The stereodynamic processes involved in each step of the catalytic cycle provide different mechanisms for enantioselection and ample opportunities for developing corresponding asymmetric reactions. Furthermore, both reacting partners, the nucleophile and allyl unit can be the site for asymmetric induction.

1.5. The Aims and Objectives of this Project

The exceptional chemoselectivity and synthetic versatility of asymmetric allylic alkylation have resulted in a number of new strategies for the synthesis of natural products and have found elegant applications. As is evident from the research work in the past years, the potential of the asymmetric allylation reactions will lead to continuing efforts to discover efficient catalysts and reaction systems. So, the objectives of this thesis are to:

- **Synthesize novel chiral diphosphine ligand**.

As we know, a variety of chiral diphospine ligands have been synthesized and successfully applied to asymmetric catalytic reactions. So, the opportunities to synthesize new chiral diphosphine ligands become very rare. It is much difficult and challenging to create a totally novel chiral diphosphine ligand (particularly with new

structure motif). However, a totally novel ligand should have some special properties in asymmetric catalysis. So one of the main purposes of this project is try to find a new method to synthesize a totally novel chiral diphosphine ligand.

- **Apply the novel diphosphine ligand to asymmetric allylic alkylations**.

Unlike that in asymmetric hydrogenation, among all the chiral diphosphine ligands, few exhibit good performance in asymmetric allylic alkylations. So, it is also a purpose for us to synthesize a proprietary diphosphine ligand which is good especially for asymmetric allylic alkylations.

Chapter 2

Synthesis of a Novel Chiral Bipyrimidyl Diphosphine ligand (PM-Phos):

5, 5′-Bis(diphenylphosphino)-1, 1′, 3, 3′-tetramethyl-4, 4′-bipyrimidine-2, 2′, 6, 6′-(1*H*, 1′*H*, 3*H*, 3′*H*)-tetrone

2.1. Chiral Diphosphine Ligands

2.1.1. Introduction

Homogeneous asymmetric catalysis involving chiral phosphine ligands is currently one of the most extensively studied areas in chemistry. As a matter of fact, the design and synthesis of chiral phosphine ligands have played a significant role in the development of efficient transition metal catalyzed reactions. Among all aspects of research in this field, much effort has been placed in the preparation and application of new chiral diphosphine ligands. So far, a number of optically pure diphosphines have been synthesized and evaluated aiming at higher enantioselectivity, such as DIPAMP,[77] DIOP,[78] Chirophos,[79] Norphos,[80] BPPM,[81] DEGphos,[82] BINAP,[83] Duphos,[84] BPE,[84] BICP,[85] SpiroOP,[86] PENNEPHOS,[87] BisP,[88] MiniPhos,[89] Binaphane,[90] PHANEPHOS[91] and TangPhos.[92] Some typical chiral diphosphines are summarized in **Figure 2-1.** Among these ligands, BINAP, a fully arylated C_2 symmetrical diphosphine is one of the most effective chiral ligands reported in the literature.

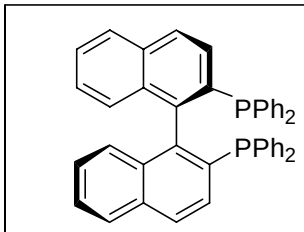

(R)-BINAP

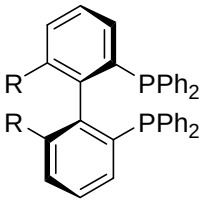

(R)-BiPHEMP

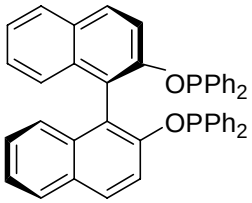

(*R*)-BINAPO

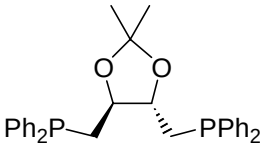

DIOP

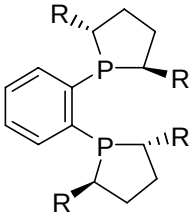

DuPhos

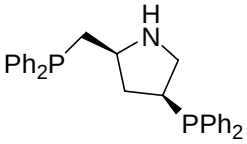

(*S*,*S*)-BPPM

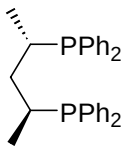

(*S*,*S*)-BDPP

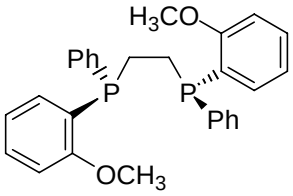

(*R*,*R*)-DiPAMP

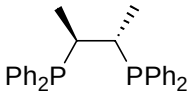

(*S*,*S*)-Chiraphos

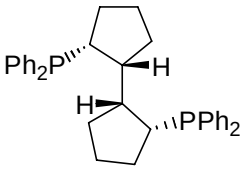

(*R*,*R*)-BICP

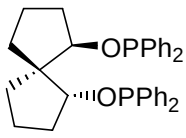

(*R*,*R*,*R*)-SpirOP

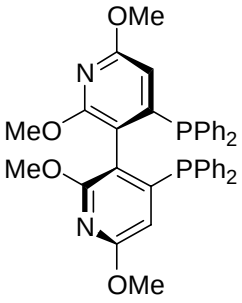

(*R*)-P-Phos

Figure 2-1. Some Chiral diphospine ligands

Recently, Pai and Chan *et al.*[93-96] successfully synthesized a novel atropisomeric heteroatom-containing diphosphine ligand P-Phos, whose ruthenium complexes were found to catalyze the asymmetric hydrogenation of a wide range of substrates with excellent enantioselectivity. This new catalyst can be recycled by a simple phase separation which makes this new ligand commercially attractive.

The search for more practical and efficient ligands is one of the main goals in asymmetric catalysis. And in light of these prominent pioneer results, the main target of this thesis is to explore the opportunities in synthesis of a novel chiral diphospine ligand and to investigate its asymmetric catalytic properties.

2.1.2. Synthetic Methods of Diphosphine Ligands

Although each chiral diphosphine ligand has its own synthetic route and resolution method, some typical methods do exist as illustrated by the synthetic method of BINAP and P-phos.

- **Synthetic methods of BINAP:**[97]

The synthetic methods of BINAP can illustrate the general methods of the synthesis of ordinary diphosphine ligands. The first practical methods for the synthesis of BINAPs were reported in 1986.[98] Since then, a series of BINAP analogues have been prepared according to the standard synthetic route (**Scheme 2-1**). However, this route requires harsh conditions for the coversion of binaphthol to the corresponding dibromide and tedious optical resolution of BINAP derivatives.

Cai *et al.*[99] of Merck developed a new method for direct asymmetric synthesis of BINAP by use of nickel-catalyzed coupling reaction of easily accessible chiral 2,2′-bis((trifluromethanesulfonyl)oxy)-1,1′-binaphthyl in the presence of DABCO (**Scheme 2-2**). Similarly, Laneman *et al.*[100] of Monsanto reported the nickel-catalyzed cross-coupling of chiral 2,2′-bis((trifluromethanesulfonyl)oxy)-1,1′-binaphthyl

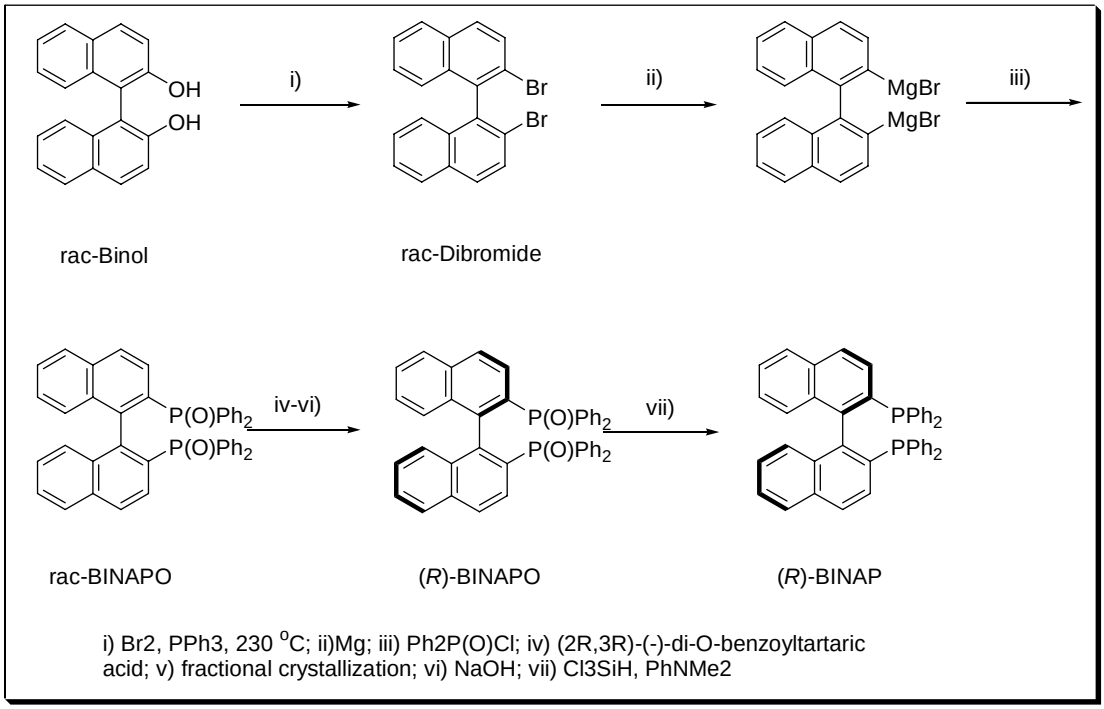

Scheme 2-1.

with chlorodiphenylphosphine in the presence of zinc. These methods, however, have some drawbacks in industrialization, such as use of pyrophoric diphenylphosphine or moisture-sensitive chlorodiphenylphosphine.

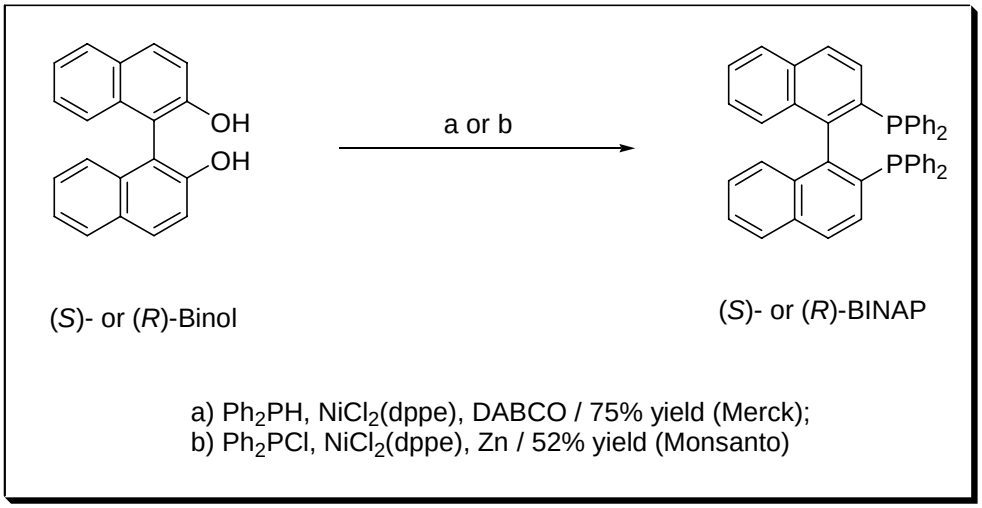

Scheme 2-2.

Recently, Sayo and Zhang *et al.*[101] reported two procedures for the synthesis of chiral BINAPs by using the metal-catalyzed coupling reaction of 2.2′-bis((trifluromethanesulfonyl)oxy)-1,1′-binaphthyl with diarylphosphine oxides, which are readily prepared by the reaction of aryl-magnisium halide with diethyl phosphate and easy to handle in large quantity. The first one is well illustrated by coupling of (*R*)- 2.2′-bis((trifluromethanesulfonyl)oxy)-1,1′-binaphthyl with diphenylphosphine oxide, which proceeded smoothly in the presence of 1,2-bis(diphenylphosphino)ethane (dppe) and nickel (II) chloride to give a mixture of (*R*)-BINAP, (*R*)-BINAP(O), (*R*)-BINAPO. This mixture was then reduced by a mixture of trichlorosilane and N,N-dimethylaniline in refluxing toluene, giving (R)-BINAP in 96% yield (**Scheme 2-3**). This procedure has been successfully applied to the synthesis of a series of known of new chiral BINAP ligands in reasonable to good yields.

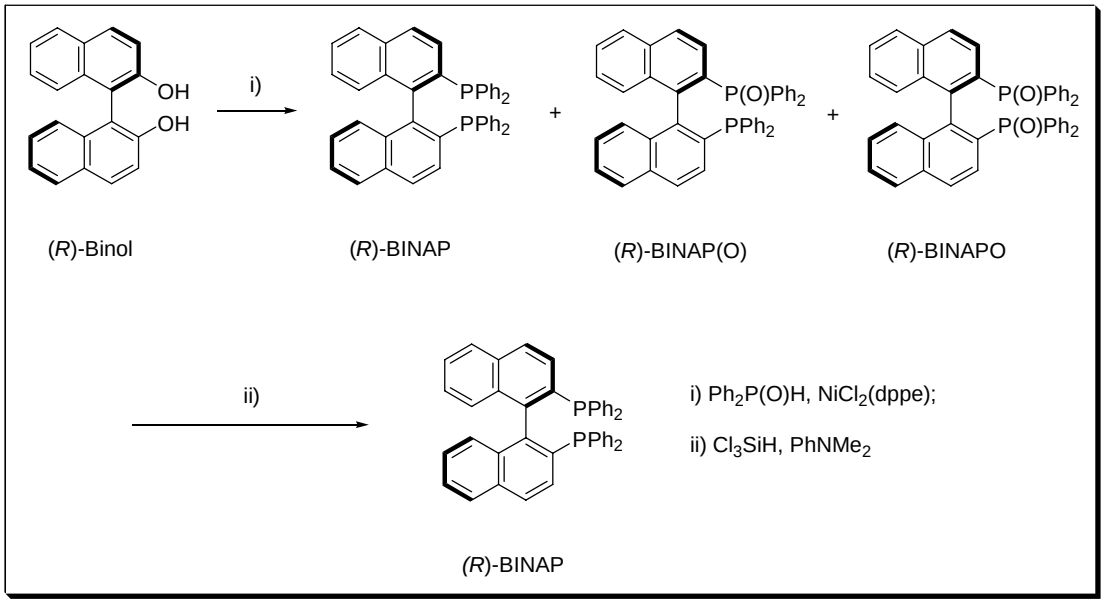

Scheme 2-3

- **Synthetic method of P-Phos**

In contrast to the tremendous success achieved in the use of chiral arylphosphine ligands in transition metal-catalyzed asymmetric reactions, chiral phosphine ligands containing heterocyclic moieties such as pyridyl groups have been relatively unexplored even though the expansion of the scope of the metal phosphine chemistry with the rich chemistry of heterocyclic functionalities is quite obvious. Some transition metal complexes with pyridylphosphine ligands had been synthesized and found to be inactive in homogeneous hydrogenations.[102] However, we have successfully developed a class of dipyridylphosphine ligands: P-Phos, Tol-P-Phos and Xyl-P-Phos and found their Ru(II) and Rh(I) complexes to be highly effective in the catalytic asymmetric hydrogenation and other reactions[93-96]. In some asymmetric reactions, its performance is better than BINAP. The reason is that the unique N-containing feature and the different hindrance (provided by OMe groups) of these

ligands favor the reactions, while the unfavorable coordination possibility of nitrogen atoms is removed by the strong shielding ability of the OMe groups.

The synthetic route for P-Phos ligand is outline in **Scheme 2-4**. The most special

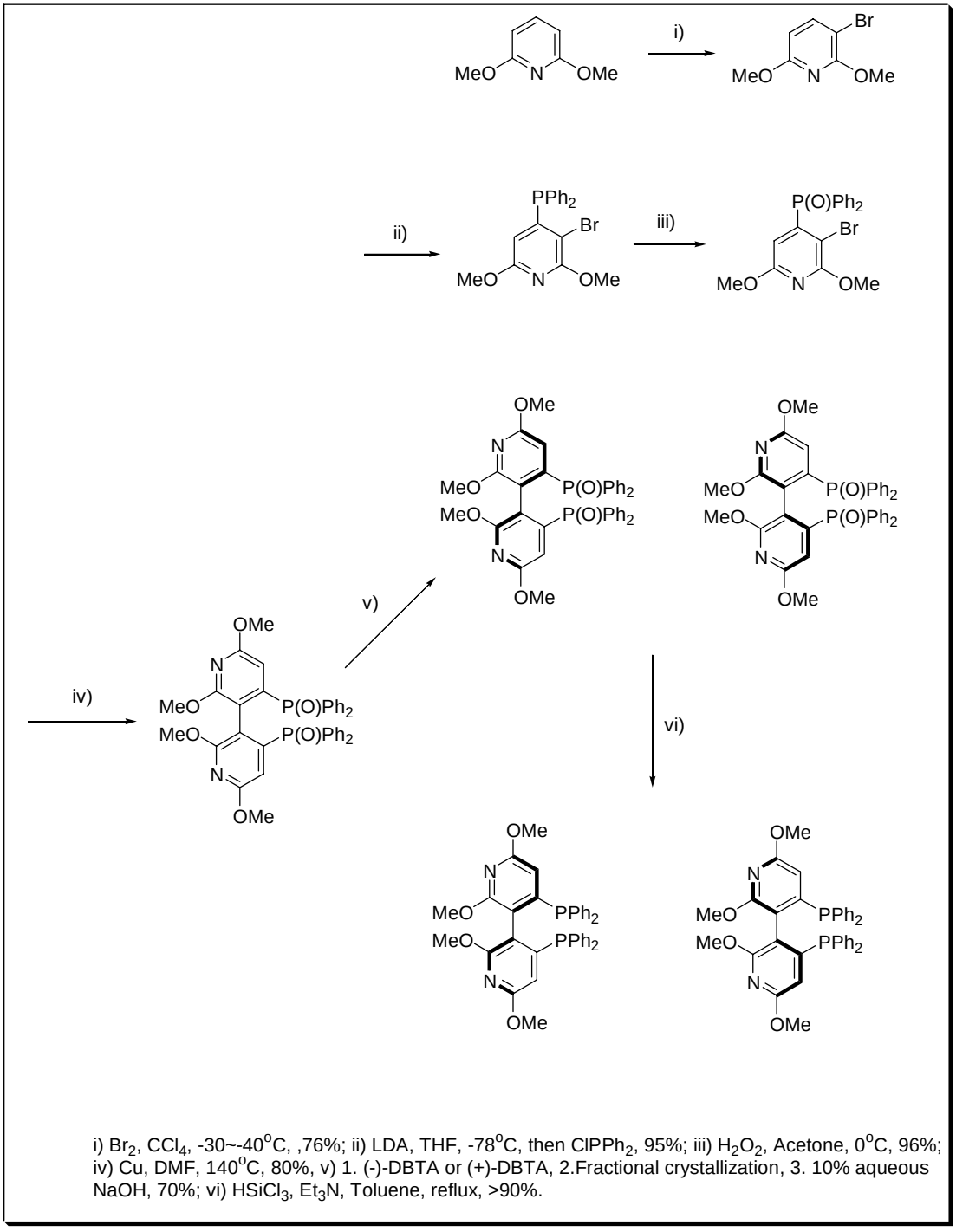

Scheme 2-4. Synthetic route of P-Phos

feature in the synthesis of this proprietary ligand is that we employed Ullmann coupling to synthesize a C_2-symmetry diphosphine ligand. Although the ligand contains nitrogen atoms which may form H-bonds with DBTA and interfere the optical resolution process, the ligand was successfully resolved by the DBTA with our efforts.

2.2. Synthesis of Novel Chiral Bipyrimidine Diphosphine ligand (PM-Phos): 5,5′-Bis(diphenylphosphino)-1,1′,3, 3′-tetramethyl-4,4′-bipyrimidine-2,2′,6,6′-(1*H*, 1′*H*, 3*H*, 3′*H*)-tetrone

2.2.1. Design of the ligand

As we know, the design and synthesis of chiral phosphine ligands have played a significant role in the development of efficient transition metal catalyzed reactions. Along with the great success in the synthesis and application of BINAP, a series of C_2-symmetry aryl diphosphine ligands have been synthesized, which can be roughly classified into the following categories:

- Binaphthyl type, such as BINAP.
- Biphenyl type, such as BIPHEMP and MeO-BIPHEP.
- Bipyridine type, such as P-PHOS, Tol-P-Phos and Xyl-P-Phos.
- Other types.

So, one question is whether there is still possibility to develop other types of C_2-symmetric aryl diphosphine ligands. Although at this time it is very difficult to

develop a new type of these ligands, the main target of this thesis was determined to seek this rare possibility. The following ligands (**Figure 2-2**) can be called as bipyrimidine, biquinoline and biisoquinoline diphosphine ligands, they may give some potential and promising leads in developing novel diphosphine ligands.

OptionButton1

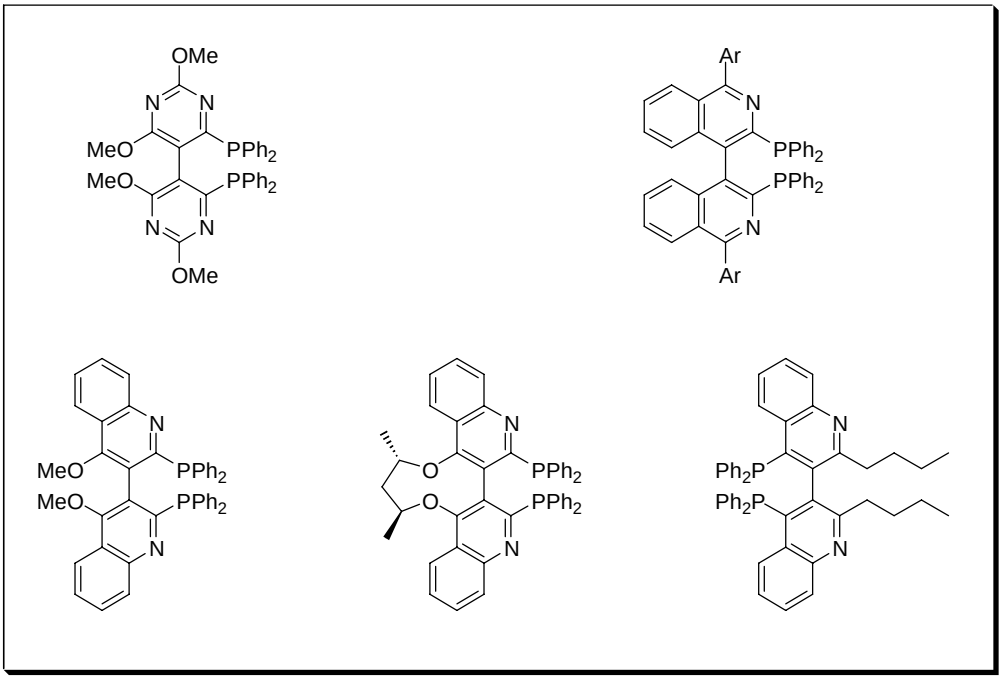

Figure 2-2. Some potential diphosphine ligands

Encouraged by the success of our proprietary diphosphine ligand P-Phos, we planned to synthesize a bipyrimidine type diphosphine ligand which was like P-Phos. This was our proposed target in an effort of developing a novel chiral diphosphine ligand. However, we enventually got a ligand with totally different structure motif, i.e., our realized target was totally different from our proposed target (**Figure 2-3**).

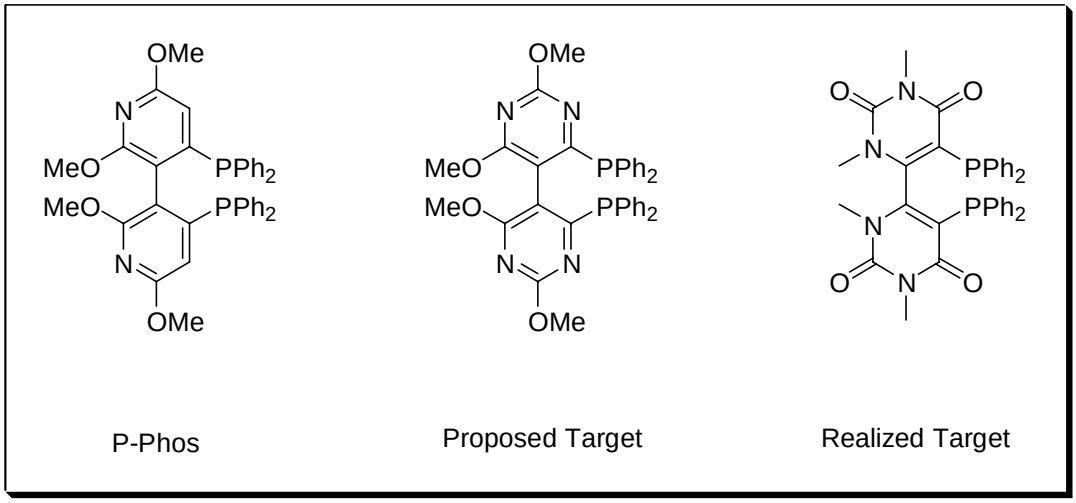

Figure 2-3. The proposed target and realized target.

2.2.2. Synthetic Route

Chiral bipyrimidine-type diphosphine ligand has not been synthesized before. Even ordinary pyrimidine phosphine ligands have not been reported so far. So it is a great adventure or challenge to try to synthesize such a ligand. As this is an unexplored field, there may be some potential opportunities. In the synthesis of this kind of ligand which is depicted in **Scheme 2-5**, we met many challenges and found very interesting chemistry, which are outlined in the followings.

- **Rearrangement in step ii) (Scheme 2-5):**

In step ii), whereby the diphenylphosphine moiety was introduced to the molecular structure of compound **2-2**, the bromine group and the diphenylphosphine substituent appeared at positions other than their expected locations. This unforeseen “exchange” was so complete that almost no unrearranged product could be found after the reaction.

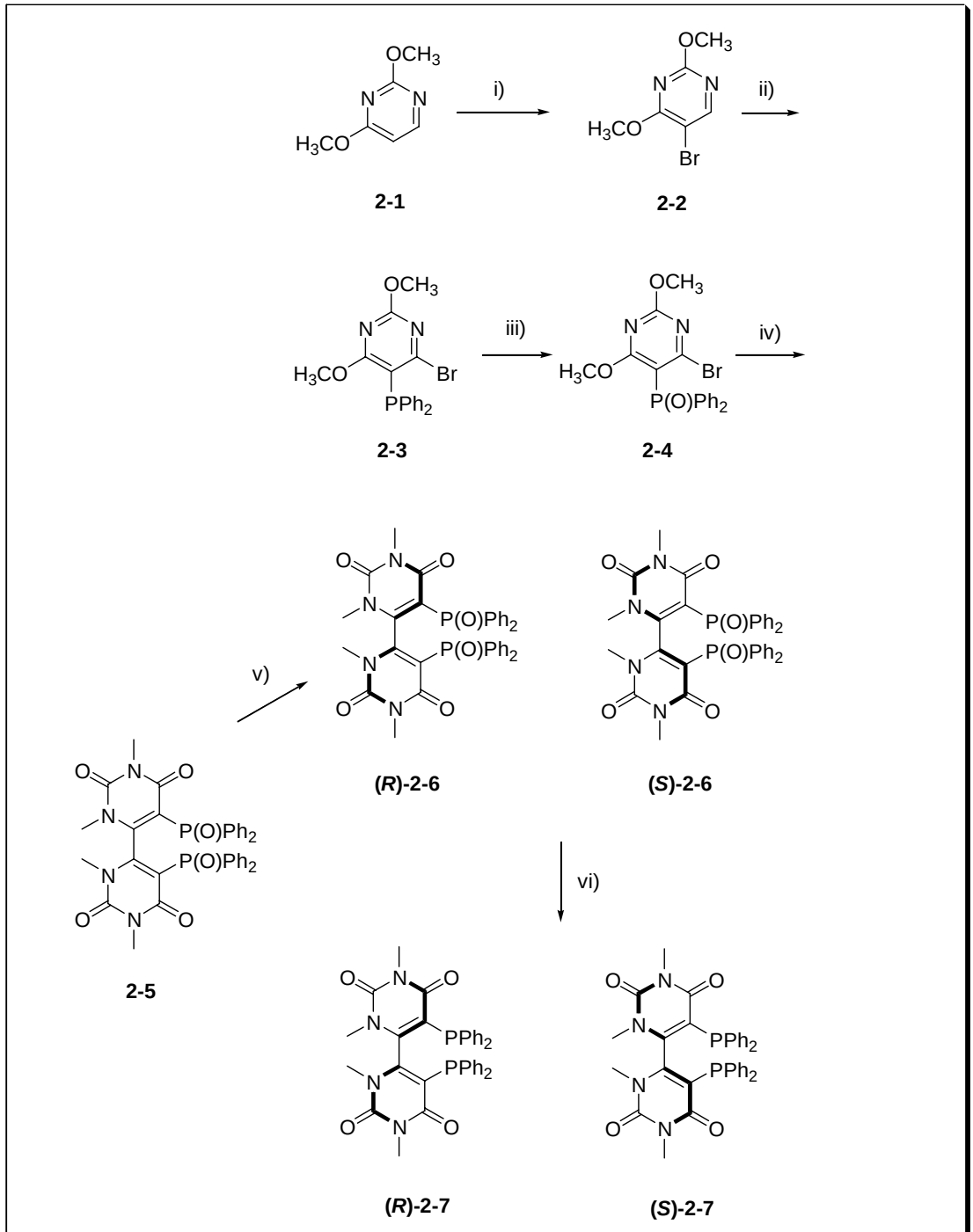

i) Br_2, CCl_4, 0^oC, 88%; ii) LDA, THF, -78^oC, then $ClPPh_2$, 76%; iii) H_2O_2, Acetone, 0^oC, 92%; iv) Cu, DMF, Na_2CO_3,140^oC, 40%, v) 1. (-)-DBTA or (+)-DBTA, 2.Fractional crystallization, 3. 10% aqueous NaOH, 75%; vi) $HSiCl_3$, Et_3N, Toluene, 140^oC in autoclave, 75%.

Scheme 2-5. Synthetic route of PM-Phos

And after recrystallization, compound **2-3** was isolated in very pure state and no unrearranged product could be detected by NMR.

In the step ii), compound **2-2** was first lithiated by LDA. In the lithiation of halopymidine compounds, halogen migration is a common phenomenon. This was first discovered by Bunnet[103] and its mechanism was explained by Queguiner *et al.*[104]. According to their explanation, a likely mechanism for step ii) is proposed as shown in **Scheme 2-6**. First, compound **2-2** was lithiated by LDA at low temperature. The lithiation was ortho directed by the bromine group to give intermediate **A**, which was not stable because of the repulsion effect of the two electron pairs. The subsequent bromine ortho-migration was sufficiently fast to give intermidiate **B**, whose negative and positive ion were stabilized by the electron-withdrawing effect of the two nitrogen atoms and the neighboring electron-donating effect of the ortho methoxy group respectively. So, the bromine migration was driven by these stabilization effects. Then, in the final step, intermediate **B** was treated with the electrophile PPh_2Cl to give product

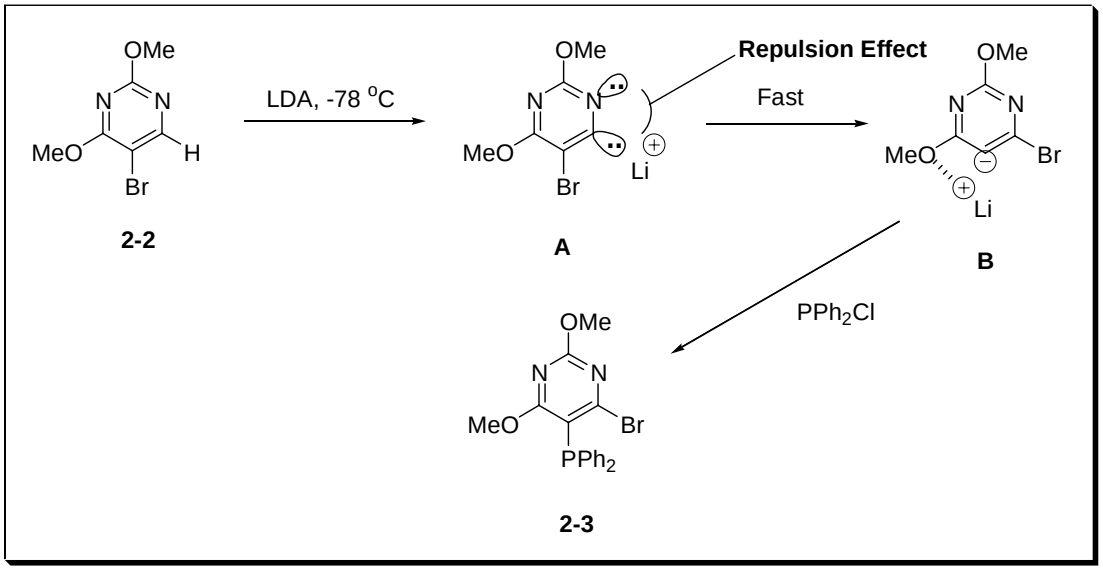

Scheme 2-6. The proposed mechanism for bromine migration in step ii).

2-3. In the synthesis of P-Phos, there is the same bromine migration problem.[105] However, as there is only one nitrogen atom in the molecular structure of the starting material of P-Phos, the repulsion effect of electron pairs does not exist and the stabilization effect of nitrogen atom is not strong enough. So, the bromine migration is not as facile as in the present case. Hence, by careful manipulation the bromine migration was avoided in the synthesis of P-Phos as shown in **Scheme 2-7**. Although in the synthesis of PM-Phos this kind of rearrangement was inevitable, it turned out to be critical to synthesize an unexpected novel ligand.

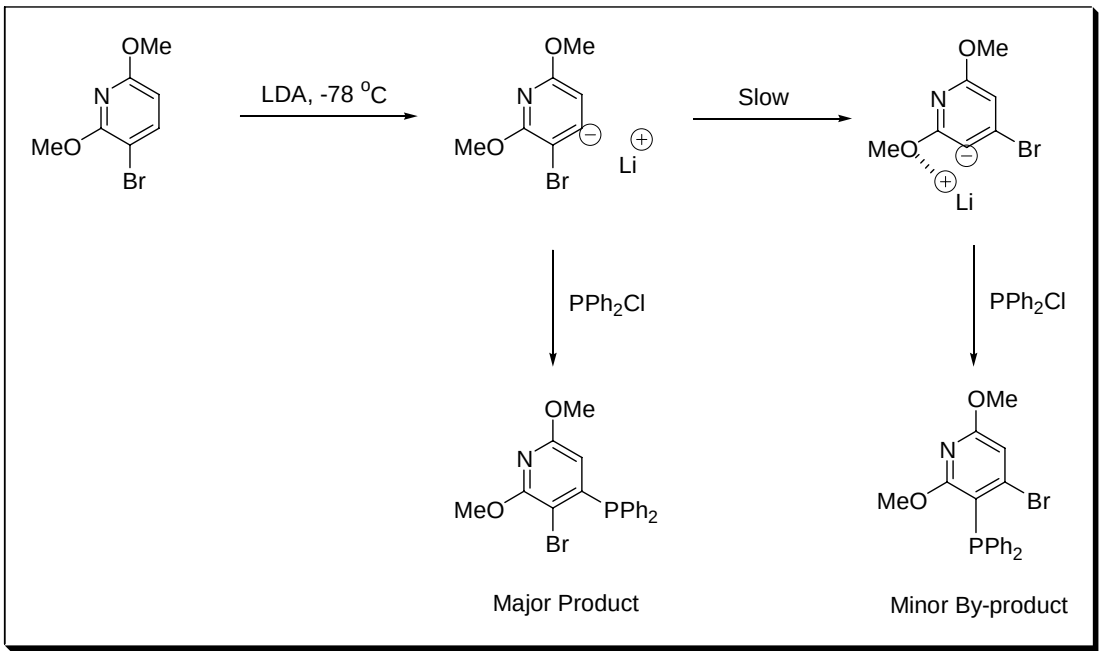

Scheme 2-7 The bromine migration in the synthesis of P-Phos

- **Rearrangement in step iv) (Scheme 2-5):**

In the coupling step, the methyl groups rearranged from the oxygen atoms to the nitrogen atoms. Thus, in this step two reactions had occurred, namely homoaryl

coupling and rearrangement, respectively. However, we do not know which reaction took place first or whether they occured simultaneously. Another very special feature is that there was no partially rearranged product; i.e., only one product **2-5** was obtained from the reaction system. This implies that the mechanism of the reaction should be very interesting and need further exploration. As this stage, it is hard for us to propose a reasonable explanation of the mechanism. However, the stabilization effects should still be the driving factor of the rearrangement. Overall, the coupling and the strange but complete rearrangement resulted in synthesis of a totally novel diphosphine dioxide **2-5**.

- **Modified Ullmann Coupling:**

It is worthy to state that under usual Ullmann coupling condition which is refluxing in DMF with copper, we could only get an unknown polymeric copper complex byproduct which could only dissolve in hydrochloric acid or aqueous ammonia solution, and we could not obtain any desired product **2-5**. Thus we developed a modified Ullmann reaction condition by the addition of sodium carbonate. This method was able to effectively facilitate the coupling of compound **2-4.** It was anticipated that by adding sodium carbonate continuous removal of the produced copper ion from the reaction system might be effected by copper carbonate precipitate formation. Sodium carbonate, potassium carbonate and sodium oxylate should have the same function, but sodium carbonate appeared to be the best. This method was initially created by us, it has not been reported before and it had been proved to be effective and critical to realize the coupling of compound **2-4**.

- **Modified reduction method**

Compound **2-5** was optically resolved successfully with the conventional DBTA reagent. However, in the final step it was very difficult to reduce compound **2-6** under the usual reduction condition which is refluxing with $SiHCl_3$ and Et_3N in toluene. The usual reduction condition is much efficient for the reduction of P-Phos-oxide, however, it had almost no effect in the reduction of compound **2-6**. We had tried other reduction methods and failed at all. And finally, we found that performing the reaction in an autoclave could solve this problem. In an autoclave, the temperature was able to be maintained thoroughly under a higher pressure, which should much favor the reaction.

2.3. Experimental

2.3.1. General Method

Unless specially noted, all experiments were carried out under a dry nitrogen atmosphere. The preparation of the samples and the setup of reactions were either performed in a nitrogen-filled continuous purge MBRAUN lab master 130 glovebox or using standard Schlenk-type techniques. Column chromatography was carried out on silica gel (Merck, 60A, 230-400 mesh). Analytical thin layer chromatography was performed on Merck silica gel 60 F-254 pre-coated plates.

2.3.2. Apparatus

Unless otherwise indicated, NMR spectra were recorded on a Varian 500 using chloroform as an internal standard for ^{1}H and ^{13}C spectra and H_3PO_4 in D_2O as an external standard for ^{31}P spectra. For all NMR spectra, signals are reported in ppm unit and coupling constants were given in hertz. Melting points were measured using an Electrothermal 9100 apparatus in capillaries and the data were uncorrected. Optical rotations were measured on a Perkin-Elmer model 341 polarimeter at 25^{o}C. spectra Mass analyses were performed on a Finnigan model Mat 95 ST mass spectrometer. HPLC analyses were performed using a Hewlett-Packard model HP 1050 LC.

2.3.3. Chemicals and Solvents

The commercial chemicals and reagents were used as received without further purification. Toluene, diethyl ether and tetrahydrofuran (THF) were refluxed and then distilled from sodium sand under nitrogen with benzophenone as indicator. Hexane, pyridine, triethylamine, dimethylformamide and dichloromethane were refluxed and then distilled from calcium hydride.

2.3.4. Preparation of 5-Bromo-2,4-dimethoxypyrimidine (2-2)

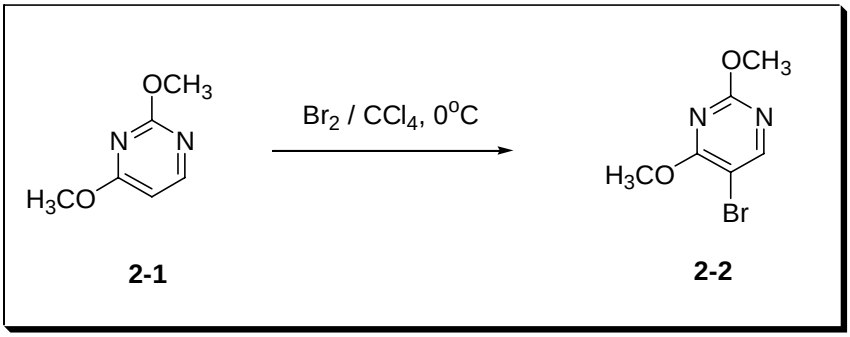

Scheme2-8

To a mixture of 2,4-dimethoxy pyrimidine (8.4 g, 60.0 mmol) and carbon tetrachloride (80 mL) with a magnetic stirrer was slowly added a solution of bromine (3.1 mL, 9.6g, 60 mmol) in carbon tetrachloride (40 mL) at 0 ^{o}C in 2 h. The reaction mixture was stirred at 0 ^{o}C for 12 h. The solution was neutralized with saturated sodium carbonate aqueous solution at 0 ^{o}C, and washed with water for three times. The organic layer was separated and dried with anhydrous sodium sulfate, the solvent carbon tetrachloride was recovered by distillation. The residue was extracted with dichloromethane, and purified by flash chromatography with dichloromethane as eluant. The eluate was concentrated *in vacuo* and the solvent was completely removed off. Finally, the residue was purified by recrystallization in hexane to give a pure product **2-2** (11.6g, yield 88%) as colorless crystal.

M.p.: 63 ^{o}C

^{1}H NMR ($CDCl_3$): δ3.71 (s, 3H, OCH_3), 3.79 (s, 3H, OCH_3), 8.02 (s, 1H).

^{13}C-NMR ($CDCl_3$): δ54.85, 55.18, 98.05, 159.09, 164.22, 166.66.

X-ray diffraction experiment:

Single crystal of **2-2** was obtained by slowly evaporating solvent from the solution of **2-2** in dichloromethane and hexane. The crystal structure determined by x-ray diffraction is exhibited in **Figure 2-4**.

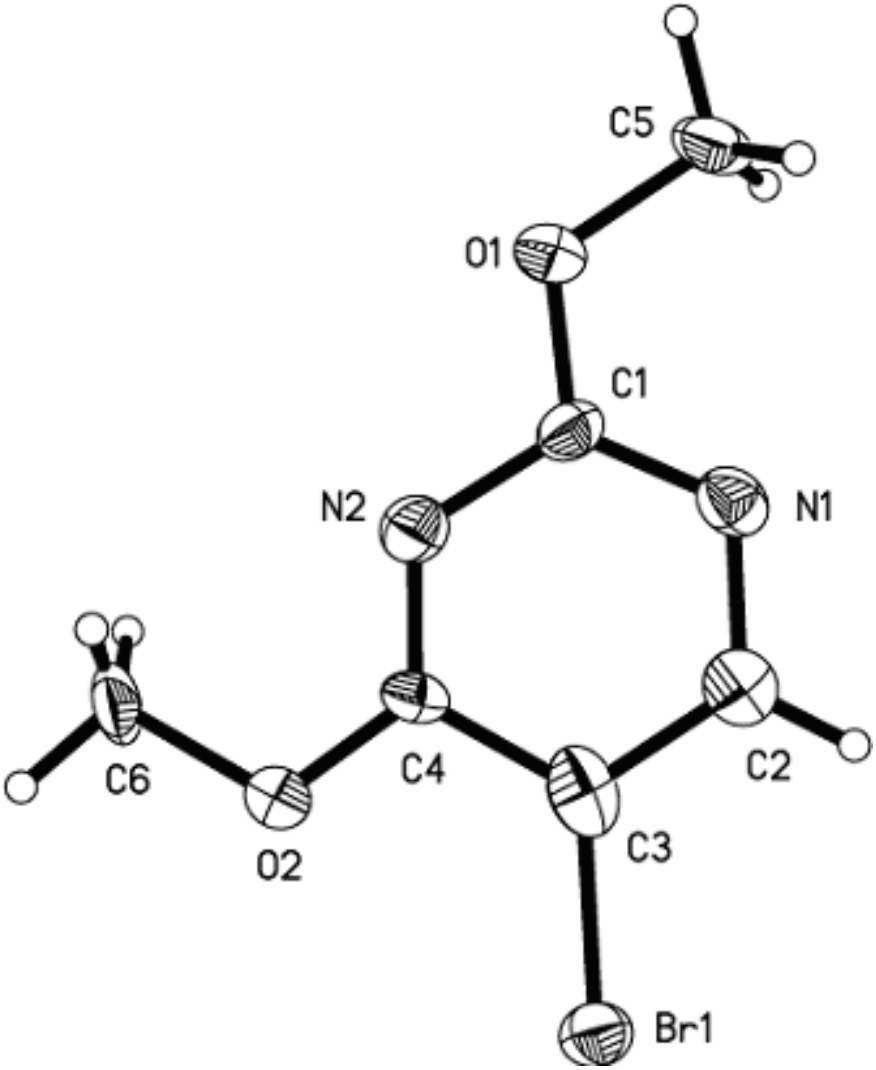

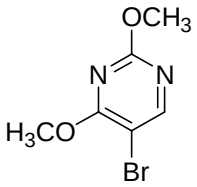

Figure 2-4. ORTEP drawing of **2-2**

Selected Crystal data for **2-2**: $C_6H_7BrN_2O_2$, M = 219.05, Orthorhombic, Space group Fdd2, *a* = 12.439(6) Å, *b* = 37.312(10) Å, *c* = 6.997(3) Å, α = 90°, β = 90°, γ = 90°, *V* = 3248(2) $Å^3$, *Z* = 16, D_c = 1.792 Mg/m^3, *T* = 294(2) K, Goodness-of-fit on F_2 1.005, R1 = 0.1130

Table 2-1. Selected Bond lengths [Å] and angles [°] for (*R*)-**2-2**.

Bond lengths [Å]			
Br(1)-C(3)	1.853(5)	O(1)-C(1)	1.329(5)
O(2)-C(4)	1.306(4)	N(1)-C(1)	1.334(6)
N(1)-C(2)	1.359(6)	N(2)-C(4)	1.267(4)
N(2)-C(1)	1.327(5)	C(2)-C(3)	1.391(6)
C(3)-C(4)	1.434(7)		
Angles [°]			
C(1)-O(1)-C(5)	121.1(4)	C(4)-O(2)-C(6)	114.1(3)
C(1)-N(1)-C(2)	115.5(4)	C(4)-N(2)-C(1)	120.2(4)
N(2)-C(1)-O(1)	115.5(4)	N(2)-C(1)-N(1)	125.7(4)
O(1)-C(1)-N(1)	118.6(3)	N(1)-C(2)-C(3)	121.7(5)
C(2)-C(3)-C(4)	116.3(4)	C(2)-C(3)-Br(1)	121.7(4)
C(4)-C(3)-Br(1)	122.0(3)	N(2)-C(4)-O(2)	125.1(4)
N(2)-C(4)-C(3)	120.5(4)	O(2)-C(4)-C(3)	114.4(3)

2.3.5. Preparation of

4-Bromo-5-(diphenylphosphino)-2,6-dimethoxypyrimidine (2-3)

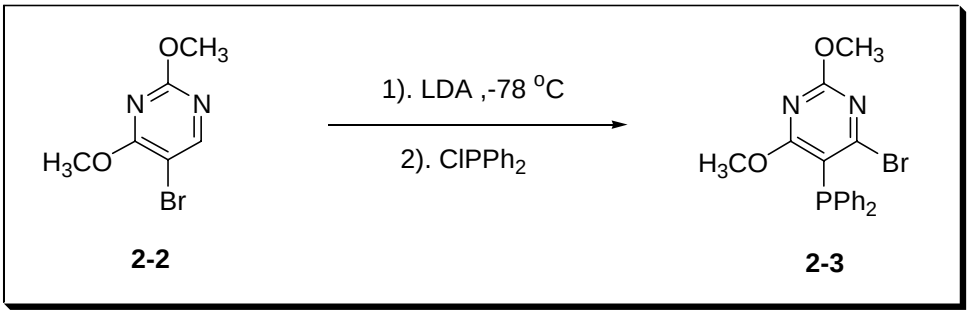

2-2 **2-3**

Scheme 2-9

To a magnetically stirred solution of 8.2 mL (58.4 mmol) of diisopropyl amine in 50 mL THF at 0 ^{o}C was dropwisely added 34.2 mL (54.7 mmol) of a solution of n-BuLi (1.6 M) in Hexane. After the addition, the resulting solution was maintained at room temperature for 1 h, then cooled down to -78 ^{o}C. To the above solution, a solution of **2-2** (10 g, 45.6 mmol) in 50 mL THF was dropwisely added in 1 h. The temperature was let to naturally rise a little until the color of the solution became dark brown, and then cooled down to -78 ^{o}C again. A solution of $ClPPh_2$ (10 mL, 55.5 mmol) in 50 mL THF was dropwisely added to the above solution. And finally the temperature naturally recovered to room temperature. The reaction mixture was allowed to maintain at ambient temperature for additional 12 h. At the end, the reaction mixture was poured into 300 mL water with vigorous stirring. The product was extracted with dichloromethane (3 x 50 mL). The combine extract was washed with water for 3 times and dried with anhydrous sodium sulfate. The solvent was

removed off *in vacuo* to give a crude product which was purified by flash chromatography with dichloromethane as eluant and then by recrystallization in the 1:1 mixture of methanol and acetone to give a pure product (14 g, 76% yield) as white crystal.

M.p.: 135-136 ^{o}C

^{1}H NMR ($CDCl_3$): δ 3.55 (s, 3H, OCH_3), 4.02 (s, 3H, OCH_3),

7.31-7.38 (m, 10H, PhH)

^{13}C-NMR ($CDCl_3$): δ 54.44, 55.77, 110.767-110.958, 128.389-128.434, 128.64, 132.561-132.721, 135.292-135.376, 162.426-162.792, 165.04, 172.267-172.290.

^{31}P-NMR ($CDCl_3$): δ -8.95 (s).

HRMS calcd for $C_{18}H_{16}BrN_2O_2P$ $(M)^+$: 403.0211; Found: 403.0251.

2.3.6. Preparation of

4-Bromo-5-(diphenylphosphinoyl)-2,6-dimethoxypyrimidine (2-4)

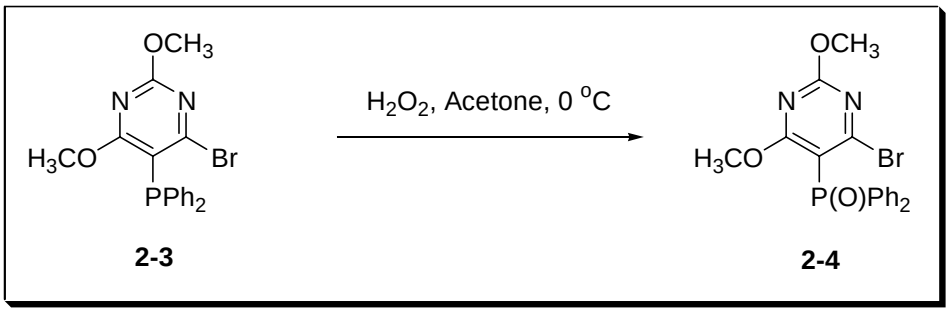

Scheme 2-10

A round bottom flask with a magnetic stirrer was charged with **2-3** (13 g) and 150 mL acetone, the reaction mixture was stirred vigorously and cooled down to 0 ^{o}C. To this mixture was slowly added 15 mL of ca. 35% hydrogen peroxide. The reaction was monitored by TLC. After the solid was completely dissolved, the reaction turned to end. After adding 100 mL water, the product was extracted with dichloromethane (3 x 50 mL). The combined extract was washed with water for three times and dried with anhydrous sodium sulfate. The solution was concentrated *in vacuo* to give a crude product which was purified by recrystallization from 1:1 ethyl acetate and hexane mixture to afford a pure product (12 g, 92% yield) as colorless crystal.

M.p.: 131-132 ^{o}C

^{1}H NMR ($CDCl_3$): δ 3.49(s, 3H), 4.02 (s, 3H), 7.43-7.46 (m, 4H), 7.50-7.54 (m, 2H), 7.67-7.72 (m, 4H)

^{13}C-NMR ($CDCl_3$): δ 54.74, 56.06, 128.56-128.66, 131.455-131.539, 131.97, 133.13, 134.03, 158.810-158.864, 165.18, 172.236-172.282

^{31}P-NMR ($CDCl_3$): δ 24.84 (s)

HRMS calcd. for $C_{18}H_{16}BrN_2O_3P$. $(M)^+$: 419.0160. Found: 419.0176.

X-ray diffraction experiment:

Single crystal of **2-4** was obtained by slowly evaporating solvent from the solution of **2-3** in dichloromethane and ethyl acetate. The crystal structure determined by x-ray diffraction is exhibited in **Figure 2-5**.

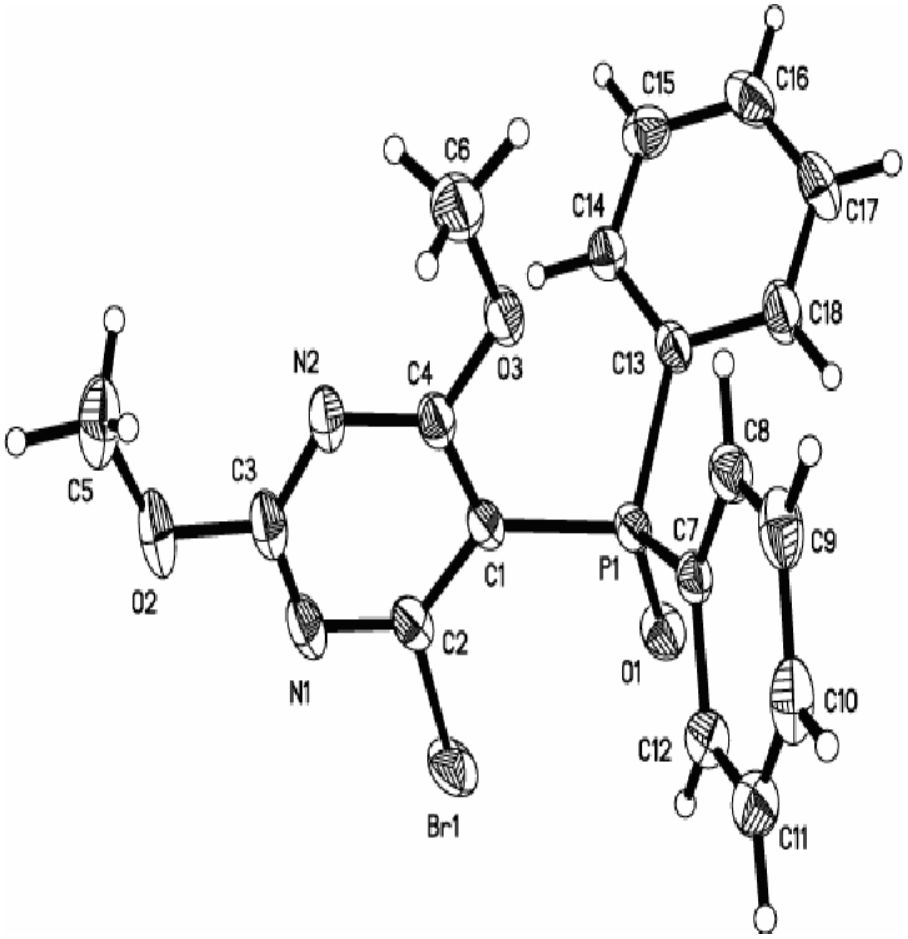

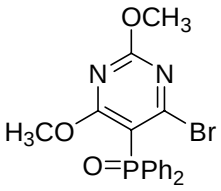

2-4

Figure 2-5. ORTEP drawing of **2-4**

Selected crystal data for **2-4**: $C_{18}H_{16}BrN_2O_3P$, M = 419.21, Triclinic, Space group P-1, *a* = 8.2552(11) Å, *b* = 8.9731(11) Å, *c* = 13.4012(16) Å, α = 79.609(3)°, β = 75.669(3)°, γ = 67.786(2)°, *V* = 886.24(19) $Å^3$, *Z* = 2, D_c = 1.571 Mg/m^3, *T* = 294(2) K, Goodness-of-fit on F_2 0.985, R1 = 0.0546

Table 2-2. Selected Bond lengths [Å] and angles [°] for **2-4**.

Bond lengths [Å]			
Br(1)-C(2)	1.889(2)	N(1)-C(3)	1.325(3)
P(1)-O(1)	1.4738(16)	N(1)-C(2)	1.334(3)
P(1)-C(13)	1.800(2)	N(2)-C(3)	1.318(3)
P(1)-C(7)	1.805(2)	N(2)-C(4)	1.327(3)
P(1)-C(1)	1.832(2)	C(1)-C(2)	1.389(3)
O(2)-C(3)	1.337(3)	C(1)-C(4)	1.405(3)
O(3)-C(4)	1.329(3)		
Angles [°]			
O(1)-P(1)-C(7)	111.54(10)	C(2)-C(1)-P(1)	126.38(18)
C(13)-P(1)-C(7)	108.69(10)	C(4)-C(1)-P(1)	120.40(15)
O(1)-P(1)-C(1)	113.33(9)	N(1)-C(2)-C(1)	124.5(2)
C(13)-P(1)-C(1)	107.93(10)	N(1)-C(2)-Br(1)	112.26(17)
C(7)-P(1)-C(1)	103.50(9)	C(1)-C(2)-Br(1)	123.28(17)
C(3)-N(1)-C(2)	115.3(2)	N(2)-C(3)-N(1)	127.6(2)
C(3)-N(2)-C(4)	115.2(2)	N(2)-C(4)-C(1)	124.7(2)
C(2)-C(1)-C(4)	112.77(19)		

2.3.7. Preparation of 5,5′-Bis(diphenylphosphinoyl)-1,1′,3,3′-tetramethyl-4,4′-bipyrimidine-2,2′,6,6′-(1*H*, 1′*H*, 3*H*, 3′*H*)-tetrone (2-5)

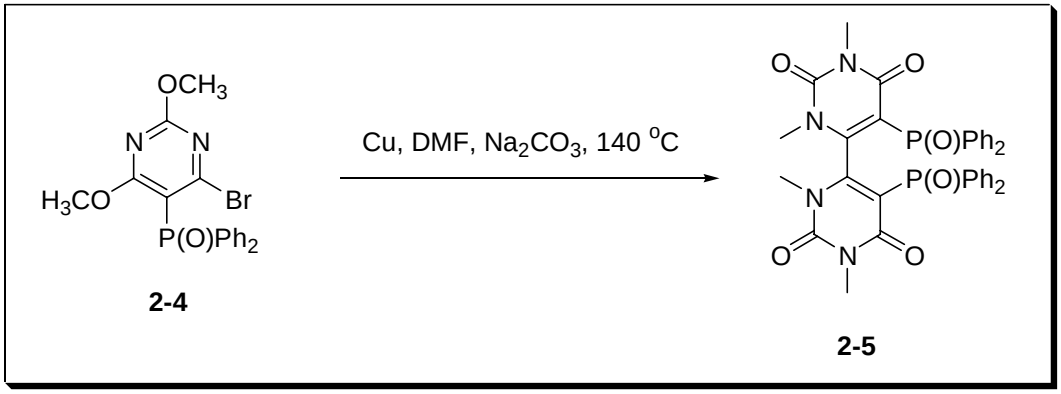

2-4 **2-5**

Scheme 2-11

Copper powder activating procedure:

Activated copper powder is essential for satisfactory yields in the Ullmann coupling reaction, and uniform results can be obtained by the following activation process. 10 g of copper powder (Acros) was treated with 100 mL of a 2 percent solution of iodine in acetone for 5-10 minutes. This resulted in the production of a rather grayish color due to the formation of copper iodide. The product was filtered off on a Buchner funnel, removed and washed by stirring with 50 mL 1:1 solution of concentrated hydrochloric acid in acetone for half an hour. The copper iodide dissolved, and the residual copper powder is filtered and washed with acetone. This washing procedure was repeated for two more times. The resulting copper powder

was then dried in a vacuum desiccator. The activated copper powder was used immediately after preparation.

Modified Ullmann Coupling Reaction:

We developed a modified Ullmann reaction condition by the addition of sodium carbonate which was proved critical to realize the coupling of compound **2-4.** A mixture of **2-4** (4.8 g, 11.5 mmol), activated copper powder (7.36 g, 115 mmol), sodium carbonate (12.2 g, 115 mmol) and 10 mL of dried DMF was stirred for 24 h under nitrogen atmosphere. The mixture was evaporated to almost dryness. The residue was boiled for a few minutes with 50 mL of chloroform, the insoluble solid was removed off by filtration and was washed with hot chloroform (2 x 25 mL). The combined filtrate was washed with 5 N aqueous ammonia (2 x 100 mL), water (2 x 100 mL) and brine (100 mL), and then dried with sodium sulfate. The solvent was evaporated *in vacuo*, and the residue was purified by flash chromotagraphy with 1:1 mixture of ethyl acetate and chloroform as eluant. The eluate was concentrated *in vacuo*, and the product was further purified by recrystallization from the solution of ethyl acetate and dichloromethane (better by solvent evaporation) to give a pure product (1.6 g, 40% yield) as colorless crystal.

M.p.: 346-347 ^{o}C (with decomposition)

^{1}H NMR ($CDCl_3$): δ 3.32 (s, 6H), 3.41 (s, 6H), 6.94-6.98 (m, 4H), 7.15-7.18 (m, 2H), 7.45-7.57 (m, 10H), 8.03-8.07 (m, 4H).

^{13}C-NMR (CD_2Cl_3): δ 28.39, 34.03, 104.21-105.11 (d, J=113Hz), 127.78-127.89 (d, J=13.9Hz), 128.16-128.26 (d, J=12.5Hz), 131.35-131.995 (d, J=81.6Hz), 131.75, 131.80-131.89 (d, J=12.1Hz), 132,22-132.91 (d, J=86.7Hz), 132.41-132.43 (d, J=2.4Hz), 133.65-133.73 (d, J=10.1Hz), 153.87-153.97 (d, J=12.6Hz), , 161.43-161.50 (d, J=9.0Hz).

^{31}P-NMR ($CDCl_3$): δ 29.06 (s)

HRMS calcd for $C_{36}H_{32}N_4O_6P_2$ $(M)^+$: 679.1875; Found: 679.1858.

X-ray diffraction experiment:

Single crystal of **2-5** was obtained by slowly evaporating solvent from the solution of **2-5** in dichloromethane and ethyl acetate. The crystal structure determined by x-ray diffraction is exhibited in **Figure 2-6.**

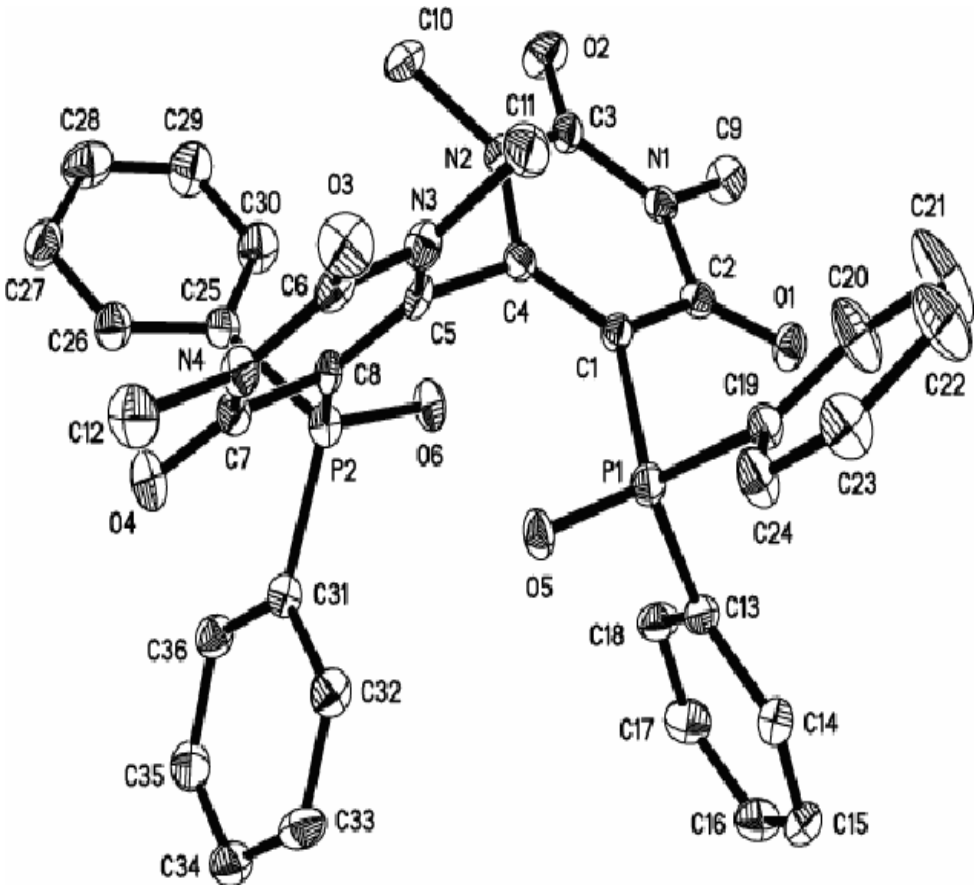

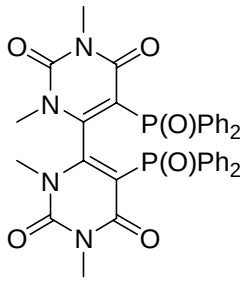

2-5

Figure 2-6. ORTEP drawing of **2-5**

Selected crystal data for **2-5**: $C_{36}H_{32}N_4O_6P_2$, M = 678.60, monoclinic, space group P2(1)/n, *a* = 12.1480(19) Å, *b* = 15.246(2) Å, *c* = 17.814(3) Å, α = 90°, β = 100.690(4)°, γ = 90°, *V* = 3242.2(9)Å^3, *Z* = 2, D_c = 1.390Mg/m^3, *T* = 294(2) K, Goodness-of-fit on F_2 0.681, R1 = 0.2392

Table 2-3. Selected Bond lengths [Å] and angles [°] for **2-5**.

Bond lengths [Å]			
P(1)-O(5)	1.491(2)	P(1)-C(13)	1.786(4)
P(1)-C(19)	1.805(4)	P(1)-C(1)	1.820(3)
N(1)-C(3)	1.376(4)	N(1)-C(2)	1.420(4)
N(2)-C(4)	1.377(4)	N(2)-C(3)	1.397(4)
C(1)-C(4)	1.337(4)	C(1)-C(2)	1.450(5)
C(4)-C(5)	1.510(5)		
Angles [°]			
O(5)-P(1)-C(13)	111.61(19)	O(5)-P(1)-C(19)	110.93(18)
C(13)-P(1)-C(19)	110.69(19)	O(5)-P(1)-C(1)	110.80(17)
C(13)-P(1)-C(1)	106.89(19)	C(19)-P(1)-C(1)	105.69(19)
C(3)-N(1)-C(2)	125.4(4)	C(3)-N(1)-C(9)	116.1(3)
C(2)-N(1)-C(9)	118.5(3)	C(4)-N(2)-C(3)	121.3(4)
C(4)-N(2)-C(10)	122.8(4)	C(3)-N(2)-C(10)	115.8(3)
C(4)-C(1)-C(2)	119.8(4)	C(4)-C(1)-P(1)	122.3(3)
C(2)-C(1)-P(1)	117.9(3)	O(1)-C(2)-N(1)	119.6(4)
O(1)-C(2)-C(1)	125.8(4)	N(1)-C(2)-C(1)	114.5(4)
O(2)-C(3)-N(1)	122.3(4)	O(2)-C(3)-N(2)	122.6(4)
N(1)-C(3)-N(2)	115.1(4)	C(1)-C(4)-N(2)	122.2(4)
C(1)-C(4)-C(5)	123.5(4)	N(2)-C(4)-C(5)	114.3(4)

2.3.8. Optical Resolution of 5,5′-Bis(diphenylphosphinoyl)-1,1′,3,3′-tetramethyl-4,4′-bipyrimidine-2,2′,6,6′-(1*H*, 1′*H*, 3*H*, 3′*H*)-tetrone (2-5)

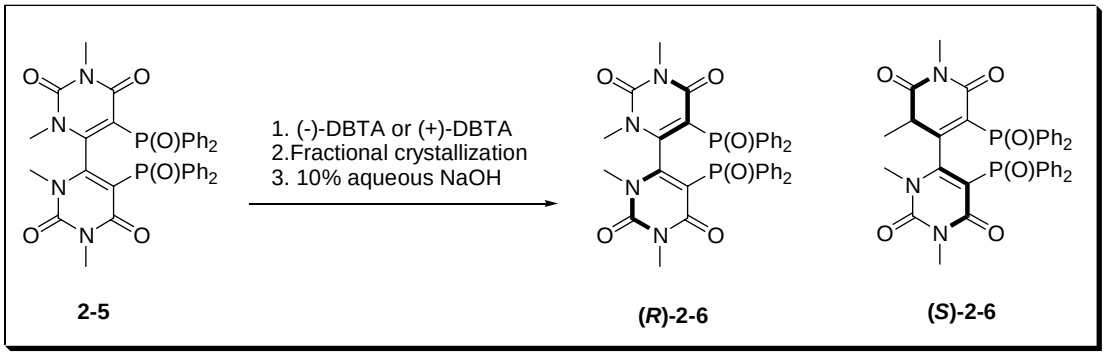

Scheme 2-12

To a mixture of **2-5** (1.4 g, 2.1 mmol) and (-)-dibenzoyl-L-tartaric acid ((-)-DBTA) (0.78 g, 2.1 mmol) was added 15 mL of ethyl acetate and 15 mL of chloroform. The mixture was heated to dissolve and reflux for 24 h. Then it was naturally cooled down to room temperature and maintained for another 48 h at ambient temperature. In this period, a 1:1 complex of **(*R*)-2-6** and (-)-DBTA formed as crystal. The complex was collected by filtration, washed for 3 times with chloroform and dried by suction. (The mother liquor and the wash solution were stored for the recovery of the other enantiomer which was further resolved by (+)-DBTA.) The complex was stirred with 20 mL 5% aqueous sodium hydroxide solution and 30 mL of chloroform until it was completely dissolved. The organic layer was separated, washed with water (3 x 20 mL), dried with anhydrous sodium sulfate

and concentrated *in vacuo* to afford a pure product (*R*)-**2-6** (1.05 g, 75% yield) as a white powder. This procedure could be repeated once more to provide an absolutely optically pure product.

$[\alpha]_D$ = -128.8º (*c* = 1, 25 ºC, $CHCl_3$).

X-ray diffraction experiment:

The crystal structure of the complex of (*S*)-**2-6** + (+)DBTA determined by x-ray diffraction experiment is exhibited in **Figure 2-7,** which also illustrate the hydrogen bond forming between the two molecules to form chain-like supramolecular structure was the driving factor of the resolution.

This material was enantiomeriacally pure (>99.9% ee) according to HPLC analysis on a DIACEL CHIRACEL AD column. The compound was eluated with a solvent system of isopropanol : hexane = 10 : 90 with a flow rate of 1.0 mL per minute. The retention time of the (*S*)-form isomer was at 43.5 minute and that of (*R*)-form isomer was at 50.6 minute **(Figure 2-8a, 2-8b**).

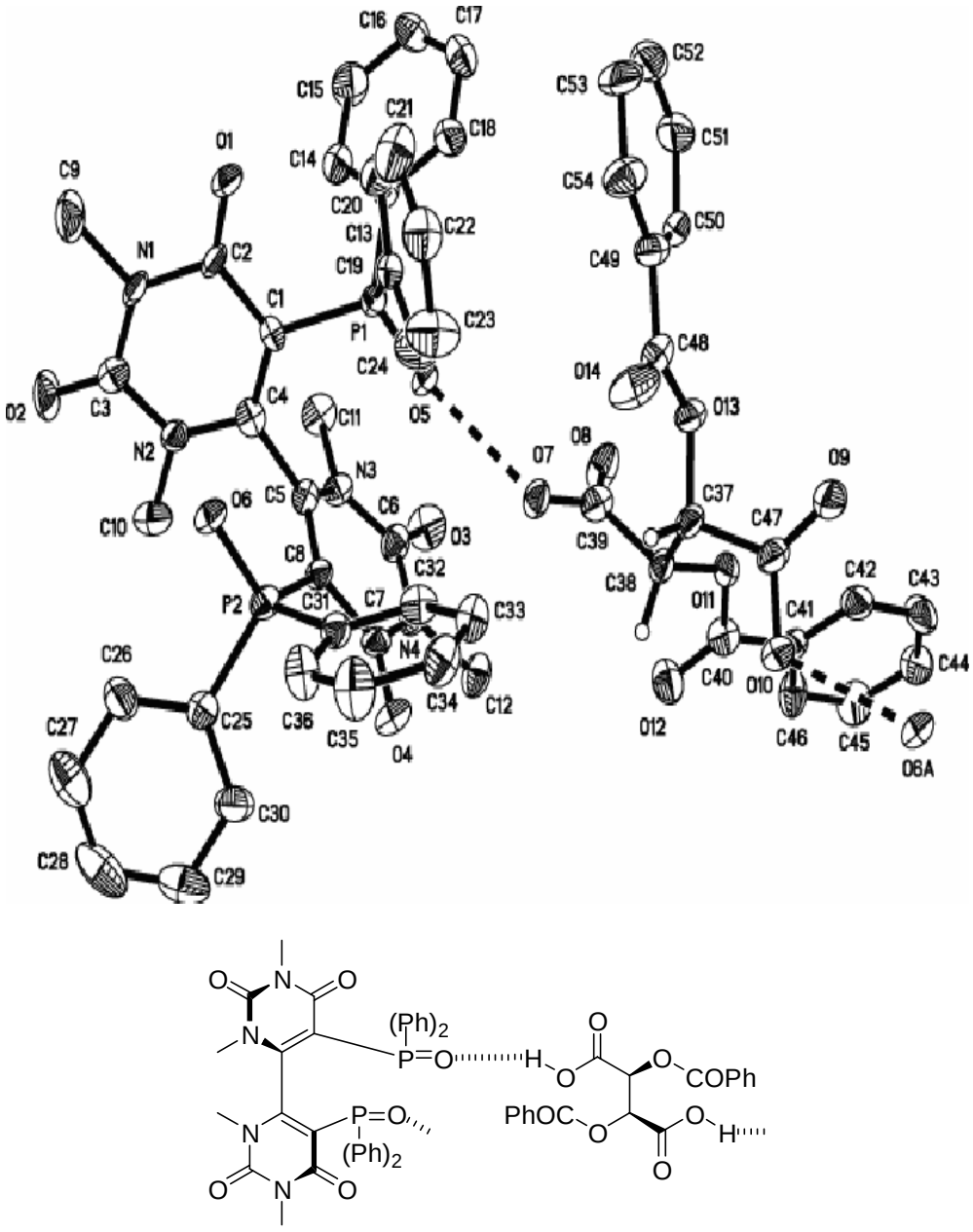

Figure 2-7. ORTEP drawing of complex (*S*)-**2-6** + (+)DBTA

Selected crystal data for (*S*)-**2-6** + (+)DBTA: $C_{55}H_{47}N_4O_{14}P_2$, M = 1156.26, orthorhombic, space group P2(1)2(1)2(1), *a* = 14.023(3) Å, *b* = 17.475(3) Å, *c* = 22.545(5) Å, α = 90°, β = 90°, γ = 90°, *V* = 3242.2(9)Å^3, *Z* = 4, D_c = 1.390 Mg/m^3, *T* = 294(2) K, Goodness-of-fit on F_2 0.775, R1 = 0.1187.

Table 2-4. Selected Bond lengths [Å] and angles [°] for (*S*)-**2-6** + (+)DBTA.

Bond lengths [Å]			
P(1)-O(5)	1.506(2)	P(1)-C(19)	1.805(4)
P(1)-C(1)	1.812(4)	P(1)-C(13)	1.821(4)
O(1)-C(2)	1.206(4)	O(2)-C(3)	1.212(5)
N(1)-C(3)	1.385(5)	N(1)-C(2)	1.428(5)
N(1)-C(9)	1.470(4)	N(2)-C(4)	1.380(5)
N(2)-C(3)	1.390(5)	N(2)-C(10)	1.467(4)
C(1)-C(4)	1.335(5)	C(1)-C(2)	1.439(5)
C(4)-C(5)	1.516(5)		
Angles [°]			
O(5)-P(1)-C(19)	111.61(17)	O(5)-P(1)-C(1)	110.18(17)
C(19)-P(1)-C(1)	107.75(18)	O(5)-P(1)-C(13)	113.30(16)
C(19)-P(1)-C(13)	107.59(19)	C(1)-P(1)-C(13)	106.11(18)
C(3)-N(1)-C(2)	125.0(3)	C(3)-N(1)-C(9)	117.1(4)
C(2)-N(1)-C(9)	117.9(3)	C(4)-N(2)-C(3)	122.4(4)
C(4)-N(2)-C(10)	122.5(3)	C(3)-N(2)-C(10)	115.1(4)
O(1)-C(2)-N(1)	119.1(4)	O(1)-C(2)-C(1)	125.5(4)
N(1)-C(2)-C(1)	115.4(4)	O(2)-C(3)-N(1)	122.4(4)
O(2)-C(3)-N(2)	122.7(5)	N(1)-C(3)-N(2)	114.8(4)
C(1)-C(4)-N(2)	122.5(4)	C(1)-C(4)-C(5)	123.3(4)
N(2)-C(4)-C(5)	114.1(4)		

No.	R.Time (min.)	Comp.	Height (uV)	Height%	Area (uV.sec)	Area%
1	3.14	Unknown	1150	0.21	6534	0.01
2	3.86	Unknown	3403	0.63	26197	0.03
3	43.46	Unknown	299283	55.60	46437559	50.12
4	50.58	Unknown	234465	43.56	46187417	49.85
Total			538302	100.00	92657706	100.00

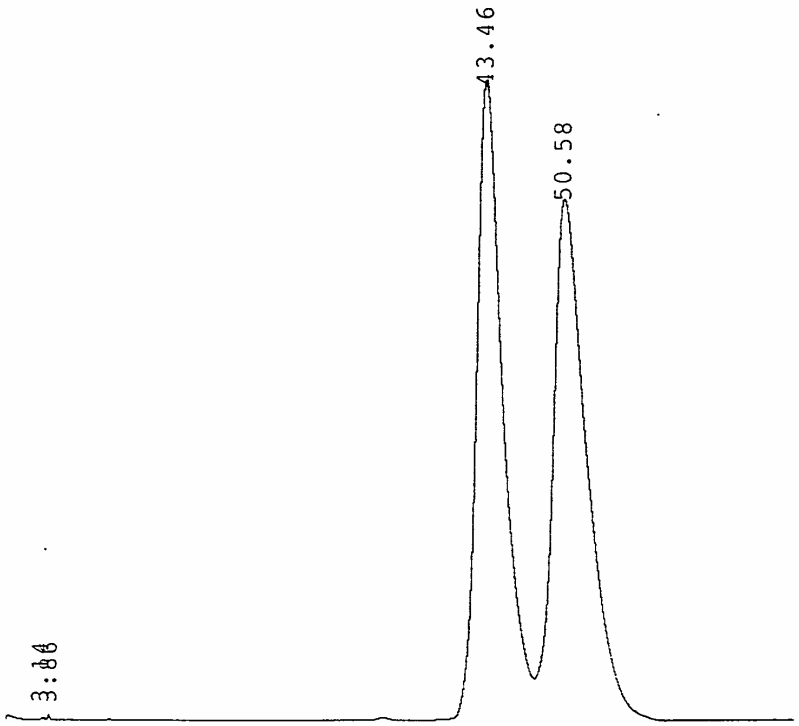

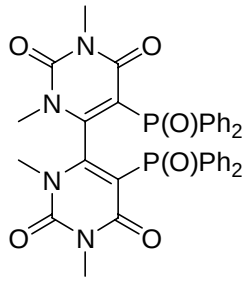

2-5

Figure 2-8a. HPLC chromatogram for **2-5**

No.	R.Time (min.)	Comp.	Height (uV)	Height%	Area (uV.sec)	Area%
1	3.13	Unknown	1894	0.28	14554	0.01
2	3.97	Unknown	25725	3.75	366742	0.24
3	49.66	Unknown	658781	95.98	150442233	99.75
Total			686400	100.00	150823529	100.00

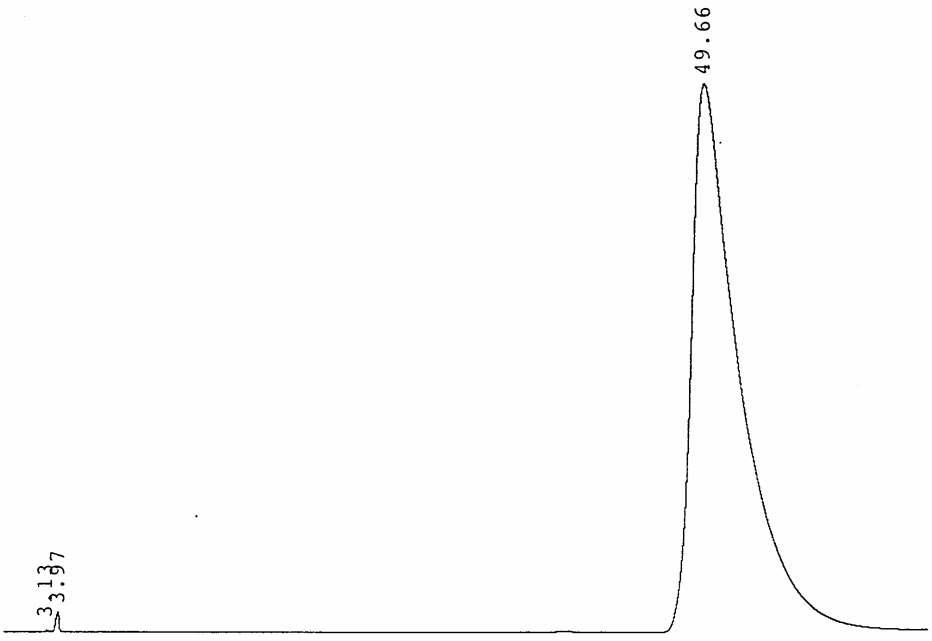

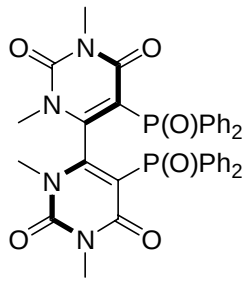

(*R*)-2-6

Figure 2-8b. HPLC chromatogram for (*R*)-**2-6**

2.3.9. Preparation of 5,5′-Bis(diphenylphosphino)-1,1′,3,3′-tetramethyl-4,4′-bipyrimidine-2,2′,6,6′-(1*H*, 1′*H*, 3*H*, 3′*H*)-tetrone (2-7)

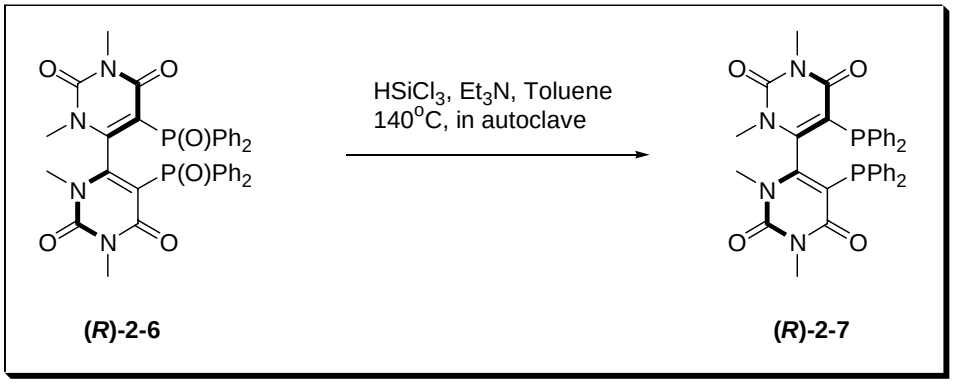

Scheme 2-13

Place 400 mg (0.6 mmol) of **2-6**, 1.2 mL (12 mmol) of trichlorosilane, 1.6 mL (12 mmol) of triethtyl amine and a magnetic stirrer in 5 mL of toluene into a glass tube equipped in an autoclave. The autoclave was then put into an oil bath at 140 ^{o}C for 3 days. After the completion of the reaction, 30 mL of chloroform was added, then with stirring vigorously 3 mL of 50% aqueous sodium hydroxide solution was added dropwisely. The mixture was filtered through a short silica gel column with suction, and washed by chloroform for 3 times. The combine filtrate was concentrated *in vacuo* to give crude product, which was purified by recrystallization with 10 mL of chloroform to afford pure product (*R*)-**2-7** (300 mg, 75% yield) (abbreviated as (*R*)-**PM-Phos**) as a colorless crystal.

M.p.: 321-322 ^{o}C (with decomposition)

^{1}H NMR ($CDCl_3$): δ 3.17 (s, 6H), 3.37 (s, 6H), 6.99-7.10 (m, 10H), 7.36-7.42 (m, 6H), 7.74-7.77 (m, 4H).

^{13}C-NMR ($CDCl_3$): δ 28.71, 34.32, 127.56, 127.83-127.86 (d, J=8.7Hz), 128.68-128.75 (d, J=8.7Hz), 130.22, 131.04-131.06 (d, J=2.9Hz), 131.18-131.20 (d, J=2.9Hz), 134.24-134.31 (d, J=8.7Hz), 135.16-135.19 (d, J=2.9Hz), 135.73-135.92 (d, J=23.9Hz), 151.55, 153.87-153.90 (d, J=4.4Hz), 154.27-154.31 (d, J=4.8Hz), 160.70

^{31}P-NMR (CD_2Cl_2): δ -12.68 (s)

HRMS calcd. for. $C_{36}H_{32}N_4O_4P_2$ $(M)^+$: 647.1977. Found: 647.1946.

$[\alpha]_D$ = 192º (*c*=1, 25 ºC, $CHCl_3$).

X-ray diffraction experiment:

Single crystal of **(*R*)-2-7** was obtained by slowly evaporating solvent from the solution of **2-7** in dichloromethane and ethyl acetate. The crystal structure determined by x-ray diffraction is exhibited in **Figure 2-9a, b.** Notable is that the pyrimidinyl ring is a slightly tortous plane rather than a perfect plane (such as the phenyl groups) This is different from that of other typical atropisomeric bisphosphand ligands such as BINAP, BIPHEP and P-Phos. The bond lengths and angles among the atoms in the pyrimidyl ring (presented in **Table 2-5**) indicate that nitrogen atoms are inequivalently sp^3 hybridised and other atoms are sp^2 hybridised. As the primidinyl ring is a slightly tortous plane, the isolated electron-pairs of nitrogen atoms should partially conjugated with other double bonds to form a 10 π-electron conjugated system.

This material was enantiomeriacally pure (>99.9% ee) according to HPLC analysis on a DIACEL CHIRACEL AD column. The compound was eluated with a solvent system of isopropanol : hexane = 10 : 90 with a flow rate of 1.0 mL per minute. The retention time of the (*S*)-form isomer was at 6.58 minute and that of (*R*)-form isomer was at 10.63 minute **(Figure 2-10a, 2-10b, 2-10c**).

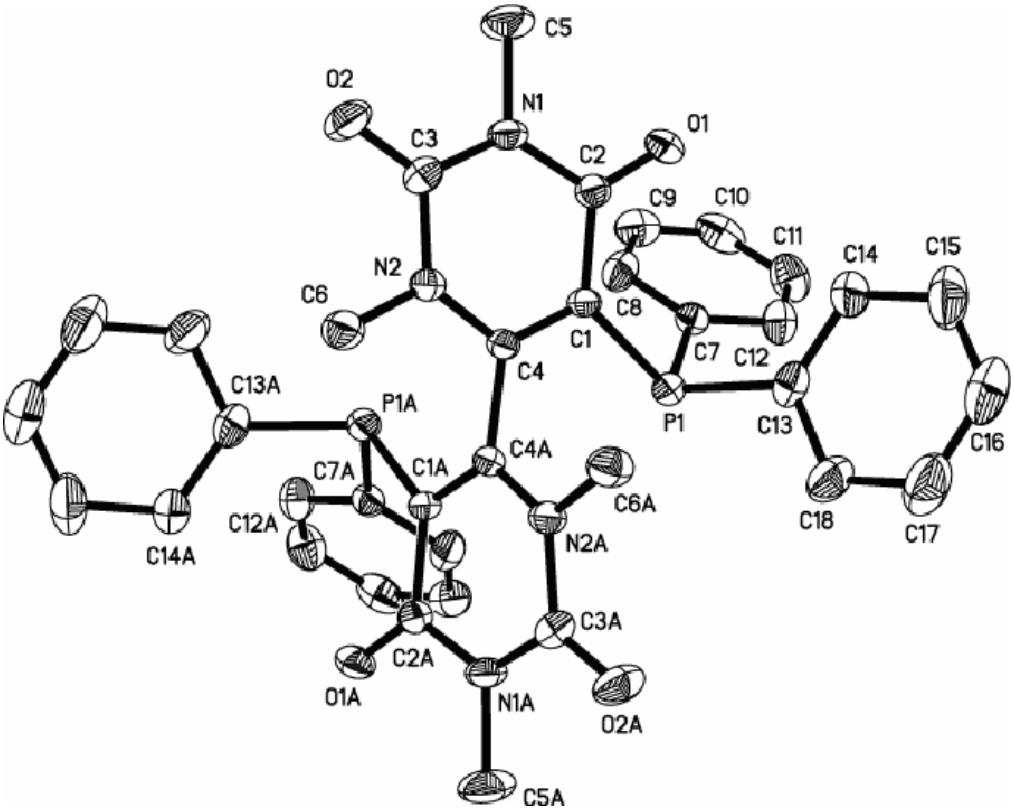

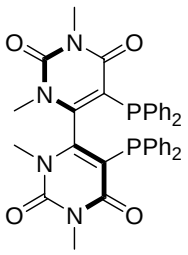

***(S)*-2-7**

Figure 2-9a. ORTEP drawing of (*R*)-**2-7**

Selected crystal data for (*R*)-**2-7**·2$CHCl_3$: $C_{38}H_{34}N_{16}O_4P_2$, M = 885.33, monoclinic, space group C_2, *a* = 22.527(5) Å, *b* = 8.2136(19) Å, *c* = 11.826(3) Å, α = 90°, β =

108.475(5), γ = 90°, V = 2075.4(8) Å^3, Z = 2, D_c = 1.417 Mg/m^3, T = 294(2) K,

Goodness-of-fit on F_2 1.036, R1 = 0.0661.

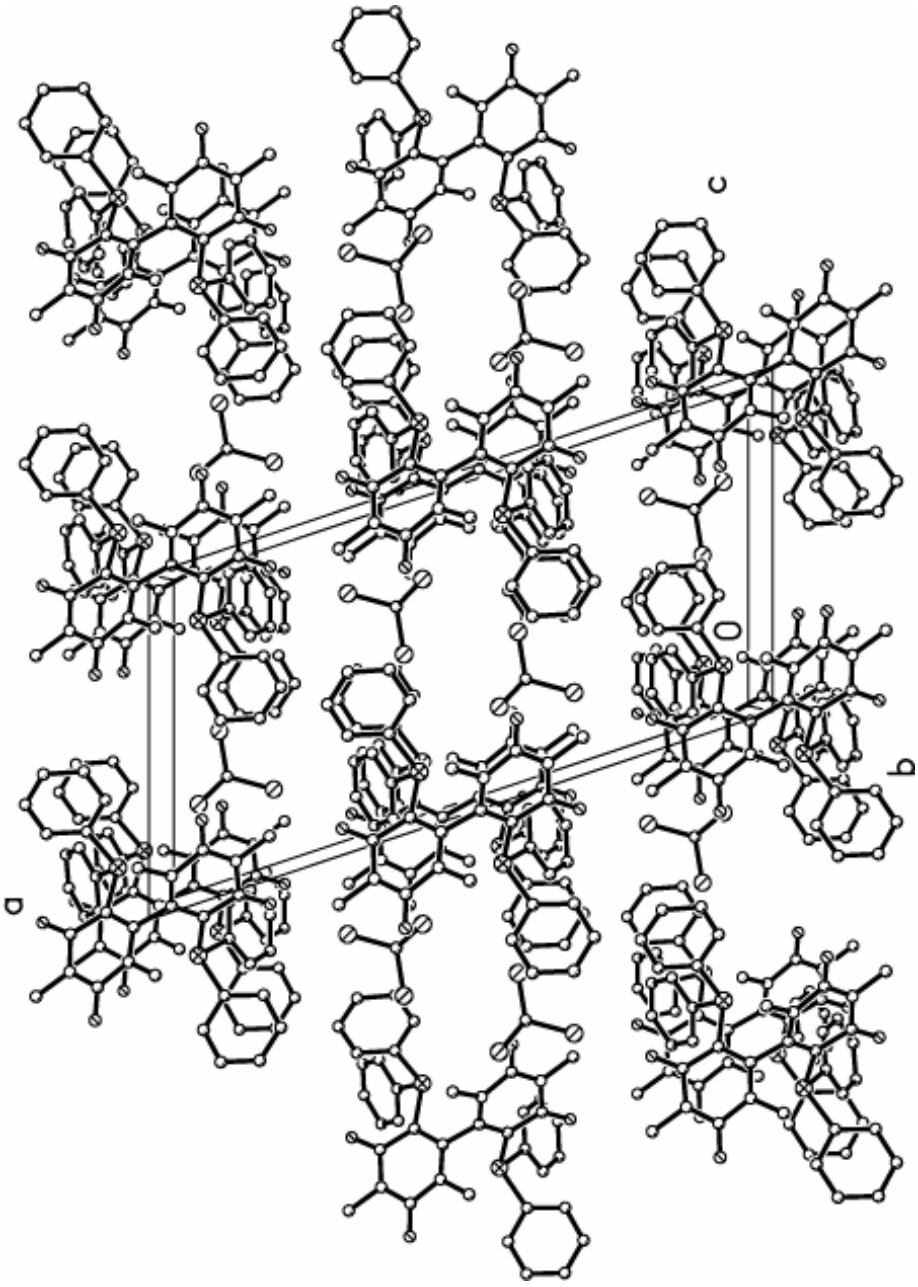

Figure 2-9b. PKB drawing of (*R*)-**2-7**·2$CHCl_3$

Table 2-5. Selected Bond lengths [Å] and angles [°] for (*R*)-**2-7**.

Bond lengths [Å]			
P(1)-C(7)	1.822(4)	P(1)-C(13)	1.842(4)
P(1)-C(1)	1.844(4)	O(1)-C(2)	1.219(5)
O(2)-C(3)	1.219(5)	N(1)-C(3)	1.378(5)
N(1)-C(2)	1.393(5)	N(1)-C(5)	1.463(5)
N(2)-C(4)	1.373(5)	N(2)-C(3)	1.389(5)
N(2)-C(6)	1.482(5)	C(1)-C(4)	1.364(5)
C(1)-C(2)	1.458(5)	C(4)-C(4)#1	1.489(7)
Angles[°]			
C(7)-P(1)-C(13)	104.27(17)	C(7)-P(1)-C(1)	101.57(17)
C(13)-P(1)-C(1)	103.86(18)	C(3)-N(1)-C(2)	124.9(3)
C(3)-N(1)-C(5)	116.8(4)	C(2)-N(1)-C(5)	118.2(4)
C(4)-N(2)-C(3)	121.2(3)	C(4)-N(2)-C(6)	122.9(3)
C(3)-N(2)-C(6)	115.8(3)	C(4)-C(1)-C(2)	118.5(3)
C(4)-C(1)-P(1)	117.4(3)	C(2)-C(1)-P(1)	124.1(3)
O(1)-C(2)-N(1)	119.7(3)	O(1)-C(2)-C(1)	124.8(4)
N(1)-C(2)-C(1)	115.5(3)	O(2)-C(3)-N(1)	122.1(4)
O(2)-C(3)-N(2)	121.7(4)	N(1)-C(3)-N(2)	116.2(3)
C(1)-C(4)-N(2)	122.0(3)	C(1)-C(4)-C(4)#1	121.2(3)
N(2)-C(4)-C(4)#1	116.7(3)		

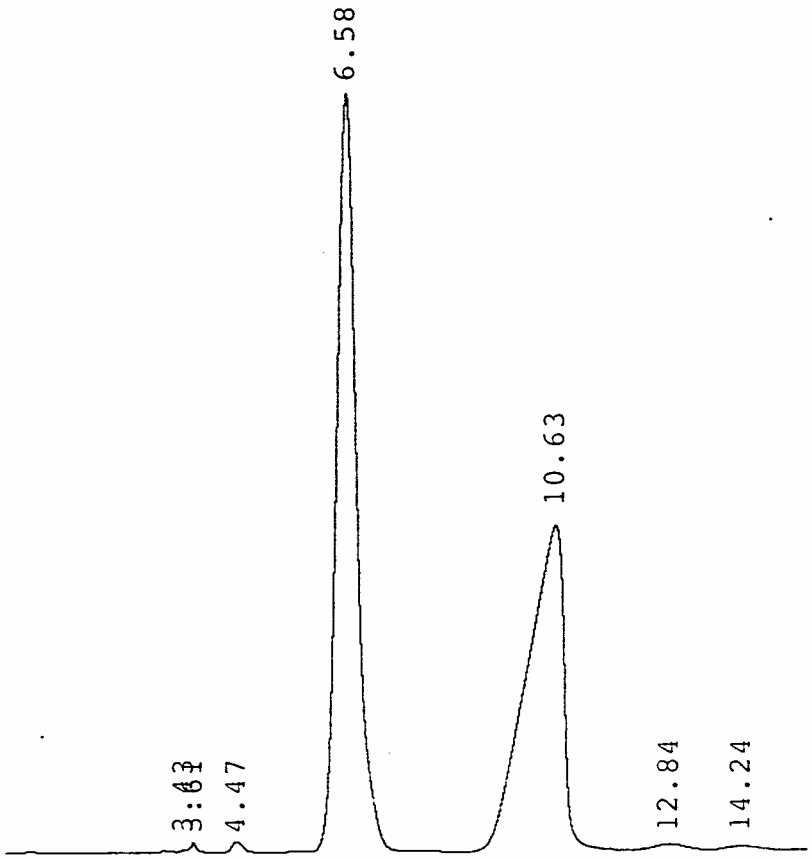

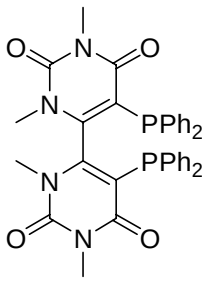

2-7

Figure 2-10a. HPLC chromatogram of racemic **2-7**

No.	R.Time (min.)	Comp.	Height (uV)	Height%	Area (uV.sec)	Area%
1	6.54	Unknown	1047157	99.96	27036130	99.97
2	9.87	Unknown	394	0.04	9196	0.03
Total			1047551	100.00	27045325	100.00

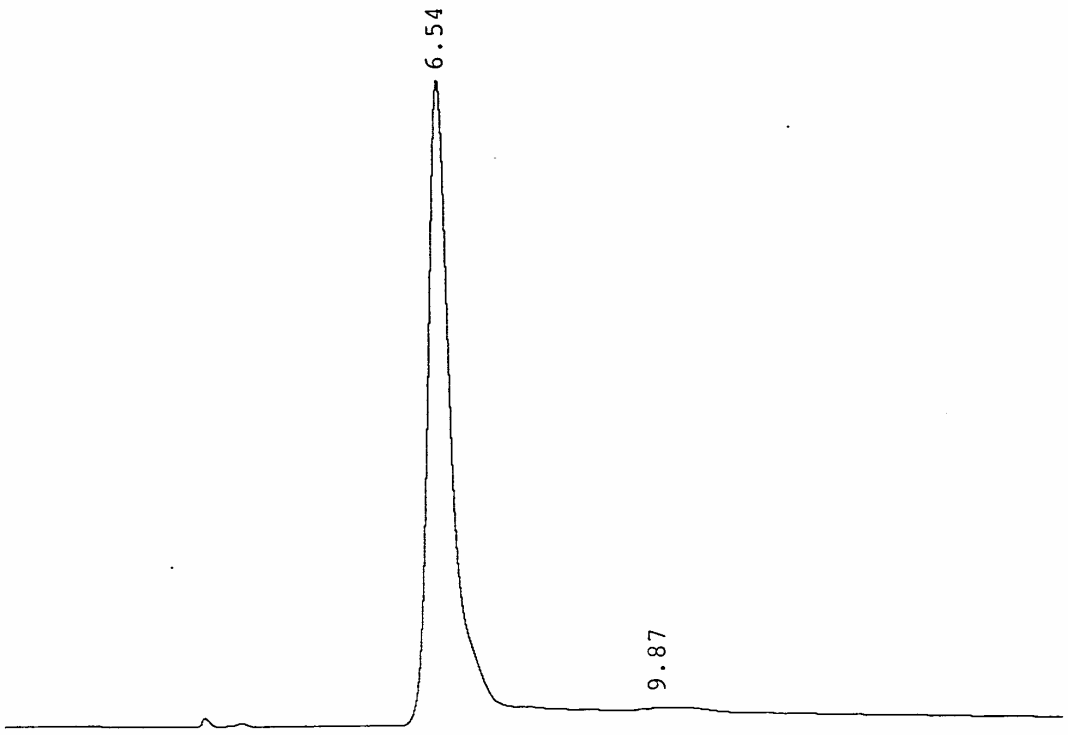

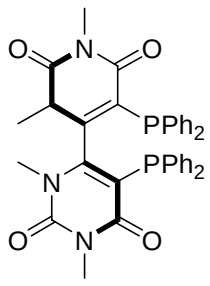

(*S*)-2-7

Figure 2-10b. HPLC chromatogram of (*S*)-**2-7**

No.	R.Time (min.)	Comp.	Height (uV)	Height%	Area (uV.sec)	Area%
1	10.55	Unknown	464352	100.00	25415385	100.00
Total			464352	100.00	25415385	100.00

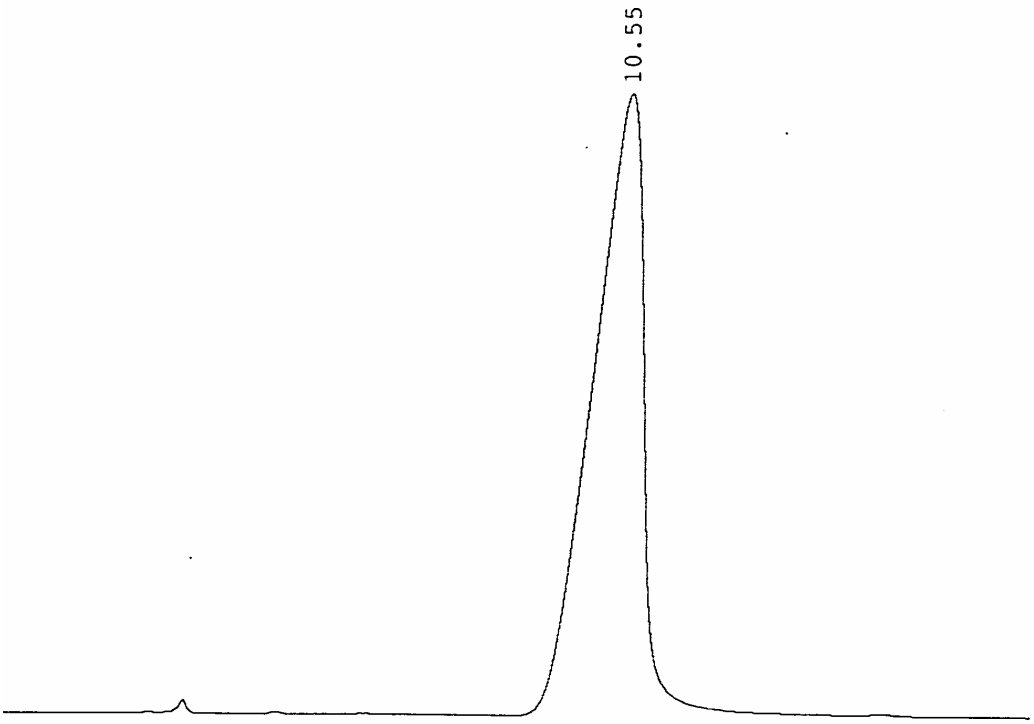

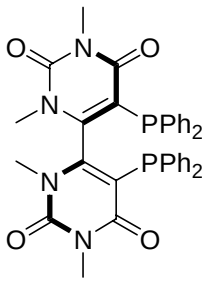

(*R*)-2-7

Figure 2-10c. HPLC chromatogram of (*R*)-**2-7**

2.4. Summary

As we know, the opportunity to synthesize a novel chiral phosphine ligand is very rare and precious at this time. In the difficult search of this rare opportunity, we developed a new proprietary ligand **PM-Phos**. The main results are outlined in the following.

- A novel chiral atropisomeric diphosphine ligand **2-7** (**PM-Phos**) has been designed and prepared. This ligand has a **new structure motif** with tetramethyl-bipyrimidine-tetrone as backbone. It is the first bipyrimidine-type diphosphine ligand.
- In the synthetic process, there were **intresting migration and rearrangement** which resulted in synthesis of an unexpected ligand.
- A **modified Ullmann coupling** procedure had been developed to realize the coupling of a pyrimidine phosphine compound for the first time.
- **Resolution and reduction**: the ligand was resolved and reduced under special conditions or with special techniques developed by us. Optically pure ligand was eventually obtained for further investigation in asymmetric catalytic reactions.
- PM-Phos has potential to form a base of a new family of chiral atropisomeric diphosphine ligands. The future work will be mainly focused on synthesis of the derivatives of PM-Phos such as Tol-PM-Phos, Xyl-PM-Phos and MeO-PM-Phos. In addition, investigation of the intricate mechanisms of the interesting migration and rearrangement will be valuable research topic.

Chapter 3
Palladium-catalyzed Allylic Alkylation and Other Asymmetric Reactions in the Presence of PM-Phos

3.1. Introduction

The development of new chiral ligands for use in asymmetric catalytic reactions has drawn considerable interest in the last two decades. In this area, palladium-catalyzed allylic alkylation is one of the most powerful tools for the controlled introduction of carbon-carbon and carbon-heteroatom bond formation, and several categories of efficient enantioselective catalysts such as C_2- and C_1-symmetric bidentate chiral ligands and non-C_2-symmetric ligands such as phosphineoxazoline have been explored for these reactions. Unlike most transition metal-catalyzed process, asymmetric allylic alkylations offer multiple mechanisms as a source of asymmetry because the enantio-discriminating event can arise in any one of many steps in the catalytic cycle. Thus, this unique feature of the asymmetric allylic alkylation reaction allows for the conversion of starting materials of various types, such as racemic, meso-, and achiral compounds, into enantiomerically enriched material. Strategies to effect such transformations derive from recognition of the stereochemical courses in each step of the catalytic cycle and analysis of symmetry elements imparted in the substrates or intermediates. Accordingly, there are several types of asymmetric allylic alkylations (AAA). As the above described situation is

much complicated, so to simplify things and to easily test the catalytic properties of our ligand (PM-Phos), we first focused on the reaction of palladium-catalyzed allylic

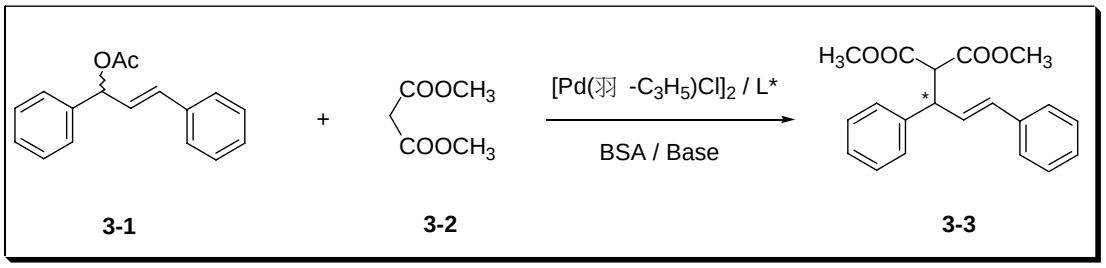

Scheme 3-1

alkylation of 1,3-diphenyl-2-propenyl acetate with dimethyl malonate (**Scheme 3-1**). This reaction is a foundamental AAA reaction and has been studied with a wide range of chiral ligands. Some typical chiral P-N ligands give good to excellent enantioselectivity in this reaction. However, ordinary chiral diphosphine ligands usually are not good for this reaction. Our ligand PM-Phos was used in this reaction and gave good to excellent enantioselectivity.

3.2. Experimental

3.2.1. Preparation of the Substrate (1,3-diphenyl-2-propenyl acetate)

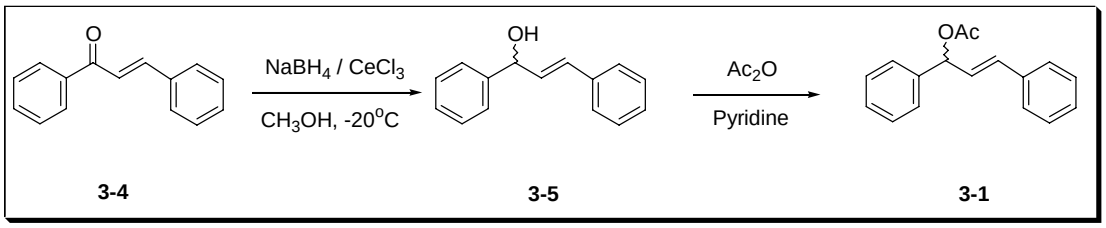

Scheme 3-2

A mixture of chalcone **3-4** (10.4 g, 50 mmol) and $CeCl_3 \cdot 6H_2O$ (17.7 g, 50 mmol) in 200 mL methanol was stirred at room temperature. When the solid dissolved, the mixture was cooled down to -20 ^oC. To the mixture, $NaBH_4$ (2.46 g, 65 mmol) was added gradually. Then the mixture was stirred at room temperature for half an hour. At the end of the reaction, 100 mL 2 N aqueous HCl solution was added, then the mixture was extracted with dichloromethane (3 x 30 mL). The combined organic layer was washed with water (3 x 100 mL) and brine. The solution was dried with anhydrous sodium sulfate and concentrated *in vacuo* to give a crude product which was purified by chromatography with 10:90 ethyl acetate and hexane mixture as eluant to afford a pure product **3-5** (1.2 g, 11% yield).

^1H NMR ($CDCl_3$): δ 2.24 (s, 1H, OH), 5.38-5.39 (d, J=7Hz, 1H), 6.37-6.42 (dd, J=16Hz, 1H), 6.68-6.71 (d, J=16Hz, 1H), 7.24-7.46 (m, 10H)

3-5 (1.2 g, 5.7 mmol) was dissolved in 5 mL of acetic anhydride and 5 mL of pyridine. This solution was stirred for 12 h. The solution was dropped into 100 mL of saturated sodium hydrogen carbonate aqueous solution with vigorous stirring. Then the mixture was extracted with dichloromethane (3 x 20 mL), washed with water for 3 times and dried with anhydrous sodium sulfate. The solvent was removed off *in vacuo* to give a crude product which was purified by chromatography with 10:90 ethyl acetate and hexane mixture as eluant to afford a pure product **3-1** (0.9g, 62% yield) as a oily liquid.

^{1}H NMR ($CDCl_3$): δ 2.14 (s, 3H), 6.33-6.37 (dd, J=16Hz, 1H), 6.44-6.45 (d, J=6.5, 1H), 6.62-6.65 (d, J=16Hz, 1H), 7.23-7.26 (m, 1H), 7.29-7.34 (m, 3H), 7.37-7.43 (m, 6H).

3.2.2. General Procedure for Palladium-catalyzed Asymmetric Allylic Alkylation in the Presence of PM-Phos (Scheme 3-1)

- **Preparation of catalyst solution:**

  A mixture of the ligand (*R*)-PM-Phos ((*R*)-**2-7**) (8.8 mg, 0.0136 mmol) and $[PdCl(\eta^3\text{-}C_3H_5)]_2$ (2.0 mg, 0.0055 mmol) in dry dichloromethane (5.5 mL) was stirred at room temperature for 1 h. The concentration of the resulting brown palladium catalyst solution was 2.0 x 10^{-3} mN.

- **Preparation of the solution of various bases:**

  The following bases ,LiOAc, NaOAc, KOAc, Cs_2CO_3 NH_4OAc, and $N(Bu)_4OH$, were dissolved to methanol to a concentration of 0.25 mN.

- **Preparation of the substrate solution:**

  The substrate **3-1** (252 mg, 1.0 mmol) was dissolved into 5 mL of dry dichloromethane. The concentration of the solution was 0.2 mM.

- **General procedure for palladium-catalyzed asymmetric allylic alkylation in the presence of PM-Phos:**

The ratio of Pd/ligand/base/substrate/dimethly malonate/BSA was 1:1.2:5:100:300:300 or 2:2.4:10:100:300:300. A typical procedure is described in the following. In a schlenk tube was added 20 μl of the base solution. The tube was evacuated and refilled with dry nitrogen for several time to totally remove off the solvent (methanol) and replace the air with nitrogen. 0.5 mL of the substrate solution and 0.5 mL of the catalyst solution were added with syringes. (The solvent dichloromethane would be removed off *in vacuo*, and then another solvent such as toluene, THF, diethyl ether could be added.) Dimethyl malonate (35 μl, 0.3 mmol) and N,O-bis(trimethylsilyl)acetamide (BSA) (75 μl, 0.3 mmol) were added with syringes. Then the solution was stirred at certain temperature. The reaction was monitored by TLC. After completion, the mixture was diluted with hexane (1.5 mL) and quenched by the addition of saturated aqueous NH_4Cl. The organic layer was washed with brine and dried with anhydrous sodium sulfate. The solution was flashed through a short silica gel column with 1:1 dichloromethane and hexane mixture as eluant. The solvent was evaporated under a reduce pressure to give a crude product which was further purified by preparative TLC (hexane: EA = 8:1) to give a pure product **3-3**.

^{1}H NMR ($CDCl_3$): δ 3.53 (s,3H), 3.70 (s, 3H), 3.94-3.96 (d, J=10.5Hz, 1H), 4.24-4.28 (dd, J=11Hz, 1H), 6.30-6.35 (dd, J= 16Hz, 1H), 6.46-6.49 (d, J=16Hz, 1H), 7.18-7.33 (m, 10H).

The enantiomeric excess was determined by HPLC (Chiralcel AD, 1.0 mL/min, hexane:2-propanol = 95:5). The absolute configuration was determined by optical rotation.

3.3. Results and Discussion

We investigated the palladium-catalyzed allylic alkylation of 1,3-diphenyl-2-propenyl acetate with dimethyl malonate, diethyl malonate, dibenzyl malonate and diethyl 2-formamidomalonate in the presence of (*R*)-**2-7**. The results are summarized in **Table 3-1** and **Table 3-2**. Some important corresponding HPLC chromatograms are listed in **Figure 3-6** to **Figure 3-20** in **Appendix II**.

3.3.1. The Effect of Structure of the Nucleophiles

We first investigated the effect of the types of malonates on the enantioselectivity of the reaction. The following four types of malonates (**Figure 3-1**) were applied to the reaction to test which one would give the best enantiomeric excess. The results are listed in the **Table 3-1**.

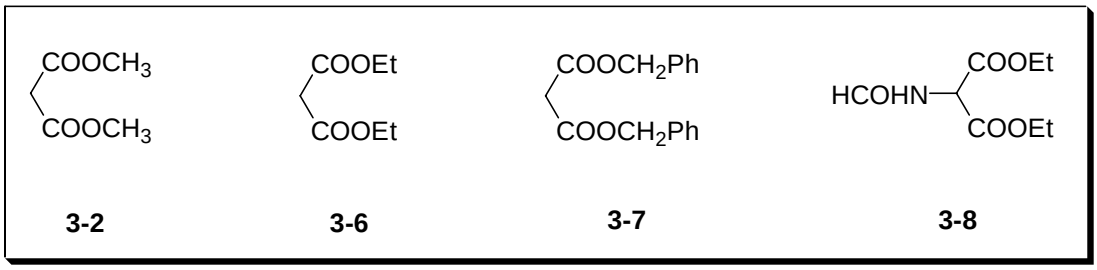

Figure 3-1

Table 3-1. Results of palladium-catalyzed asymmetric allylic alkylation of 1,3-diphenyl-2-propenyl acetate with various dialkyl malonate in the presence of (*R*)-**2-7**.

Entry	Ligand	Solvent	Base	Pd/Sub	Temperature (^oC)	Nucleophile	Product	Ee %
1	(*R*)-**2-7**	CH_2Cl_2	LiOAc	1/100	25	**3-2**	**3-3**	82.6
2	(*R*)-**2-7**	CH_2Cl_2	LiOAc	1/100	25	**3-6**	**3-9**	76.3
3	(*R*)-**2-7**	CH_2Cl_2	LiOAc	1/100	25	**3-7**	**3-10**	71.7
4	(*R*)-**2-7**	CH_2Cl_2	LiOAc	1/100	25	**3-8**	**3-11**	77.0

To ensure the completion of the reaction, the reaction time was 24 h for all entries.

Table 3-1 shows that under identical conditions the bulkier nucleophile gave lower enantiomeric excess. So we focused our investigation only on the reaction with dimethyl malonate.

3.3.2. The Effect of Solvent on the Enantioselectivity

In **Table 3-2**, entries 1-4 show that the best solvent was CH_2Cl_2 (**Figure 3-2**).The reaction not only proceeded much faster, but also gave better enantioselectivity in CH_2Cl_2 than in other solvent. CH_2Cl_2 is a non-polar solvent, and more importantly, it is the best solvent for the ligand (*R*)-**2-7** or even for the corresponding palladium catalyst and the reaction intermediates. The solubility of (*R*)-**2-7** in THF and toluene is almost equally bad, but THF is more polar. So, in THF the enantioselectivity was the worst. Hence, we can conclude that for this reaction an appropriate solvent is a non-polar solvent with good solubility for **2-7**.

Table 3-2. Results of palladium-catalyzed asymmetric allylic alkylation of 1,3-diphenyl-2-propenyl acetate with dimethyl malonate in the presence of (*R*)-**2-7**.

Entry	Ligand	Solvent	Base	Pd [b]/Sub	Temperature (^oC)	Time (h)	Conv. %	Ee [a] %
1	(*R*)-**2-7**	THF	LiOAc	1/100	25	20	40	69.6
2	(*R*)-**2-7**	Toluene	LiOAc	1/100	25	20	77	80.7
3	(*R*)-**2-7**	Ether	LiOAc	1/100	25	20	98	80.0
4	(*R*)-**2-7**	CH_2Cl_2	LiOAc	1/100	25	1.5	100	82.6
5	(*R*)-P-Phos	CH_2Cl_2	LiOAc	1/100	25	1.5	100	61.5
6	(*S*)-BINAP	CH_2Cl_2	LiOAc	1/100	25	20	100	80.2
7	(*R*)-**2-7**	CH_2Cl_2	NaOAc	1/100	25	2	100	**85.2**
8	(*R*)-**2-7**	CH_2Cl_2	KOAc	1/100	25	1.5	100	82.2
9	(*R*)-**2-7**	CH_2Cl_2	Cs_2CO_3	1/100	25	1.5	100	81.0
10	(*R*)-**2-7**	CH_2Cl_2	NH_4OAc	1/100	25	2	100	85.1
11	(*R*)-**2-7**	CH_2Cl_2	$N(Bu)_4OH$	1/100	25	3	100	85.1
12	(*R*)-**2-7**	CH_2Cl_2	LiOAc	1/100	0	4	100	86.1
13	(*R*)-**2-7**	CH_2Cl_2	NaOAc	1/100	0	10	100	**88.5**
14	(*R*)-**2-7**	CH_2Cl_2	KOAc	1/100	0	10	95	86.5
15	(*R*)-**2-7**	CH_2Cl_2	Cs_2CO_3	1/100	0	10	100	86.8
16	(*R*)-**2-7**	CH_2Cl_2	NH_4OAc	1/100	0	10	90	88.5
17	(*R*)-**2-7**	CH_2Cl_2	$N(Bu)_4OH$	1/100	0	20	99	88.7
18	(*R*)-**2-7**	CH_2Cl_2	LiOAc	1/50	-40	24	98	92.3
19	(*R*)-**2-7**	CH_2Cl_2	NaOAc	1/50	-40	24	96	**95.2**

20	(*R*)-**2-7**	CH_2Cl_2	KOAc	1/50	-40	24	92	93.6
21	(*R*)-**2-7**	CH_2Cl_2	Cs_2CO_3	1/50	-40	24	94	93.4
22	(*R*)-**2-7**	CH_2Cl_2	NH_4OAc	1/50	-40	24	44	94.6
23	(*R*)-**2-7**	CH_2Cl_2	$N(Bu)_4OH$	1/50	-40	24	Too low	
24	(*R*)-**2-7**	CH_2Cl_2	LiOAc	1/25	-78	24	Too low	

[a]The configuration of the product is (*S*)-form for all entry except entry 6. For entry 6, the configuration is (*R*)-form. [b] The palladium source was $[PdCl(\eta^3\text{-}C_3H_5)]_2$.

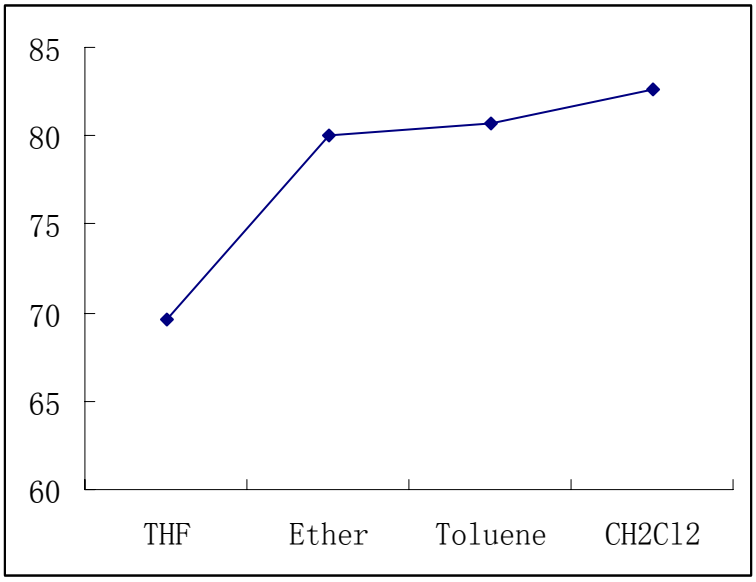

Figure 3-2. The solvent effect on enantioselectivity

3.3.3. The Effect of the Types of Base Additives

5 types of base additive were tested. An overall conclusion drawn from the results in the **Table 3-2** and **Figure 3-3** is that with LiOAc the conversion was the best and with NaOAc the enantioselectivity was the best. The optimal base was NaOAc,

because at lower temperature the reaction with NaOAc not only proceeded comparatively fast, but also afforded the best enantiomeric excess.

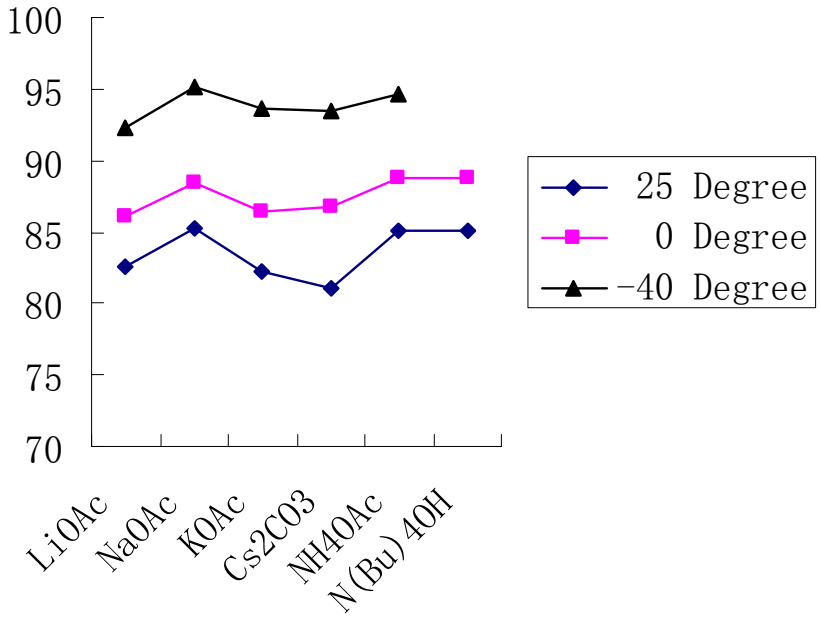

Figure 3-3. The effect of base additive and temperature on the enantioselectivity

3.3.4. The Effect of Temperature

With a decreasing temperature, the reaction rate became lower but the enantioselectivity increased. This is the general situation for asymmetric catalytic reactions. However, if the temperature became too low such as -78 ^{o}C, the reaction proceeded very slowly or almost stopped. The optimal temperature was about -40 ^{o}C for this reaction. At this temperature, the enantiomeric excess obtained was up to 95% and the conversion was nearly complete in 24 h with NaOAc as base additive. This result is almost excellent especially for a C_2-symmetry diphosphine ligand.

3.3.5. The Results of PM-Phos Compared with the Results of other Typical Phosphine Ligand

Entries 4, 5 and 6 in **Table 3-2** indicates that in the reaction of palladium-catalyzed allylic alkylation of 1,3-diphenyl-2-propenyl acetate with dimethyl malonate, the result of PM-Phos was better than those of BINAP and P-Phos under the same reaction conditions. The catalytic activity of both PM-Phos and P-Phos were almost equally good, but the enantioselectivity of PM-Phos was better than that of P-Phos (82.6% ee vs 61.5% ee). Compared to the results of BINAP, the enantioselectivity of PM-Phos was just a little better, but its activity was much better.

For this reaction, some chiral dinitrogen or P-N-chelate ligands give excellent enantioselectivity, up to 99% ee can be obtained. **Figure 3-4** listes some typical examples of these ligands which represent the best results in this field.

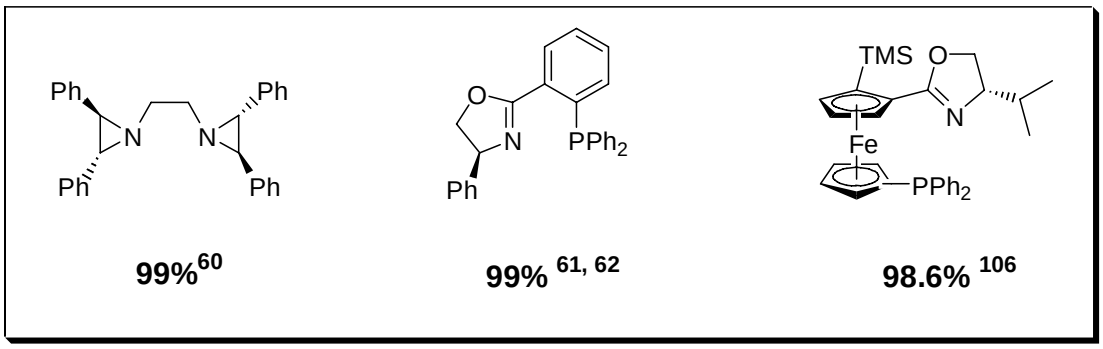

Figure 3-4. Some excellent ligands and the enantiomeric excess values obtained in the reaction of palladium-catalyzed allylic alkylation of 1,3-diphenyl-2-propenyl acetate with dimethyl malonate.

Ordinary chiral diphosphine ligands usually are not good for this reaction. However, our ligand PM-Phos was used in this reaction and gave good to

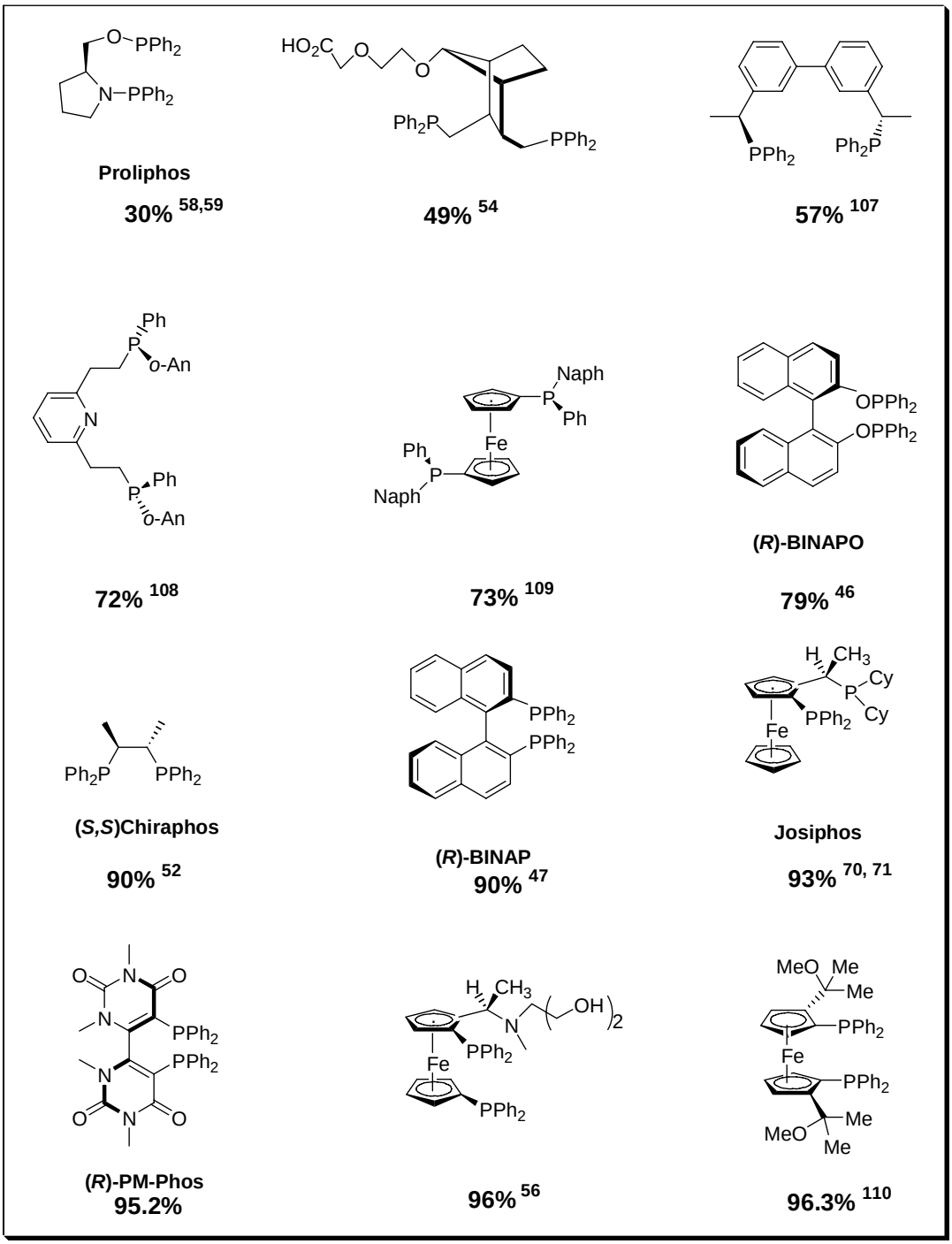

Figure 3-5 Typical diphosphine ligands and the optimal enantiomeric excess values obtained in the reaction of palladium-catalyzed allylic alkylation of 1,3-diphenyl-2-propenyl acetate with dimethyl malonate.

excellent enantioselectivity. **Figure 3-5** exhibits some typical diphosphine ligands and the optimal enantiomeric excess values they gave in this reaction. Actually, the enantioselectivity of PM-Phos is not the best among these chiral diphosphine ligands, but it is among the fewer best chiral diphosphine ligands for asymmetric allylic alkylation with enantiomeric excess values up to 95%.

3.4. Other Asymmetric Reactions Catalyzed with PM-Phos

3.4.1. Palladium-Catalyzed Enantioselective Alkylation Ring Opening of Oxabenzonorbornadiene

3.4.1.1. Introduction

The use of stereochemically rigid oxabicyclic templates to achieve stereoselective functional group introduction in carbocyclic products has been investigated for some years. The products from ring opening of these substrates are potentially very useful in the synthesis of many natural products. Over the past five years, several metal-catalyzed asymmetric ring cleaving reactions have been developed to generate ring-opened products in high yield and enantiomeric excess.[111] Usually, three different transition metals have been employed, namely nickel, palladium and rhodium, leading to synthetically useful transformations. These reactions can be carried out with a range of nucleophiles including hydride, stabilized and nonstabilized carbanions, alcohols, amines, and carboxylates. As a result, the

oxabicyclic template has become increasingly common as a starting material in the preparation of both cyclic and acyclic compounds.

To investigate the application of our proprietary ligand PM-Phos in other palladium-catalyzed reactions, we studied the alkylation ring opening of 7-oxabenzonorbornadiene with diethylzinc reagents. This reaction was recently reported by Lautens *et al.*.[111] As depicted by **Scheme 3-3**, the reaction of 7-oxabenzonorbornadiene with Et_2Zn in the presence of chiral ligand ((*R*)-P-Phos and (*R*)-PM-Phos) provided the corresponding alcohol which enantiomeric excess was determined by HPLC.

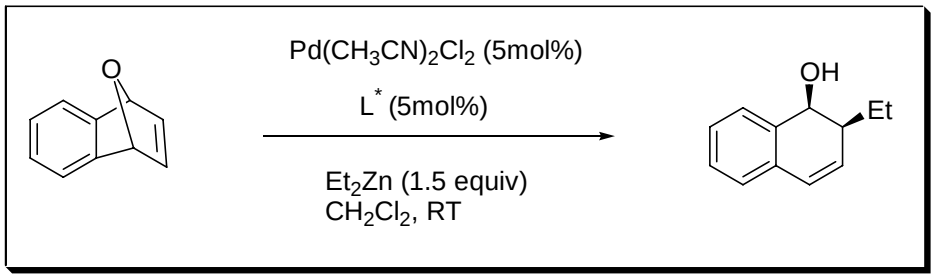

Scheme 3-3

3.4.1.2. Experimental

General Procedure for the enantioselective alkylation ring opening of oxabenzonorbornadiene: A dried round bottom flask was charged, under nitrogen, with bis(acetonitrile)palladium dichloride (5 mol%) and the appropriate ligand (5%). 1 mL of distilled dichloromethane was added and the solution stirred at room temperature for two hours. To this solution was added at room temperature via canula a solution of oxabenzonorbornadiane (1 mmol) in dichloromethane (30 mL) followed

by a solution of diethylzinc in toluene. The resulting solution was allowed to stired at room temperature until completion monitored by TLC analysis. The flask was opened to air and few drops of water were added. This solution was stirred for half an hour, filter through a short plug of celite and concentrated. The conversion was determined by NMR. The crude mixture was purified by flash chromatography on silica gel to afford the dihydronaphthalene. The ee value was determined using HPLC analysis on a CHIDRACEL OD column, λ=254 nm. Retention times in 1% iPrOH in hexanes were 20 min and 22 min (major). 1H NMR (500 MHz, CDCl3) δ 7.31 (1H, d, J=6.9Hz), 7.28-7.19 (2H, m), 7.10 (1H, d, J = 7.1Hz), 6.52 (1H, dd, J = 9.7, 2.5 Hz), 5.81 (1H, dd, J = 9.6, 1.8 Hz), 4.62 (1H, dd, J = 7.3, 4.5 Hz), 2.39-2.32 (1H, m), 1.84 (1H, dquin, J = 13.6, 7.5 Hz), 1.63 (1H, dquin, J = 13.6. 7.5 Hz), 1.52 (1H, d, J = 7.3 Hz), 1.11 (3H, t, J = 7.4)

3.4.1.3. Results and Discussion

Table 3-3 exhibits the results of Pd-catalyzed ring opening reaction of 7-oxabenzonorbornadiene with diethylzinc reageats in the presence of chiral diphosphine ligands. Both (*R*)-BINAP and (*R*)-P-Phos gave 99% conversion and 91% ee. However, PM-Phos gave lower conversion and poor enantioselectivity in this reaction. The possible reason is that under stronger basic condition (such as addition of diethylzinc solution), PM-Phos was not stable and could transform to unknown compound other than the original form, and hence PM-Phos could only give negative results in this reaction. This will be investigated in future work.

Table 3-3. Pd-catalyzed ring opening reaction of 7-oxabenzonobornadiene with diethylzinc reageats in the presence of chiral diphosphine ligands

Entry	Ligand	Time (h)	Conversion (%)	Ee (%)
1	(*R*)-BINAP	24	99	91
2	(*R*)-P-Phos	24	99	91
3	(*R*)-PM-Phos	24	85	22

3.4.2. Rhodium and Ruthenium-catalyzed Asymmetric Hydrogenation

Typical chiral diphosphine ligands such as BINAP and P-Phos are substantially used in rhodium and ruthenium-catalyzed asymmetric hydrogenation of prochiral olefinic substrates such as α−acetaminoacrylate, acrylic acids, β-keto esters, ketones and so on, and always exhibit excellent enantioselectivity and catalytic activity. PM-Phos may be considered as a typical chiral diphosphine ligand, and should demonstrate similar activity and enantioselectivity for asymmetric hydrogenation. However, when it was tested in rhodium and ruthenium-catalyzed hydrogenation of some typical substrates according to Noyori's methods,[112] negative results were achieved. Either no activity or specially low enantioselectivity was observed. In the ruthenium-catalyzed asymmetric hydrogenation of methyl acetoacetate, ee value achieved was only 40%. Both in the ruthenium-catalyzed hydrogenation of 2-(6′-methoxy-2′-naphthyl)propenoic acid (dehydronaproxen) and rhodium-catalyzed asymmetric hydrogenation of (*E*)-methyl 3-phenyl-2-acetaminoacrylate, there was no conversion as determined by NMR. These unusual results imply there was different

catalytic mechanism and coordination mode of PM-Phos in asymmetric hydrogenation compared to P-Phos and BINAP. The detailed reasons and mechanism for these special strange results will be investigated in the future.

3.5. Summary

With the palladium-catalyzed allylic alkylation of 1,3-diphenyl-2-propenyl acetate with dimethyl malonate as a model reaction, the asymmetric induction properties of PM-Phos preliminarily tested. The results demonstrate that some progress have been achieved as outlined in the follows.

- PM-Phos can cooperate with palladium to afford an efficient catalyst for asymmetric allylic alkylation.

- For the palladium-catalyzed allylic alkylation of 1,3-diphenyl-2-propenyl acetate with malonates, the optimal nucleophile is dimethyl malonate, the optimal solvent is CH_2Cl_2 and the optimal base additive is NaOAc.

- The catalytic activity of the PM-Phos palladium complex is excellent especially at room temperature. The enantioselectivity of the complex is fair at room temperature, but good at 0°C, and almost excellent at a still lower temperature (up to 95% ee at -40 °C).

- PM-Phos has the potential to be applied to other palladium-catalyzed asymmetric reactions such as asymmetric allylic amination for further exploration. On the other hand, there are also opportunities to develop derivatives of PM-Phos such as Tol-PM-Phos of Xyl-PM-Phos to seek better catalytic activity and enantioselectivity in the future work.

In summary, we have successfully developed a novel, unique and efficient chiral diphosphine ligand for asymmetric allylic alkylation.

Chapter 4

Synthesis of Novel Chiral Amino Alcohol Ligands and their Application in Asymmetric Catalysis

4.1. Introduction

Chiral amino alcohols and their derivatives are useful ligands in asymmetric synthesis and catalysis,[113, 114] especially in the asymmetric borane reduction of ketones[115] and the organozinc addition to carbonyl compounds.[116] One of the most successful methods in the asymmetric borane reduction of ketones is based on the use of chiral 1,3,2-oxazaborolidines as catalysts[117, 118] (**Figure 4-1**), which were prepared from β-amino alcohols (usually derived from α-amino acids). During the last decade, many amino acids such as L-valine, L-proline, L-cysteine,[119] and L-methionine[120] have been used in preparing 1,3,2-oxazaborolidine catalysts. Most of the tested amino alcohols contained only one stereogenic center, although a limited number of amino alcohols possessing two stereogenic centers exhibited higher enantioselectivities in the asymmetric borane reduction of acetophenone. [121] To expand the scope of these studies, it is of interest to develop new amino alcohols with two stereogenic centers and to test their synergistic effects. In this research field, we mainly focused on the preparation of the two diastereomers of new chiral amino alcohols containing two stereogenic centers and their application in the borane reduction of ketones and the addition of diethylzinc to aldehydes.

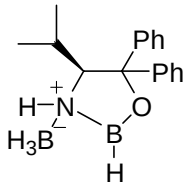

Figure 4-1. a chiral 1,3,2-oxazaborolidine

4.2. Synthesis of Novel Amino Alcohol Ligands

4.2.1. The Synthetic Route

In our initial study we chose L-valine as a starting material because of its ample availability and low cost. L-valine had previously been used in the preparation of α,α-diphenyl-β-amino alcohol which was used as a chiral auxiliary for the enantioselective borane reduction of aromatic ketones with good to excellent enantioselectivities.[122] In this study, we synthesized the new amino alcohols **4-6a** and **4-6b** according to the synthetic route developed by Reetz et al (**Scheme 4-1**).[123]

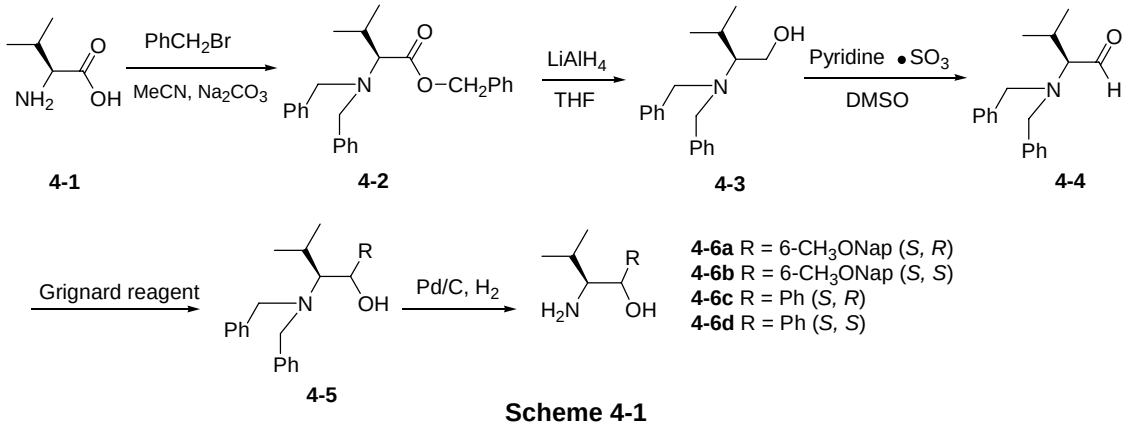

Scheme 4-1

The reaction of amino acid with benzyl bromide in the presence of sodium carbonate produced N, N-dibenzyl benzylamino-L-valine benzyl ester which, on treatment with $LiAlH_4$, gave amino alcohol **4-3** in 90% yield. Compound **4-3** was transformed to amino aldehyde **4-4** in almost quantitative yield via the oxidation with sulfur trioxide pyridine complex in DMSO. The reaction of compound **4-4** with Grignard reagent gave the new amino alcohol **4-5** and the de-benzylation of it produced ligands **4-6** in 60-80% yield. In contrast to the oily liquid form of **4-6c** and **4-6d**, the mixtures of the diastereomers **4-6a** and **4-6b** were easily separated by crystallization. The *R*-configuration of the new stereogenic center in the amino alcohol **4-6c** was confirmed by single crystal X-ray diffraction analysis (Figure 1).[124] For the purpose of comparison, amino alcohol **4-7** with one stereogenic center was prepared according to a method reported by Itsuno *et al*. (**Scheme 4-2**)[122]

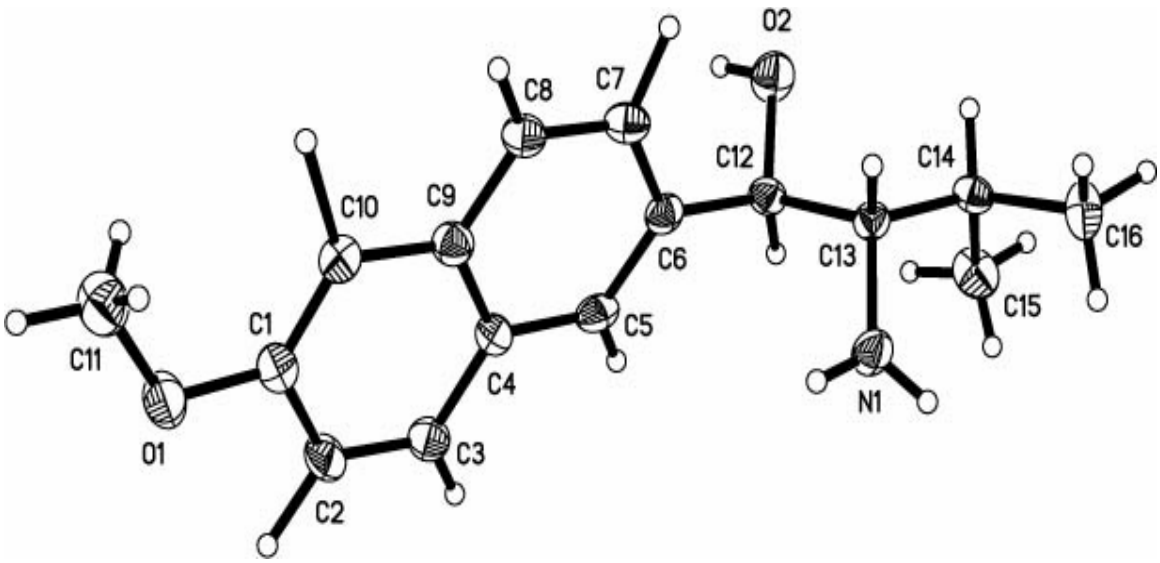

Figure 4-2. The ORTEP drawing of amino alcohol **4-6a**

Table 4-1. Selected bond lengths [Å] and angles [°] for **4-6a**.

Bond lengths [Å]			
O(2)-C(12)	1.436(3)	N(1)-C(13)	1.475(3)
C(6)-C(12)	1.503(3)	C(12)-C(13)	1.543(3)
C(13)-C(14)	1.528(3)	C(14)-C(16)	1.545(4)
C(14)-C(15)	1.546(4)		
Angles [°]			
O(2)-C(12)-C(6)	111.0(2)	O(2)-C(12)-C(13)	109.5(2)
C(6)-C(12)-C(13)	112.7(2)	N(1)-C(13)-C(14)	111.2(2)
N(1)-C(13)-C(12)	110.6(2)	C(14)-C(13)-C(12)	112.8(2)
C(13)-C(14)-C(16)	112.6(2)	C(13)-C(14)-C(15)	112.4(2)
C(16)-C(14)-C(15)	109.3(2)		

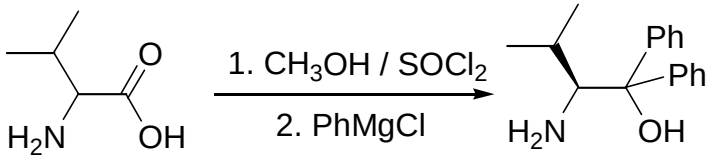

4-7

Scheme 4-2

4.2.2 Experimental

General procedures:

Unless otherwise indicated, all reactions were carried out under nitrogen atmosphere. Melting points were measured using an electrothermal 9100 apparatus in capillaries and the data were uncorrected. Optical rotations were measured on a Perkin-Elmer model 341 polarimeter at 20^{o}C. NMR spectra were recorded on a Varian 500 spectrometer. Mass analyses were performed on a Finnigan model Mat 95 ST mass spectrometer. HPLC analyses were performed using a Hewlett-Packard model HP 1050 LC interfaced to a HP 1050 series computer workstation. GC analyses were performed using a Hewlett-Packard HP 4890A apparatus. The prochiral ketones and aldehydes used for catalytic asymmetric reactions were distilled or re-crystallized before use and all other chemicals were purchased from Acros or Aldrich and were used as received.

Preparation of (*S*)-2-(N,N-Dibenzylamino)-3-methylbutan-1-ol (4-3).

To a suspension of 17.5g (165 mmol) anhydrous sodium carbonate in 300 mL of acetonitrile, 5.85g L-valine (50 mmol) was added at room temperature. The mixture was stirred for half an hour followed by the slow addition of 29.5g (173 mmol) of benzyl bromide. The reaction mixture was refluxed for 24 h and then cooled to room temperature. Water was added until the solution became clear. The organic layer was separated and the aqueous layer was extracted with ethyl acetate (3×100 mL). The combined organic layers were washed with brine and dried over sodium sulfate. The solvents were removed under reduced pressure and the crude product was purified by

flash chromatography to afford 17.6g of N,N-(dibenzylamino)-L-valine benzyl ester (91% yield). ^{1}H NMR ($CDCl_3$): δ 0.780-0.792 (d, *J* = 6.0 Hz, 3H), 1.026-1.039 (d, *J* = 6.5 Hz, 3H), 2.195-2.198 (m, 1H), 2.913-2.935 (d, *J* = 11.0 Hz, 1H), 3.285-3.313 (d, *J* = 14.0 Hz, 2H), 3.972-4.000 (d, *J* = 14.0 Hz, 2H), 5.166-5.191 (d, *J* = 12.5 Hz, 1H), 5.297-5.322 (d, *J* = 12.5 Hz, 1H), 7.218-7.459 (m, 15H). ^{13}C NMR ($CDCl_3$): δ 19.595, 19.966, 27.349, 54.702, 65.722, 68.217, 126.948, 128.242, 128.351, 128.600, 128.697, 128.861, 136.214, 139.559, 171.867.

A solution of 7.74g (20 mmol) N,N-(Dibenzylamino)-L-valine benzyl ester in 30 mL dry THF was added to a stirred suspension of lithium aluminum hydride (1.52g, 40 mmol) in 20 mL of THF at 0^{o}C. The reaction mixture was warmed to room temperature and was stirred for another 12 h before being quenched at 0^{o}C by careful addition of water (1.5 mL), aqueous NaOH (15% w/v, 1.5 mL) and water (4.5 mL) in sequence. The resulting white suspension was filtered and the solid residue was washed with THF (3×50 mL). The combined organic solutions were dried over sodium sulfate and concentrated under reduced pressure to yield the crude amino alcohol. Purification of the crude product by column chromatography on silica eluted with hexane/ethyl acetate (3/1) afforded 4.58g amino alcohol **4-3** (81% yield). ^{1}H NMR ($CDCl_3$): δ 0.949-0.963 (d, *J* = 7.0 Hz, 3H), 1.214-1.200 (d, 7.0 Hz, 3H), 2.082-2.151 (m, 1H), 2.584-2.627 (m, 1H), 3.153 (s, 1H), 3.524-3.565 (m, 1H), 3.668-3.698 (m, 1H), 3.766-3.793 (d, *J* = 13.5 Hz, 2H), 3.928-3.954 (d, *J* = 13.0 Hz, 2H), 7.260-7.396 (m, 10H). ^{13}C NMR ($CDCl_3$): δ 20.039, 22.479, 27.470, 54.258, 59.146, 64.665, 127.015, 128.314, 129.092, 139.741. Ms: 284 (M+1).

(*S*)-2-(N,N-Dibenzylamino)-3-methylbutan-1-al (4-4).

A solution of 4.37g pyridine-sulfur trioxide (27.5 mmol) in DMSO (16.5 mL) was added over 20 min to a solution of 4.67g (*S*)-2-(N,N-dibenzylamino)-3-methylbutan-1-ol (16.5 mmol) and 4.2 mL of triethylamine (30.2 mmol) in 16.5 mL DMSO at 0^{o}C. The mixture was stirred and was allowed to warm to room temperature for 9 h, quenched with ice-water (30 mL) and extracted with ethyl acetate (3×50 mL). The combined organic layers were washed with water, brine and dried over sodium sulfate. The solvent was evaporated under reduced pressure and the crude amino aldehyde was dried further under high vacuum for 12 h and was used without further purification. (95% yield) ^{1}H NMR ($CDCl_3$): δ 0.869-0.883 (d, *J* = 7.5 Hz, 3H), 1.079-1.092 (d, *J* = 7.5 Hz, 3H), 2.265-2.310 (m, 1H), 2.714-2.739 (dd, *J* = 3.0 Hz, 1H), 3.698-3.725 (d, *J* = 13.5 Hz, 1H), 4.013-4.041 (d, *J* = 13.5 Hz, 1H), 7.236-7.378 (m, 10 H), 9.858-9.852 (d, *J* = 3.0 Hz, 1H).

Preparation of amino alcohols with two stereocentres (4-6).

A Grignard reagent prepared from magnesium (50 mmol) and 2-bromo-6-methoxynaphthalene or phenyl bromide (45 mmol) in 50 mL dry THF was added to N,N-dibenzylamino aldehyde **4-4** (20 mmol in 50 mL of dry THF) over 30 min at 0^{o}C. The solution was stirred at this temperature for 3 h and another 5 h at room temperature. The solution was cooled to 0^{o}C and was hydrolyzed with a saturated NH_4Cl solution. The organic layer was separated and the aqueous layer was extracted with ethyl acetate. The combined organic layers were washed with brine and dried over Na_2SO_4. After the solvent was evaporated under reduced pressure, the product was

purified by column chromatography to afford 6.85g of the 1-[2′-(6′-methoxynaphthyl)]-2-(N,N-dibenzylamino)-3-methyl-butan-1-ol (78% yield). ^{1}H NMR ($CDCl_3$): . 0.994-1.010 (d, 3H), 1.068-1.082 (d, 3H), 2.385-2.401 (m, 1H), 2.925-2.945 (m, 1H), 3.618-3.647 (d, 2H), 3.886-3.914 (d, 2H), 3.960 (s, 3H), 5.125-5.134 (d, 2H), 7.15-7.65 (m, 16H).

In a 50 mL stainless steel autoclave were added 1.32g (3 mmol) of the N,N-dibenzylamino alcohol and 0.2g of 10% Pd/C in a solution of 20 mL methanol and acetic acid (0.21g, 3.5 mmol). The vessel was pressurized with 500 psi of hydrogen and the reaction was carried out at ambient temperature for 48 h. The solution was filtered and concentrated under reduced pressure. The residue was treated with ammonia solution and was worked up to afford a mixture of 1-[2′-(6′-methoxynaphthyl)]-2-amino-3-methylbutan-1-ol (1*R*,2*S*:1*S*,2*S* = 87:13, determined by ^{1}H NMR spectrum). Crystallization from dichloromethane and hexane gave **4-6a** (0.59g, 75% yield) as a white crystalline solid. M.p.: 108-109 ºC. $[\alpha]_D$ = -20.6º (*c*=1, 25 ºC, CH_3OH). ^{1}HNMR ($CDCl_3$): δ 0.901-0.914 (d, *J* = 6.5 Hz, 3H), 1.036-1.050 (d, *J* = 7.0 Hz, 3H), 1.731- 1.770 (m, 1H), 2.817-2.841 (t, *J* = 6.0 Hz, 1H), 7.120-7.161 (m, 2H), 7.740-7.460 (m, 2H), 7.702-7.719 (m, 2H). Ms: 242 [(M+1)-18, 55%], 260 (M+1, 100%). Anal. Calcd. for $C_{16}H_{21}NO_2$: C, 74.10; H, 8.16; N, 5.40. Found: C, 74.27; H, 8.06; N, 5.21. In the NMR spectra of the crude hydrogenated products, compound **4-6b** was observed: ^{1}H NMR ($CDCl_3$) δ 0.85 (d), 0.95 (d), 1.70 (m), 2.89 (m), 3.9 (s), 4.96 (d), 7.1-7.8 (m).

Preparation of 1*R*-[2′-(6′-methoxynaphthyl)]-2*S*-pyrrolidinyl-3-methylbutan-1-ol (4-8).

To a solution of **4-6a** (0.52g, 2 mmol) in 50 mL acetonitrile, sodium carbonate (0.75g, 7 mmol) was added. The mixture was stirred at room temperature for 15 min and then followed by the addition of 0.238g 1,4-dibromobutane (1.1 mmol). The reaction mixture was refluxed for 24 hours and was cooled to ambient temperature. Water was added until the solution became clear. The organic layer was separated and the aqueous layer was extracted with ethyl acetate (2×15 mL). The combined organic layers were washed with brine and dried over sodium sulfate. The solvents were removed under reduced pressure and the crude product was purified by flash chromatography to afford the amino alcohol **4-8** (5.7g, 90% yield). M.p.: 70-71 ºC. $[\alpha]_D$ = -14.9º (*c*=1, 25 ºC, CH_3OH). ^{1}H NMR ($CDCl_3$): δ 0.876-0.890 (d, *J* = 7.0 Hz, 3H), 1.039-1.054 (d, *J* = 7.5Hz, 3H), 1.727-1.767 (m, 4H), 1.867-2.042 (m, 1H), 2.667-2.713 (m, 3H), 2.776-2.802 (m, 2H), 3.910 (s, 3H), 5.144-5.121 (d, *J* = 3.5Hz, 1H), 7.124-7.150 (m, 2H), 7.420-7.440 (m, 1H), 7.677-7.733 (q, *J* = 8.5Hz 2H), 7.801 (s, 1H). ^{13}C NMR ($CDCl_3$): δ 20.360, 22.036, 23.906, 28.065, 51.708, 55.333, 72.401, 72.886, 105.661, 118.709, 124.720, 125.206, 126.317, 128.788, 129.492, 133.682, 138.041, 157.495. Ms: 314 (M+1, 100%). Exact mass calcd. for $C_{20}H_{27}NO_2$: 313.2042; Found: 313.2036.

4.3. Results and discussion

4.3.1. Enantioselective reduction of acetophenone with borane

The results of the enantioselective reduction of acetophenone with borane catalyzed by amino alcohol **4-6a, 4-6c** and **4-7** were summarized in **Table 4-2**. Both ligands **4-6a** and **4-6c**, which possessed two stereogenic centers, showed higher enantioselectivity than ligand **4-7** (entries 3, 6 vs. 7). The highest ee value achieved with chiral ligand **4-6a** indicated that the large group in compound **4-6a** was favorable for higher enantioselectivity (entry 3 vs. 6). This result is consistent with the mechanism proposed by Corey *et al*.[125] A possible transition state of the key reaction intermediate is shown in Figure 2. The acetophenone binds to the oxazaborolidine that is *cis* to the vicinal BH_3 group. This manner of binding minimizes the unfavorable steric interactions between the oxazaborolidine and the acetophenone. The smaller methyl group of the acetophenone points to the β-face of the oxazaborolidine which is more sterically crowded, and the larger phenyl group points to the α-face of oxazaborolidine which is less sterically hindered. Therefore, it can be explained that the relatively large naphthyl substituent in ligand **4-6a** enhances this orientation of the acetophenone. On the other hand, if one more phenyl group is attached to the α-face of the carbonyl carbon (ligand **4-7**), the previous preferential orientation of the acetophenone will be less dominant, and thus lower ee is observed in the product.

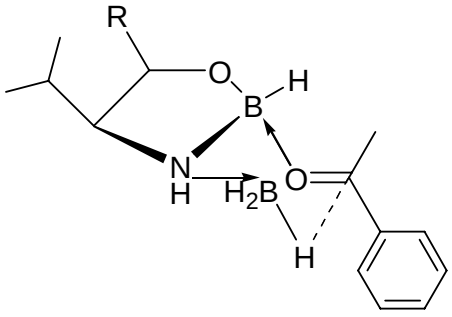

Figure 4-2. R = Ph, 6-CH_3ONap

Table 4-2. The enantioselective borane reduction of aromatic ketones using chiral amino alcohol ligands.

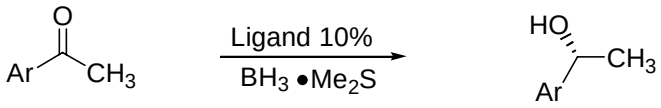

Entry	Ligand	Ketones	T (^{o}C)	Conc. of ligands (mol%)	Conv. (%)	ee (%)[a,b]
1	**4-6a**	$PhCOCH_3$	0	10	80	90
2	**4-6a**	$PhCOCH_3$	25	10	95	92
3	**4-6a**	$PhCOCH_3$	50	10	100	94
4	**4-6a**	$PhCOCH_3$	50	5	100	93
5	**4-6a**	$PhCOCH_3$	50	20	100	95
6	**4-6c**	$PhCOCH_3$	50	10	100	89
7	**4-7**	$PhCOCH_3$	50	10	100	81
8	**4-6a**	$PhCOCH_2Cl$	50	10	100	93
9	**4-6a**	*p*-$NO_2PhCOCH_3$	50	10	100	97
10	**4-6a**	*o*-$CH_3PhCOCH_3$	50	10	100	87

[a]The ee values were determined by GLC analysis with a Chrompack Chirasil-Dex CB column. [b]All products were in *R* configuration as determined by comparison with authentic samples.

4.3.2. Asymmetric Dialkylzinc Additions to Aldehydes

Amino alcohols constitute an important part of the chiral ligands developed for dialkylzinc additions to aldehydes. The first highly enantioselective catalytic addition of dialkylzincs to aromatic aldehydes was reported by Noyori using camphor-derived homochiral amino alcohol (2*S*)-3-*exo*-(dimethylamino)isoborneol (DAIB)[126] as the chiral auxiliary. After this important discovery, a large number of highly enantioselective chiral catalysts have been developed.[127] It was reported that the bulkiness and the electronic effect of the substituents on the nitrogen atom of the chiral amino alcohols might affect the formation and the stability of the six-membered transition states. N-Alkyl substituents must possess at least one β-carbon atom to give high enantioselectivity. Suitably large N-alkyl substituents limited the approach of the nucleophiles to one of the enantiotopic faces of the aldehyde, leading to high enantioselectivity.[128] We prepared amino alcohol **4-8** by cycloalkylating ligand **4-6a** using 1,4-dibromobutane in the presence of a base. (**Scheme 4-3**).

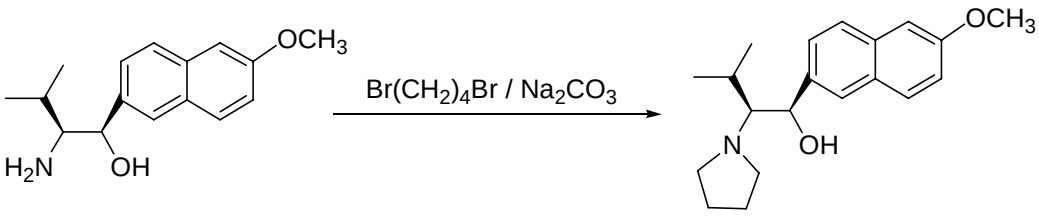

4-6a **4-8**

Scheme 4-3

The results of the enantioselective addition of diethylzinc to aldehydes accelerated by amino alcohol **4-8** were listed in **Table 4-3**. Moderate to excellent enantioselectivities were achieved. It was found that the reaction temperature had little influence on the

enantioselectivities (entries 1 – 2), while the increase of the size of the aldehyde slightly increased the enantioselectivity. (entry 3) These results were consistent with the mechanism proposed by Noyori that a larger substituent on the aromatic aldehyde favored the *anti* coordination of the aryl aldehyde (with respect to the chiral ligand) and enhanced the *si* face addition of the ethyl group to the aldehyde.[129, 130] *meta*- and *para*-chlorobenzaldehydes gave products with the highest ee's (up to 98%, entries 6–7). It was possible that the electron-withdrawing group on the phenyl ring made the carbonyl carbon more susceptible to the nucleophilic attack by the ethyl group in the diethylzinc.

Table 4-3. Enantioselective addition of diethylzinc to aldehyde catalyzed by ligand **4-8**

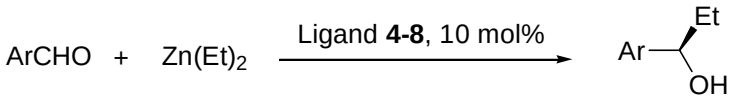

Entry	Aldehyde	Conc. of ligand (mol%)	Temperature (^{o}C)	ee (%)[a,b]
1	C_6H_5CHO	10	0	84
2	C_6H_5CHO	10	25	83
3	2-NapCHO	10	25	87
4	*o*-OCH_3C6H_5CHO	10	25	86
5	*o*-ClC_6H_5CHO	10	25	85
6	*m*-ClC_6H_5CHO	10	25	96
7	*p*-ClC_6H_5CHO	10	25	98

[a] The conversions were 95-100% in all cases. [b] All products were in *R* configuration and the ee values were determined by HPLC and GLC analysis

4.4. Synthesis of Other Amino Alcohol ligands

Encouraged by the above stated success in synthesis of an efficient novel amino alcohol ligand and to investigate the structural effect on the ligand and hence provide

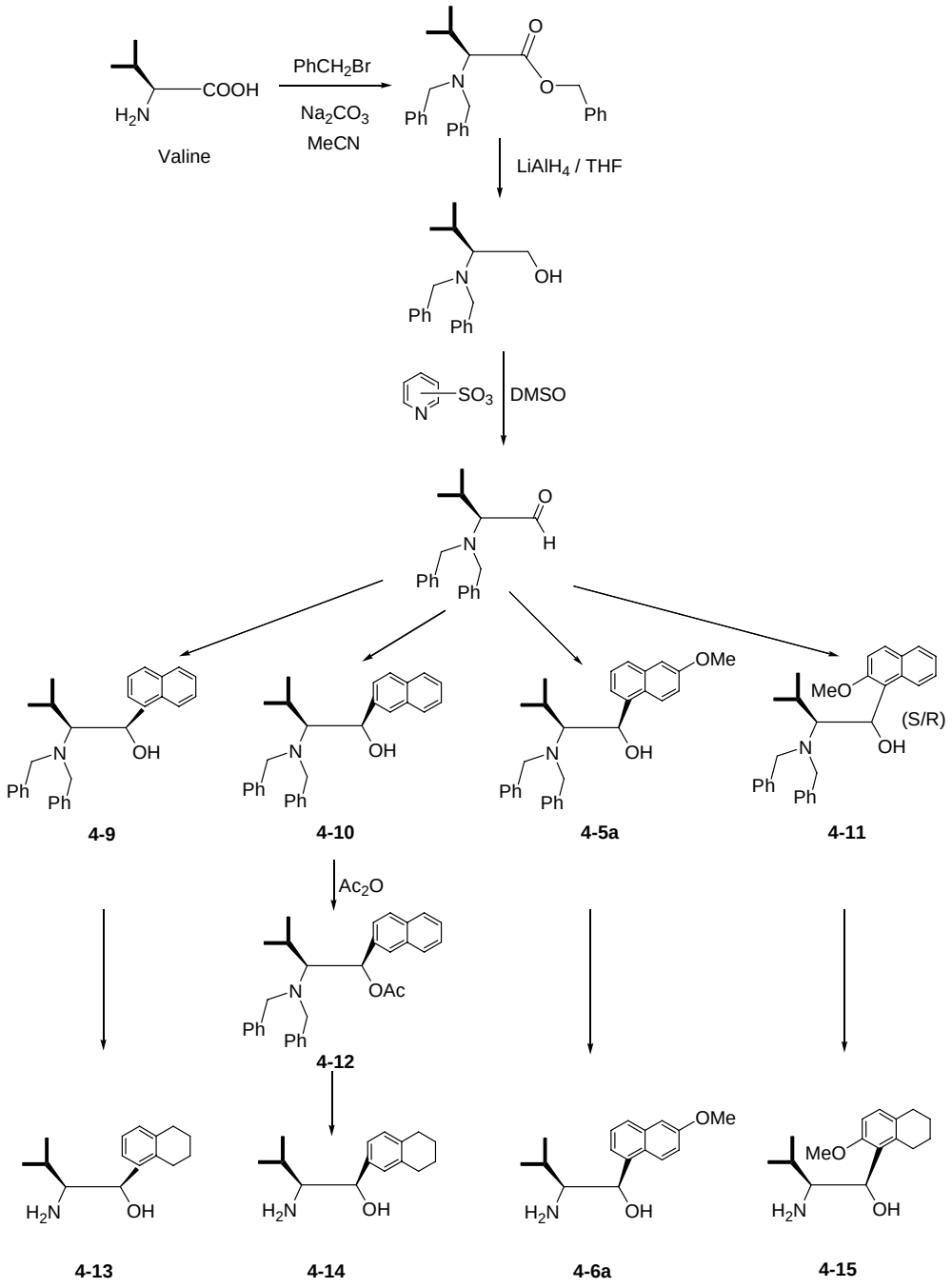

Scheme 4-4

better opportunities for the rational design of efficient ligands, some analogues of ligand **4-6a** were synthesized according to the synthetic routes shown in **Scheme 4-4**. The structures of the corresponding ligands or their derivatives have been determined by x-ray diffraction experiments and are listed in **Figure 4-4** to **Figure 4-7.** Their catalytic properties in asymmetric reactions such as enantioselective borane reduction of acetophenone and diethylzinc addition to aldehydes will be investigated in future work.

In the future work, there is also possibility to synthesize some new excellent P-N ligands based on **4-6a** or its analogues for palladium-catalyzed asymmetric allylic substitutions.

4.5. Summary

In summary, the diastereomers of a new type of amino alcohols with two stereogenic centers were synthesized from L-valine. The enantioselective borane reduction of acetophenone catalyzed by the amino alcohols with (*S*,*R*)-configuration (**4-6a** and **4-6c)** provided high ee's (up to 97%) in the production of chiral secondary alcohols. The enantioselective diethylzinc addition to aldehydes catalyzed by the N,N-cycloalkylated amino alcohol **4-8** also provided the corresponding chiral secondary alcohols with good to excellent ee's (up to 98%).

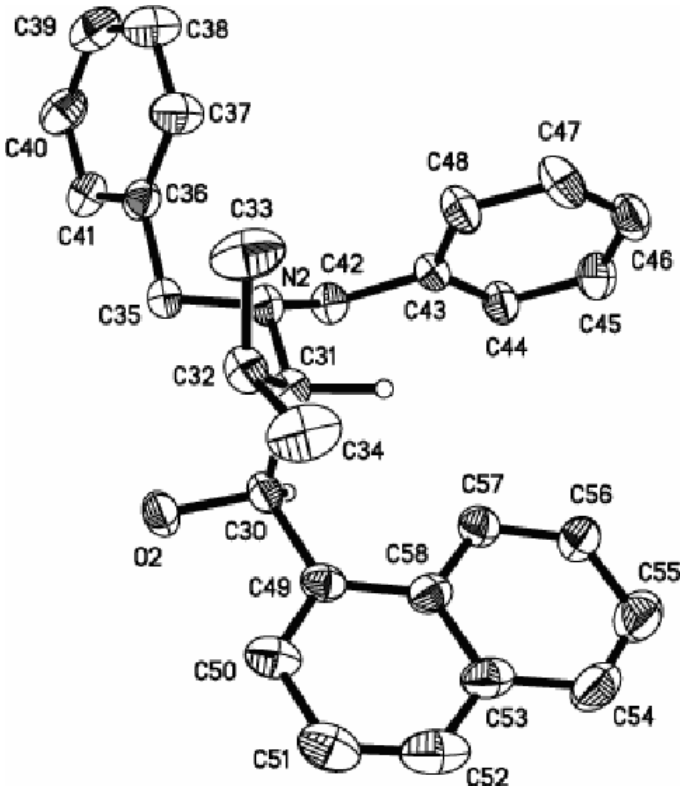

Figure 4-4. ORTEP drawing of **4-9**

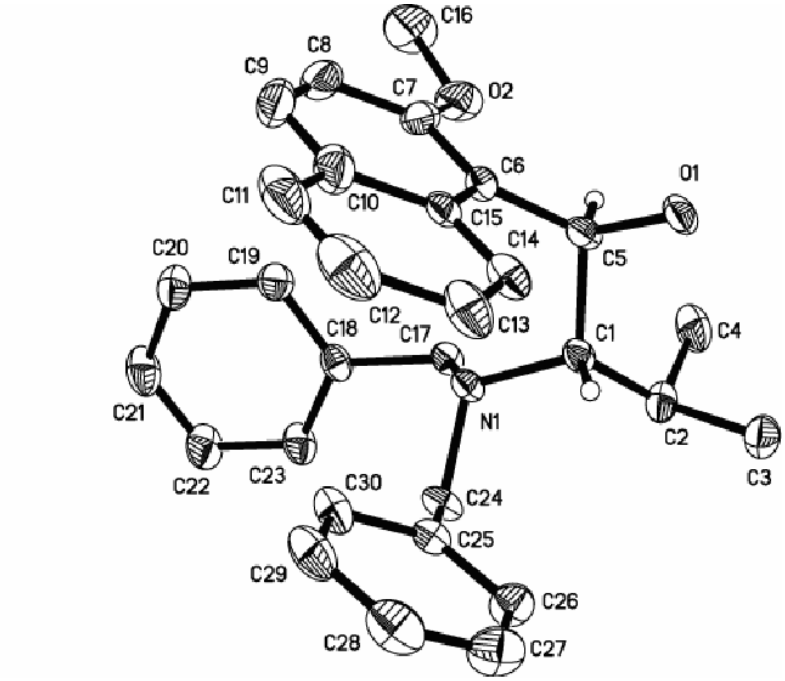

Figure 4-5. ORTEP drawing of **4-11**

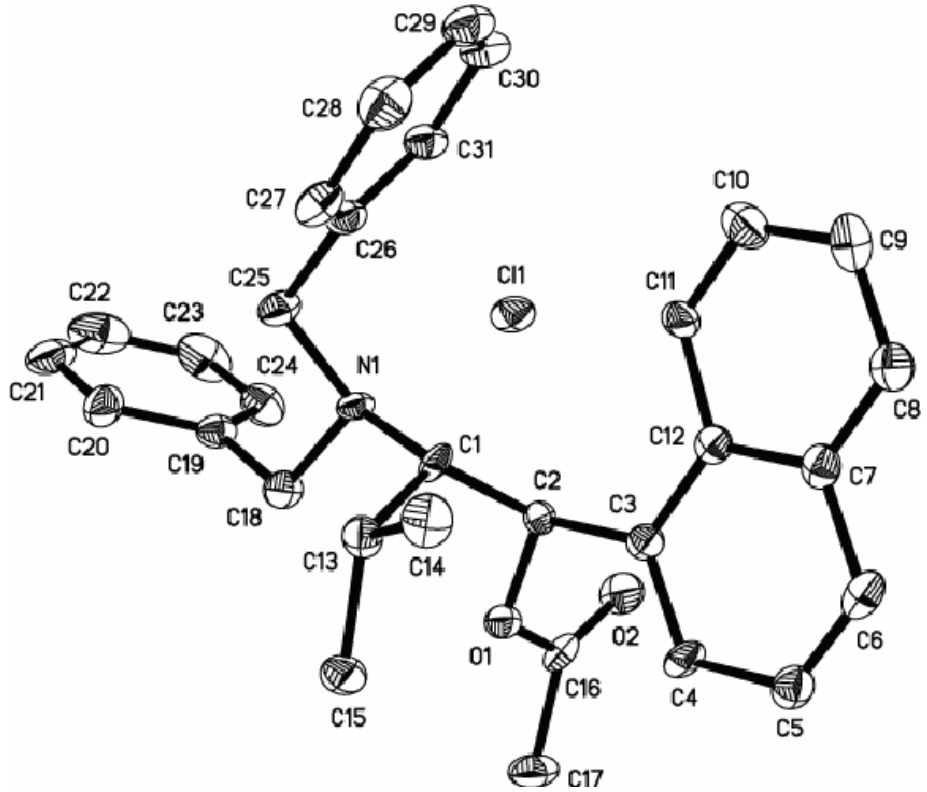

Figure 4-6. ORTEP drawing of **4-12**

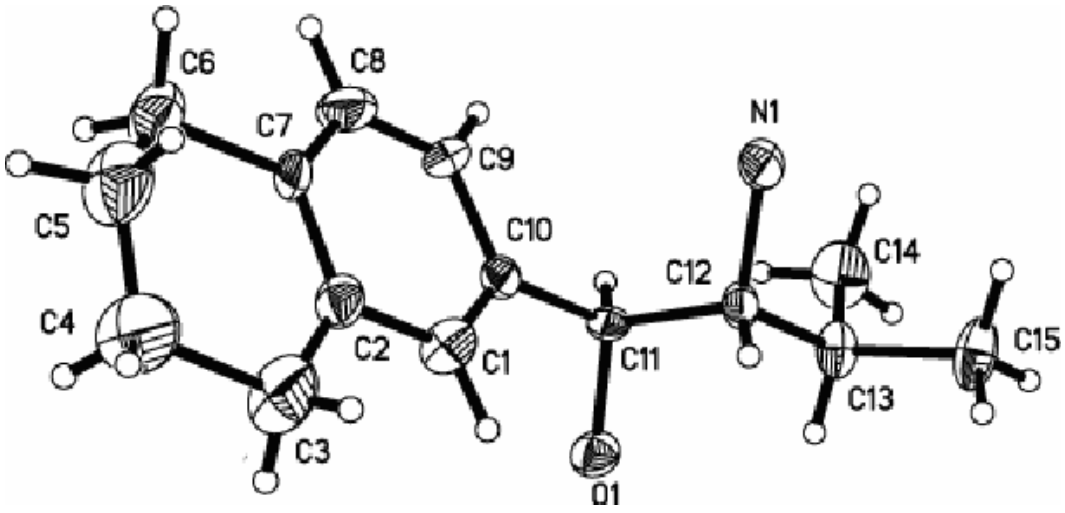

Figure 4-7. ORTEP drawing of **4-14**

Chapter 5
Ion Exchanger Immobilized Chiral Catalysts and their Application in Asymmetric Hydrogenation

5.1. Asymmetric Hydrogenation and Immobilization

5.1.1 Asymmetric Hydrogenation

Asymmetric hydrogenation by chiral transition metal catalysts has been the most extensively studied reaction in the field of asymmetric catalysis because of its great importance. The first enantioselective hydrogenation of unsaturated compounds appeared in the late 1930's using metallic catalysts deposited on chiral supports. This method attracted attention from a synthetic point of view when its enantioselectivity exceeded 60% ee in the mid-50's. In 1968, Knowles and Horner independently reported homogeneous asymmetric hydrogenation with Rh complexes bearing chiral tertiary phosphines as the first example of homogeneous asymmetric hydrogenation catalysts. Knowles *et al*. further developed the catalyst system for the commercial production of L-Dopa.

Among various chiral catalysts in asymmetric hydrogenation, rhodium(I) complexes with chiral phosphine ligands have been the most extensively used. A breakthrough in this area came when Kagan devised DIOP, a C_2 -symmetry chiral diphosphine obtained from natural tartaric acid. The DIOP-Rh(I) complex catalyzed the hydrogenation of α-(acylamino)acrylic acids and esters to produce the

corresponding amino acid derivatives in up to 80% ee. Today, a series of naturally and non-naturally occurring amino acids can be prepared in greater than 90% ee by using chiral phosphine-Rh catalysts (**Scheme 5-1 and Table 5-1**).

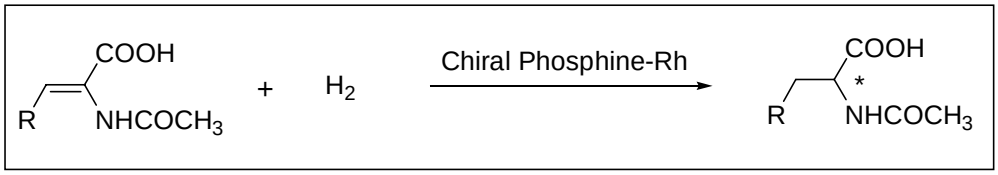

Scheme 5-1

Table 5-1. Enantioselective hydrogenation of α-(acylamino)acrylic acids

Phosphine Ligands	Ee% (R=Ph)	Ee%(R=H)
(R,R)-DIOP	85 (*R*)	73*(R)*
R,R)-DIPAMP	96(*S*)	94(*S*)
(S,S)-CHIRAPHOS	99(*R*)	91(*R*)
(S,S)-CYCPHOS	88(*R*)	---[a]
(S,S)-NORPHOS	95(*S*)	90(*R*)
(S,S)-BDPP	92(*R*)	---[a]
(S,S)-BPPM	91(*R*)	98.5(*R*)
(S)-(R)-BPPFA	93(*S*)	---[a]
(S)-BINAP	100(*R*)[b]	98(*R*)[b]
(S,S)-Et-DuPHOS	99(*S*)	99.4(*S*)
(R,R)-BICP	96.8(S)	---[a]
(*R*)-spirOP	97.9(*R*)	99.9(*R*)

[a] Data not available; [b] Hydrogenation of N-benzoyl derivative.

However, the catalytic activity and enantioselectivity of rhodium system are quite substrate dependent and only gave good results in the preparation of amino acids. Recently, chiral ruthenium-diphosphine complexes have been developed and have opened new frontiers for the catalytic asymmetric hydrogenation reaction. The ruthenium catalysts containing BINAP ligand have been found to give good to excellent results in the hydrogenation of a variety of substrates which are useful intermediate for the production of high value pharmaceuticals. The most famous examples using BINAP-Ru(II) as catalyst is the synthesis of naproxen which has already been industrialized.

5.1.2 Homogeneous and Heterogeneous Catalysts

Homogeneous catalysts not only show high catalytic activity and selectivity but also have a well-defined molecular structure. So, structural variation can be made in order to optimize the catalytic activity and steroselectivity. However, one of the major problems in homogeneous catalysis is the separation and recycling of the expensive catalyst. The strengths and weaknesses of homogeneous and heterogeneous catalysis are summarized in **Table 5-2.**

In homogeneous catalysis, especially in asymmetric catalytic reaction, the catalysts are usually expensive, and so it is crucial to retrieve the chiral ligands as well as the transition metals. Therefore, separation and reuse of homogeneous catalysts is a desirable and urgent necessity. On the other hand, catalyst recycling is not a problem in heterogeneous processes. The catalyst either remains on the solid bed of the reactor

after reaction or can be recovered readily from a catalyst suspension by filtration of centrifugation with subsequent recycling.

Table 5-2. Advantages and disadvantages of homogeneous and heterogeneous catalysis

Capability	Homogeneous catalysis	Heterogeneous catalysis
Activity	high	variable
Selectivity	high	variable
Reaction conditions	mild	harsh
Service of catalyst	variable	long
Sensitivity to catalyst poisons	Low	high
Diffussion	none	may be important
Catalyst recycling	expensive	unnecessary
Variability of steric and electronic properties	possible	not possible
Mechanistic understanding	plausible	more or less impossible (except for model system)

5.1.3. Methodology for Asymmetric Catalyst Immobilization and Recycling

As stated above, one of the serious problems in homogeneous catalysis is the separation of the reaction products from the expensive catalyst and recycling of the catalyst. Basically, several methods have been devised to overcome this difficulty.

5.1.3.1. Immobilized Asymmetric catalysts

Catalysts are anchored on a stationary (insoluble) supports such as organic polymers (for example, cross-linked polystyrene) or inorganic carrier (for example, silica gel). In this case, the molecules of catalysts are covalently connected to the surface of the support. With this kind of catalyst, catalysis reaction proceeds heterogeneously, and after completion of reaction catalysts can be filtered off and reused for next catalytic reaction run.

- **Insoluble Polymer-supported Asymmetric Catalysts**

Insoluble polymer-supported asymmetric catalysts have been attracting much interest at the present time due to their easy separation and recycling ability. The use of these catalysts has been extensively studied. Some typical examples of these catalysts for asymmetric hydrogenation are listed in **Figure 5-1**.

The most important factors in asymmetric catalysis are activity and stereoselectivity of catalysts. However, usually immobilization of the catalysts involves the loss of some degree of enantioselectivity and catalytic activity. The insoluble polymer-supported catalysts often give lower catalytic activities and/or enantioselectivities compared to those of homogeneous catalysts. And in most case, recycling is accompanied by metal leaching. In fact, the catalytic activity and stereoselectivity of these heterogeneous catalysts remain far from satisfactory due to the limited mobility and accessibility of the catalytic sites. So far, a catalyst of industrial (economical) importance is still unknown. Catalytic activity, selectivity and catalyst leaching remain the central problem.

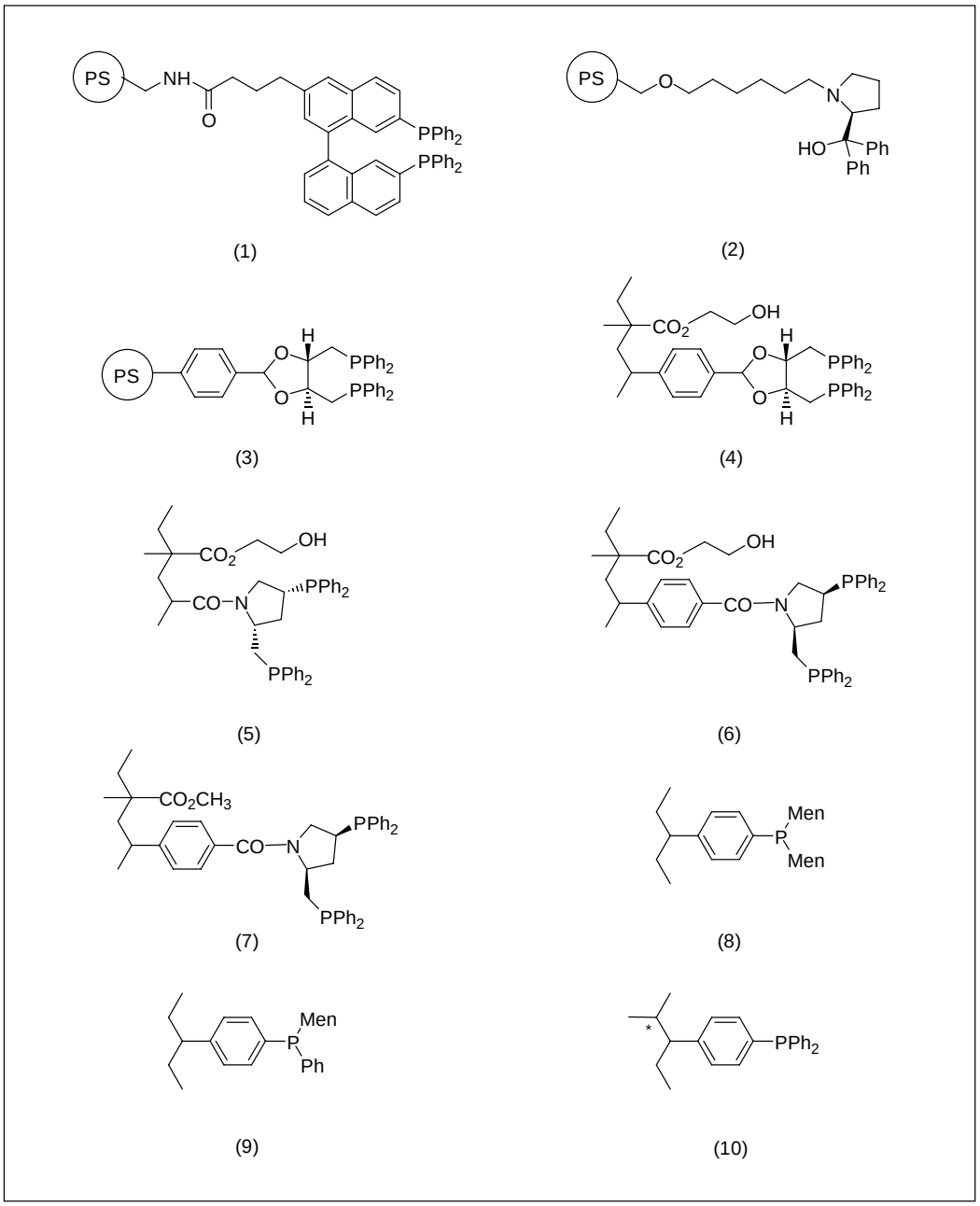

Figure 5-1. Ligands immobilized on organic supports used as asymmetric hydrogenation catalysts.

The weakness of the insoluble polymer-supported asymmetric catalysts as compared to their homogeneous counterparts is due to the following reasons:

1. The limited accessibility of the active site

The homogeneous catalysts are usually covalently bounded to the polymer chains; and the extensive cross-linking and steric hindrance of the polymer matrix may restrict the freedom and mobility of the catalytic site.

2. Catalyst leaching

Leaching normally results from the dissociation of the catalytic metal from one of the anchored ligands, thus liberating the active molecular catalyst. Leaching can also originate from structure changes with concomitant weakening of certain bonds (especially the specific bonding type between catalyst and support) during the catalytic cycle.

3. The mechanical properties problem (poor stability)

The structure of the polymer often changes during the catalytic cycle, for example, polystyrene beads collapse and shrink in polar solvent, which prevent entry of the substrate to the catalytic site.

4. Limited polymer capacity and difficult characterization

The surface area of the insoluble polymer resins often limits the quantities of the supported catalysts. The chemical modification to bind a catalyst onto the polymer also affects the polymer capacity. Usually common method such as NMR can not be used to characterize the modification and the structure of the polymer-supported catalysts.

Therefore, many studies focus on developing new polymer supports in which the mobility and accessibility of the bound chiral catalyst can be enhanced. Typically, there are two main methods to alleviate this problem.

1. Catalyst bound to polymer via a " spacer"

As stated above, the steric hindrance of the polymer support may restrict the freedom and mobility of the catalytic site. This is probably the main reason why there is a decrease of catalytic activity and enantioselectivity of polymeric catalysts. For example, quinine (monomer) catalyzed asymmetric Michael addition for 5 h affords the product with 55% ee in 93% yiels, whereas the corresponding polymeric quinine catalyzed the same reaction requires a much longer reaction time (48 h) and affords the product with only 24% ee.

In order to alleviate the restriction of the catalytic site, the chiral catalyst is anchored on polymer via a spacer which can separate the catalytic site from the polymer matrix. Soai *et al.*[131] reported an enantioselective addition of diethylzinc to

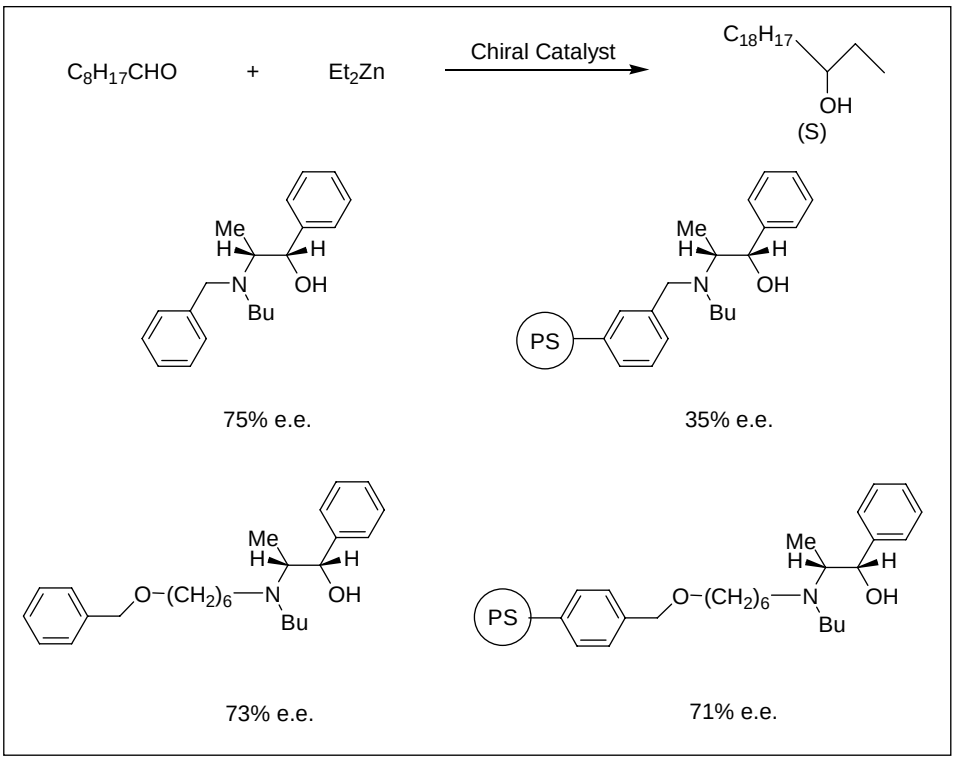

Figure 5-2

aldehydes using chiral polymer catalysts possessing an olygomethylene spacer (**Figure 5-2**). N-Butylnorphedrine was supported on a polystyrene resin via a spacer with six methylene groups and afforded a more enantioselective catalysts than those without such olygomethylene spacer.

Usually, porous and rigid polymers are used as catalyst supports. For example, cross-linked polystyrene (PS) is one of the most widely used polymer supports for the attachment of phosphine ligands through chemical modifications. However, poor results are usually obtained in asymmetric synthesis with polystyrene containing chiral phoshine ligands. Recently, Nagel *et al.* [132] reported the PEG-PS-supported chiral phosphine Rh(I) catalyst (**Scheme 5-2**). The grafted polyethylene glycol (spacer) exhibits good swelling properties in most organic solvents,[133] and this may enhance the mobility an accessibility of the active site. This catalyst was used for the hydrogenation of dehydroamino acids with 96% ee. However, the recovered polymeric catalyst did not show any activity, probably due to the poor stability of the polymer support.

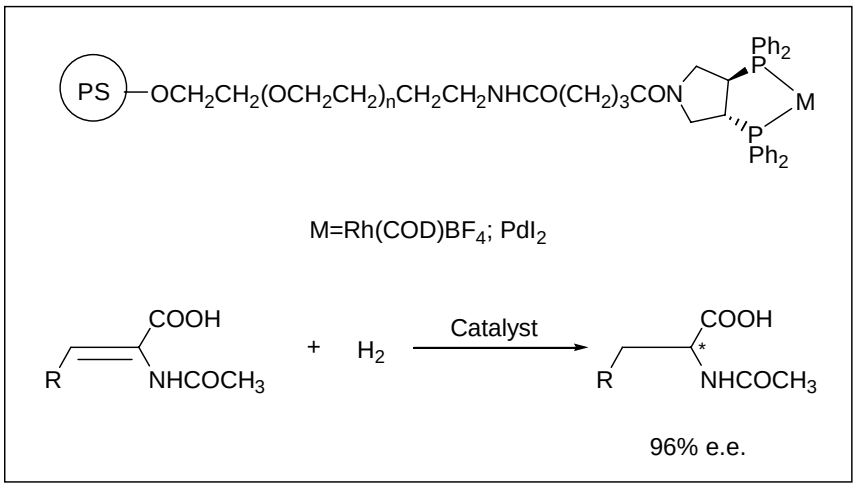

Scheme 5-2

Another example with good results is the catalyst (1) shown in **Figure 5-1**. With this catalyst, optical yields up to 100% are obtained in heterogeneous hydrogenation of α-(acetylamino)cinnamic acid and its methyl ester.

2. New polymer as catalyst support

Chiral catalyst supported on polymer is located in "new" environment. As explained in the previous section, the polymer matrix may restrict the mobility and accessibility of the active sites and consequently result in the decrease of catalytic activity and selectivity. On the other hand, the support may provide unique microenvironment for the catalytic reactions such that stereroselectivity and reactivity may be enhanced in a favorable case. Therefore, the success of synergistic effect of the support on the catalyst is often affected by the choice of polymer, with regard to mechanical stability, swellability, compatibility with a range of hydrophilic and/of hydrophobic solvents. For example, Salvadori *et al.*[134] reported an insoluble polymer-bound Cinchona alkaloid ligand for the symmetric dihydroxylation of olefins with similar reactivity as that of the corresponding homogeneous catalyst (**scheme 5-3**). The polyhydroxymethacrylic backbone offers a favorable microenvironment to the chiral catalytic sites. This suggests that once an appropriate support which is compatible with the reaction medium is found, the reactivity of the soluble or insoluble ligand is very similar.

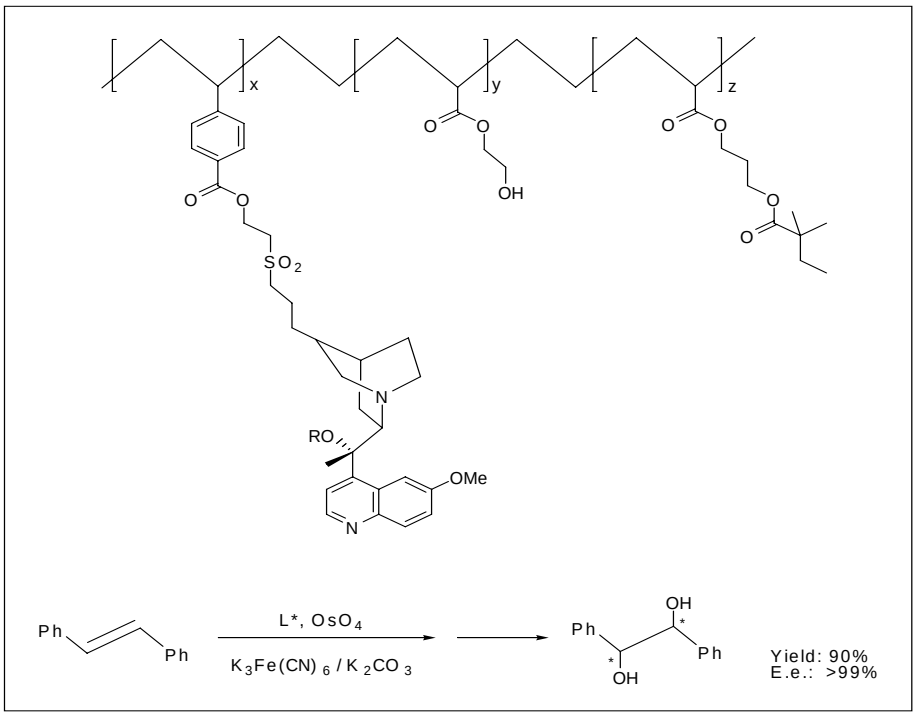

Scheme 5-3

Yang *et al.*[135] recently reported another outstanding example that the Ti complex of the following immobilized ligand (**Scheme 5-4** and **Table 5-3**) is substantially more enantioselective for the asymmetric addition of diethylzinc to aldehydes than its "free" analogue complex. A profound solvent effect was observed in the study,

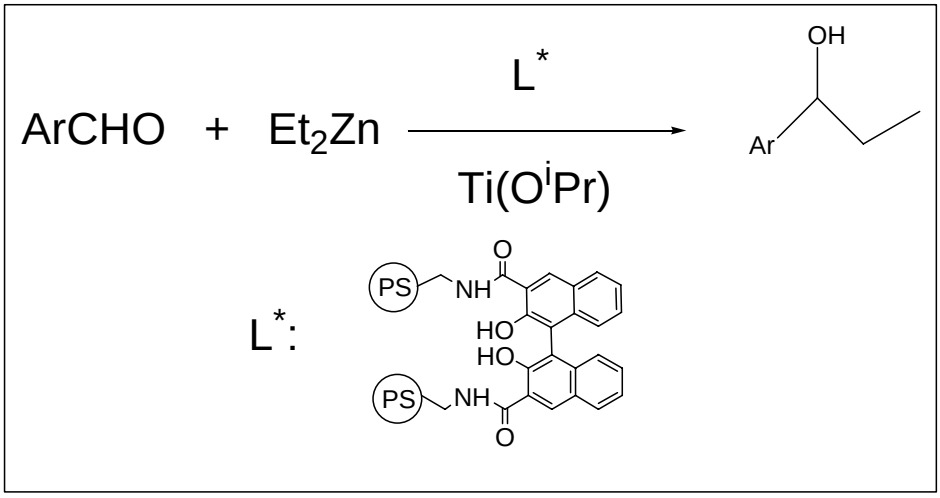

Scheme 5-4

and dichloromethane was found to be superior to other common organic solvent. The enantioselectivity also varied significantly when different levers of ligands were used. The optimum amount of ligand is 20 mol%. Interestingly, with this polymer-supported catalyst, similar results were obtained for substrates with identical substituents at the ortho, meta, or para position of the aromatic aldehydes. To learn about the influence of the polymer on the enantioselectivity, the author also studied the reaction of diethylzinc with benzaldehyde using a homogeneous BINOL derivative having a $CONHCH_2C_6H5$ groups at the 3,3′ positions of BINOL. Though this catalyst could provide a faster reaction, the enantioselectivity (63% ee) is much lower than that of the immobilized catalyst (97%ee). These results demonstrate that under some circumstances the hindrance of polymeric support may have a favorable effect on the enantioselectivity of the corresponding immobilized catalysts.

Table 5-3.

Entry	Ar	Time	Yield (%)	Ee (%) (L*)	Ee (%) (BINOL)
1	Ph	24	93	97	91.9
2	2-MeOPh	25	92	91	68.6
3	3-ClPh	24	89	94	88.2
4	4-ClPh	30	88	92	88.1
5	2-MeOPh	24	92	89	
6	3-MeOPh	28	78	92	94.0
7	4-MeOPh	48	90	83	79.0
8	3-NO_2Ph	54	88	99	70.0

- **Silica Gel Supported Asymmetric Catalysts**

An alternative way to immobilize catalysts is to connect them to silica gel. This kind of immobilized catalysts is also studied extensively and intensively. Usually silica gel has a very large surface (between 200 and 800 m^2/g). So the catalytic ability of catalysts should not be sacrificed too much when them are connected to the surface of silica gel. And catalysts can be immobilized on silica gel by a standard procedure which involves coupling of trichlorosilane or trialkyloxysilane on silica gel particles.

In **Figure 5-3** typical silica gel supported catalysts and ligands are listed, among which, few give good results. For example, Zhou *et al.* [136] recently reported that catalyst (1) (shown in **Figure 5-3**) is an effective catalyst for asymmetric epoxidation of unfunctionalised alkenes and gave significantly higher ee than the free complex.

Another example with good results is the catalyst (2)[137] (shown in **Figure 5-3**). The catalyst was used for the hydrogenation of α-(acetylamino)cinnamic acid and its methyl ester in methanolic solution. The optical yields were comparable to the homogeneous case although they varied considerably with silica of different pore size with the ester as substrate; this was not observed with the acid. The longer and more flexible the link between the silica and ligand, the higher the optical purity of the products was obtained. Up to100% ee was achieved with α-(acylamino)acrylic acid esters, 97% with the acids. The resulting catalyst was much less active, even though it was washed thoroughly with methanol. The maximum rate of the hydrogenation is about four times slower if the coupling on silica was done in dichloromethane rather

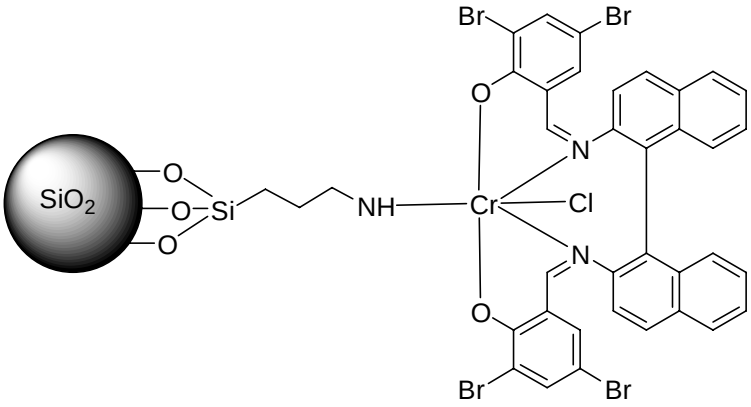

(1)

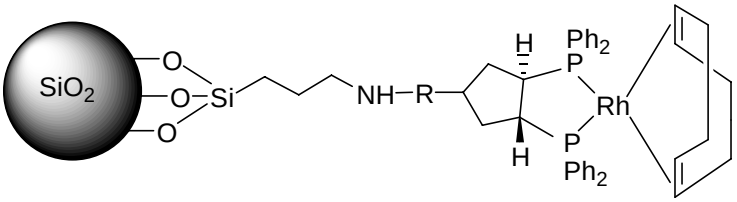

(2)

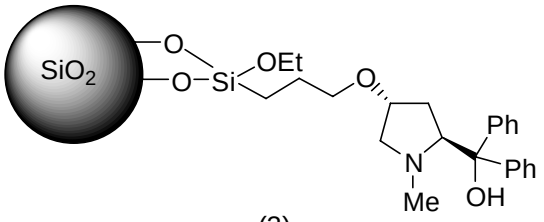

(3)

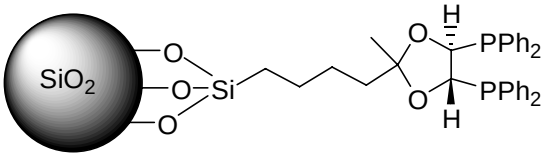

(4)

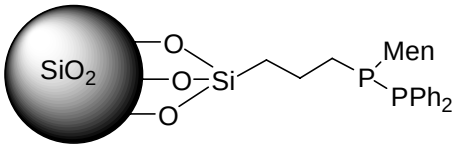

(5)

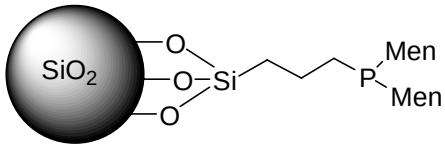

(6)

Figure 5-3.

than in methanol. The catalyst was reused three times. In the third run the activity and selectivity decreased considerably.

5.1.3.2. Soluble Polymer(or dendrimer)-bound Asymmetric Catalyst

Another approach to polymeric catalyst is the use of soluble polymer as catalyst support. The molecules of catalyst are covalently connected to the backbone of soluble polymers to form main-chain or side-chain soluble polymer-bound catalyst. Such catalyst has the following advantages over the insoluble polymer-supported catalysts.

- One-phase catalysis / two phase separation

The catalytic reaction can be carried out in a homogeneous manner and the interaction between the polymer backbone and the active sites is negligible. Therefore, the soluble polymer-bound catalysts provide high catalytic activity and stereoselectivity as effectively as a free homogeneous catalyst. Separation of the catalyst from reaction products can be achieved by taking advantage of the properties of the polymer, e.g., by addition of a bad solvent of change temperature to precipitate the polymeric catalyst. So, the catalyst can be separated from the reaction mixture and can be reused for next catalytic reaction run. This technique can compromise the advantages of homogeneouse and heterogeneous catalysts, i.e., high activity and high stereoselectivity with easiness of separation of and recycle of the catalyst.

- Tailor-made choices

Because the polymeric ligand or catalyst is soluble in a proper organic solvent, the common method such as NMR can be used to characterize it. Thus, the modification of such catalyst may be controlled (The homogeneous catalysis has its greatest potential in step-by-step improvements; in contrast, the heterogeneous catalysis is still in the status of empiricism). Furthermore, the easy modification of such catalyst provides an opportunity to study the polymer effect in which the presence of polymer may improve the reactivity and stereoselectivity of the supported catalyst.

- Physical stability

The traditional insoluble polymer-supported catalyst, in most cases, may deterioate after a few cycles. While the catalytic reaction catalyzed by the soluble polymer-bound catalysts can operate in an unhindered manner as homogeneous catalyst. Thus the deterioration caused by mechanic stirring or solvent can be minimized.

Recently, dendritic asymmetric catalysts are attracting some research interest. And the “ one phase catalysis / two phase separation” can also be applied to this kind of special modified catalyst.

Even though, there is a principle disadvantage of the soluble polymer (or dendrimer)-bound asymmetric catalyst, that is, their synthesis are usually difficult and recycling process is also troublesome.

Figure 5-4 listed several typical soluble polymer (or dendrimer)-bound asymmetric catalysts which exhibit good results in asymmetric catalysis. The catalyst (1) integrated a chiral ligand to the terminal of a soluble polymer (MeO-PEG) so that

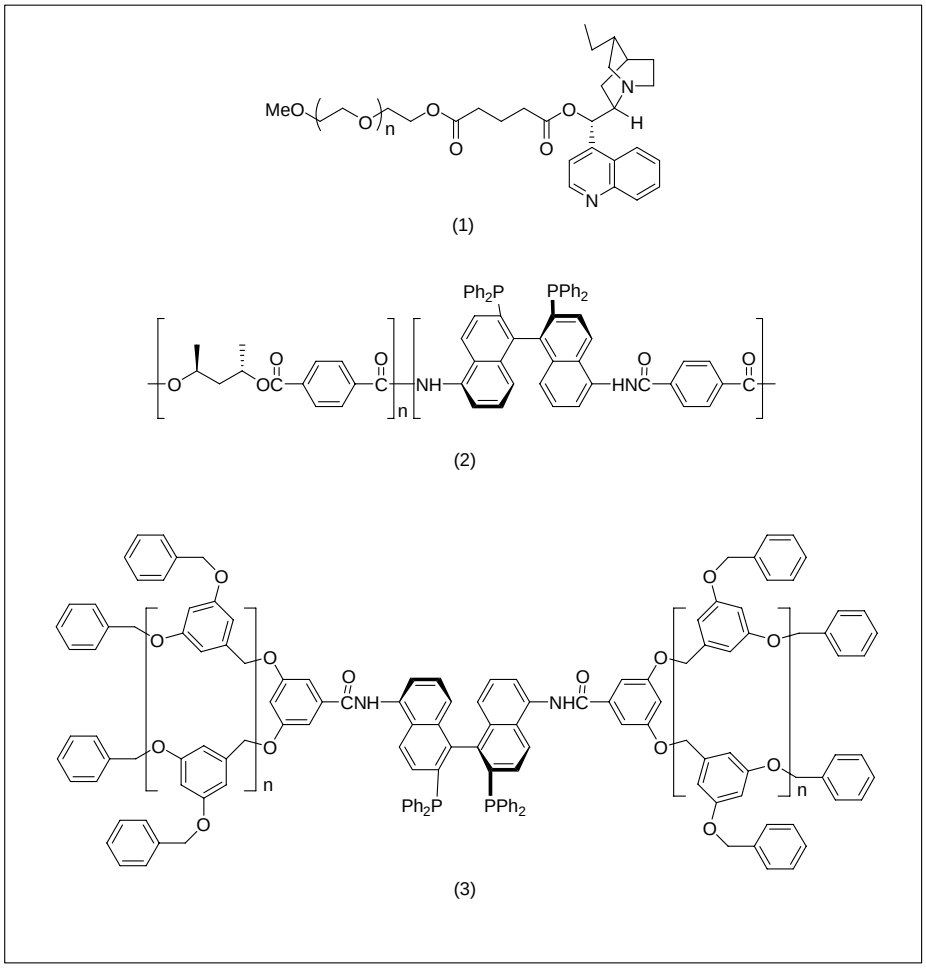

Figure 5-4

asymmetric dihydroxylation can operate in an unhindered manner on a polymer a support.[138] The soluble polymer-bound ligand provides all advantages that an insoluble support can offer, while also being as effective as a free ligand both in reactivity and selectivity. And reported by Fan *et al.*, [139] the Ru(II) complex of polymeric ligand (2) was found to be substantially more active than the corresponding

monomeric or free catalyst (BINAP-Ru complex) and to give almost the same enantioselectivity in 10 recycle runs as BINAP-Ru complex can give. This result really has the potential not only for laboratory research but also for industrial application.

5.1.3.3. Water-soluble Asymmetric Catalyst

Asymmetric catalyst can be made water-soluble by sulfonation or ammoniumization. Water- soluble catalysts are poorly soluble in organic media. And hence, asymmetric catalysis could be carried out in a two-phase system (aqueous and organic phase) and decantation would allow an easy separation and recovery of the catalyst.

In this field, sulfonated BINAP takes the most important part (**scheme 5-9**). Reported by Wan and Davis, [140] Rh(I) complex of this ligand is the first to perform asymmetric hydrogenation in neat water with optical yields as high as those obtained in nonaqueous solvent. And its Ru(II) complex is shown to be an excellent asymmetric hydrogenation catalyst for 2-acylamino acid precursors and methylenesuccinic acid in both methanolic and in neat water solvent systems; enantiomeric excesses approaching 90% have been obtained on aqueous and methanolic solvents.

Wan and Davis[141] also developed a so-called “supported aqueous-phase catalyst” for asymmetric hydrogenation of dehydronaproxen with sulfonated BINAP. The water-soluble complex, [Ru(BINAP-4SO_3Na)(benzene)Cl]Cl, was control-pore glass,

while the reactants and products remain within a hydrophobic held in a thin film of water on a porous hydrophilic support such as silica or organic phase. This new technique does not require covalent modification of the catalyst and provides a large interfacial area between the catalytic phase and the solvent. This heterogeneous catalyst gave enantioselectivity of only about 70% ee. When PEG was used as the hydrophilic liquid phase instead of water, the modified catalyst could give enantioselectivity up to 96% ee.

Davis' "supported aqueous-phase catalysis" system is excellent in designing. However, a rather non-polar solvent should be employed to for hydrophobic phase, and in non-polar solvent the hydrogenation of dehydronaproxen just gives comparatively low enantioselectivity and reactivity (especially when sulfonated BINAP is used as catalyst). If the best solvent (Methanol) is used, the aqueous phase (water of PEG) will be destroyed and the reaction will practically proceed homogeneously. So Davis' system shouldn't be a really practical method in asymmetric hydrogenation of dehydronaproxen.

5.1.3.4. Ion Exchanger Immobilized Asymmetric Catalyst

Chiral metal complex catalyst usually carries electronic charges, and hence can be attracted by ion exchangers. This special method was firstly developed by Selke *et al*..[142, 143, 144] The application of silica-based cation exchangers (SiO_2)-O-$C_6H_4SO_3H$ for immobilization of the cationic rhodium(I) chelate in methanol gives rise to heterogenized solvolyzed species carrying two hydroxy groups and showing enhanced

enantioselectivity in the hydrogenation of N-acetylamino-acrylic acid esters of up to 95% ee compared with 91% ee for the corresponding homogeneous

catalyst. The high activity of the heterogenized catalyst may be increased more than five-fold by preloading the exchanger with alkali or ammonium ions, thus approaching the level of homogeneous ones. The high leaching of rhodium may be minimized by using cation exchanger preloaded with aniline. And most importantly, the heterogenized catalyst was recycled for 20 runs with no loss of enantioselectivity. When the commercially available sulfonated polystyrene resin was adopted as cation exchanger instead of that based on silica gel, similar good results had been achieved.

4.1.3.5. Other Immobilization Methods

Vankelecom *et al* developed another new technique to immobilize chiral catalysts in membranes (chiral catalytic membranes) that can be regenerated and reused. Chiral [Rh(BINAP)(cymene)Cl] was occluded in an elastic type polydimethylsiloxane (PDMS) membrane. This process does not require covalent modification of the ligand. The membrane-supported chiral catalyst was effective in the asymmetric hydrogenation of methyl acetoacetate. Similarly, the absorption of N,N′-bis(3,5-di-tert-butylsalicylidene)chloro-1,2-cyclohexanediamine-manganese(Jac obsen catalyst) on PDMS membrane was effective in asymmetric epoxidation of olefins. However, the reactivity and enantioselectivity of the catalysts were lower than those of the corresponding homogeneous catalysts.

In addition, “heterogeneous modification” of homogeneous catalysts has used the supramolecular concepts of sol-gel entrapment, templates, and host-guest interactions.

5.1.4. Aims of this Study

To combine the advantages of various immobilization methods and to overcome their disadvantages, in this study, we aim at:

- Synthesis of cation and anion exchangers based on silica gel.
- Synthesis of water-soluble ligands including sulfonated BINAP and P-phos.
- Immobilization of water-soluble catalysts on ion exchangers and their application in asymmetric hydrogenation.

5.2. Asymmetric Hydrogenation of Dehydronaproxen Catalyzed by Ruthenium Complex of Sulfonated BINAP Immobilized by Anion Exchanger

5.2.1. Experimental

5.2.1.1. Synthesis of Anion Exchanger Based on Silica Gel

Anion exchanger based on silica gel can be commercially purchased or synthesized easily. Anion exchanger based on silica gel (**5-1**) was prepared by the procedure shown in **Scheme 5-5.** Silica gel (Meck 60, 60-200μm) and γ-aminopropyltriethoxysilane were purchased commercially. 10 g of silica gel (pre-dried in vacuum oven at 200 ^{o}C for 24 h) was placed into a 250 mL round bottom flask, 150 mL of dried and freshly distilled toluene was added, and then with stirring

4.42 g (20 mmol) of γ-aminopropyltriethoxysilane was added. The mixture was refluxed for 24 h. After the reaction, the resulting silica gel was filtered out with suction and washed with dried toluene for five times and then with acetone for 5 times. This γ-aminopropyl-modified silica gel was placed into a round bottom flask with100 mL of acetone, 14.2 g (100 mmol) of CH_3I and 13.8 g (100 mmol) of K_2CO_3, then, the mixture was refluxed for 24 h without stirring. The mixture was cooled down, filtered by suction, washed with acetone for 5 times and poured into 250 mL of de-ionized water. Then the produced anion exchanger was filtered, washed with de-ionized water and acetone and then dried *in vacuo* at 80 ^oC to afford 11.5 g of anion exchanger **5-1**.

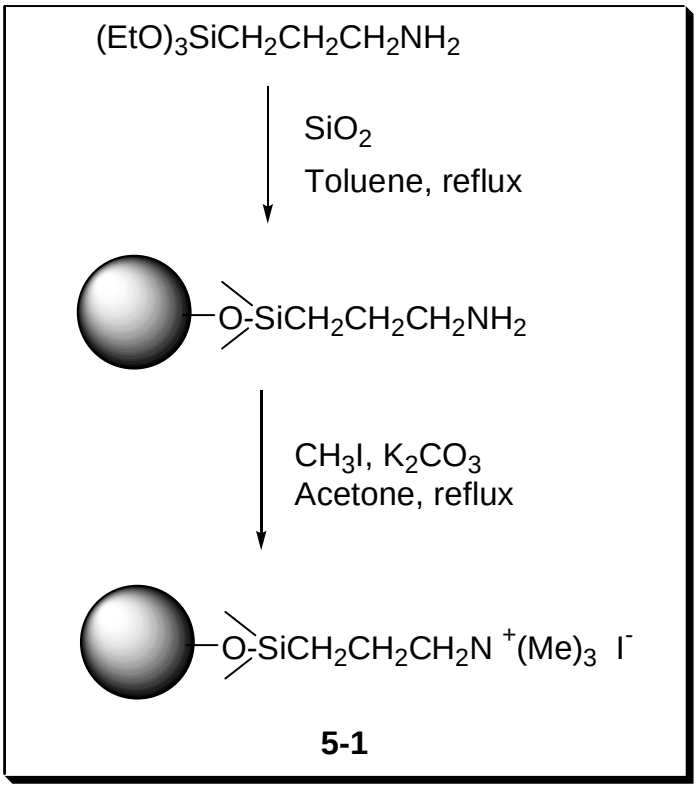

Scheme 5-5. Synthesis of Anion Exchanger (**5-1**)

5.2.1.2. Synthesis of Sulfonated BINAP Ruthenium Complex

BINAP was sulfonated according to Davis' method[145] (shown in **Scheme 5-6).** The sulfonation was accomplished by dissolving (*S*)-BINAP (0.25 g) in concentrated sulfuric acid (1 mL) with subsequent dropwise addition of 4 mL fuming sulfuric acid (40% wt% sulfuric trioxide in concentrated sulfuric acid) during one hour at 0 ^{o}C and the mixture was stirred for 3 days at 10 ^{o}C under nitrogen. The reaction was quenched by pouring the solution into 25 mL of ice-cooled water and the product neutralized by dropwise addition of aqueous sodium hydroxide (50 wt% NaOH) until a pH of 8 was reached. The volume of the solution was reduced to 6 mL *in vacuo* and methanol (25 mL) was added to precipitate any sodium sulfate present. Sulfonated (*S*)-BINAP (*S*)-**5-2** (0.35 g, 84% yield) was then recovered as a white powder by vacuum drying the filtered methanolic solution. The ^{31}P NMR spectra showed a single major resonance at δ -11.1 with a second small peak around δ -12.7. This indicated the product was not a completely pure compound. Because of the difference in π-stabilization energy, the phenyl rings in BINAP are relatively more reactive towards electrophilic aromatic substitute by sulfur trioxide as compare to the naphthyl rings. Thus, the major species obtained in sulfonation was assumed by Davis as the product (*S*)-**5-2** with only four phenyl rings in BINAP being sulfonated under this condition.

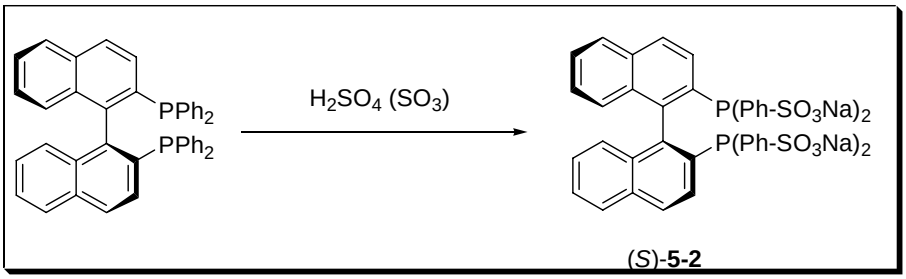

Scheme 5-6. Synthesis of Sulfonated BINAP (**5-2**)

Ruthenium complex of sulfonated BINAP was also synthesized by Davis' procedure[146, 147](shown in **Scheme 5-7**). $[Ru(benzene)Cl_2]_2$ (5 mg, 0.001 mmol) was treated with two equivalents of (*S*)-BINAP-4SO_3Na (20.6 mg, 0.002 mmol) in

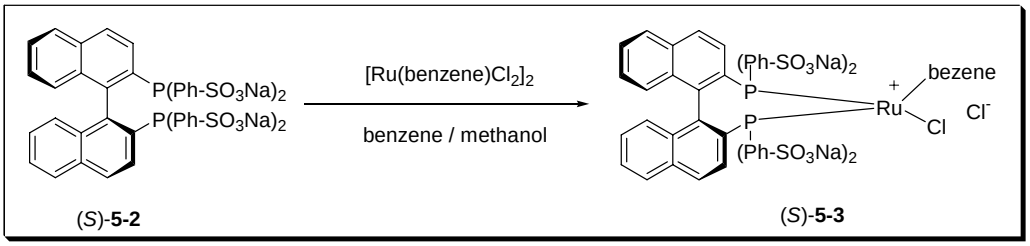

Scheme 5-7. Synthesis of catalyst (*S*)-**5-3**

4.5 mL of 1:8 benzene/methanol mixture at 55-60 ^oC for 1 h. The resulting clear, brown solution of {Ru[(*S*)-BINAP-4SO_3Na](benzene)Cl}Cl was vacuum dried at room temperature to give catalyst (*S*)-**5-3**. The solid was re-dissolved in 2.0 mL methanol as catalyst solution for the next step use.

5.2.1.3. Asymmetric Hydrogenation of Dehydronaproxen with Anion Exchanger Immobilized {Ru[(*S*)-BINAP-4SO_3Na](benzene)Cl}Cl

Since naproxen and many other chiral 2-arylpropionic acids are high-valued pharmaceutical products, there is always great economic incentive for the development of a practical process for the expensive catalyst immobilization and recycling. As we know anion exchanger can immobilize sulfonated type catalyst very

efficiently, so our main purpose was to test the activity and recylability of catalyst **5-3** when it was immobilized by anion exchanger **5-1**.

Asymmetric hydrogenations of 2-(6′-methoxy-2′-naphthyl)propenoic acid (dehydronaproxen) (**Scheme 5-8**) were conducted in a 50 mL glass tube inside a stainless autoclave. A typical procedure is as the follows: 2-(6′-methoxy-2′-naphthyl)propenoic acid (10 mg, 0.044 mmol), a solution of 5.0 x 10^{-3} M of (*S*)-**5-3** in methanol (88 μl, 4.4x10^{-4} mmol) and methanol (2 mL) were added to a glass tube and then placed into an 50 mL autoclave under a nitrogen atmosphere. Hydrogen was initially introduced into the autoclave at a pressure of 200 psi, the pressure was then reduced to 1 atm by carefully releasing the stop valve. This procedure was repeated for three times and the vessel was finally pressurized to 1000 psi. The reaction mixture was stirred at room temperature for certain time before releasing the H_2. After that, the autoclave was brought to drybox again. Under nitrogen atmosphere, anion exchanger **5-1** (100 mg) was added and stirred for half an hour to allow the immobilization complete. Then, the mixture was filtered and the immobilized catalyst **5-1**/(*S*)-**5-3** was used as catalyst for the next hydrogenation run. The configuration of the product was in S form. The conversion was determined by NMR analysis. The ee values were determined by HPLC analysis after converting the product to its corresponding methyl ester. HPLC condition: Daicel Chiracel OD column, 25 cm x 4.6 mm, 25 ^{o}C; eluent 1:99 2-propanol-hexane; flow rate, 1 mL/min; detection, 254 nm light.

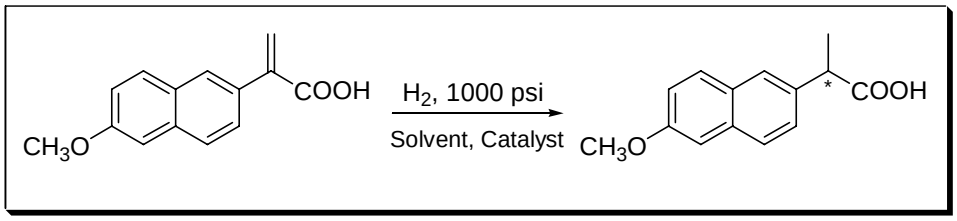

Scheme 5-8

5.2.2. Results and Discussion:

Table 5-4. The effects of water on the hydrogenation of dehydronaproxen.

Entry	Solvent Ratio CH_3OH / H_2O		Catalyst	Time (h)	Conv. %	ee %
1	1	0	(*S*)-**5-3**: homo	6	100	84.7
2	9	1	(*S*)-**5-3**: homo	20	100	84.7
3	3	1	(*S*)-**5-3**: homo	20	100	78.0
4	1	1	(*S*)-**5-3**: homo	20	Poor	
5	1	0	**5-1**/(*S*)-**5-3:** hetero	24	56	
6	9	1	**5-1**/(*S*)-**5-3**: hetero	24	96	85.1
7	3	1	**5-1**/(*S*)-**5-3**: hetero	24	100	78.9
8	1	1	**5-1**/(*S*)-**5-3**: hetero	24	100	74.9
9*	0	1	**5-1**/(*S*)-**5-3**: hetero	24	100	33

The experiment of entry 9 was carried out at 90 °C. The molar ratio of substrate / catalyst / ion exchanger was 100:1:100. The conversion was determined by NMR and the ee values were determined by HPLC. The configuration of the product was in S form.

Table 5-4 exhibits the results of the experiments. The catalyst is a strongly polar and water soluble compound. When treated with the anion exchanger, it was strongly absorbed by the exchanger and tightly attached onto the surface of the ion exchanger. So, ^{31}P NMR spectra of the solution indicated the disappearance of phosphine after immobilization. This means the immobilization process was very efficient. However, the catalytic activity was seriously sacrificed. In order to recover the catalytic activity of the immobilized catalyst, we had to add water to release the catalyst relatively. And hence our experiments were firstly designed to test the effects of water on the catalytic activity and enantioselectivity of the homogeneous and heterogeneous catalysts.

As shown in **Table 5-4**, with the addition of water, the ee values decreased steadily for both homogeneous and heterogeneous catalysts. But for heterogeneous catalysts, the addition of water improved its catalytic activity (Entry 5, 6, 7). This was because the tightly immobilized catalyst was freed somewhat by water. However, large excess of water decreased the enantioselectivity for both homogeneous and heterogeneous catalyst in the same way.

Another interesting result was that with large water-to-methanol ratio (for example 1:1), heterogeneous catalyst was more active than the homogeneous catalyst (Entry 4 and Entry 8). This result can be explained by the fact that the ion exchanger can improve the solubility of the substrate in the solvent. In a solvent of 1:1 water and methanol mixture, the substrate wasn't able to dissolve and hence the conversion of the reaction was very low. However, with the addition of ion exchanger, the substrate

was attracted to the large surface of the silica gel-based ion exchanger along with the catalyst, and the catalytic reaction took place on the surface of the ion exchanger. So, under this condition a special reaction mechanism might occur, i.e., the giant surface of the silica gel-based ion exchanger rather than the solution was the reaction platform, and hence the environment on the surface of the ion exchanger might affect the reaction.

Entry 9 shows that at higher temperature, the reaction was able to proceed smoothly in pure water with the addition of ion exchanger. However, the enantioselectivity decreased significantly.

Though the immobilized catalyst could be recycled for several times with 9:1 methanol and water mixture as solvent, the enantioselectivity was just fair. So although this method is a good way for sulfonated catalyst immobilization and recycling, it is not practical as the catalytic activity is sacrificed too seriously.

5.3. Ruthenium Complex of P-Phos Recycled by Cation Exchanger for Asymmetric Hydrogenation of β-ketoesters

5.3.1. Experimental

5.3.1.1. Synthesis of Cation Exchanger Based on Silica Gel

Cation exchanger based on silica gel (**5-4**) was synthesized according to Capka's method.[148] The preparation procedure is shown in **Scheme 5-9**. Silica gel (Meck 60, 60-200 μm) and 3-phenoxypropyltrichlorosilane were purchased commercially. 10g

of silica gel (pre-dried in vacuum oven at 200 ^{o}C for 24 h) was placed into a 250 mL round bottom flask, 150 mL of dried and freshly distilled toluene was added, and then with stirring 5.4 g (20 mmol) of 3-phenoxypropyltrichlorosilane was added. The mixture was refluxed for 24 h. After the reaction, the mixture was filtered with suction and washed with dried toluene for five times and then with acetone for 5 times. The resulting silica gel was then placed into a round bottom flask and 20 mL of concentrated sulfuric acid (98%) was added. Then the mixture was kept at room temperature for 7 days. And finally, the mixture was filtered with suction and washed with deionized water for 10 times. The resulting cation exchanger (in acid form) was neutralized with 0.1 N NaOH aqueous solution, washed 10 times with de-ionized water and 5 times with methanol to afford the target cation exchanger (**5-4**). The capacity of **5-4** was estimated by the following titration procedure: 500 mg of the exchanger (in acid form) was suspended in 20 mL of de-ionized water, an excess of 0.1 N NaOH aqueous solution was added, after 10 minutes it was titrated with 0.1 N HCl solution with bromocesol purple as indicator. The capacity of **5-4** was determined to be 1.57 mmol/g.

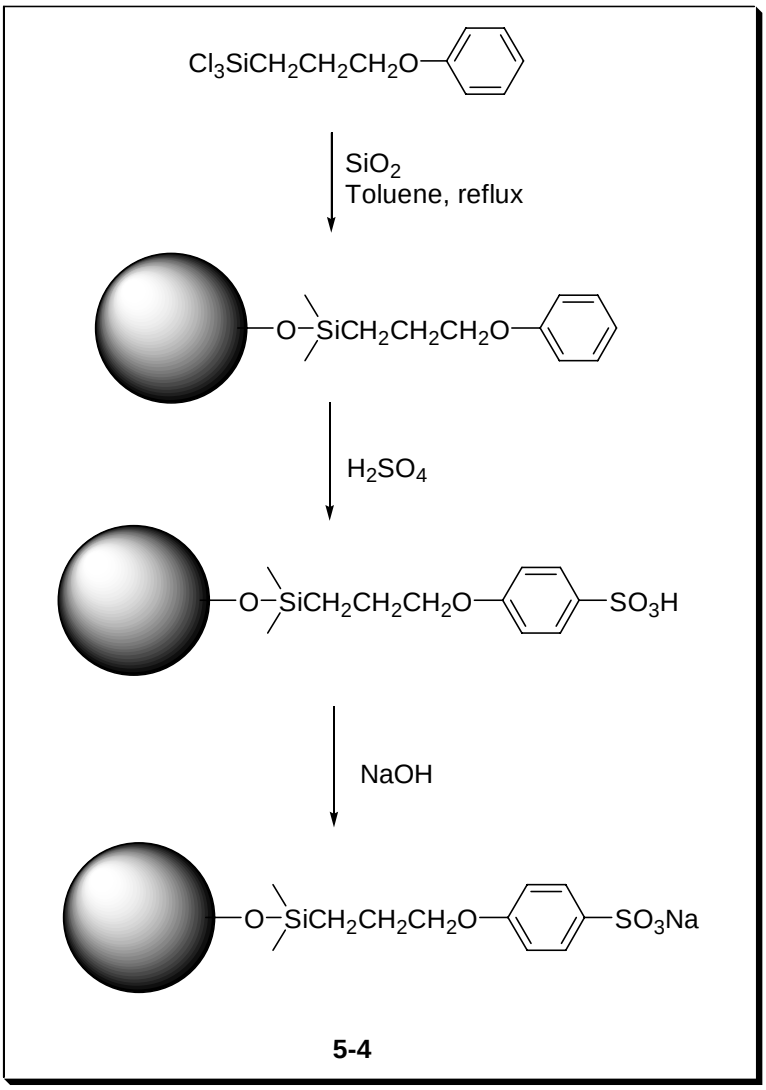

Scheme 5-9. Synthesis of cation exchanger **5-4**

5.3.1.2. Synthesis of Ruthenium Complexes of (*S*)-P-Phos and (*S*)-BINAP

Ruthenium complexes of (*S*)-P-Phos and (*S*)-BINAP were also synthesized by Noyori's method[112] (**Scheme 5-10**). $[Ru(benzene)Cl_2]_2$ (5 mg, 0.001 mmol) was treated with two equivalents of (*S*)-P-Phos or (*S*)-BINAP in 4.5 mL of benzene/methanol solvent mixture at 55-60 ^oC for 1 h. The resulting clear, brown solution of {Ru[(*S*)-P-Phos](benzene)Cl}Cl or {Ru[(*S*)-BINAP](benzene)Cl}Cl was

vacuum dried at room temperature to give catalyst (*S*)-**5-5** or (*S*)-**5-6**. The solid was re-dissolved in 2.0 mL methanol as catalyst solution for the next step.

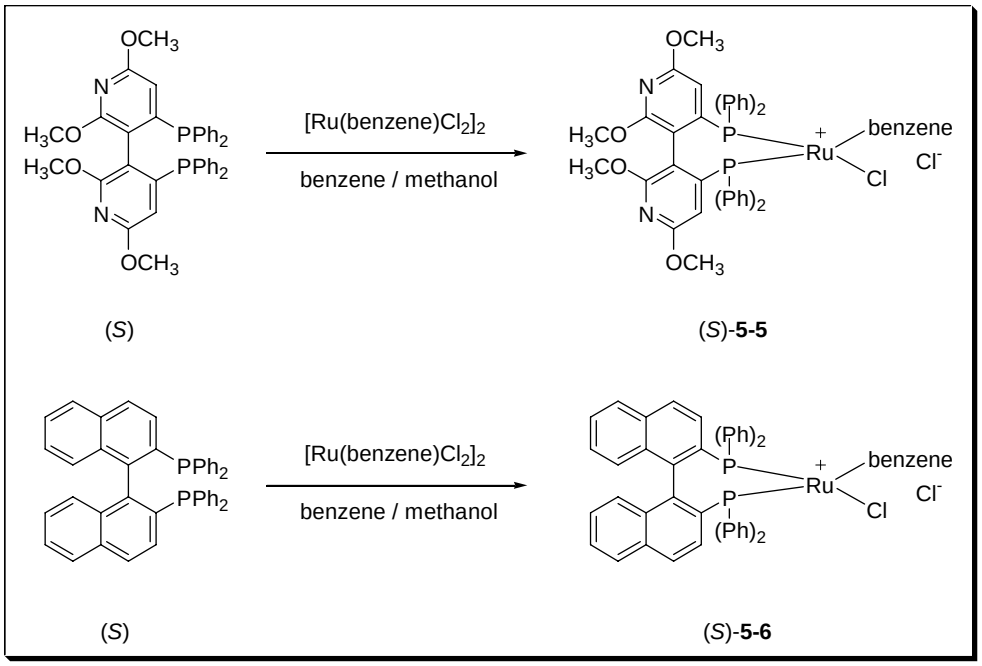

Scheme 5-10. Synthesis of catalyst (*S*)-**5-5** and (*S*)-**5-6**

5.3.1.3. Asymmetric Hydrogenation of β-ketoesters Catalyzed by Ruthenium Complexes of (*S*)-P-Phos and (*S*)-BINAP and Catalyst Recycling.

Nitrogen containing ligands such as P-Phos can combine with protons and carry positive electric charges, and hence can be attracted by cation exchanger to realize immobilization and separation more efficiently. The ruthenium complexes of P-Phos and BINAP were excellent catalysts for asymmetric hydrogenation of β-ketoesters (**Scheme 5-11**). After the reaction, the catalysts could be separated easily by a column packed with silica-gel based cation exchanger (**5-4**) and used again for the next recycling run of the reaction with a slight loss of enantioselectivity and activity.

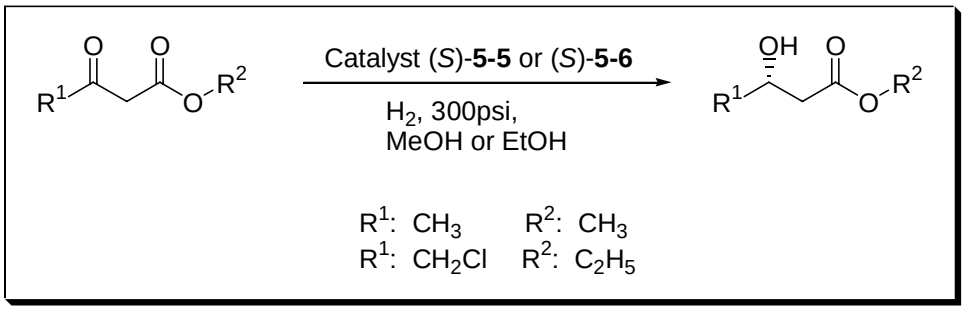

Scheme 5-11. Asymmetric hydrogenation of β-ketoesters

The ratio of substrate to catalyst is 200:1. The substrate (0.5 mmol) was placed in an autoclave with 2 mL of solvent, the catalyst solution was added. The autoclave was charged with hydrogen (usually 300 psi), then the reaction was carried out at appropriate temperature. After the reaction, the solvent (methanol or ethanol) was evaporated *in vacuo*, and 2 mL of dichloromethane was added, then the solution was passed through a column of 200mg of the ion exchanger (**5-4**) and washed by additional 3 mL of dichloromethane. The catalyst was attracted by the ion exchanger, whereas, the product was eluated out. In the end, 2 mL of methanol or ethanol was added as eluant to release and wash out the catalyst, the substrate was added to the subsequent solution, and then placed into an autoclave for the next recycling reaction run. The conversion was determined by NMR. The ee values determined by chiral GC analysis with a 25 m x 0.25 mm Chrompack Chirasil-DEX CB column after converting to the corresponding acetyl derivatives.

5.3.2. Results and discussion:

The results of asymmetric hydrogenation of β-ketoesters and catalyst recycling are outlined in **Table 5-5, Figure 5-5** and **Figure 5-6**.

Table 5-5. The results of asymmetric hydrogenation of β-ketoesters catalyzed by ruthenium complexes of (*S*)-P-Phos and (*S*)-BINAP and catalyst recycling.

Catalyst	Substrate		Solvent	Tem.	Time	ee % (conv. %)			
	R^1	R^2		°C	(h)	R0	R1	R2	R3
(*S*)-**5-5**	CH_3	CH_3	CH_3OH	60	5	99.3	96.2	95.6	94.2 (98)
(*S*)-**5-6**	CH_3	CH_3	CH_3OH	60	5	98.3	87.9	86.6	86.1 (82)
(*S*)-**5-5**	$ClCH_2$	C_2H_5	C_2H_5OH	70	10	96.5	96.0	94.8	94.3 (100)
(*S*)-**5-6**	$ClCH_2$	C_2H_5	C_2H_5OH	70	10	95.8	93.9	93.0	93.6 (87)

R0, R1, R2 and R3 were the initial and the subsequent recycling reaction runs.

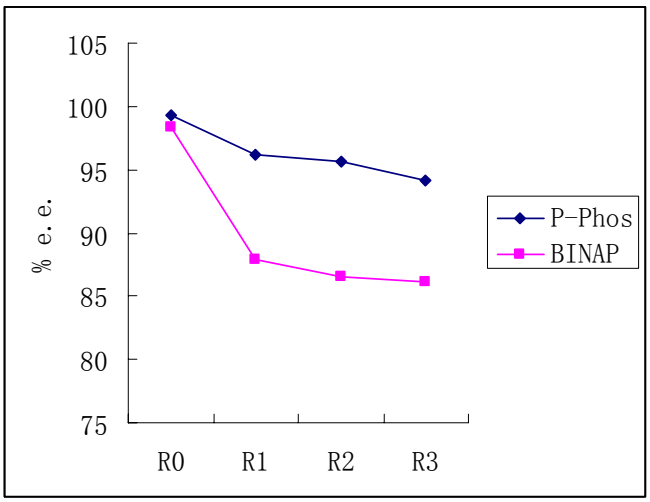

Figure 5-5. Catalyst recycling results for substrate methyl acetoacetate.

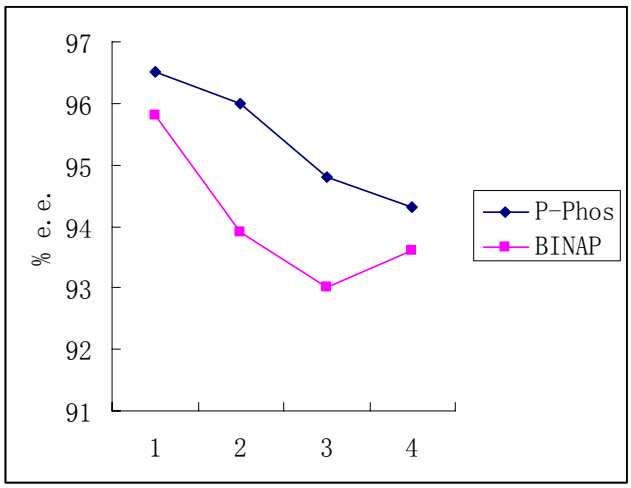

Figure 5-6. Catalyst recycling results for substrate ethyl chloroacetoacetate.

To develop a new asymmetric catalyst recycling method, our proprietary bipyridyl C_2-chiral diphosphine ligand P-Phos was employed and silica gel based ion exchanger was synthesized. The ruthenium complex of (*S*)-P-Phos was applied to the asymmetric hydrogenation of β-ketoesters. The enantioselectivity was excellent. In the hydrogenation of methyl acetoacetate, up to 99% ee was obtained in the initial reaction run. After the reaction, the catalyst was separated by a column packed with silica gel based cation exchanger. Then it was eluated by polar solvent (methanol or ethanol) and used again in the subsequent recycling runs of the reaction. The results show that the catalyst was able to be recycled for several times by this method, but the enantioselectivity and activity decreased slightly (as indicated in **Table 5-5**). This method shows industrialization potential especially to the synthesis of the precursor of L-carnitine from the substrate ethyl chloroacetoacetate.

The ruthenium complex of BINAP could also be recycled in this way, however, the enantioselectivity and activity dropped more rapidly than that of P-Phos in the recycling runs of the same reaction (as shown in **Figure 5-5, Figure 5-6**).

The results compared with other relevant catalyst recycling methods:

To the best of our knowledge, the successful examples of immobilization and recycling of chiral complex catalysts by ion exchangers were reported only by Selke *et al*..[142, 143, 144] They developed the chiral diphosphite ligands Ph-β-glup-OH (as shown in **Figure 5-7**), whose rhodium complex [Rh(COD)Ph-β-glup-OH]BF_4 was a very efficient asymmetric catalyst for hydrogenation of dehydroaminoacid derivatives. When the complex catalyst was treated with silica gel-based cation exchanger (SiO_2)-O-$C_6H_4SO_3H$ in methanol, it would be immobilized by the ion exchanger. In the hydrogenation of N-acetylaminoacrylic acid esters, the heterogenized catalyst exhibited high enantioselectivity (up to 95% ee) and almost the same activity as the corresponding homogeneous catalyst. The catalyst was able to be recycled simply by filtration and reusing for more than 20 times with almost no loss of enantioselectivity, but the catalytic activity steadily decreased because of catalyst leaching problem.

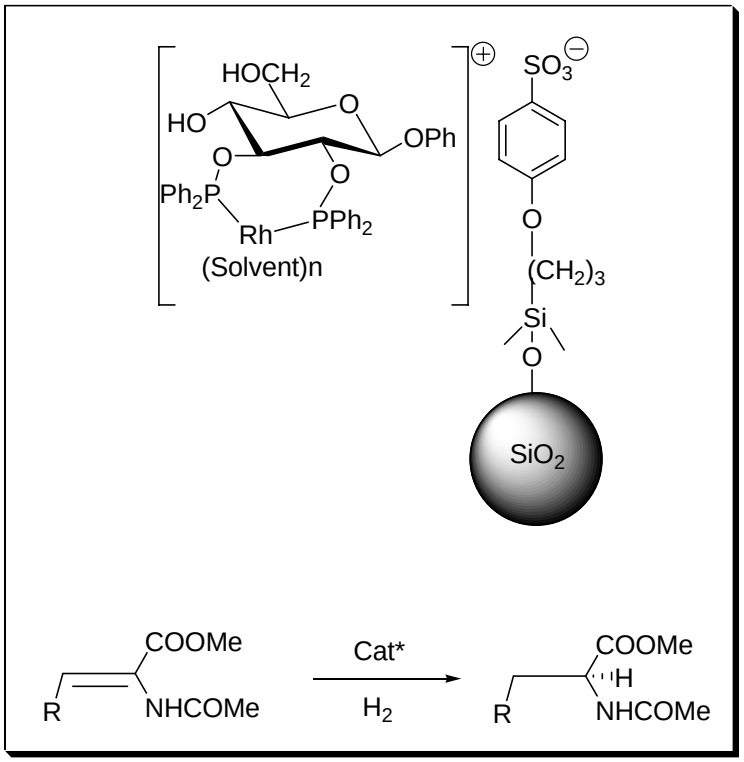

Figure 5-7

This is one of the best results so far in the research field of immobilization and recycling of asymmetric catalyst. And the reason for such an excellent result is that the molecules of the catalyst are attracted to the support electronically rather than connected to the support by covalent bonds, and hence they have comparatively large freedom and flexibility for reactivity and stereoselectivity. The disadvantage of this system is that catalyst leaching and decreasing in catalytic ability is considerable. Although this method for chiral complex catalyst immobilization and recycling achieved great success in the asymmetric hydrogenation of dehydroaminoacid derivatives, so far the authors haven't reported its utility in the ruthenium-catalyzed asymmetric hydrogenation of other common substrates such as dehydronaproxen and β-ketoesters. Usually the catalytic activity of ruthenium complexes of chiral

diphosphine ligands in asymmetric hydrogenation is comparatively lower than that of the corresponding rhodium complexes. When ruthenium complexes are heterogenized by ion exchangers, their catalytic activity may be sacrificed so much that this immobilization and recycling method is not appropriate for ruthenium complexes. According to our results, as long as the ruthenium complex of P-Phos was immobilized by silica gel-based cation exchanger (**5-4**), low catalytic activity would be obtained. So, we had to separate the ruthenium complex of P-Phos first by employing the ion exchanger, and then used it again in homogeneous way in subsequent recycling runs. This method should alleviate the leaching problem in Selke's case. However, as the catalyst deterioration can not be avoided completely because of some harmful process such as oxidation, decomplexation and so on, the catalytic activity and enantioselectivity of the complex decreased steadily as demonstrated in **Figure 5-5** and **Figure 5-6**.

Recently, Lemaire *et al.*[149, 150, 151] reported the best results of immobilization and recycling of chiral diphosphine ruthenium complex catalysts in asymmetric hydrogenation of β-ketoesters. Based on their proprietary *diam*-BINAP monomer, a series of BINAP polymeric derivatives (polyamide, polyureas, PEG-derivatives, *etc.* as shown in **Figure 5-8**) had been synthesized and employed in the ruthenium-catalyzed asymmetric hydrogenation of methyl acetoacetate. The catalysts were efficient, usually gave 98%-99% ee values in this reaction. And by precipitation and filtration, the catalysts were used for several times without loss of neither

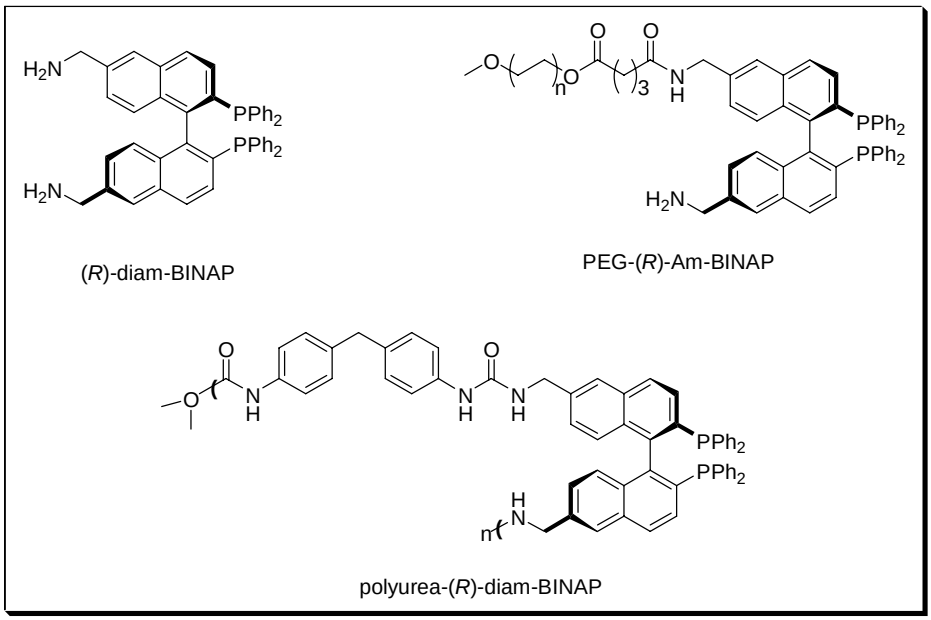

Figure 5-8

enantioselectivity nor activity. These results are better than ours. However, the synthesis of polymeric BINAP derivatives is not easy and hence the corresponding catalysts are much more expensive. So, our method, which just employs much cheaper ion exchanger to realize catalyst immobilization and recycling, should be a more **cost-effective** way especially for industrialization.

5.4. Summary

The heterogenizaton of enantioselective but rather expensive homogeneous catalysts by the use of insoluble supports as a means to make economical industrial application is a challenge. The advantage of heterogenized asymmetric catalysts is the convenience of separation and recycling of catalysts, whereas the main disadvantage is the lower catalytic activity and enantioselectivity normally observed. In our efforts addressed to this challenge, we developed a method which employed silica gel-based

anion and cation exchangers to immobilize catalysts in asymmetric hydrogenation. The main results demonstrated that:

- In the asymmetric hydrogenation of dehydronaproxen catalyzed by ruthenium complex of sulfonated BINAP (*S*)-**5-3**, the anion exchanger (**5-1**) was able to immobilize the catalyst very efficiently. However, as the catalyst was attracted too tightly onto the surface of the anion exchanger, the accessibility or availability of the catalytic sites was limited a lot, and hence the catalytic activity was sacrificed seriously. By adding some water, the catalytic activity recovered somewhat, but the enantioselectivity decreased with the addition of water.
- In asymmetric hydrogenation of β-ketoesters catalyzed by ruthenium complexes of P-Phos and BINAP, the cation exchanger (**5-4**) was able to separate the catalysts (*S*)-**5-5** and (*S*)-**5-6** efficiently for recycling. Both catalysts were able to be reused by this method for several times. With P-Phos, just a slight loss of enantioselectivity and activity was observed in the subsequent recycling runs. But with BINAP, the enantioselectivity and activity dropped more rapidly. These results demonstrate that the special feature of P-Phos (nitrogen-containing) favors the stability and recyclability of its ruthenium complex as chiral catalyst in asymmetric hydrogenation.

References

1. a) Ojima, I. Ed. *Catalytic Asymmetric Synthesis*; Wiley-VCH: New York, **2000**.
   b) Brown, J. M. in *Comprehensive Asymmetric Catalysis* (Eds.: E. N. Jacobsen, A. Pfaltz, H. Yamamoto), Springer, Berlin, **1999**, p. 121.
2. a) Noyori, R. *Asymmetric Catalysis in Organic Synthesis*; Wiley & Sons: New York, **1994**.
   b) Ohkuma, T.; Kitamura, M.; Noyori, R. *Catalytic Asymmetric Synthesis*, Wiley-VCH, Weinheim, **2000.**
3. Stephenson, G. R., Ed. *Advanced Asymmetric Synthesis*; Chapman & Hall: London, **1996**.
4. Trost, B. M.; Vranken, D. L. V. *Chem. Rev*. **1996**, 96, 395-422.
5. Jacobsen, E. N.; Zhang, W.; Muci, A. R.; Ecker, J. R. *J. Am. Chem. Soc.* **1991**, *113*, 7063.
6. Kolb, H. C.; VanNieuwenhze, M. S.; Sharpless, K. B. *Chem. Rev.* **1994**, *94*, 2483.
7. Noyori, R. In *Asymmetric Catalysis in Organic Synthesis*; John Wiley & Sons, Inc.: New York, **1994**; Chapter 2.
8. Consiglio, G.; Waymouth, R. M. *Chem. Rev.* **1989**, *89*, 257.
9. Fiaud, J. C. In *Metal-Promoted Selectivity in Organic Synthesis*; Graziani, M., Hubert, A. J., Noels, A. F., Eds.; Kluwer Academic Publishers: Dordrecht, **1991**.
10. Heumann, A.; Reglier, M. *Tetrahedron* **1995**, *51*, 975.
11. Hayashi, T. In *Catalytic Asymmetric Synthesis*; Ojima, I., Ed.; VCH Publishers, Inc.: New York, **1993**.
12. Reiser, O. *Angew. Chem., Int. Ed. Engl.* **1993**, *32*, 547.
13. Trost, B. M. In *Advances in Natural Product Chemistry*; Atta-Ur-Rahman, Ed.; Harwood Academic Publishers: Chur, **1992**; pp 19-34.
14. Trost, B. M. *Tetrahedron* **1977**, *33*, 2615.
15. Trost, B. M. *Acc. Chem. Res.* **1980**, *13*, 385.
16. Tsuji, J. *Organic Synthesis with Palladium Compounds*; Springer-Verlag: New York, **1980**.

17. Trost, B. M. In *Stereochemistry of Organic and Bioorganic Transformations*; Bartmann, W., Sharpless, K. B., Eds.; VCH: New York, **1986**.
18. Trost, B. M. *Pure Appl. Chem.* **1981**, *53*, 2357.
19. Trost, B. M.; Verhoeven, T. R. In *Comprehensive Organometallic Chemistry*; Wilkinson, G., Ed.; Pergamon Press: Oxford, **1982**; Vol. 8, Chapter 57.
20. Tsuji, J. *Pure Appl. Chem.* **1982**, *54*, 197.
21. Tsuji, J. *Tetrahedron* **1986**, *42*, 4361.
22. Trost, B. M. *Chemtracts: Org. Chem.* **1988**, *1*, 415.
23. Trost, B. M. *Angew. Chem., Int. Ed. Engl.* **1989**, *28*, 1173.
24. Trost, B. M. *ACS Adv. Chem. Ser*. **1992**, *230*, 463.
25. Godleski, S. A. In *Comprehensive Organic Synthesis*; Trost, B. M., Fleming, I., Semmelhack, M. F., Eds.; Pergamon Press: Oxford, 1991; Vol. 4, Chapter 3.3.
26. Trost, B. M.; Strege, P. E. *J. Am. Chem. Soc.* **1977**, *99*, 1649.
27. Trost, B. M.; *J. Am. Chem. Soc.J. Am. Chem. Soc*. **1980**, 102, 4730.
28. Yamamoto. K.; Deguchi, R.; Ogimura, Y.; Tsuji, J. *Chemistry Lett*. **1982**, 1657
29. Hayashi, T.; Yamamoto, A.; Hagihara. T. *J. Org. Chem*. **1986**, 51,723.
30. Granberg, K. L.; Backvall, J. E. *J. Am. Chem. Soc.* **1992**, 114,6858.
31. Trost, B. M.; Strege, P. E. *J. Am. Chem. Soc.* **1975**, 972534.
32. Trost, B. M.; Verhoeven, T. R. J. *Org. Chem*. **1971**, 41, 3215.
33. Hayashi, T.; Hagihara, T.; Konishi, M.; Kumada, M. *J. Am. Chem. Soc.* **1983**,105, 7767.
34. Templ. J. S.; Schwartz, J. *J. Am. Chem. Soc.* **1980**, 102, 7318.
35. Matsushida, H.; Negishi, E. *J. Chem. Soc., Chem. Commun*. **1982**, 160.
36. Temple, J. S.; *et al*. *J. Am. Chem. Soc.* **1982**, 104, 1310.
37. Labadie, J. W.; Stille, J. K. *J. Am. Chem. Soc.* **1983**, 105, 6129.
38. Goliaszewshi, A.; Schwartz, J. *J. Am. Chem. Soc.* **1984**, 106, 5028.
39. Keinan, E.; Roth, Z. J. *Org. Chem* **1983**, 48, 1769.
40. Fiaud, J.-C.; Legros, J, -Y. J. *Org. Chem.* **1987**, 52, 1907.
41. Hayashi, T. *Pure Appl. Chem*. **1988**, 60, 7.
42. Sawamura, M.; Ito, Y. *Chem. Rev.* **1992**, 92, 857.

43. Pfaltz, A. *Acc. Chem. Res*. **1993**, 26, 339.

44. Trost, M. B. *Acc. Chem. Res*. **1989**, 89, 1581.

45. Trost, B. M.; Murphy, D. J. *Organometallics* **1985**, *4*, 1143.

46. Trost, B. M.; Singleton, D. Unpublished work.

47. Brown, J. M.; Hulmes, D. I.; Guiry, P. J. *Tetrahedron* **1994**, *50*, 4493.

48. Bovens, M.; Togni, A.; Venanzi, L. M. *J. Organomet. Chem.* **1993**, *451*, C28.

49. Wimmer, P.; Widhalm, M. *Tetrahedron: Asymmetry* **1995**, *6*, 657.

50. Togni, A. *Tetrahedron: Asymmetry* **1991**, *2*, 683.

51. Kang, J.; Cho, W. O.; Cho, H. G. *Tetrahedron: Asymmetry* **1994**, *5*, 1347.

52. Yamaguchi, M.; Shima, T.; Yamagishi, T.; Hida, M. *Tetrahedron: Asymmetry* **1991**, *2*, 663.

53. Frost, C.; Williams, M. J. *Tetrahedron Lett.* **1993**, *34*, 2015.

54. Yamazaki, A.; Morimoto, T.; Achiwa, K. *Tetrahedron: Asymmetry* **1993**, *4*, 2287.

55. Hayashi, T.; Yamamoto, A.; Hagihara, T.; Ito, Y. *Tetrahedron Lett.* **1986**, *27*, 191.

56. Hayashi, T. *Pure Appl. Chem.* **1988**, *60*, 7.

57. Yamaguchi, M.; Shima, T.; Yamagishi, T.; Hida, M. *Tetrahedron Lett.* **1990**, *31*, 5049.

58. Cesarotti, E.; Grassi, M.; Prati, L.; Demartin, F. *J. Chem. Soc., Dalton Trans.* **1991**, 2073.

59. Petit, M.; Montreaux, A.; Petit, F.; Pfeiffer, G. *Nouv. J. Chem.* **1983**, *7*, 593.

60. Andersson, P. G.; Harden, A.; Tanner, D.; Norby, P. O. *Chem. Eur. J.* **1995**, *1*, 12.

61. von Matt, P.; Pfaltz, A. *Angew. Chem., Int. Ed. Engl.* **1993**, *32*, 566.

62. Dawson, G. J.; Frost, C. G.; Williams, J. M. J.; Coate, S. W. *Tetrahedron Lett.* **1993**, *34*, 3149.

63. Sprinz, J.; Kiefer, M.; Helmchen, G.; Reggelin, M.; Huttner, G.; Walter, O.; Zsolnai, L. *Tetrahedron Lett.* **1994**, *35*, 1523.

64. Pfaltz, A. *Acc. Chem. Res.* **1993**, *26*, 339.

65. Allen, J. V.; Coote, S. J.; Dawson, G. J.; Frost, C. G.; Martin, C. J.; Williams, J.

66. Allen, J. V.; Bower, J. F.; Williams, J. M. J. *Tetrahedron: Asymmetry* **1994**, *5*, 1895.

67. Kubota, H.; Koga, K. *Tetrahedron Lett.* **1994**, *35*, 6689.

68. Leutenegger, U.; Umbricht, G.; Fahrni, C.; von Matt, P.; Pfaltz, A. *Tetrahedron* **1992**, *48*, 2143.

69. Gamez, P.; Dunjic, B.; Fache, F.; Lemaire, M. *J. Chem. Soc., Chem. Commun.* **1994**, 1417.

70. Abbenhius, H. C. L.; Burckhardt, U.; Gramlich, V.; Kollner, C.; Pregosin, P. S.; Salzman, R.; Togni, A. *Organometallics* **1995**, *14*, 759.

71. Pregosin, P. S.; Salzmann, R.; Togni, A. *Organometallics* **1995**, *14*, 842.

72. Brenchley, G.; Merifield, E.; Wills, M.; Fedouloff, M. *Tetrahedron Lett.* **1994**, *35*, 2791.

73. Kubota, H.; Nakajima, M.; Koga, K. *Tetrahedron Lett.* **1993**, *34*, 8135.

74. Auburn, P. R.; Mackenzie, P. B.; Bosnich, B. *J. Am. Chem. Soc.* **1985**, *107*, 2033.

75. Yamazaki, A.; Morimoto, T.; Achiwa, K. *Tetrahedron: Asymmetry* **1993**, *4*, 2287.

76. Hayashi, T.; Iwamura, H.; Naito, M.; Matsumoto, Y.; Uozumi, Y.; Miki, M.; Yanagi, K. *J. Am. Chem. Soc.* **1994**, *116*, 775.

77. Knowles, W. S. *Acc. Chem. Res.* **1983**, 16, 106.

78. Kagan, H. B.; Dang, T. P. *J. Am. Chem. Soc.* **1972**, 94, 6429.

79. Fryzuk, M. D.; Bosnich, B. *J. Am. Chem. Soc.* **1977**, 99, 6262.

80. Brunner, H.; Pieronczyk, W.; Schönhammer, B.; Streng, K,; Bernal, I,; Korp, J. *Chem. Ber.* **1981**, 103, 2280.

81. Achiwa, K. *J. Am. Chem. Soc.* **1976**, 98, 8265.

82. Nagel, U.; Kinzel, E.; Andrade, J.; Prescher, G. *Chem. Ber.* **1986**, 119, 3326.

83. Miyashita, A.; Yasuda, A.; Takaya, H.; Toriumi, K.; Ito, T.; Noyori, R. *J. Am. Chem. Soc.* **1980**, 102, 7932.

84. Burk, M. J.; Lee, J. R.; Martinez, J. P. *J. Am. Chem. Soc.* **1994**, 116, 10847.

85. a) Zhu, G.; Cao, P.; Jiang, Q.; Zhang, X. *J. Am. Chem. Soc.* **1997**, 119, 1799;
b) Zhu, G.; Zhang, X. *J. Org. Chem.* **1998**, 63, 9590.

86. Chan, A. S. C.; Hu, W.; Pai, C. C.; Lau, C. P. *J. Am. Chem. Soc.* **1997**, 119, 9570.

87. Jiang, Q.; Jiang, Y.; Xiao, D.; Cao, P.; Zhang, X. *Angew. Chem.* **1998**, 110, 1203.

88. a) Imamoto, T.; Watanabe, J.; Yoshiyuki, W.; Masuda, H.; Yamada, H.; Tsuruta, H.; Matsukawa, S.; Yamaguchi, K. *J. Am. Chem. Soc.* **1998**, 120, 1635;

b) Gridnev, I. D.; Yasutake, M.; Higashi, N.; Imamoto, T. *J. Am. Chem. Soc.* **2001**, 123, 5268;

c) Gridnev, I. D.; Yamanoi, Y.; Higashi, N.; Tsuruta, H.; Yasutake, M.; Imamoto, T. *Adv. Synth. Catal.* **2001**, 343, 118.

89. Yamanoi, Y.; Imamoto, T. *J. Org. Chem.* **1999**, 64,2988.

90. Xiao, D.; Zhang, Z,; Zhang, X. *Org. Lett.* **1999**, 1, 1679.

91. Pye, P. J. *et al*. *J. Am. Chem. Soc.* **1997**, 119, 6207.

92. Tang, W.; Zhang, X. *Angew. Chem. Int. Ed.* **2002**, 41, 9.

93. Chan, A. S. C.; Pai, C.-C. US Patent 5,886,182, **1999**.

94. Pai, C. C.; Lin, C. W.; Lin, C. C.; Chen, C. C.; Chan, A. S. C.; Wong, W. T. *J. Am. Chem. Soc.* **2000**, 122, 11513.

95. Wu, J.; Chen, H; Zhou, Z. Y.; Yeung, C. H.; Chan, A. S. C. *Synlett* **2001**, 1050.

96. Wu, J.; Chen, H.; Kwok, W. H.; Guo, R. W.; Zhou, Z. Y.; Yeung, C, H.; Chan, A. S. C. *J. Org. Chem.* **2002**, 67, 7908-7910.

97. Kumobayashi, H. *et al. Synlett* **2001**, SI, 1055-1064.

98. Takaya, H.; Mashima, K.; Koyano, K.; Yagi, M.; Kumobayashi, H.; Noyori, R. *J. Org. Chem.* **1986**, 51, 629.

99. Cai, D. *et al*. *J. Org. Chem.* **1994**, 59, 7180.

100. Ager, D. J. *et al*. Chem. Commun. **1997**, 2359.

101. Zhang, X; Sayo, N. United States Patent 5,693,868, 1997; 5,922,918, **1999**.

102. a) Guzzo P. R.; Miller, M. J. *J. Org. Chem.* 1994, 59, 4862.

b) Pommier, A.; Pons, J. M. *Synthesis* **1994**, 1294.

c) Case-green, S. C.; Davies, S. G.; Hedgecock C. J. R. *Synlett* **1991**, 781.

d) Taber, D. F.; Silverberg L. J.; Robinson, E. D. *J. Am. Soc. Chem.* **1991**, 113, 6639

103. Bunett, J. F. *Acc. Chem. Res*. **1972**, 5, 139.

104. a) Mallet, M.; Queguiner, G. *Tetrahedron* **1982**, 38, 3035.

b) Mallet, M.; Queguiner, G. *Tetrahedron* **1985**, 41, 3433.

c) Mallet, M.; Queguiner, G. *Tetrahedron* **1986**, 42, 4253.

d) Mallet, M.; Branger, G.; Marsais, F.; Queguiner, G. *J. Organomet. Chem.* **1990**, 382, 319.

105. Wu, J.; Guo, R. W.; Zhou, Z. Y.; Chen, H.; Yeung, C. H. *Acta Cryt.* **2003**, E59, o493-o494.

106. Deng, W. P.; You, S. L.; Hou, X. L.; Dai, L. X.; Yu, Y. H.; Xia, W.; Sun, J. *J. Am. Chem. Soc*. **2001**, 123, 6508-6519.

107. Longmire, J. M.; Zhu, G. X.; Zhang, X. M. *Tetrahedron Letters* **1997**, 38, 375-378.

108. Zhu, G. X.; Terry, M. T.; Zhang, X. M.; *Tetrahedron Letters* **1996**, 37, 4475-4478.

109. Nettekoven, U.; Widhalm, M.; Kamer, P. C. J.; van Leeuwen, P. *Tetrahedron: Asymmetry* **1997**, 8, 3185-3188.

110. Kang, J.; Lee, J. H.; Choi, J. S. *Tetrahedron: Asymmetry* **2001**, 12, 33-35.

111. a) Lautens, M.; Renaud, J. L. ; Hiebert, S. *J. Am. Chem. Soc*. **2000**, 122, 1084-1085.

b) Lautens, M.; Hiebert, S.; Renaud, J. L. *J. Am. Chem. Soc*. **2001**, 123, 6834-6839.

c) Bertozzi, F.; Pineschi, M.; Macchia, F.; Arnold, L. A.; Minnaard, A. J. ; Feringa, B. L. *Org. Lett*. **2002**, 16, 2703-2705.

d) Lautens, M.; Fagnou, K.; Hiebert, S. *Acc. Chem. Res*. **2003**, 36, 48-58.

112. a) Kitamura, M.; Tokunaga, T.; Takaya, H.; Noyori, R. *Tetrahedron Lett.* **1991**, 32, 4163-4166.

b) Mashima, K.; Kusano, K.; Ohta, T.; Noyori, R. ; Takaya, H. *J. Chem. Soc., Chem. Commun*. **1989**, 1208-1210.

113. Fache, F.; Schulz, E.; Tommasino, M. L.; Lemaire, M. *Chem. Rev*. 2**000**, *100*, 2159.

114. Pu, L.; Yu, H. B. *Chem. Rev*. **2001**, *101*, 757

115. Corey, E. J.; Helal, C. J. *Angew. Chem. Int. Ed. Engl.* **1998**, *37*, 1986.

116. Pu, L.; Yu, H.-B. *Chem. Rev.* **2001**, *101*, 757.

117. a) Itsuno, S.; Ito, K.; Hirao, A.; Nakahama, S. *J. Chem. Soc., Perkin Trans. I* **1984**, 2887.

b) Itsuno, S.; Ito, K.; Hirao, A.; Nakahama, S. *J. Org. Chem*. **1984**, *49*, 555.

118. a) Corey, E. J.; Bakshi, R. K.; Shibata, S. *J. Am. Chem. Soc*. **1987**, *109*, 5551.

b) Corey, E. J.; Azimioara, M.; Sarshar, S. *Tetrahedron Letters* **1992**, *33*, 3429.

119. a) Mehler, T.; Martens, J. *Tetrahedron: Asymmetry* **1993**, *4*, 2299.

b) Li, X.; Xie, R. *Tetrahedron: Asymmetry* **1996**, *7*, 2779.

120. Mehler, T.; Martens, J. *Tetrahedron: Asymmetry* **1993**, *4*, 1983.

121. a) Jiang, Y.; Qin, Y.; Mi, A.; Huang, Z. *Tetrahedron: Asymmetry* **1994**, *5*, 1211.

b) Quallich, G. J.; Woodall, T. M. *Tetrahedron Lett.* **1993**, *34*, 785.

c) Masui, M.; Shioiri, T. *Synlett*. **1996**, 49.

122. Itsuno, S.; Nakano, M.; Miyazaki, K; Masuda, H.; Ito, K. *J. Chem. Soc., Perkin Trans. I*. **1985**, 2039.

123. Reetz, M. T.; Drews, M. W.; Schmitz, A. *Angew. Chem., Int. Ed. Engl*. **1987**, *26*, 1141.

124. Crystallographic data (excluding structure factors) for compound **6a** has been deposited with the Cambridge Crystallographic Data Center as supplementary publication numbers CCDC 173445. Copies of the data can be obtained, free of charge, on application to CCDC, 12 Union Road, Cambridge, CB2 1EZ, UK.

125. Corey, E. J.; Bakshi, R. K.; Shibata, S. *J. Am Chem. Soc*. **1987**, *109*, 5551.

126. Kitamura, M.; Suga, S.; Kawai, K.; Noyori, R. *J. Am. Chem. Soc*. **1986**, *108*, 6071.

127. Pu, L.; Yu, H.-B. *Chem. Rev*. **2001**, *101*, 757.

128. Soai, K.; Niwa, S. *Chem. Rev*. **1992**, *92*, 833.

129. Yamakawa, M.; Noyori, R. *Organometallics* **1999**, *18*, 128.

130. Yamakawa, M.; Noyori, R. *J. Am. Chem. Soc*. **1995**, *117*, 6327.

131. Watanabe, M.; Soai, K. *J. Chem. Soc., Perkin Trans*. 1, **1994**, 837.

132. Nagel, U.;Leipold, J. *Chem. Ber*. **1995**, 129, 815.

133. Nagel, U. *Angew. Chem, Int. Ed. Engl*. **1984**, 23, 435.

134. Salvadori, P., Pini, D.; Petri, A. *J. Am. Chem. Soc*. **1997**, 119.6929.

135. Yang, X. W.; Chan, A. S. C. *J. Org. Chem*. **2000**, 65,295-296.

136. Zhou, X. G.; Che, C. M. *Chem. Commun*. **1999**, 1789-1790.

137. Nagel, U.; Kinzel, E. *J. Chem. Soc., Chem Commun*. **1986**, 1098-1099.

138. Bolm, C.; Gerlach, A. *Angew. Chem. Int. Ed. Engl*. **1997**, 36, 714.

139. Fan, Q. H.; Chan, A. S. C. *J. Am. Chem. Soc*. **1999**, 121, 7407-7408.

140. Wan, K. T.; Davis, M. E. *J. Chem. Soc., Chem. Commun*. **1993**, 1262-1264.

141. Wan, K. T.; Davis, M. E. *Nature* **1994**, 370, 449-450.

142. Selke, R. *J. Mol. Cat*. **1986**, 37, 227-234.

143. Selke, R.; Haupke, K.; Krause H. W. *J. Mol. Cat*. **1989**, 56, 315-328.

144. Selke, R.; Capka, M. *J. Mol. Cat*. **1990**, 63 319-334.

145. Wan, K. T.; Davis, M. E. *J. Chem. Soc. Chem. Commun.* **1993**, 1262.

146. Wan, K. T.; Davis, M. E. *Tetrahedron: Asymmetry*. **1993**, 12, 2461-2468.

147. Wan, K. T.; Davis, M. E. *J. Cat*. **1994**, 148, 1-8.

148. Selke, R.; Capka, M. *J. Mol. Cat.* **1990**, 63, 319-334.

149. Halt,R. T.; Colasson, B.; Schulz, E.; Spagnol, M.; Lemaire, M. *Tetrahedron Lett.* **2000**, 41, 643-646.

150. Guerreiro, P.; Ratovelomanana-Vida, V.; Genet, J. P.; Dellis, P. *Tetrahedron Lett.* **2001**, 42, 3423-3426.

151. Saluzzo, C.; Lamouille, T.; Guyader, F.; Lemaire, M. *Tetrahedron: Asymmetry* **2002**, 13, 1141-1146.

Appendix I

^{1}H, ^{13}C and ^{31}P NMR Spectra

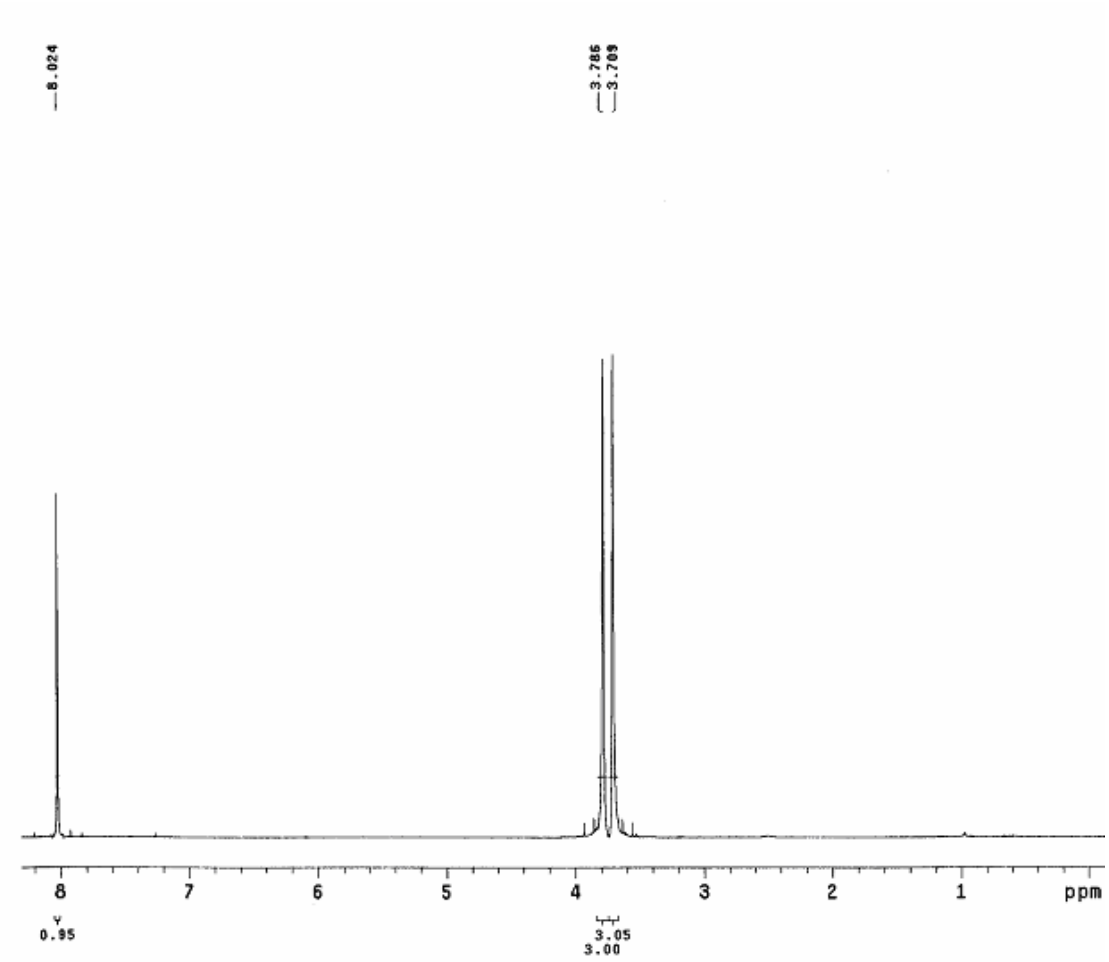

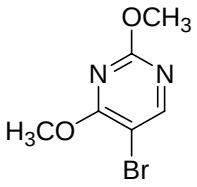

2-2

Fig. 1. ^{1}H NMR of **2-2**

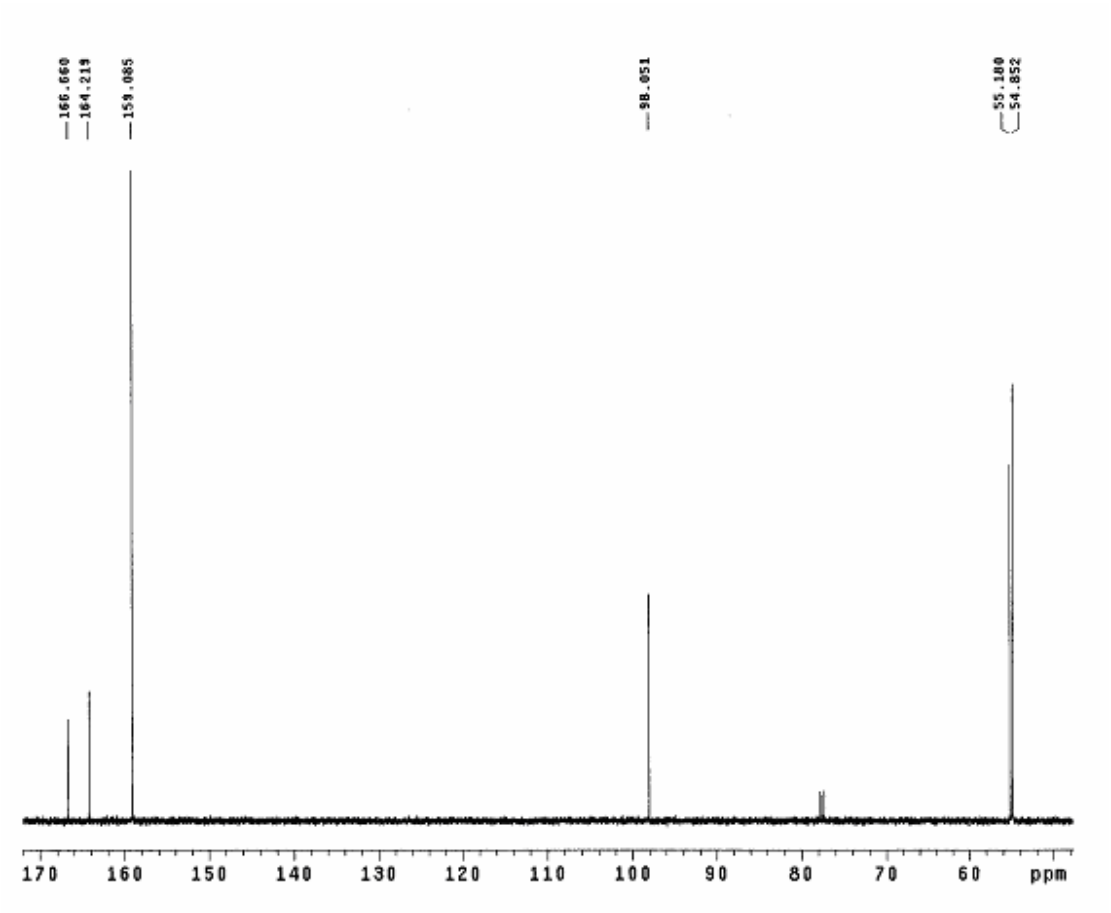

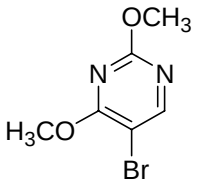

2-2

Fig. 2. ^{13}C NMR of **2-2**

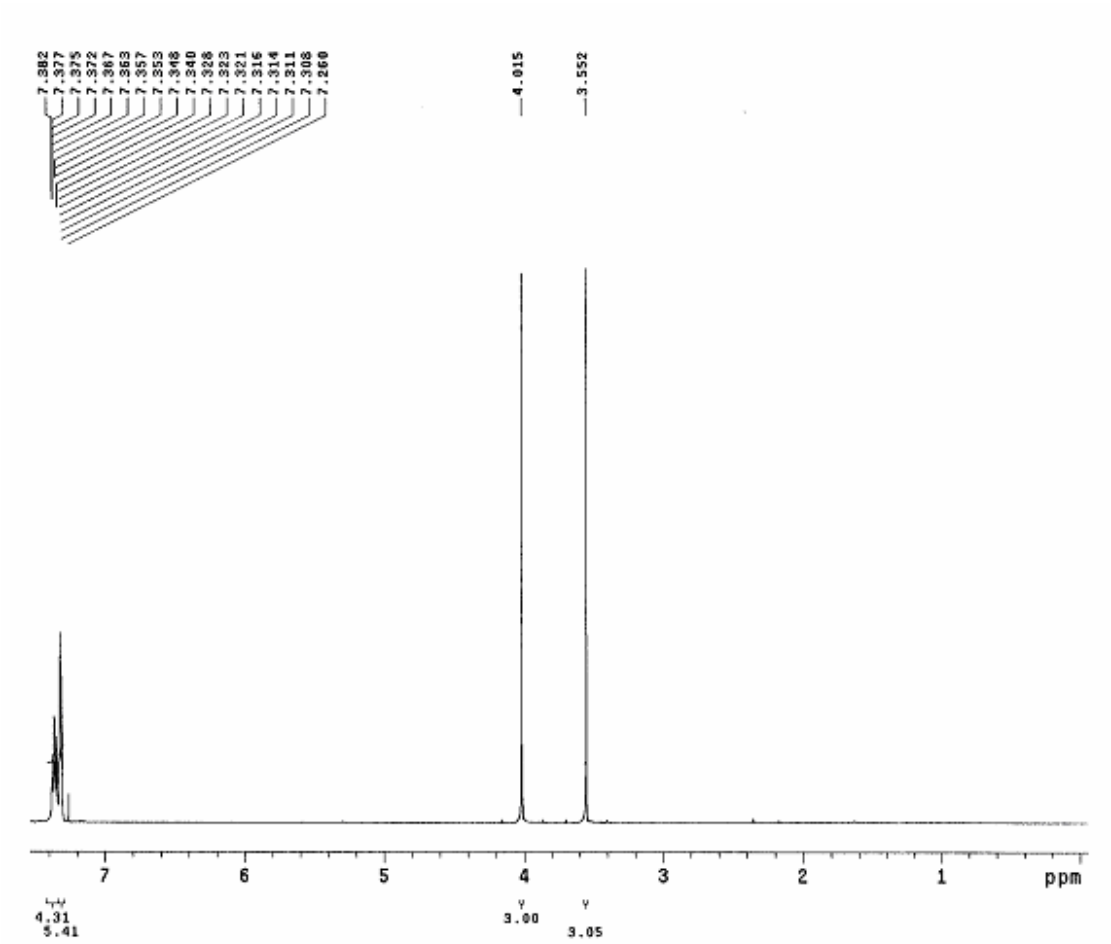

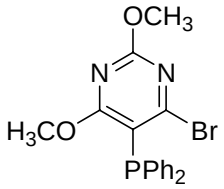

2-3

Fig. 3. ^{1}H NMR of **2-3**

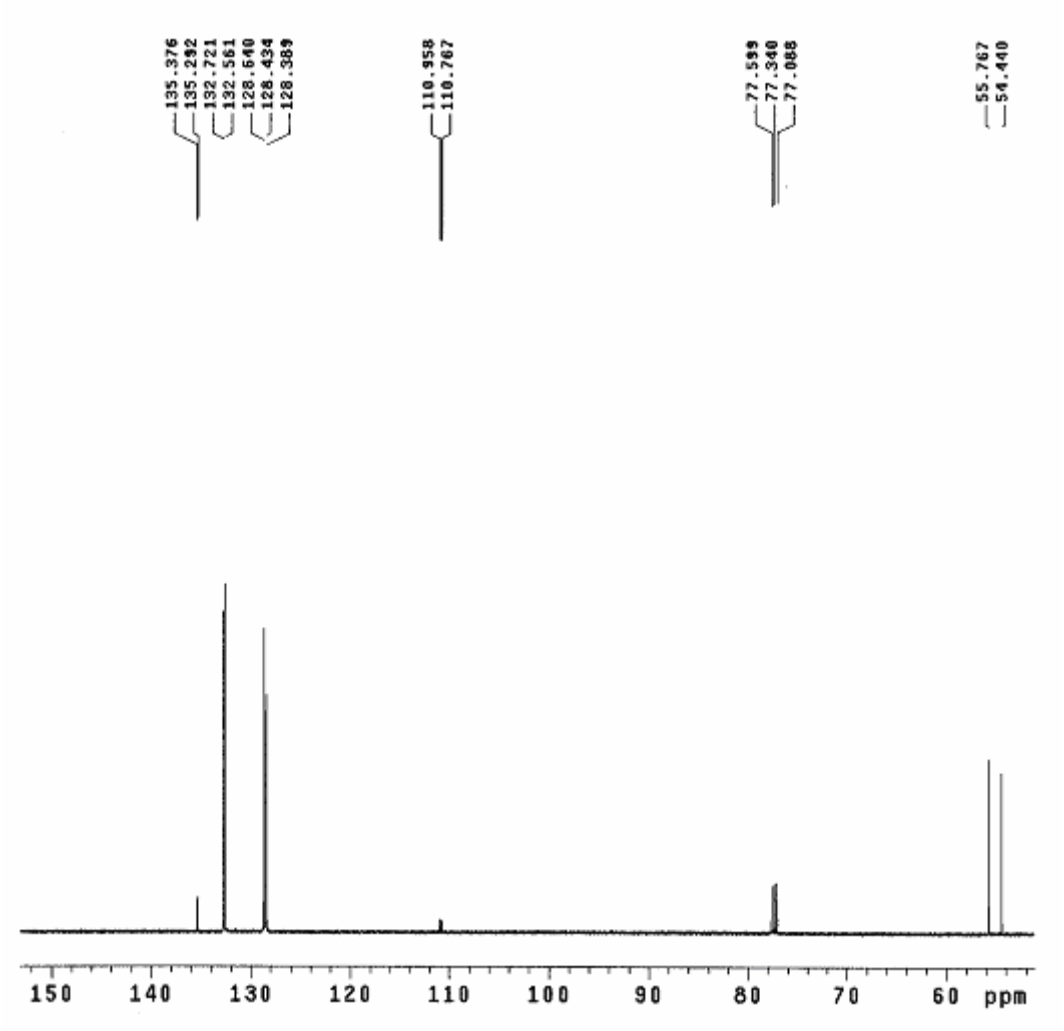

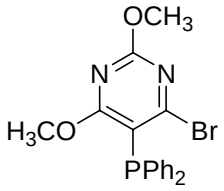

2-3

Fig. 4. ^{13}C NMR of **2-3**

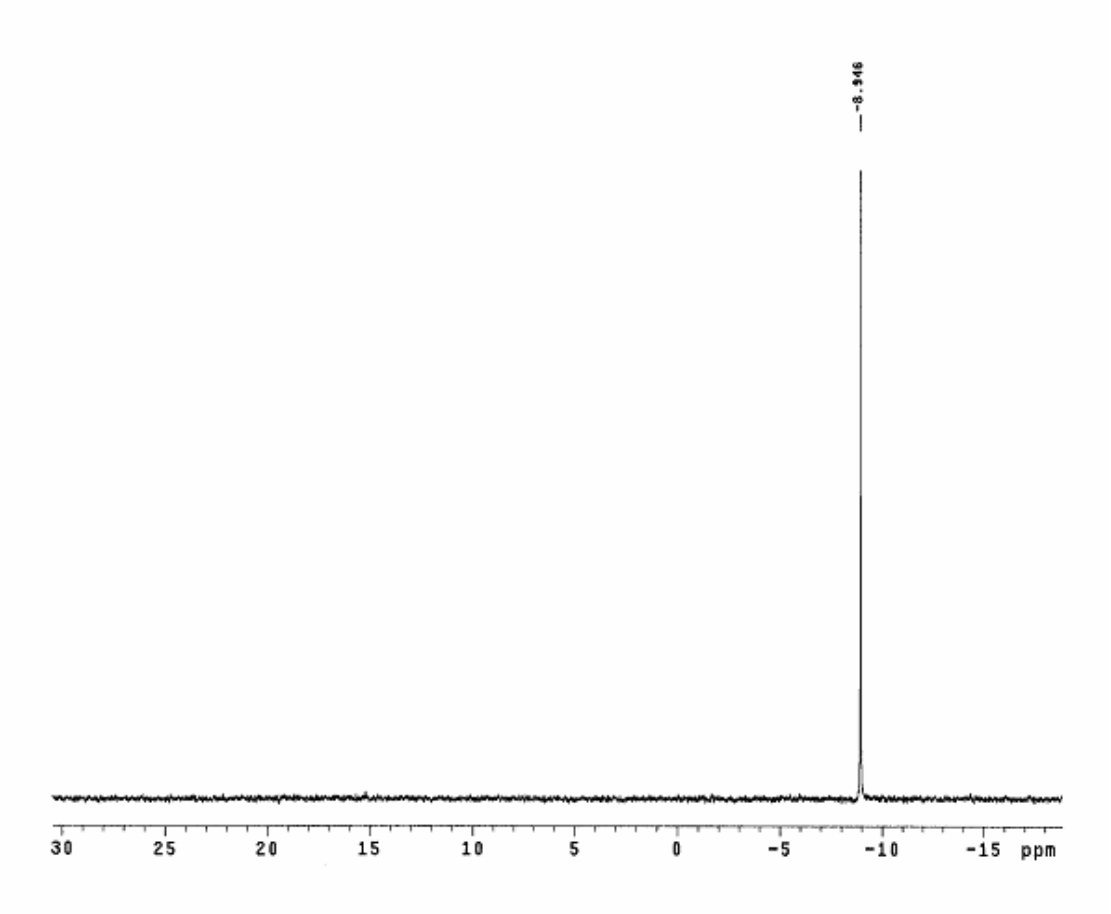

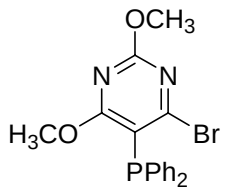

2-3

Fig. 5. ^{31}P NMR of **2-3**

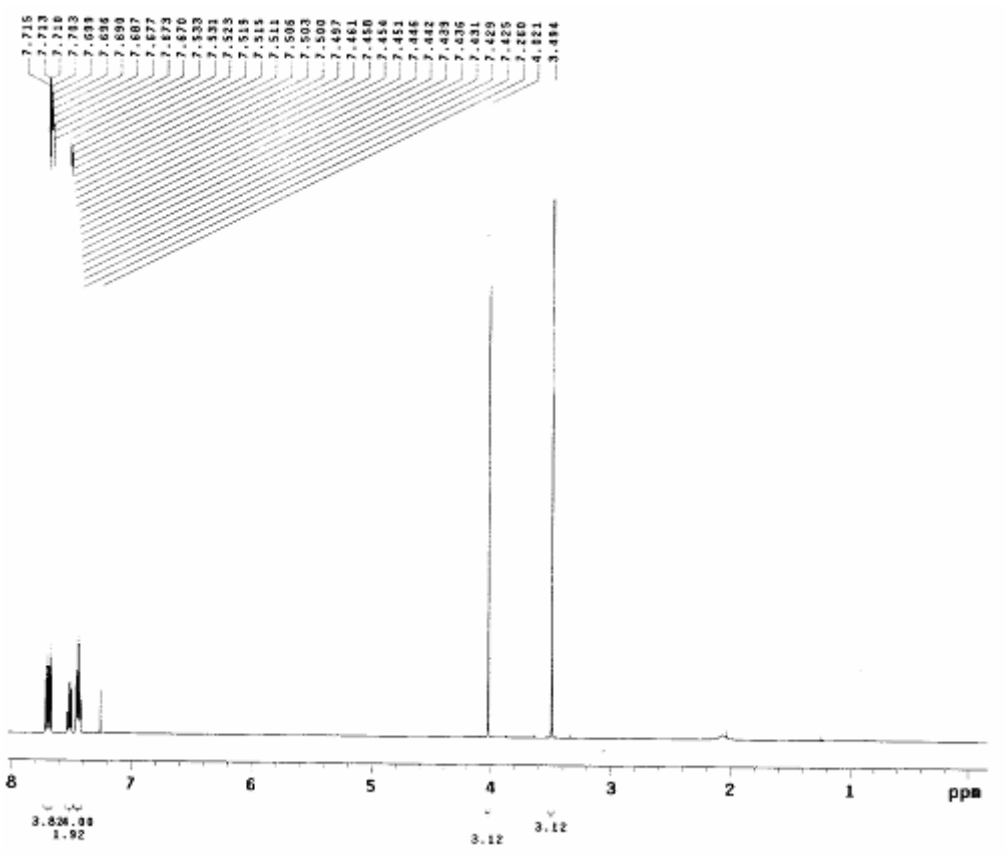

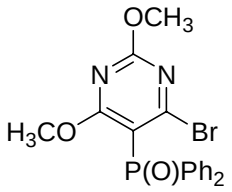

2-4

Fig. 6. ^{1}H NMR of **2-4**

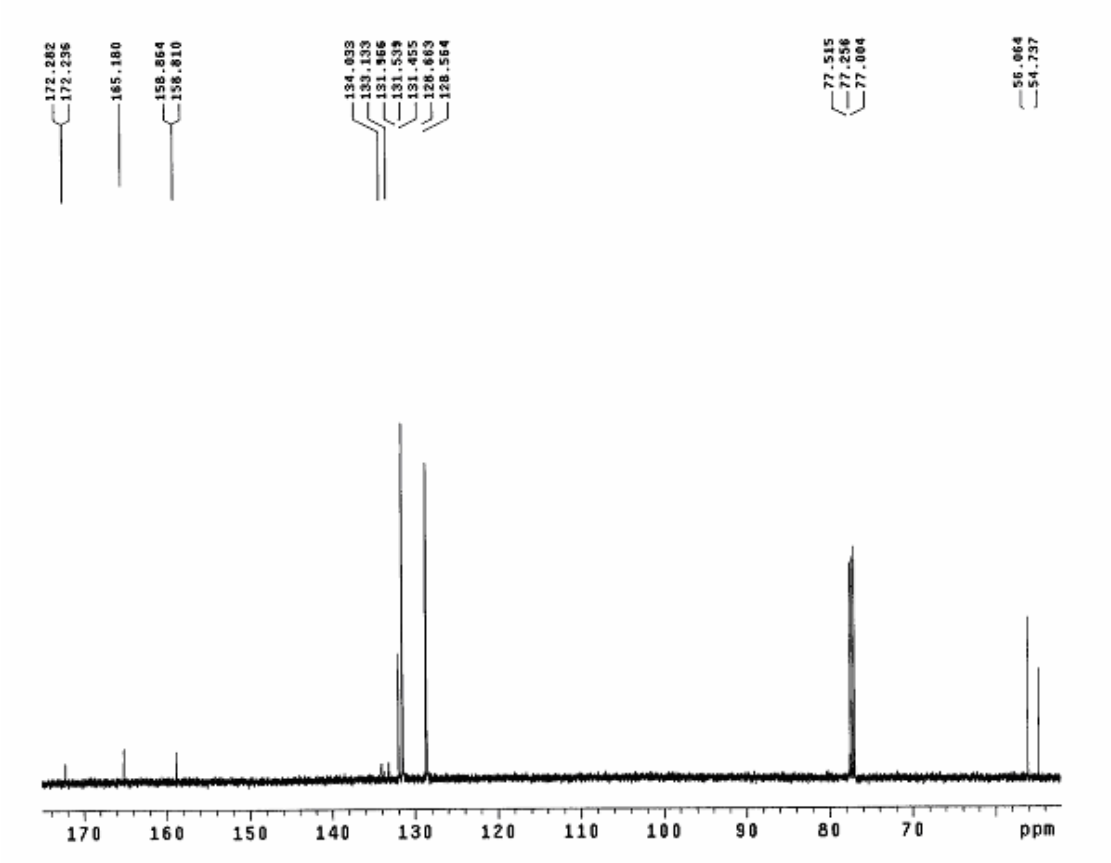

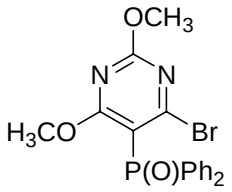

2-4

Fig. 7. ^{13}C NMR of **2-4**

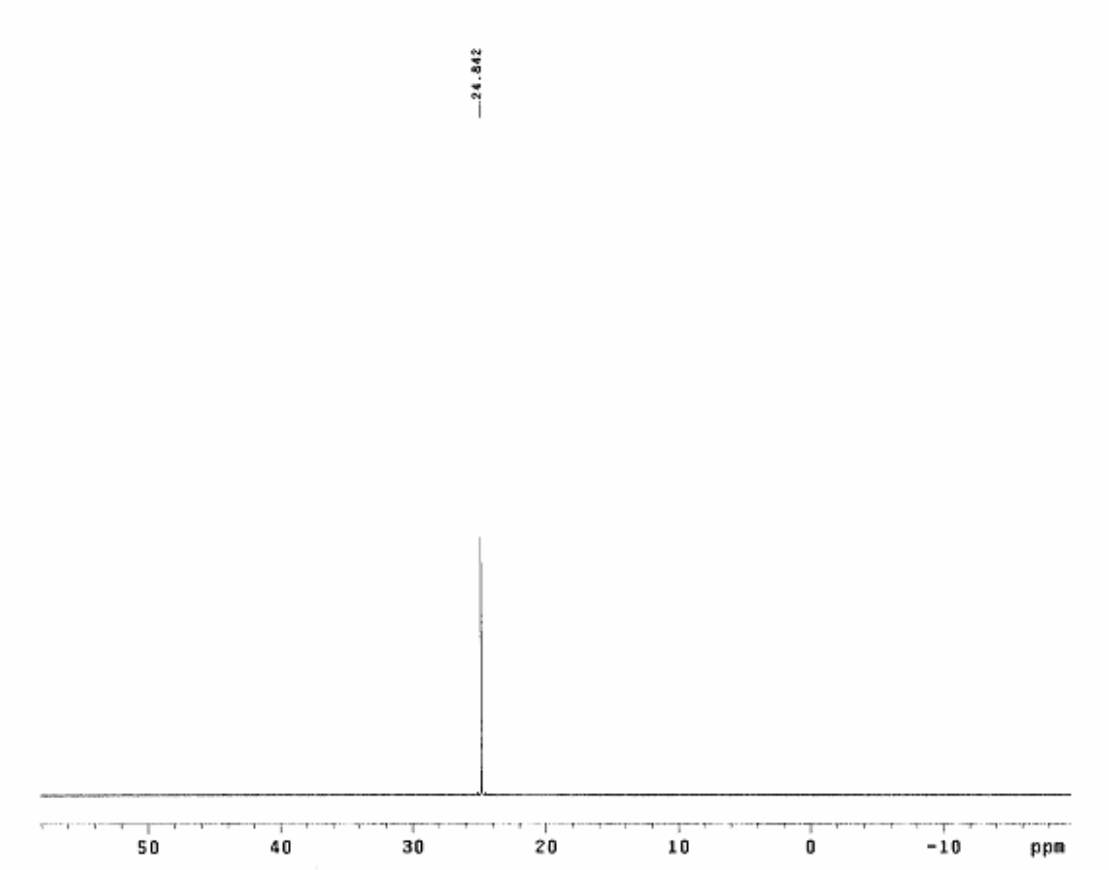

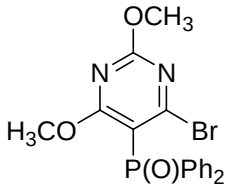

2-4

Fig. 8. ^{31}P NMR of **2-4**

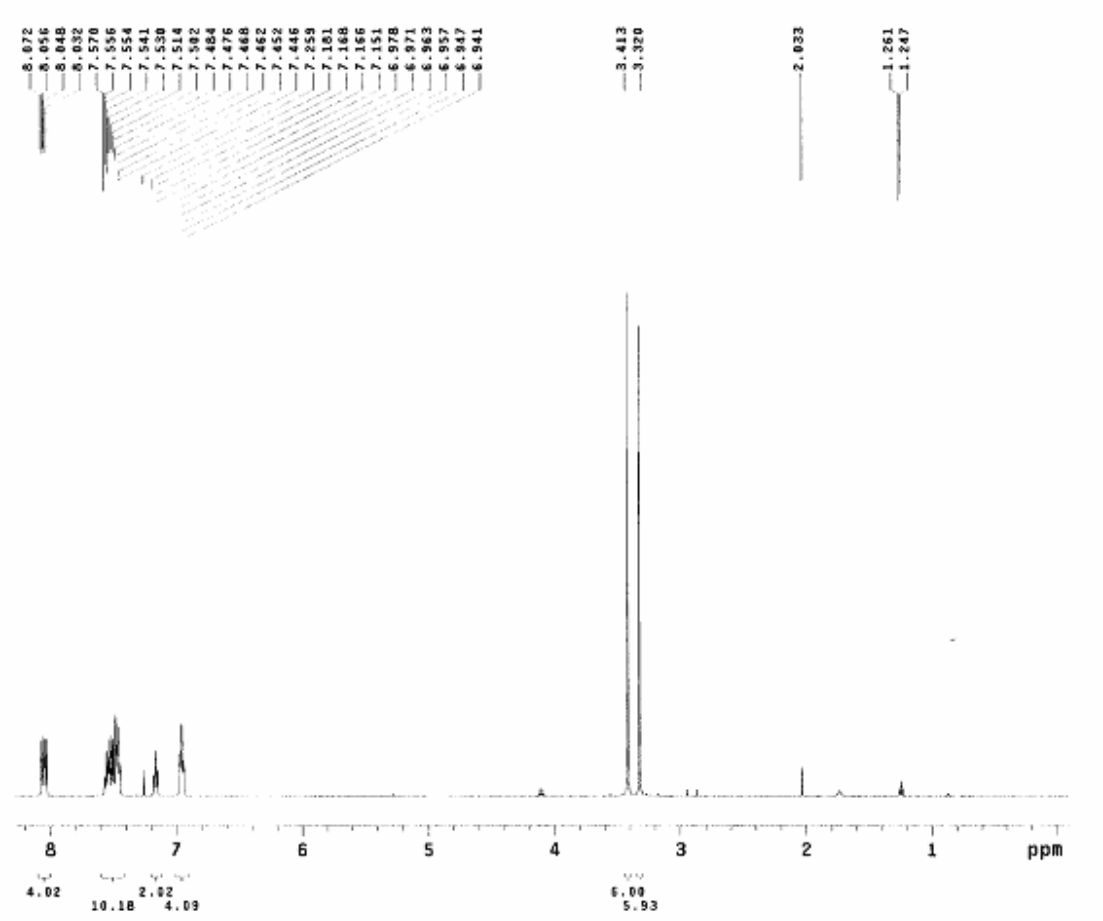

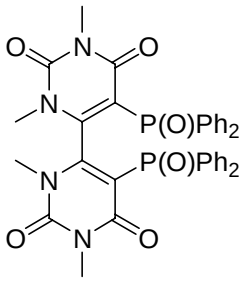

2-5

Fig. 9. ^{1}H NMR of **2-5**

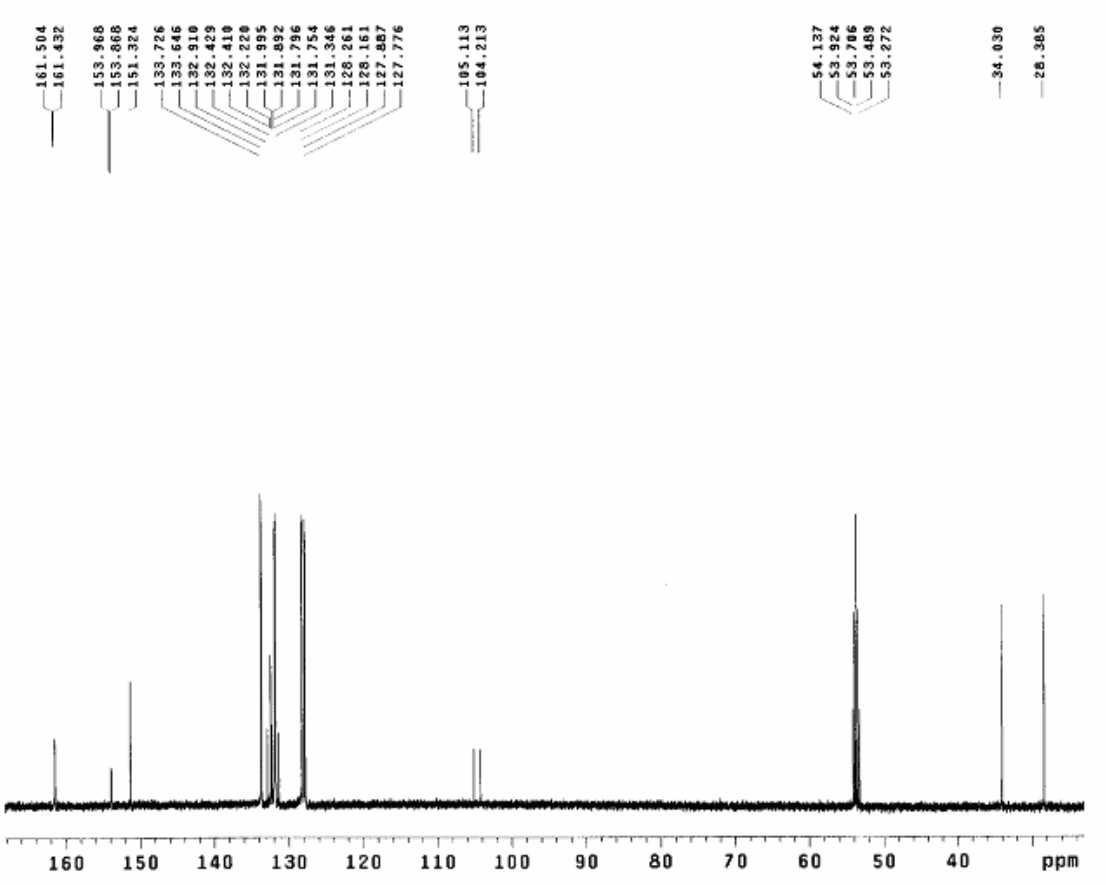

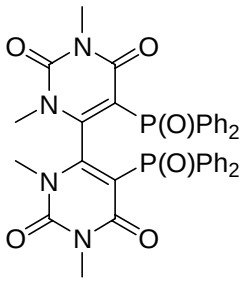

2-5

Fig. 10. ^{13}C NMR of **2-5**

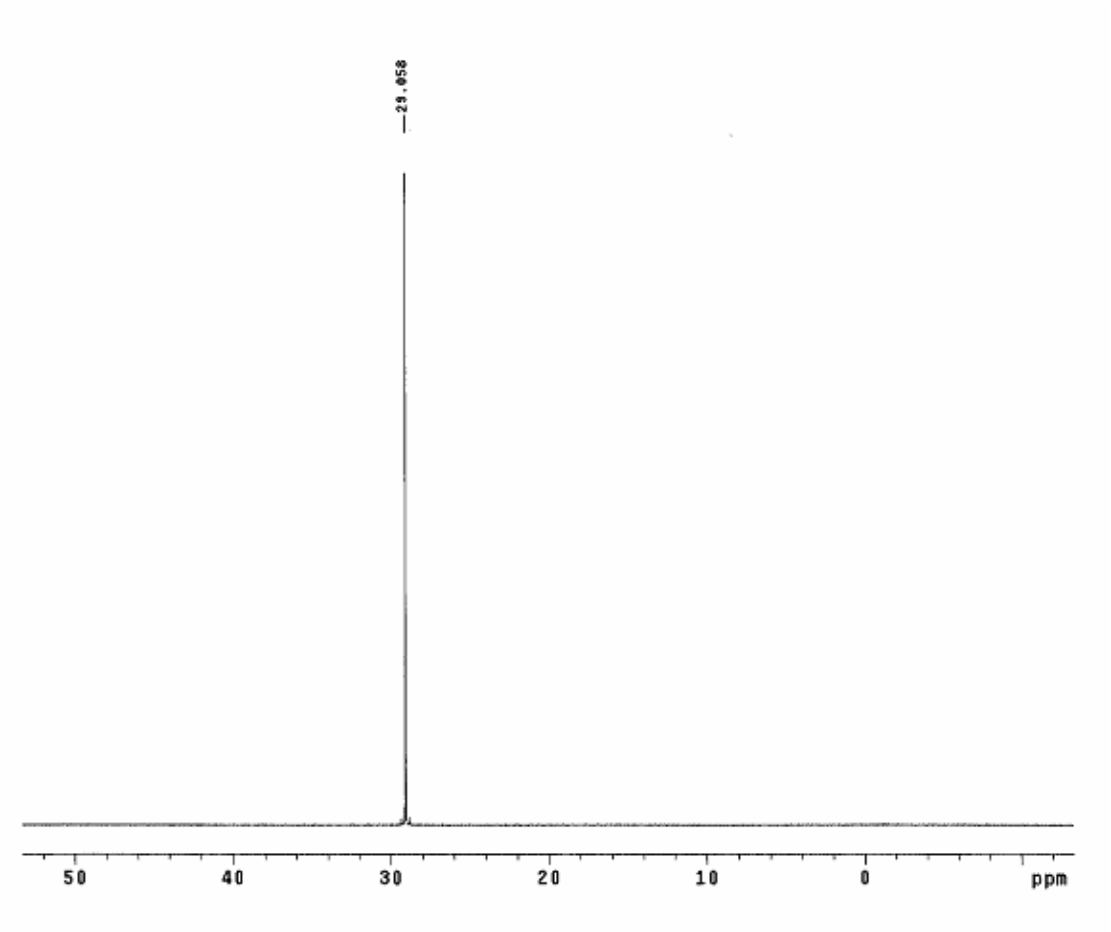

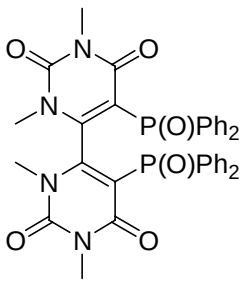

2-5

Fig. 11. ^{31}P NMR of **2-5**

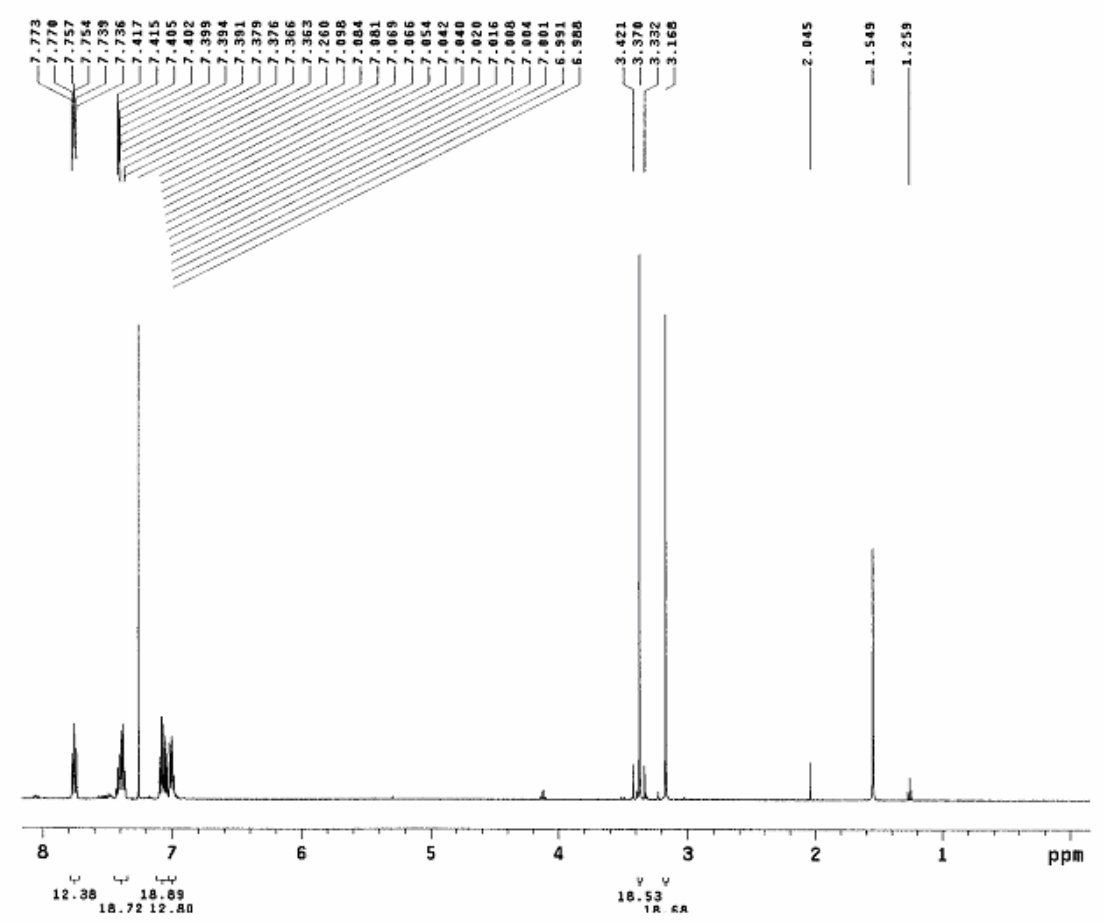

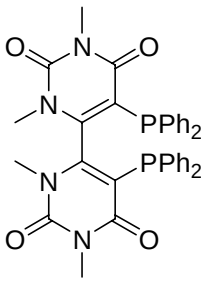

2-7

Fig. 12. ^{1}H NMR of **2-7**

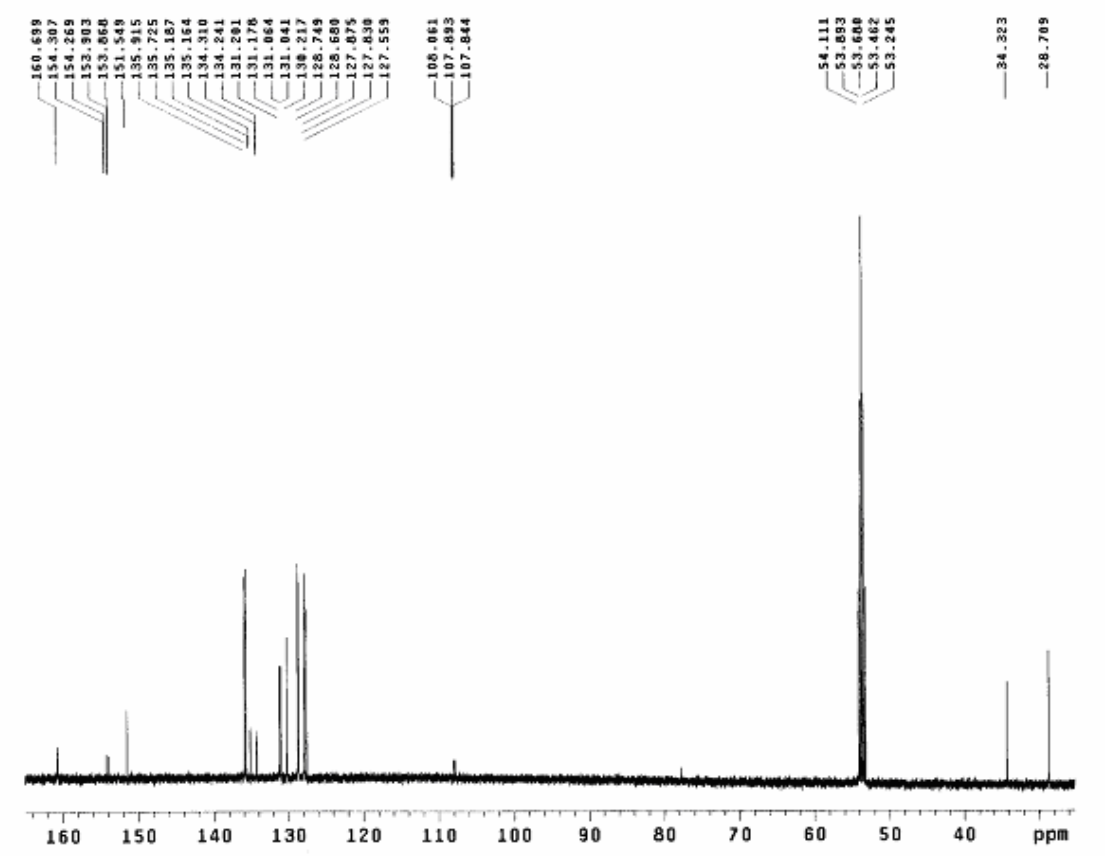

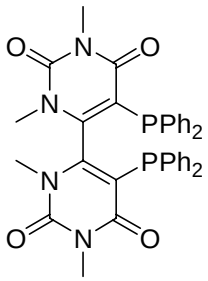

2-7

Fig. 13. ^{13}C NMR of **2-7**

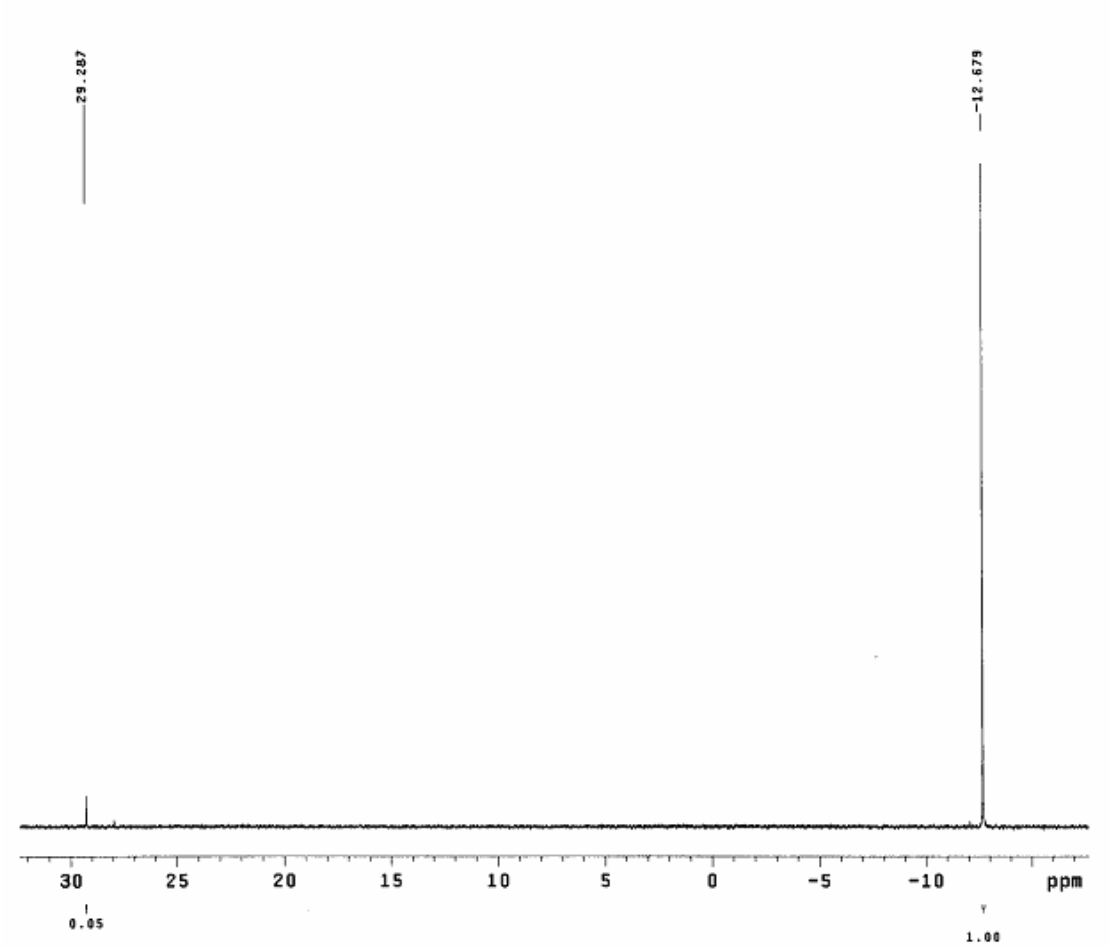

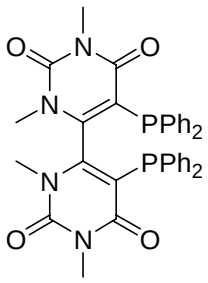

2-7

Fig. 14. ^{31}P NMR of **2-7**

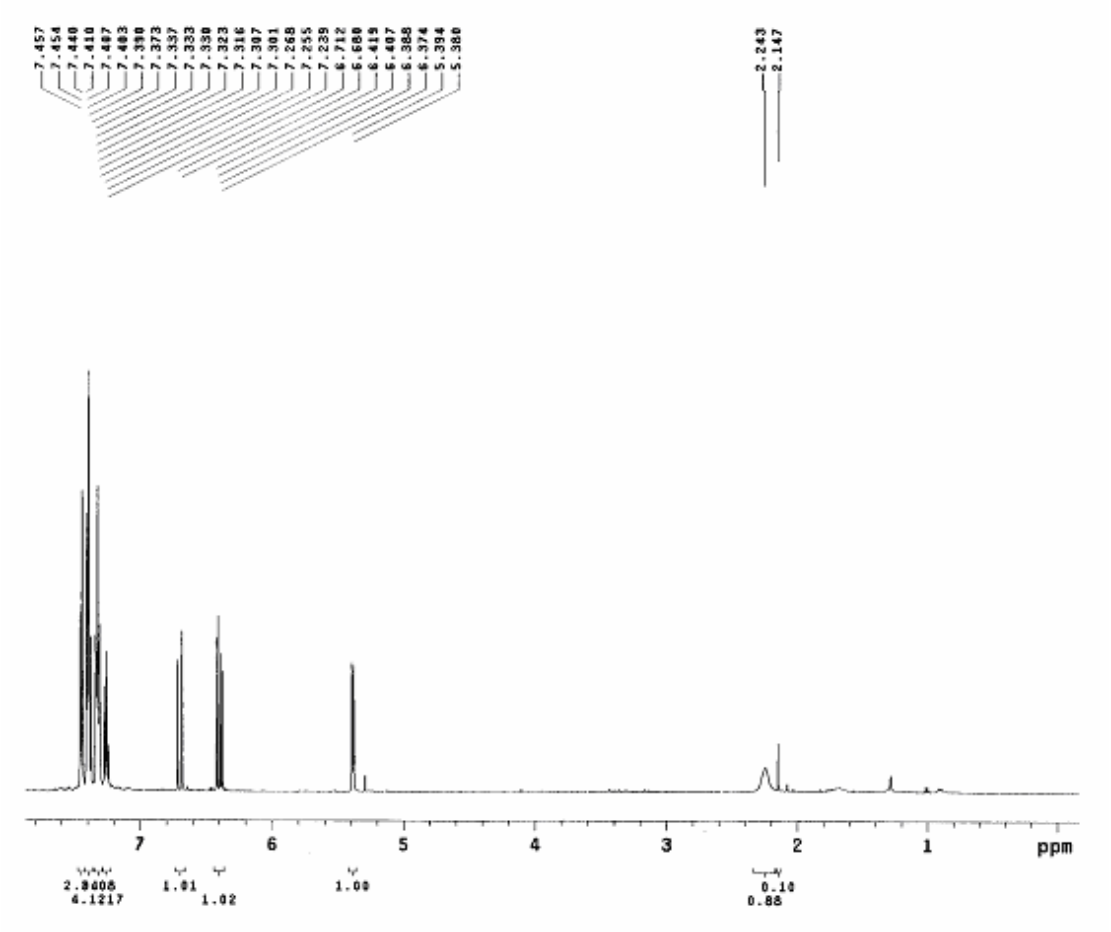

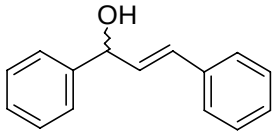

3-5

Fig. 15. ^{1}H NMR of **3-5**

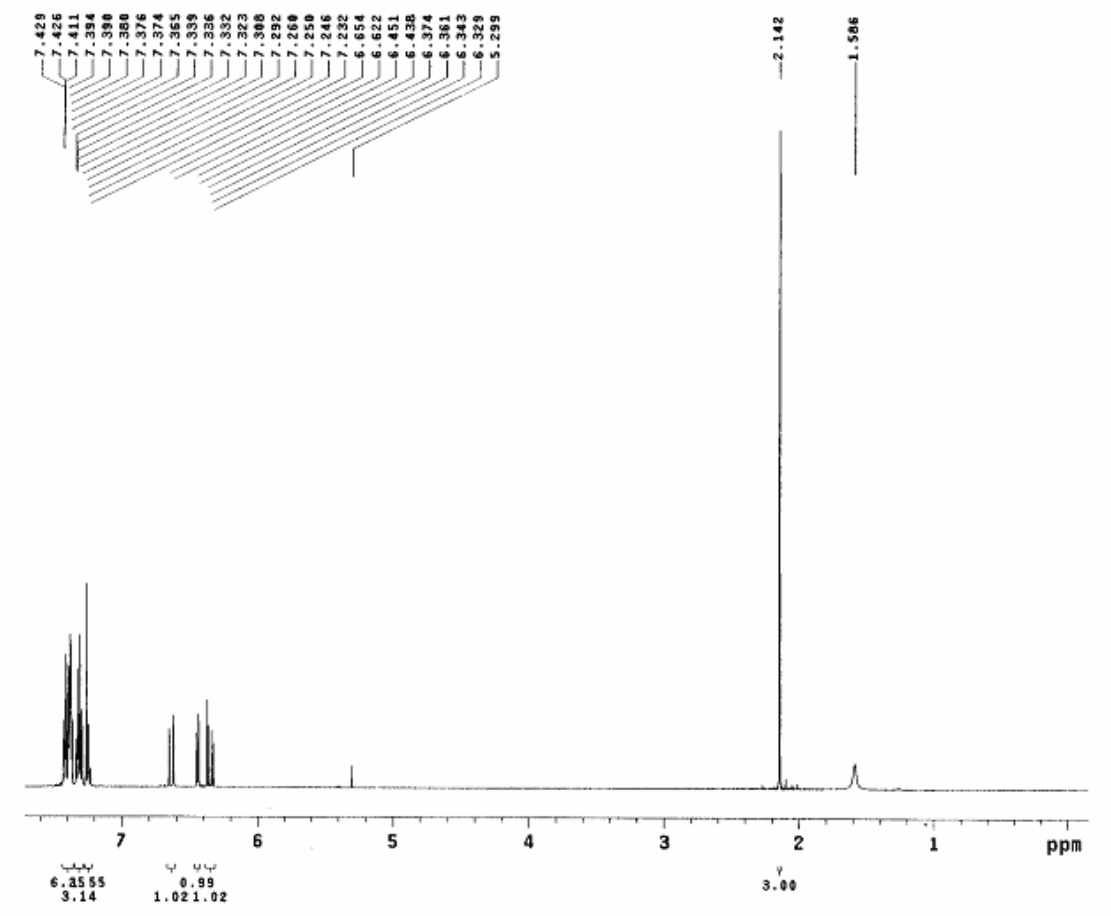

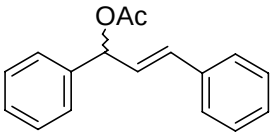

3-1

Fig. 16. ^{1}H NMR of **3-1**

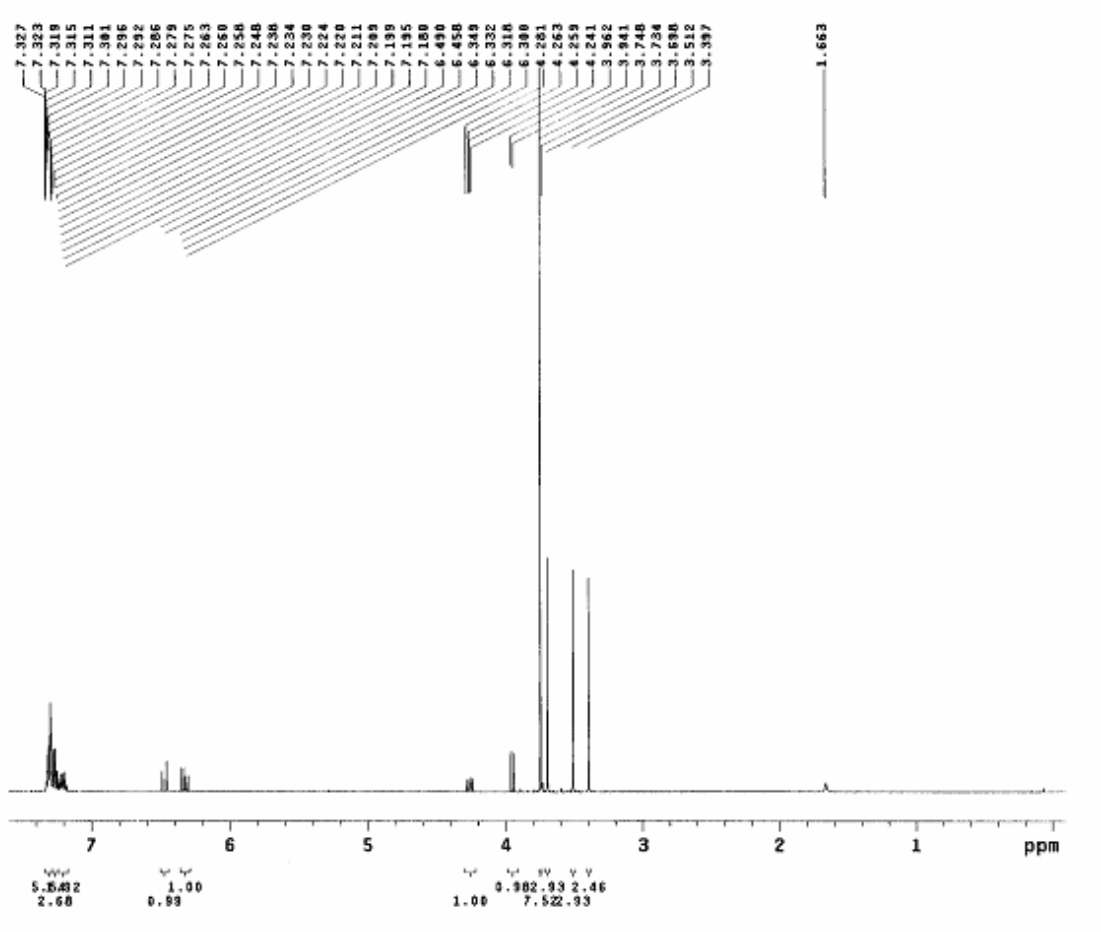

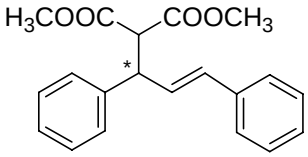

3-3

Fig. 17. ^{1}H NMR of **3-3**

Appendix II

HPLC Chromatograms for Palladium-catalyzed Allylic Alkylation in the Presence of (R)-PM-Phos

No.	R.Time (min.)	Comp.	Height (uV)	Height%	Area (uV.sec)	Area%
1	15.50	Unknown	681777	55.94	32417478	49.78
2	22.43	Unknown	537082	44.06	32703813	50.22
Total			1218860	100.00	65121291	100.00

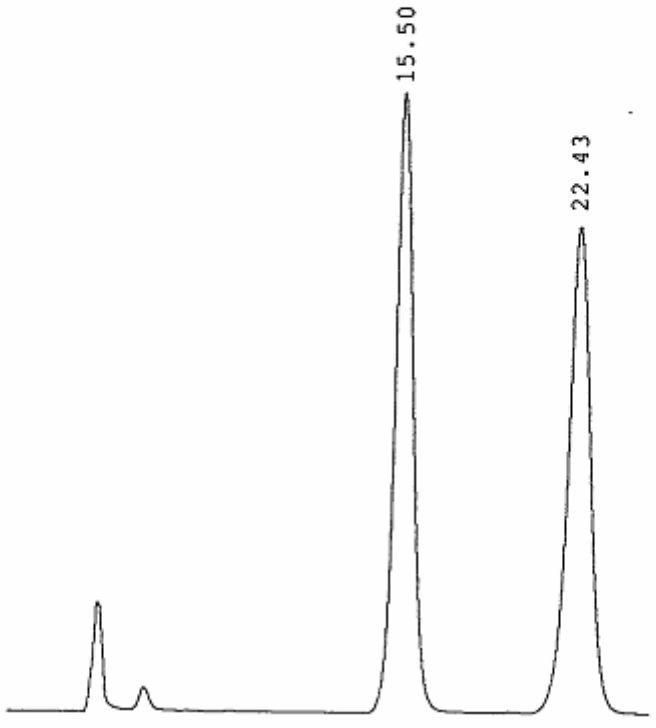

Figure 3-6. HPLC chromatogram of racemic **3-3**

No.	R.Time (min.)	Comp.	Height (uV)	Height%	Area (uV.sec)	Area%
1	10.59	Unknown	166613	56.28	5071552	50.61
2	14.52	Unknown	129429	43.72	4949860	49.39
Total			296042	100.00	10021412	100.00

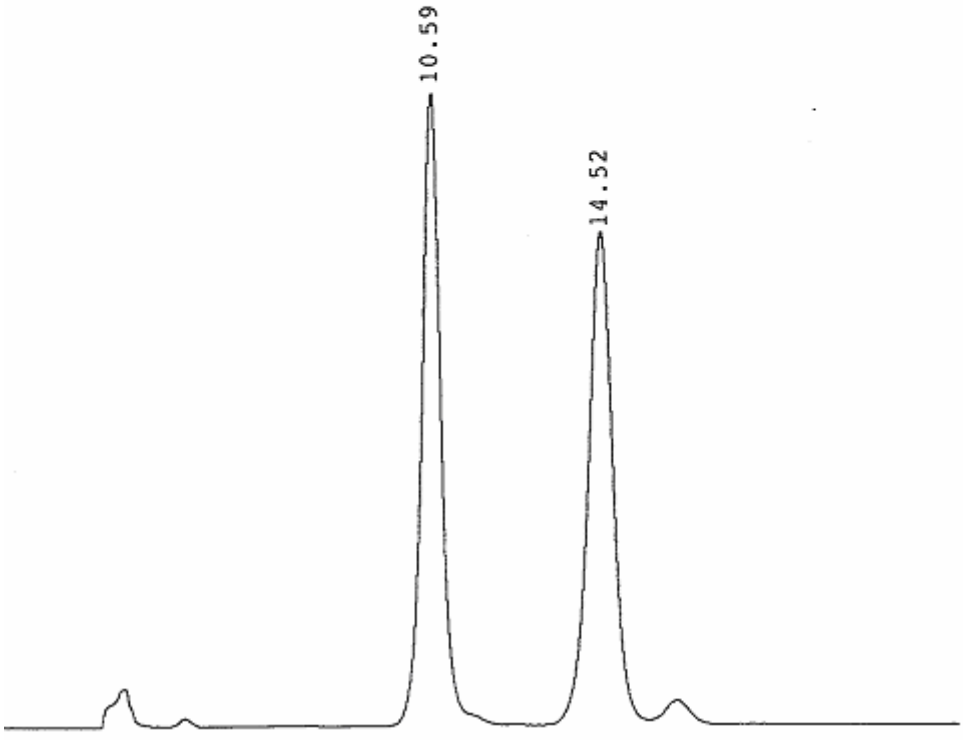

Figure 3-7. HPLC chromatogram of racemic **3-9**

No.	R.Time (min.)	Comp.	Height (uV)	Height%	Area (uV.sec)	Area%
1	23.60	Unknown	255504	54.47	15080615	48.80
2	29.53	Unknown	213557	45.53	15824476	51.20
Total			469061	100.00	30905091	100.00

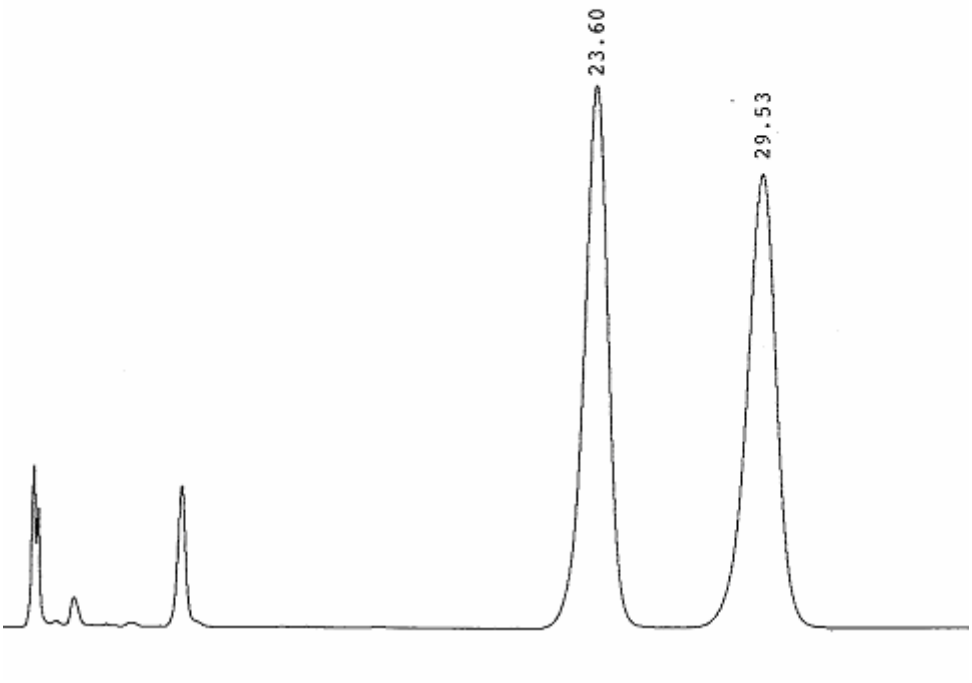

Figure 3-8. HPLC chromatogram of racemic **3-10**

No.	R.Time (min.)	Comp.	Height (uV)	Height%	Area (uV.sec)	Area%
1	32.30	Unknown	703312	57.74	96086407	50.00
2	50.10	Unknown	514826	42.26	96073508	50.00
Total			1218139	100.00	192159915	100.00

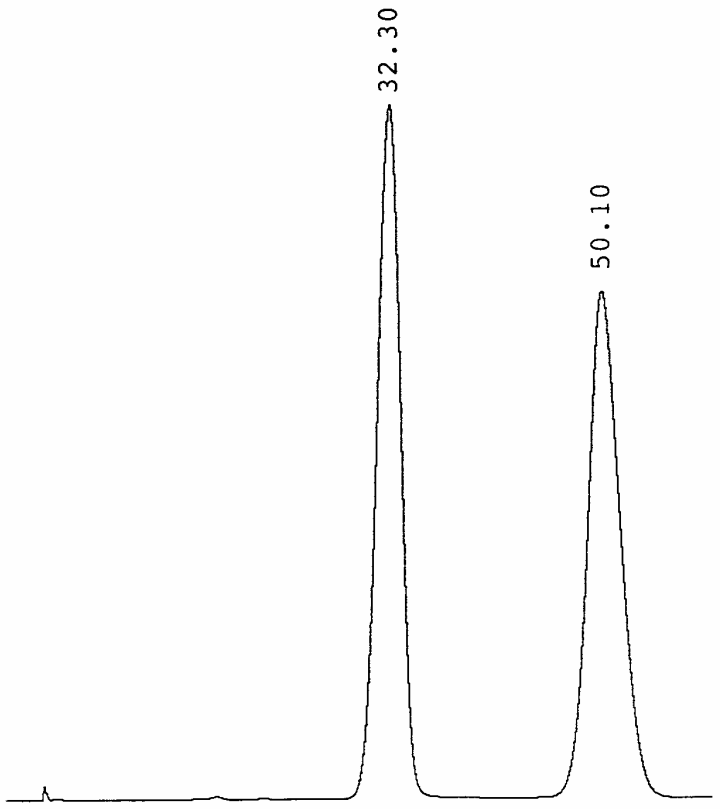

Figure 3-9. HPLC chromatogram of racemic **3-11**

No.	R.Time (min.)	Comp.	Height (uV)	Height%	Area (uV.sec)	Area%
1	10.63	Unknown	169549	14.00	5972143	11.82
2	14.58	Unknown	1041895	86.00	44558835	88.18
Total			1211443	100.00	50530977	100.00

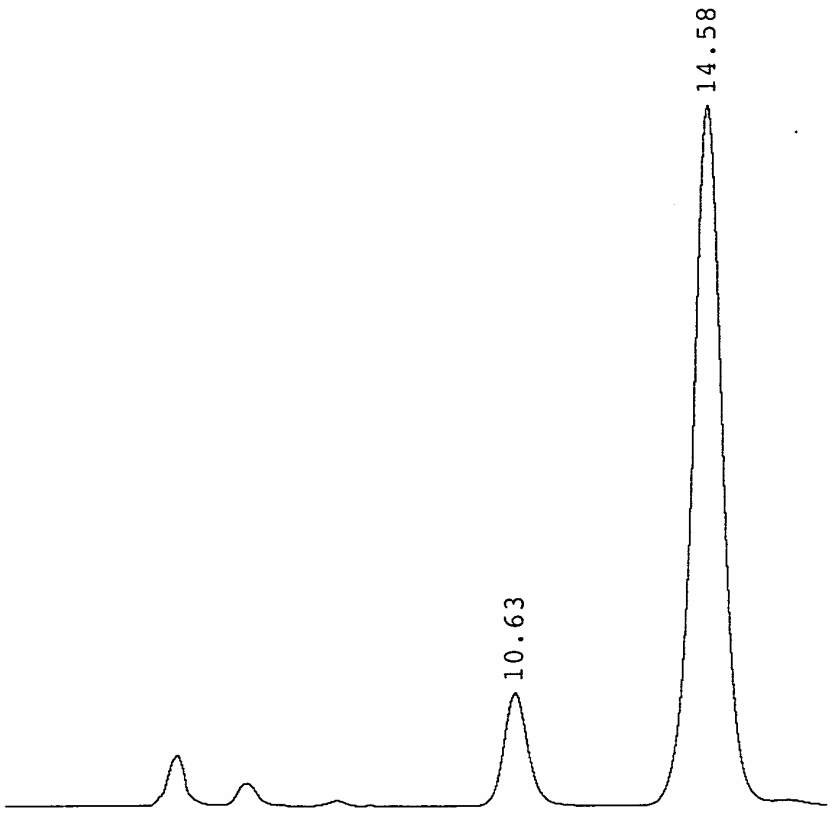

Figure 3-10. HPLC chromatogram for **Entry 2** in **Table 3-1**

No.	R.Time (min.)	Comp.	Height (uV)	Height%	Area (uV.sec)	Area%
1	23.43	Unknown	133315	17.09	8409980	14.13
2	29.37	Unknown	646575	82.91	51108153	85.87
Total			779889	100.00	59518133	100.00

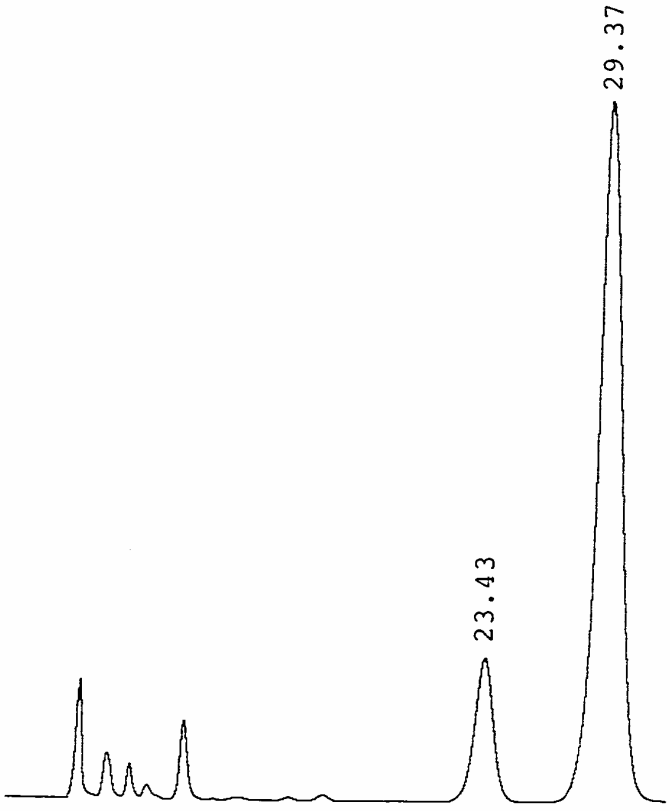

Figure 3-11. HPLC chromatogram for **Entry 3** in **Table 3-1**

No.	R.Time (min.)	Comp.	Height (uV)	Height%	Area (uV.sec)	Area%
1	32.60	Unknown	958823	90.79	126344977	88.52
2	50.67	Unknown	97281	9.21	16379516	11.48
Total			1056105	100.00	142724493	100.00

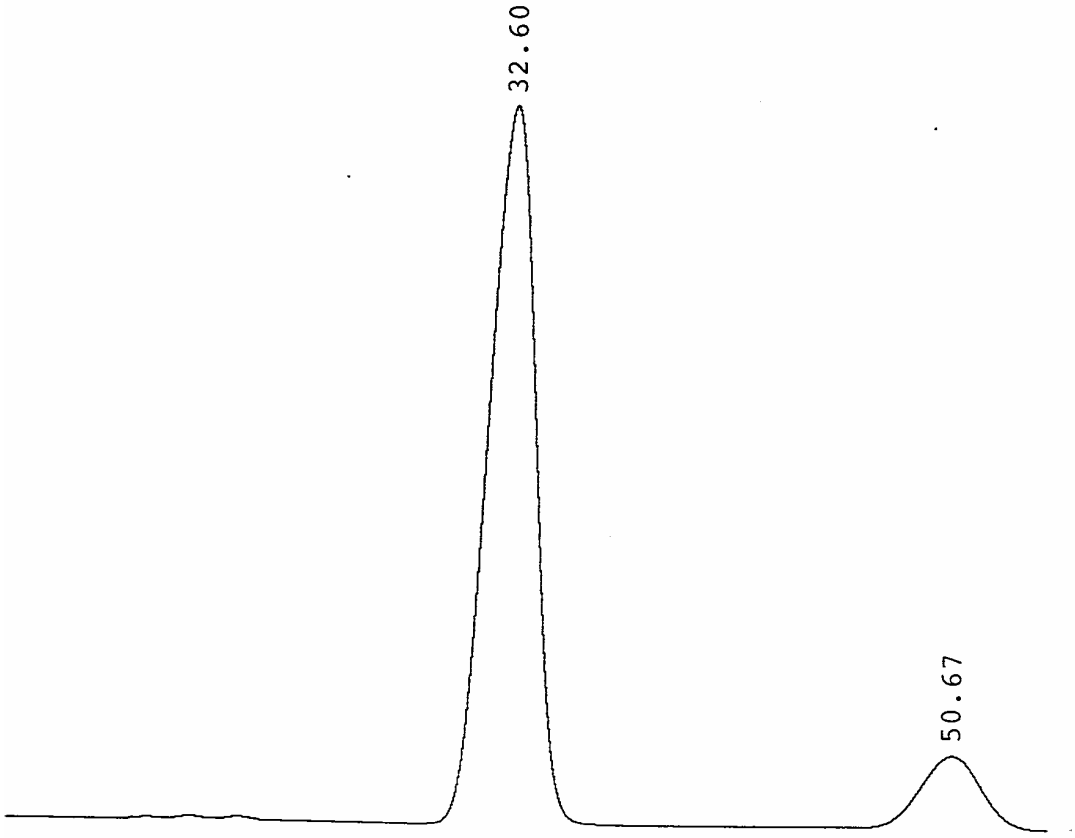

Figure 3-12. HPLC chromatogram for **Entry 4** in **Table 3-1**

No.	R.Time (min.)	Comp.	Height (uV)	Height%	Area (uV.sec)	Area%
1	15.83	Unknown	113398	11.12	5353341	8.71
2	22.81	Unknown	906248	88.88	56094281	91.29
Total			1019646	100.00	61447621	100.00

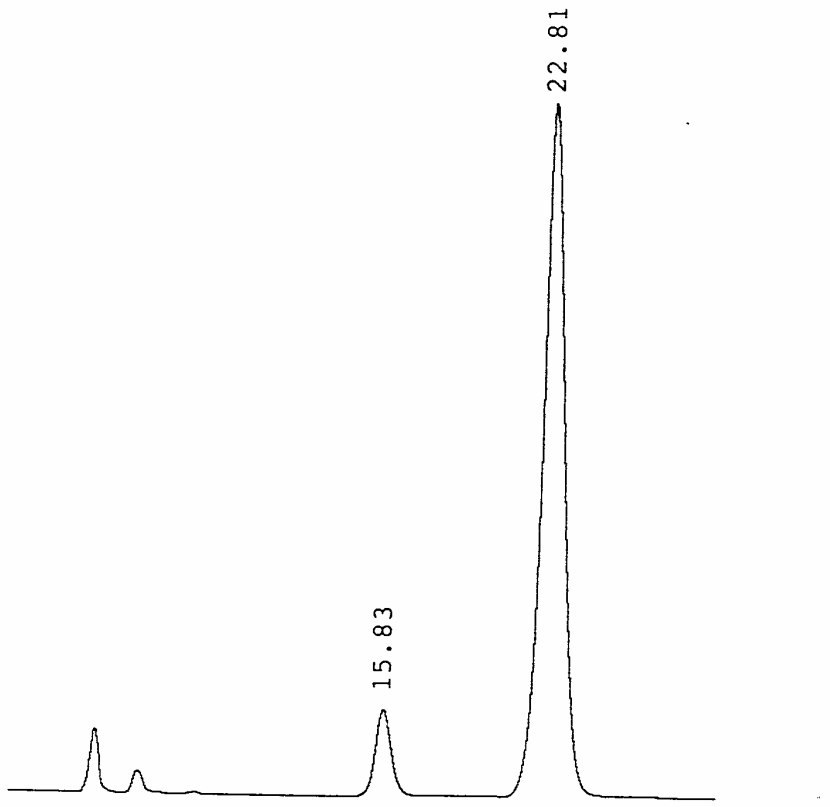

Figure 3-13. HPLC chromatogram for **Entry 4** in **Table 3-2**

No.	R.Time (min.)	Comp.	Height (uV)	Height%	Area (uV.sec)	Area%
1	15.54	Unknown	622326	24.74	25759647	19.24
2	22.18	Unknown	1892895	75.26	108138345	80.76
Total			2515221	100.00	133897992	100.00

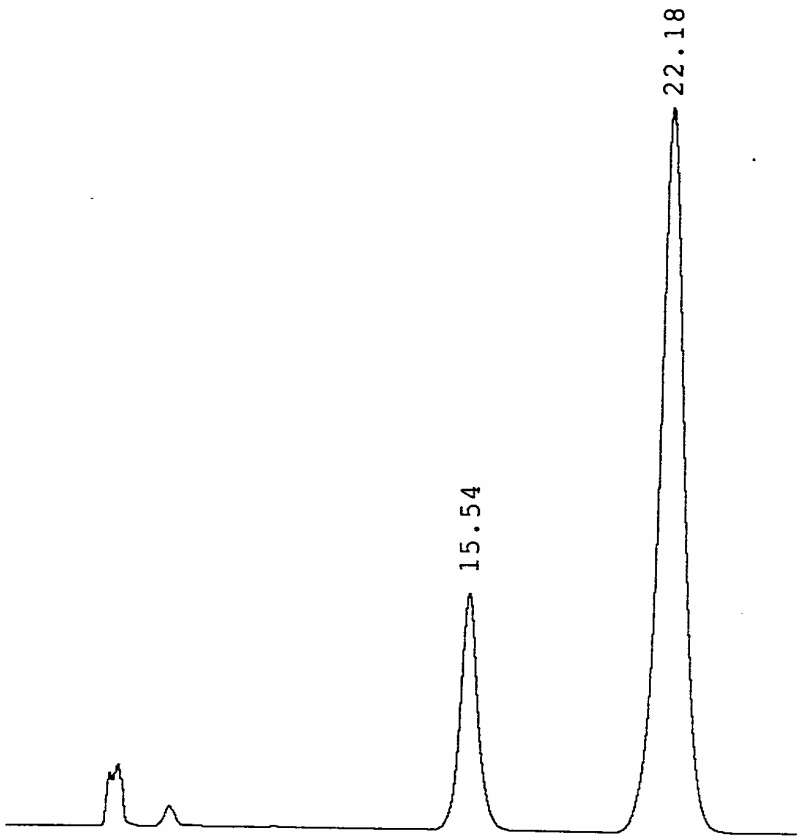

Figure 3-14. HPLC chromatogram for **Entry 5** in **Table 3-2**

No.	R.Time (min.)	Comp.	Height (uV)	Height%	Area (uV.sec)	Area%
1	15.55	Unknown	228457	91.58	11422917	90.12
2	22.48	Unknown	21009	8.42	1252752	9.88
Total			249467	100.00	12675669	100.00

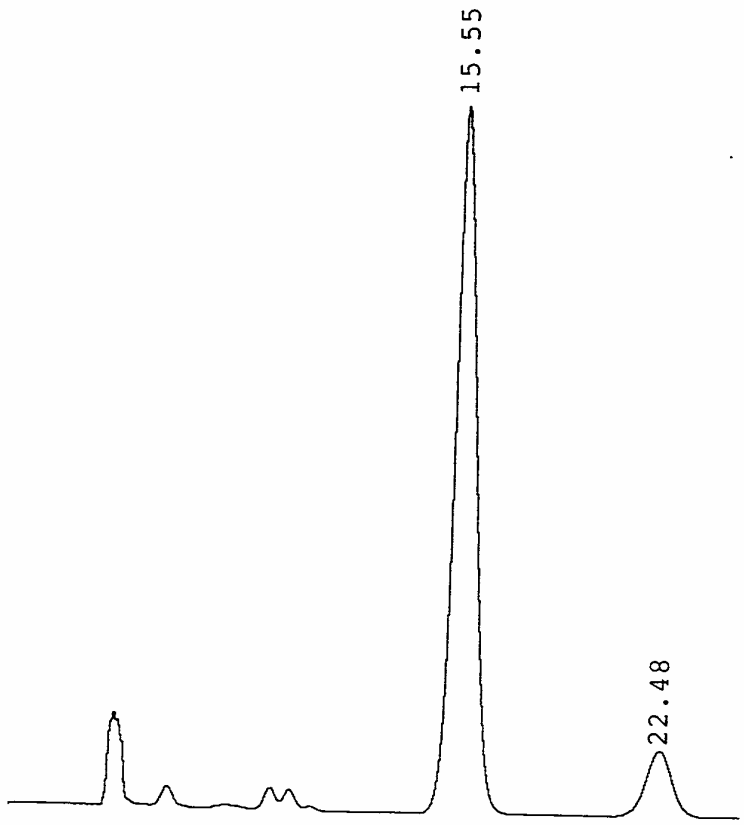

Figure 3-15. HPLC chromatogram for **Entry 6** in **Table 3-2**

No.	R.Time (min.)	Comp.	Height (uV)	Height%	Area (uV.sec)	Area%
1	15.76	Unknown	57888	9.36	2671368	7.40
2	22.55	Unknown	560269	90.64	33424641	92.60
Total			618157	100.00	36096009	100.00

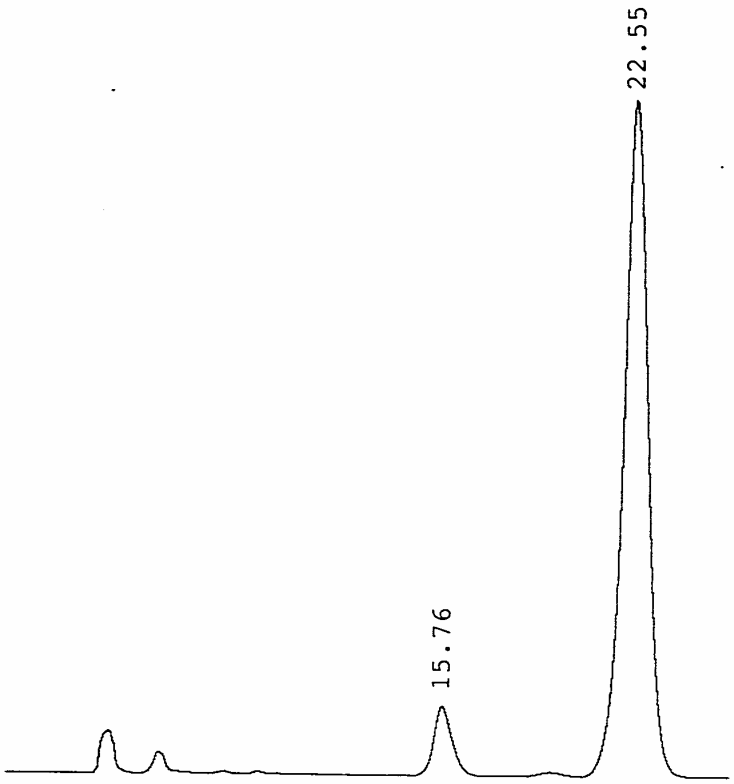

Figure 3-16. HPLC chromatogram for **Entry 7** in **Table 3-2**

No.	R.Time (min.)	Comp.	Height (uV)	Height%	Area (uV.sec)	Area%
1	15.39	Unknown	84475	8.83	3990332	6.95
2	22.06	Unknown	871896	91.17	53417916	93.05
Total			956371	100.00	57408248	100.00

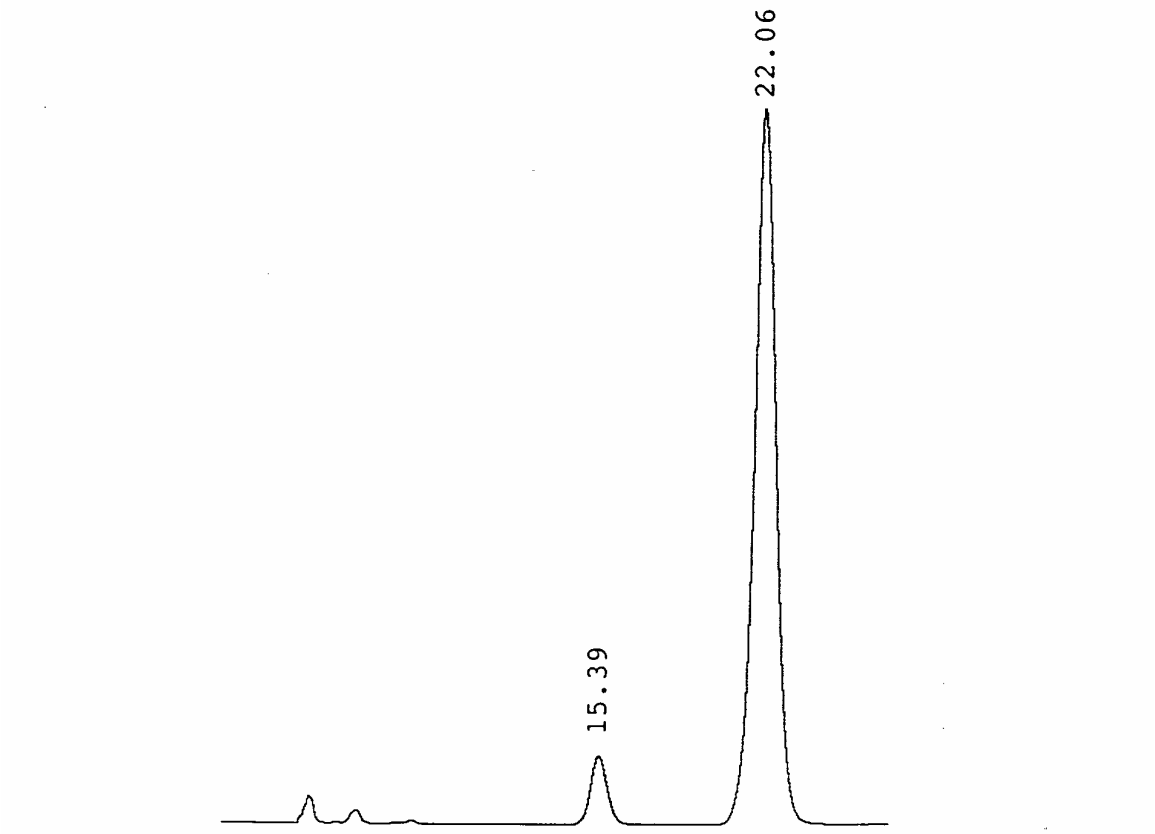

Figure 3-17. HPLC chromatogram for **Entry 12** in **Table 3-2**

No.	R.Time (min.)	Comp.	Height (uV)	Height%	Area (uV.sec)	Area%
1	15.58	Unknown	82679	7.34	4287584	5.75
2	21.93	Unknown	1043988	92.66	70302183	94.25
Total			1126667	100.00	74589767	100.00

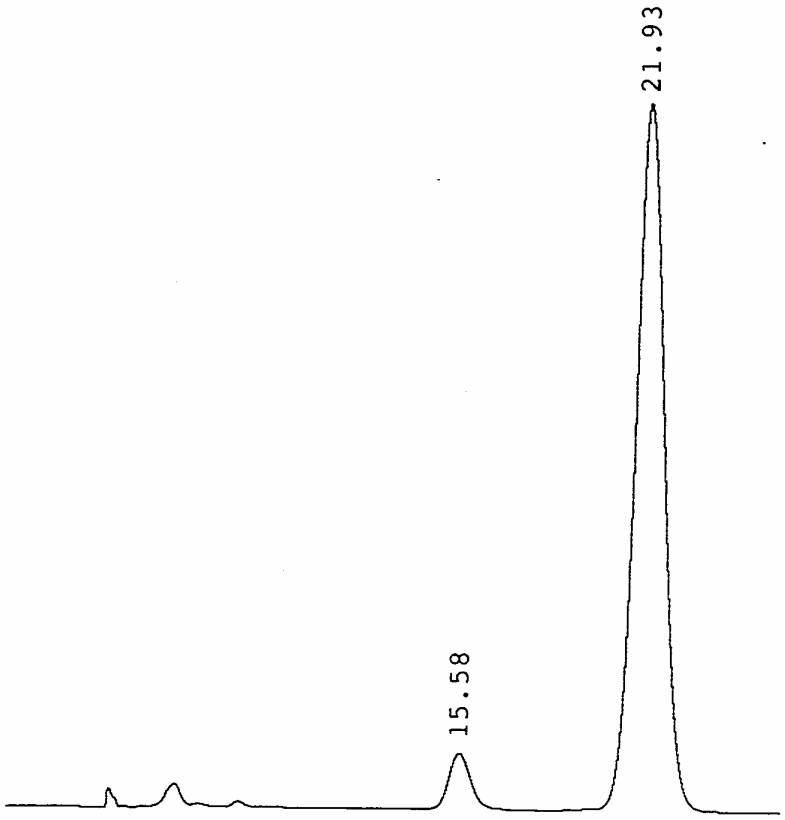

Figure 3-18. HPLC chromatogram for **Entry 13** in **Table 3-2**

No.	R.Time (min.)	Comp.	Height (uV)	Height%	Area (uV.sec)	Area%
1	15.59	Unknown	18212	5.31	755786	3.84
2	22.40	Unknown	324952	94.69	18931430	96.16
Total			343164	100.00	19687216	100.00

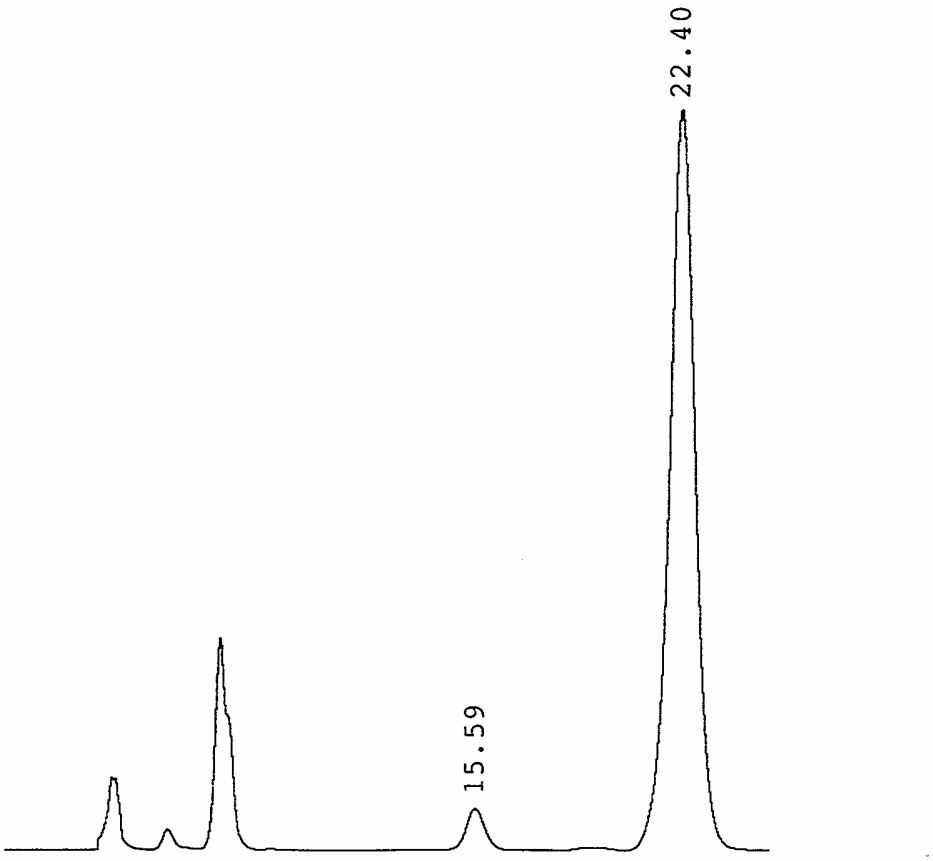

Figure 3-19. HPLC chromatogram for **Entry 18** in **Table 3-2**

No.	R.Time (min.)	Comp.	Height (uV)	Height%	Area (uV.sec)	Area%
1	15.68	Unknown	26816	3.47	1130286	2.39
2	22.53	Unknown	746724	96.53	46067089	97.61
Total			773540	100.00	47197374	100.00

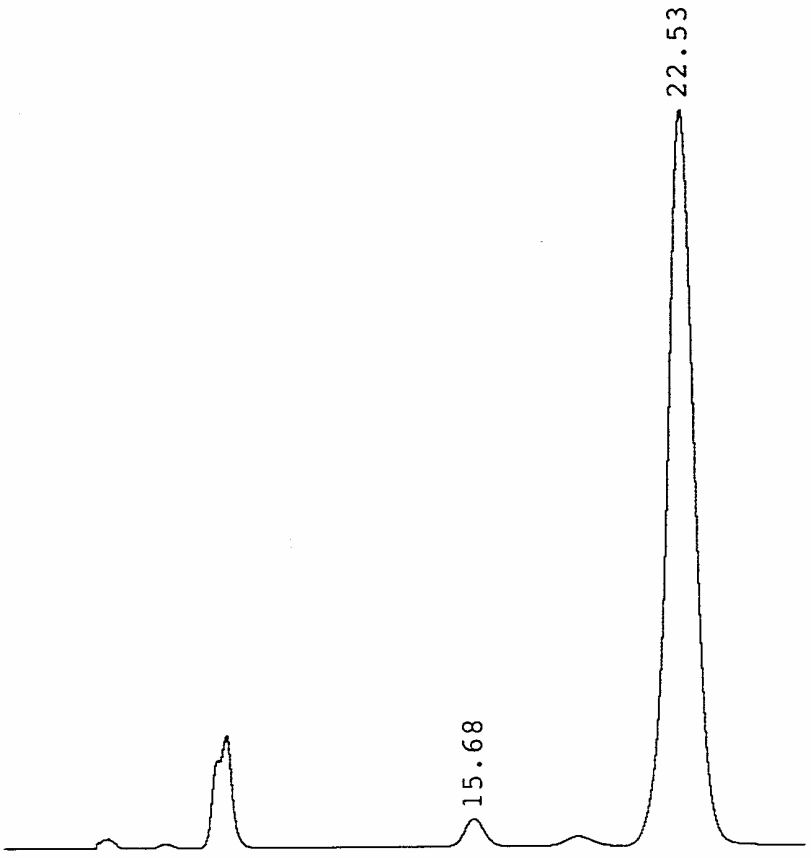

Figure 3-20. HPLC chromatogram for **Entry 19** in **Table 3-2**

Appendix III

X-ray Diffraction Data for Compound

2-2, 2-4, 2-5, (*R*)-2-7, 4-6a

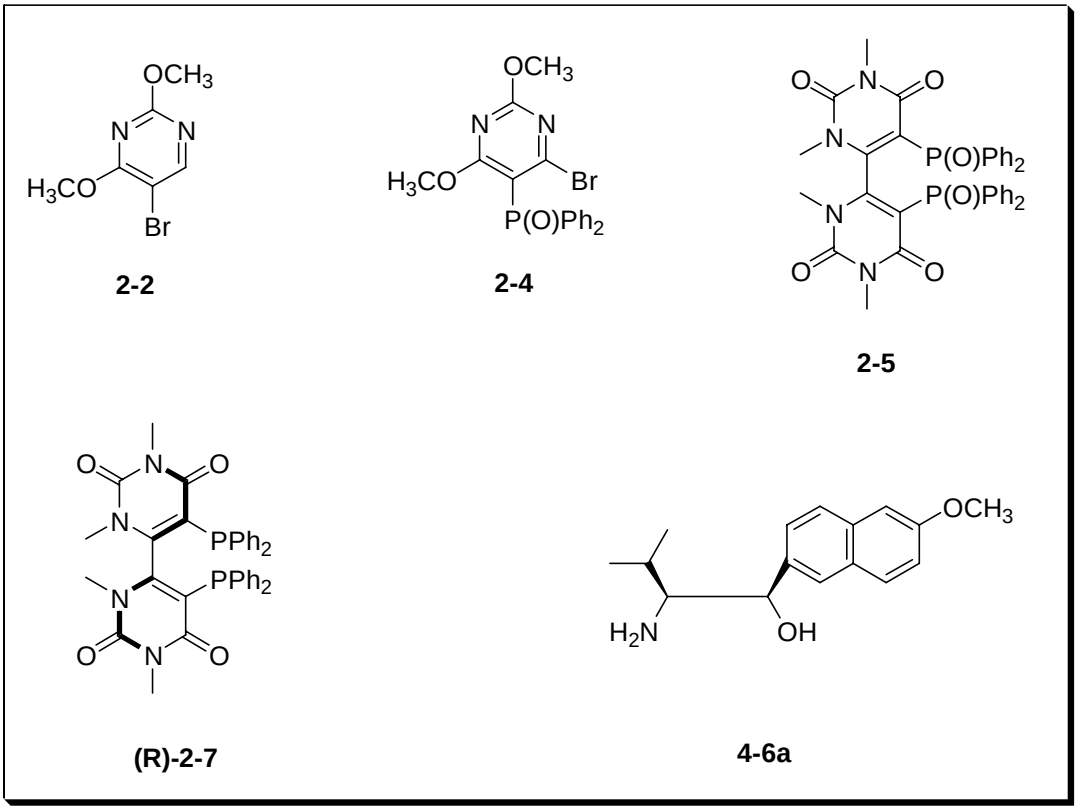

1. X-ray Diffraction Data for Compound 2-2:

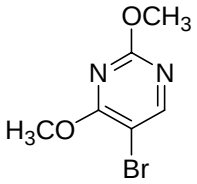

2-2

Table 1. Crystal data and structure refinement for **2-2.**

Identification code	**2-2**	
Empirical formula	$C_6 H_7 Br N_2 O_2$	
Formula weight	219.05	
Temperature	294(2) K	
Wavelength	0.71073 Å	
Crystal system	Orthorhombic	
Space group	Fdd2	
Unit cell dimensions	a = 12.439(6) Å	α= 90°.
	b = 37.312(10) Å	β= 90°.
	c = 6.997(3) Å	γ = 90°.
Volume	3248(2) $Å_3$	
Z	16	
Density (calculated)	1.792 Mg/m_3	
Absorption coefficient	5.014 mm^{-1}	
F(000)	1728	
Crystal size	0.38 x 0.32 x 0.28 mm_3	
Theta range for data collection	2.18 to 27.57°.	
Index ranges	-14<=h<=16, -48<=k<=40, -4<=l<=9	
Reflections collected	5307	
Independent reflections	1485 [R(int) = 0.0654]	
Completeness to theta = 27.57°	99.7 %	
Absorption correction	Semi-empirical from equivalents	
Max. and min. transmission	0.3341 and 0.2517	
Refinement method	Full-matrix least-squares on F_2	
Data / restraints / parameters	1485 / 1 / 100	
Goodness-of-fit on F_2	1.005	
Final R indices [I>2sigma(I)]	R1 = 0.0637, wR2 = 0.1409	
R indices (all data)	R1 = 0.1130, wR2 = 0.1568	
Absolute structure parameter	0.00	
Largest diff. peak and hole	0.995 and -0.506 $e.Å^{-3}$	

Table 2. Atomic coordinates (x 10^4) and equivalent isotropic displacement parameters ($Å^2$x 10^3)
for **2-2**. U(eq) is defined as one third of the trace of the orthogonalized U_{ij} tensor.

	x	y	z	U(eq)
Br(1)	2662(1)	331(1)	4644(1)	75(1)
O(1)	1564(3)	1701(1)	8195(5)	75(1)
O(2)	1458(3)	488(1)	8231(4)	66(1)
N(1)	2375(3)	1413(1)	5690(6)	69(1)
N(2)	1522(3)	1099(1)	8211(5)	60(1)
C(1)	1850(3)	1397(1)	7351(8)	58(1)
C(2)	2628(3)	1091(1)	4894(8)	69(1)
C(3)	2327(3)	769(1)	5740(7)	72(2)
C(4)	1742(3)	795(1)	7501(6)	52(1)
C(5)	1835(3)	2036(1)	7392(9)	73(2)
C(6)	845(4)	517(1)	10001(8)	90(2)

Table 3. Bond lengths [Å] and angles [°] for **2-2**.

Br(1)-C(3)	1.853(5)
O(1)-C(1)	1.329(5)
O(1)-C(5)	1.412(5)
O(2)-C(4)	1.306(4)
O(2)-C(6)	1.459(6)
N(1)-C(1)	1.334(6)
N(1)-C(2)	1.359(6)
N(2)-C(4)	1.267(4)
N(2)-C(1)	1.327(5)
C(2)-C(3)	1.391(6)
C(2)-H(2A)	0.9300
C(3)-C(4)	1.434(7)
C(5)-H(5A)	0.9600
C(5)-H(5B)	0.9600
C(5)-H(5C)	0.9600
C(6)-H(6A)	0.9600
C(6)-H(6D)	0.9600
C(6)-H(6B)	0.9600
C(1)-O(1)-C(5)	121.1(4)
C(4)-O(2)-C(6)	114.1(3)
C(1)-N(1)-C(2)	115.5(4)
C(4)-N(2)-C(1)	120.2(4)
N(2)-C(1)-O(1)	115.5(4)
N(2)-C(1)-N(1)	125.7(4)
O(1)-C(1)-N(1)	118.6(3)
N(1)-C(2)-C(3)	121.7(5)
N(1)-C(2)-H(2A)	119.2
C(3)-C(2)-H(2A)	119.2
C(2)-C(3)-C(4)	116.3(4)
C(2)-C(3)-Br(1)	121.7(4)
C(4)-C(3)-Br(1)	122.0(3)
N(2)-C(4)-O(2)	125.1(4)
N(2)-C(4)-C(3)	120.5(4)
O(2)-C(4)-C(3)	114.4(3)
O(1)-C(5)-H(5A)	109.5
O(1)-C(5)-H(5B)	109.5
H(5A)-C(5)-H(5B)	109.5
O(1)-C(5)-H(5C)	109.5
H(5A)-C(5)-H(5C)	109.5
H(5B)-C(5)-H(5C)	109.5

O(2)-C(6)-H(6A)	109.5
O(2)-C(6)-H(6D)	109.5
H(6A)-C(6)-H(6D)	109.5
O(2)-C(6)-H(6B)	109.5
H(6A)-C(6)-H(6B)	109.5
H(6D)-C(6)-H(6B)	109.5

Symmetry transformations used to generate equivalent atoms:

Table 4. Anisotropic displacement parameters ($Å^2 \times 10^3$) for **2-2.** The anisotropic displacement factor exponent takes the form: $-2\pi^2[h^2 a^{*2} U_{11} + ... + 2 h k a^* b^* U_{12}]$

	U_{11}	U_{22}	U_{33}	U_{23}	U_{13}	U_{12}
Br(1)	68(1)	62(1)	94(1)	-8(1)	15(1)	2(1)
O(1)	89(2)	51(1)	84(2)	-2(1)	14(2)	5(2)
O(2)	74(2)	56(1)	70(2)	1(1)	13(2)	1(1)
N(1)	61(2)	53(2)	92(3)	7(2)	4(2)	4(2)
N(2)	56(2)	50(2)	72(2)	-3(2)	10(2)	4(2)
C(1)	50(2)	50(2)	74(3)	-13(2)	1(2)	2(2)
C(2)	58(2)	75(2)	75(3)	9(3)	-10(3)	-4(2)
C(3)	44(2)	82(3)	89(3)	19(2)	-19(2)	-18(2)
C(4)	48(2)	38(2)	71(3)	3(2)	-6(2)	-4(2)
C(5)	74(3)	45(2)	99(3)	3(3)	12(3)	5(2)
C(6)	122(3)	67(2)	81(3)	8(3)	56(3)	6(3)

Table 5. Hydrogen coordinates (x 10^4) and isotropic displacement parameters ($Å^2$x 10^3) for **2-2**.

	x	y	z	U(eq)
H(2A)	3012	1087	3754	83
H(5A)	1568	2225	8196	109
H(5B)	1518	2056	6145	109
H(5C)	2602	2055	7287	109
H(6A)	668	281	10456	135
H(6D)	196	649	9767	135
H(6B)	1267	639	10945	135

Table 6. Torsion angles [°] for **2-2**.

C(4)-N(2)-C(1)-O(1)	179.0(4)
C(4)-N(2)-C(1)-N(1)	3.2(7)
C(5)-O(1)-C(1)-N(2)	-178.0(4)
C(5)-O(1)-C(1)-N(1)	-1.9(6)
C(2)-N(1)-C(1)-N(2)	-3.4(6)
C(2)-N(1)-C(1)-O(1)	-179.1(4)
C(1)-N(1)-C(2)-C(3)	1.9(6)
N(1)-C(2)-C(3)-C(4)	-0.4(6)
N(1)-C(2)-C(3)-Br(1)	179.5(3)
C(1)-N(2)-C(4)-O(2)	-180.0(4)
C(1)-N(2)-C(4)-C(3)	-1.3(6)
C(6)-O(2)-C(4)-N(2)	-0.1(6)
C(6)-O(2)-C(4)-C(3)	-178.8(4)
C(2)-C(3)-C(4)-N(2)	0.1(6)
Br(1)-C(3)-C(4)-N(2)	-179.8(3)
C(2)-C(3)-C(4)-O(2)	178.9(4)
Br(1)-C(3)-C(4)-O(2)	-1.0(5)

Symmetry transformations used to generate equivalent atoms:

2. X-ray Diffraction Data for Compound 2-4

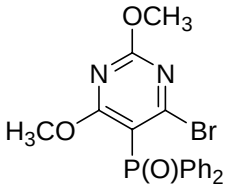

2-4

Table 1. Crystal data and structure refinement for **2-4**.

Identification code	2-4	
Empirical formula	C18 H16 Br N2 O3 P	
Formula weight	419.21	
Temperature	294(2) K	
Wavelength	0.71073 Å	
Crystal system	Triclinic	
Space group	P-1	
Unit cell dimensions	a = 8.2552(11) Å	α= 79.609(3)°.
	b = 8.9731(11) Å	β= 75.669(3)°.
	c = 13.4012(16) Å	γ = 67.786(2)°.
Volume	886.24(19) $Å^3$	
Z	2	
Density (calculated)	1.571 Mg/m^3	
Absorption coefficient	2.429 mm^{-1}	
F(000)	424	
Crystal size	0.30 x 0.28 x 0.24 mm^3	
Theta range for data collection	3.15 to 27.54°.	
Index ranges	-9<=h<=10, -5<=k<=11, -17<=l<=17	
Reflections collected	6072	
Independent reflections	4031 [R(int) = 0.0169]	
Completeness to theta = 27.54°	98.3 %	
Absorption correction	Empirical	
Max. and min. transmission	0.5933 and 0.5294	
Refinement method	Full-matrix least-squares on F^2	
Data / restraints / parameters	4031 / 0 / 226	
Goodness-of-fit on F^2	0.985	
Final R indices [I>2sigma(I)]	R1 = 0.0349, wR2 = 0.0776	
R indices (all data)	R1 = 0.0546, wR2 = 0.0820	
Largest diff. peak and hole	0.400 and -0.301 $e.Å^{-3}$	

Table 2. Atomic coordinates (x 10^4) and equivalent isotropic displacement parameters ($Å^2$x 10^3)
for **2-4**. U(eq) is defined as one third of the trace of the orthogonalized U_{ij} tensor.

	x	y	z	U(eq)
Br(1)	6697(1)	3286(1)	2564(1)	69(1)
P(1)	6466(1)	7328(1)	1927(1)	37(1)
O(1)	6107(2)	6461(2)	1220(1)	51(1)
O(2)	7893(3)	3689(2)	5890(2)	73(1)
O(3)	6921(2)	8410(2)	3772(1)	50(1)
N(1)	7261(3)	3754(2)	4360(2)	54(1)
N(2)	7392(2)	6096(2)	4871(1)	47(1)
C(1)	6730(3)	6193(2)	3194(2)	39(1)
C(2)	6901(3)	4579(3)	3461(2)	45(1)
C(3)	7488(3)	4575(3)	5011(2)	51(1)
C(4)	7009(3)	6879(3)	3971(2)	41(1)
C(5)	8163(4)	4448(4)	6660(2)	80(1)
C(6)	7397(4)	9093(3)	4499(2)	67(1)
C(7)	8562(3)	7653(2)	1439(2)	37(1)
C(8)	8958(3)	8956(3)	1587(2)	44(1)
C(9)	10638(4)	9031(3)	1199(2)	55(1)
C(10)	11945(3)	7801(3)	666(2)	58(1)
C(11)	11573(3)	6514(3)	487(2)	58(1)
C(12)	9891(3)	6436(3)	875(2)	48(1)
C(13)	4717(3)	9256(2)	2137(2)	39(1)
C(14)	3302(3)	9482(3)	2975(2)	46(1)
C(15)	1876(3)	10933(3)	3015(2)	57(1)
C(16)	1869(4)	12154(3)	2229(2)	62(1)
C(17)	3251(4)	11937(3)	1397(2)	67(1)
C(18)	4672(3)	10492(3)	1346(2)	54(1)

Table 3. Bond lengths [Å] and angles [°] for **2-4**.

Br(1)-C(2)	1.889(2)
P(1)-O(1)	1.4738(16)
P(1)-C(13)	1.800(2)
P(1)-C(7)	1.805(2)
P(1)-C(1)	1.832(2)
O(2)-C(3)	1.337(3)
O(2)-C(5)	1.436(4)
O(3)-C(4)	1.329(3)
O(3)-C(6)	1.438(3)
N(1)-C(3)	1.325(3)
N(1)-C(2)	1.334(3)
N(2)-C(3)	1.318(3)
N(2)-C(4)	1.327(3)
C(1)-C(2)	1.389(3)
C(1)-C(4)	1.405(3)
C(5)-H(5A)	0.9600
C(5)-H(5B)	0.9600
C(5)-H(5C)	0.9600
C(6)-H(6A)	0.9600
C(6)-H(6B)	0.9600
C(6)-H(6C)	0.9600
C(7)-C(8)	1.385(3)
C(7)-C(12)	1.396(3)
C(8)-C(9)	1.378(3)
C(8)-H(8A)	0.9300
C(9)-C(10)	1.376(4)
C(9)-H(9A)	0.9300
C(10)-C(11)	1.376(4)
C(10)-H(10A)	0.9300
C(11)-C(12)	1.380(3)
C(11)-H(11A)	0.9300
C(12)-H(12A)	0.9300
C(13)-C(18)	1.385(3)
C(13)-C(14)	1.386(3)
C(14)-C(15)	1.385(3)
C(14)-H(14A)	0.9300
C(15)-C(16)	1.375(4)
C(15)-H(15A)	0.9300
C(16)-C(17)	1.365(4)
C(16)-H(16A)	0.9300
C(17)-C(18)	1.380(3)
C(17)-H(17A)	0.9300

C(18)-H(18A)	0.9300
O(1)-P(1)-C(13)	111.44(9)
O(1)-P(1)-C(7)	111.54(10)
C(13)-P(1)-C(7)	108.69(10)
O(1)-P(1)-C(1)	113.33(9)
C(13)-P(1)-C(1)	107.93(10)
C(7)-P(1)-C(1)	103.50(9)
C(3)-O(2)-C(5)	118.5(2)
C(4)-O(3)-C(6)	118.42(17)
C(3)-N(1)-C(2)	115.3(2)
C(3)-N(2)-C(4)	115.2(2)
C(2)-C(1)-C(4)	112.77(19)
C(2)-C(1)-P(1)	126.38(18)
C(4)-C(1)-P(1)	120.40(15)
N(1)-C(2)-C(1)	124.5(2)
N(1)-C(2)-Br(1)	112.26(17)
C(1)-C(2)-Br(1)	123.28(17)
N(2)-C(3)-N(1)	127.6(2)
N(2)-C(3)-O(2)	119.1(3)
N(1)-C(3)-O(2)	113.3(2)
O(3)-C(4)-N(2)	118.3(2)
O(3)-C(4)-C(1)	117.01(18)
N(2)-C(4)-C(1)	124.7(2)
O(2)-C(5)-H(5A)	109.5
O(2)-C(5)-H(5B)	109.5
H(5A)-C(5)-H(5B)	109.5
O(2)-C(5)-H(5C)	109.5
H(5A)-C(5)-H(5C)	109.5
H(5B)-C(5)-H(5C)	109.5
O(3)-C(6)-H(6A)	109.5
O(3)-C(6)-H(6B)	109.5
H(6A)-C(6)-H(6B)	109.5
O(3)-C(6)-H(6C)	109.5
H(6A)-C(6)-H(6C)	109.5
H(6B)-C(6)-H(6C)	109.5
C(8)-C(7)-C(12)	118.6(2)
C(8)-C(7)-P(1)	126.32(17)
C(12)-C(7)-P(1)	115.10(17)
C(9)-C(8)-C(7)	120.5(2)
C(9)-C(8)-H(8A)	119.8
C(7)-C(8)-H(8A)	119.8
C(10)-C(9)-C(8)	120.2(2)
C(10)-C(9)-H(9A)	119.9

C(8)-C(9)-H(9A)	119.9
C(11)-C(10)-C(9)	120.4(2)
C(11)-C(10)-H(10A)	119.8
C(9)-C(10)-H(10A)	119.8
C(10)-C(11)-C(12)	119.5(2)
C(10)-C(11)-H(11A)	120.3
C(12)-C(11)-H(11A)	120.3
C(11)-C(12)-C(7)	120.8(2)
C(11)-C(12)-H(12A)	119.6
C(7)-C(12)-H(12A)	119.6
C(18)-C(13)-C(14)	119.0(2)
C(18)-C(13)-P(1)	117.38(17)
C(14)-C(13)-P(1)	122.94(16)
C(13)-C(14)-C(15)	119.9(2)
C(13)-C(14)-H(14A)	120.1
C(15)-C(14)-H(14A)	120.1
C(16)-C(15)-C(14)	120.2(2)
C(16)-C(15)-H(15A)	119.9
C(14)-C(15)-H(15A)	119.9
C(17)-C(16)-C(15)	120.4(2)
C(17)-C(16)-H(16A)	119.8
C(15)-C(16)-H(16A)	119.8
C(16)-C(17)-C(18)	120.0(2)
C(16)-C(17)-H(17A)	120.0
C(18)-C(17)-H(17A)	120.0
C(17)-C(18)-C(13)	120.6(2)
C(17)-C(18)-H(18A)	119.7
C(13)-C(18)-H(18A)	119.7

Symmetry transformations used to generate equivalent atoms:

Table 4. Anisotropic displacement parameters ($Å^2 \times 10^3$) for **2-4**. The anisotropic displacement factor exponent takes the form: $-2\pi^2[h^2 a^{*2} U_{11} + ... + 2 h k a^* b^* U_{12}]$

	U_{11}	U_{22}	U_{33}	U_{23}	U_{13}	U_{12}
Br(1)	90(1)	34(1)	85(1)	-7(1)	-22(1)	-21(1)
P(1)	44(1)	29(1)	40(1)	-1(1)	-13(1)	-12(1)
O(1)	62(1)	43(1)	57(1)	-8(1)	-23(1)	-21(1)
O(2)	83(1)	67(1)	64(1)	35(1)	-29(1)	-31(1)
O(3)	74(1)	35(1)	44(1)	2(1)	-24(1)	-19(1)
N(1)	53(1)	39(1)	62(1)	15(1)	-12(1)	-15(1)
N(2)	49(1)	47(1)	41(1)	11(1)	-13(1)	-16(1)
C(1)	39(1)	29(1)	45(1)	1(1)	-9(1)	-10(1)
C(2)	35(1)	35(1)	58(2)	2(1)	-6(1)	-11(1)
C(3)	43(1)	51(2)	50(2)	17(1)	-10(1)	-15(1)
C(4)	38(1)	38(1)	42(1)	3(1)	-9(1)	-10(1)
C(5)	80(2)	102(2)	53(2)	18(2)	-30(2)	-27(2)
C(6)	94(2)	52(2)	64(2)	-8(1)	-32(2)	-25(1)
C(7)	45(1)	33(1)	33(1)	1(1)	-14(1)	-12(1)
C(8)	53(1)	37(1)	45(1)	-3(1)	-13(1)	-18(1)
C(9)	73(2)	55(2)	53(2)	11(1)	-25(1)	-39(1)
C(10)	49(2)	71(2)	52(2)	20(1)	-16(1)	-26(1)
C(11)	54(2)	55(2)	52(2)	1(1)	-2(1)	-12(1)
C(12)	54(1)	42(1)	47(1)	-5(1)	-9(1)	-15(1)
C(13)	44(1)	31(1)	42(1)	2(1)	-17(1)	-11(1)
C(14)	51(1)	42(1)	43(1)	-1(1)	-13(1)	-14(1)
C(15)	48(1)	59(2)	58(2)	-16(1)	-12(1)	-8(1)
C(16)	61(2)	38(1)	80(2)	-6(1)	-28(2)	-1(1)
C(17)	71(2)	40(1)	79(2)	17(1)	-28(2)	-9(1)
C(18)	53(1)	45(1)	54(2)	10(1)	-11(1)	-13(1)

Table 5. Hydrogen coordinates (x 10^4) and isotropic displacement parameters ($Å^2$x 10^3) for **2-4**.

	x	y	z	U(eq)
H(5A)	8448	3674	7245	120
H(5B)	7094	5334	6878	120
H(5C)	9129	4843	6374	120
H(6A)	7277	10197	4258	100
H(6B)	8610	8485	4565	100
H(6C)	6621	9053	5160	100
H(8A)	8083	9787	1952	53
H(9A)	10889	9914	1298	66
H(10A)	13087	7841	426	70
H(11A)	12447	5702	107	70
H(12A)	9640	5562	759	58
H(14A)	3310	8661	3510	55
H(15A)	922	11083	3574	68
H(16A)	918	13132	2265	74
H(17A)	3235	12763	865	80
H(18A)	5608	10347	776	65

Table 6. Torsion angles [°] for **2-4**.

O(1)-P(1)-C(1)-C(2)	10.8(2)
C(13)-P(1)-C(1)-C(2)	134.72(19)
C(7)-P(1)-C(1)-C(2)	-110.18(19)
O(1)-P(1)-C(1)-C(4)	-177.47(16)
C(13)-P(1)-C(1)-C(4)	-53.55(19)
C(7)-P(1)-C(1)-C(4)	61.54(18)
C(3)-N(1)-C(2)-C(1)	-1.1(3)
C(3)-N(1)-C(2)-Br(1)	177.54(16)
C(4)-C(1)-C(2)-N(1)	1.0(3)
P(1)-C(1)-C(2)-N(1)	173.27(17)
C(4)-C(1)-C(2)-Br(1)	-177.50(15)
P(1)-C(1)-C(2)-Br(1)	-5.2(3)
C(4)-N(2)-C(3)-N(1)	0.5(3)
C(4)-N(2)-C(3)-O(2)	179.06(19)
C(2)-N(1)-C(3)-N(2)	0.3(4)
C(2)-N(1)-C(3)-O(2)	-178.32(19)
C(5)-O(2)-C(3)-N(2)	1.6(3)
C(5)-O(2)-C(3)-N(1)	-179.7(2)
C(6)-O(3)-C(4)-N(2)	5.3(3)
C(6)-O(3)-C(4)-C(1)	-173.1(2)
C(3)-N(2)-C(4)-O(3)	-178.87(19)
C(3)-N(2)-C(4)-C(1)	-0.6(3)
C(2)-C(1)-C(4)-O(3)	178.19(18)
P(1)-C(1)-C(4)-O(3)	5.4(3)
C(2)-C(1)-C(4)-N(2)	-0.1(3)
P(1)-C(1)-C(4)-N(2)	-172.88(16)
O(1)-P(1)-C(7)-C(8)	148.05(18)
C(13)-P(1)-C(7)-C(8)	24.8(2)
C(1)-P(1)-C(7)-C(8)	-89.76(19)
O(1)-P(1)-C(7)-C(12)	-33.06(18)
C(13)-P(1)-C(7)-C(12)	-156.32(15)
C(1)-P(1)-C(7)-C(12)	89.13(17)
C(12)-C(7)-C(8)-C(9)	-1.1(3)
P(1)-C(7)-C(8)-C(9)	177.81(16)
C(7)-C(8)-C(9)-C(10)	-0.5(3)
C(8)-C(9)-C(10)-C(11)	2.1(4)
C(9)-C(10)-C(11)-C(12)	-2.1(4)
C(10)-C(11)-C(12)-C(7)	0.5(4)
C(8)-C(7)-C(12)-C(11)	1.0(3)
P(1)-C(7)-C(12)-C(11)	-177.94(17)
O(1)-P(1)-C(13)-C(18)	-75.36(19)
C(7)-P(1)-C(13)-C(18)	47.97(19)

C(1)-P(1)-C(13)-C(18)	159.59(17)
O(1)-P(1)-C(13)-C(14)	95.40(19)
C(7)-P(1)-C(13)-C(14)	-141.28(18)
C(1)-P(1)-C(13)-C(14)	-29.7(2)
C(18)-C(13)-C(14)-C(15)	-0.4(3)
P(1)-C(13)-C(14)-C(15)	-170.97(17)
C(13)-C(14)-C(15)-C(16)	-0.5(4)
C(14)-C(15)-C(16)-C(17)	1.0(4)
C(15)-C(16)-C(17)-C(18)	-0.5(4)
C(16)-C(17)-C(18)-C(13)	-0.4(4)
C(14)-C(13)-C(18)-C(17)	0.8(3)
P(1)-C(13)-C(18)-C(17)	172.0(2)

Symmetry transformations used to generate equivalent atoms:

Table 7. Hydrogen bonds for **2-4** [Å and °].

D-H...A	d(D-H)	d(H...A)	d(D...A)	<(DHA)

3. X-ray Diffraction Data for Compound 2-5

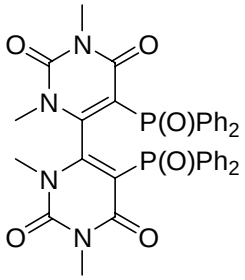

2-5

Table 1. Crystal data and structure refinement for **2-5**.

Identification code	2-5	
Empirical formula	C36 H32 N4 O6 P2	
Formula weight	678.60	
Temperature	294(2) K	
Wavelength	0.71073 Å	
Crystal system	Monoclinic	
Space group	P2(1)/n	
Unit cell dimensions	a = 12.1480(19) Å	α= 90°.
	b = 15.246(2) Å	β= 100.690(4)°.
	c = 17.814(3) Å	γ = 90°.
Volume	3242.2(9) Å^3	
Z	4	
Density (calculated)	1.390 Mg/m^3	
Absorption coefficient	0.188 mm^{-1}	
F(000)	1416	
Crystal size	0.28 x 0.24 x 0.20 mm^3	
Theta range for data collection	2.24 to 27.59°.	
Index ranges	-15<=h<=9, -19<=k<=19, -23<=l<=21	
Reflections collected	22067	
Independent reflections	7488 [R(int) = 0.1594]	
Completeness to theta = 27.59°	99.6 %	
Absorption correction	Semi-empirical from equivalents	
Max. and min. transmission	0.9633 and 0.9491	
Refinement method	Full-matrix least-squares on F^2	
Data / restraints / parameters	7488 / 0 / 437	
Goodness-of-fit on F^2	0.681	
Final R indices [I>2sigma(I)]	R1 = 0.0537, wR2 = 0.0657	
R indices (all data)	R1 = 0.2392, wR2 = 0.0865	
Largest diff. peak and hole	0.253 and -0.335 e.Å^{-3}	

Table 2. Atomic coordinates (x 10^4) and equivalent isotropic displacement parameters ($Å^2$x 10^3)
for **2-5**. U(eq) is defined as one third of the trace of the orthogonalized U_{ij} tensor.

	x	y	z	U(eq)
P(1)	-990(1)	5661(1)	3299(1)	44(1)
P(2)	1145(1)	4598(1)	1686(1)	45(1)
O(1)	-2953(2)	6242(2)	2041(1)	51(1)
O(2)	-2688(2)	4110(2)	303(2)	71(1)
O(3)	190(3)	2619(2)	4315(2)	71(1)
O(4)	2722(2)	3545(2)	2899(2)	62(1)
O(5)	89(2)	5241(2)	3654(1)	50(1)
O(6)	184(2)	5159(2)	1343(1)	54(1)
N(1)	-2764(3)	5205(2)	1151(2)	42(1)
N(2)	-1645(3)	3969(2)	1505(2)	45(1)
N(3)	-423(3)	3389(2)	3239(2)	47(1)
N(4)	1475(3)	3082(2)	3612(2)	48(1)
C(1)	-1579(3)	5135(2)	2397(2)	36(1)
C(2)	-2465(3)	5589(3)	1887(2)	40(1)
C(3)	-2378(4)	4413(3)	933(3)	47(1)
C(4)	-1184(3)	4376(3)	2180(2)	39(1)
C(5)	-195(4)	3899(2)	2640(2)	39(1)
C(6)	423(5)	3005(3)	3770(3)	49(1)
C(7)	1750(4)	3531(3)	2993(2)	42(1)
C(8)	845(4)	3960(2)	2488(2)	33(1)
C(9)	-3558(3)	5664(2)	575(2)	58(1)
C(10)	-1347(3)	3072(2)	1316(2)	63(1)
C(11)	-1572(4)	3285(3)	3391(2)	68(2)
C(12)	2389(3)	2642(2)	4138(2)	73(2)
C(13)	-806(4)	6794(2)	3095(2)	45(1)
C(14)	-811(3)	7425(3)	3656(2)	60(1)
C(15)	-550(4)	8290(3)	3512(3)	76(2)
C(16)	-261(4)	8521(3)	2838(3)	85(2)
C(17)	-238(4)	7902(3)	2287(3)	76(2)
C(18)	-494(4)	7037(3)	2422(2)	58(1)
C(19)	-2026(4)	5532(2)	3898(2)	45(1)
C(20)	-3136(4)	5572(3)	3671(2)	84(2)
C(21)	-3859(4)	5363(4)	4156(3)	116(2)
C(22)	-3453(4)	5156(3)	4907(3)	93(2)
C(23)	-2336(5)	5145(3)	5148(3)	70(2)
C(24)	-1617(4)	5329(3)	4660(2)	63(1)
C(25)	1471(4)	3813(3)	1003(2)	48(1)
C(26)	2339(4)	3218(3)	1139(2)	59(1)

C(27)	2491(4)	2599(3)	582(3)	73(2)
C(28)	1725(5)	2580(3)	-94(3)	83(2)
C(29)	879(5)	3175(4)	-234(3)	82(2)
C(30)	746(4)	3791(3)	304(3)	70(2)
C(31)	2366(4)	5231(2)	2041(2)	44(1)
C(32)	2466(4)	5675(3)	2724(2)	60(1)
C(33)	3385(5)	6205(3)	2965(3)	72(2)
C(34)	4211(4)	6312(3)	2538(3)	73(2)
C(35)	4103(4)	5881(3)	1864(3)	69(2)
C(36)	3199(4)	5336(3)	1615(2)	59(1)

Table 3. Bond lengths [Å] and angles [°] for **2-5**.

P(1)-O(5)	1.491(2)
P(1)-C(13)	1.786(4)
P(1)-C(19)	1.805(4)
P(1)-C(1)	1.820(3)
P(2)-O(6)	1.485(2)
P(2)-C(31)	1.784(4)
P(2)-C(25)	1.802(4)
P(2)-C(8)	1.820(4)
O(1)-C(2)	1.216(4)
O(2)-C(3)	1.208(4)
O(3)-C(6)	1.214(4)
O(4)-C(7)	1.224(4)
N(1)-C(3)	1.376(4)
N(1)-C(2)	1.420(4)
N(1)-C(9)	1.451(4)
N(2)-C(4)	1.377(4)
N(2)-C(3)	1.397(4)
N(2)-C(10)	1.469(4)
N(3)-C(5)	1.389(4)
N(3)-C(6)	1.390(5)
N(3)-C(11)	1.479(4)
N(4)-C(6)	1.364(5)
N(4)-C(7)	1.389(4)
N(4)-C(12)	1.475(4)
C(1)-C(4)	1.337(4)
C(1)-C(2)	1.450(5)
C(4)-C(5)	1.510(5)
C(5)-C(8)	1.344(5)
C(7)-C(8)	1.442(5)
C(9)-H(9A)	0.9600
C(9)-H(9B)	0.9600
C(9)-H(9C)	0.9600
C(10)-H(10A)	0.9600
C(10)-H(10B)	0.9600
C(10)-H(10C)	0.9600
C(11)-H(11A)	0.9600
C(11)-H(11B)	0.9600
C(11)-H(11C)	0.9600
C(12)-H(12A)	0.9600
C(12)-H(12B)	0.9600
C(12)-H(12C)	0.9600

C(13)-C(18)	1.375(5)
C(13)-C(14)	1.388(4)
C(14)-C(15)	1.393(5)
C(14)-H(14A)	0.9300
C(15)-C(16)	1.358(5)
C(15)-H(15A)	0.9300
C(16)-C(17)	1.365(5)
C(16)-H(16A)	0.9300
C(17)-C(18)	1.387(5)
C(17)-H(17A)	0.9300
C(18)-H(18A)	0.9300
C(19)-C(20)	1.335(5)
C(19)-C(24)	1.391(4)
C(20)-C(21)	1.379(5)
C(20)-H(20A)	0.9300
C(21)-C(22)	1.374(5)
C(21)-H(21A)	0.9300
C(22)-C(23)	1.345(6)
C(22)-H(22A)	0.9300
C(23)-C(24)	1.372(5)
C(23)-H(23A)	0.9300
C(24)-H(24A)	0.9300
C(25)-C(26)	1.378(5)
C(25)-C(30)	1.385(5)
C(26)-C(27)	1.406(5)
C(26)-H(26A)	0.9300
C(27)-C(28)	1.378(5)
C(27)-H(27A)	0.9300
C(28)-C(29)	1.359(6)
C(28)-H(28A)	0.9300
C(29)-C(30)	1.373(5)
C(29)-H(29A)	0.9300
C(30)-H(30A)	0.9300
C(31)-C(32)	1.378(5)
C(31)-C(36)	1.383(5)
C(32)-C(33)	1.381(5)
C(32)-H(32A)	0.9300
C(33)-C(34)	1.376(5)
C(33)-H(33A)	0.9300
C(34)-C(35)	1.354(5)
C(34)-H(34A)	0.9300
C(35)-C(36)	1.383(5)
C(35)-H(35A)	0.9300
C(36)-H(36A)	0.9300

O(5)-P(1)-C(13)	111.61(19)
O(5)-P(1)-C(19)	110.93(18)
C(13)-P(1)-C(19)	110.69(19)
O(5)-P(1)-C(1)	110.80(17)
C(13)-P(1)-C(1)	106.89(19)
C(19)-P(1)-C(1)	105.69(19)
O(6)-P(2)-C(31)	111.88(17)
O(6)-P(2)-C(25)	111.05(19)
C(31)-P(2)-C(25)	109.1(2)
O(6)-P(2)-C(8)	111.96(19)
C(31)-P(2)-C(8)	106.56(19)
C(25)-P(2)-C(8)	106.05(17)
C(3)-N(1)-C(2)	125.4(4)
C(3)-N(1)-C(9)	116.1(3)
C(2)-N(1)-C(9)	118.5(3)
C(4)-N(2)-C(3)	121.3(4)
C(4)-N(2)-C(10)	122.8(4)
C(3)-N(2)-C(10)	115.8(3)
C(5)-N(3)-C(6)	122.0(4)
C(5)-N(3)-C(11)	122.0(4)
C(6)-N(3)-C(11)	115.8(4)
C(6)-N(4)-C(7)	125.3(4)
C(6)-N(4)-C(12)	117.0(4)
C(7)-N(4)-C(12)	117.7(4)
C(4)-C(1)-C(2)	119.8(4)
C(4)-C(1)-P(1)	122.3(3)
C(2)-C(1)-P(1)	117.9(3)
O(1)-C(2)-N(1)	119.6(4)
O(1)-C(2)-C(1)	125.8(4)
N(1)-C(2)-C(1)	114.5(4)
O(2)-C(3)-N(1)	122.3(4)
O(2)-C(3)-N(2)	122.6(4)
N(1)-C(3)-N(2)	115.1(4)
C(1)-C(4)-N(2)	122.2(4)
C(1)-C(4)-C(5)	123.5(4)
N(2)-C(4)-C(5)	114.3(4)
C(8)-C(5)-N(3)	121.5(4)
C(8)-C(5)-C(4)	122.7(4)
N(3)-C(5)-C(4)	115.8(4)
O(3)-C(6)-N(4)	125.0(5)
O(3)-C(6)-N(3)	119.7(5)
N(4)-C(6)-N(3)	115.2(4)
O(4)-C(7)-N(4)	119.8(4)

O(4)-C(7)-C(8)	123.4(4)
N(4)-C(7)-C(8)	116.8(4)
C(5)-C(8)-C(7)	118.6(4)
C(5)-C(8)-P(2)	121.9(3)
C(7)-C(8)-P(2)	119.5(3)
N(1)-C(9)-H(9A)	109.5
N(1)-C(9)-H(9B)	109.5
H(9A)-C(9)-H(9B)	109.5
N(1)-C(9)-H(9C)	109.5
H(9A)-C(9)-H(9C)	109.5
H(9B)-C(9)-H(9C)	109.5
N(2)-C(10)-H(10A)	109.5
N(2)-C(10)-H(10B)	109.5
H(10A)-C(10)-H(10B)	109.5
N(2)-C(10)-H(10C)	109.5
H(10A)-C(10)-H(10C)	109.5
H(10B)-C(10)-H(10C)	109.5
N(3)-C(11)-H(11A)	109.5
N(3)-C(11)-H(11B)	109.5
H(11A)-C(11)-H(11B)	109.5
N(3)-C(11)-H(11C)	109.5
H(11A)-C(11)-H(11C)	109.5
H(11B)-C(11)-H(11C)	109.5
N(4)-C(12)-H(12A)	109.5
N(4)-C(12)-H(12B)	109.5
H(12A)-C(12)-H(12B)	109.5
N(4)-C(12)-H(12C)	109.5
H(12A)-C(12)-H(12C)	109.5
H(12B)-C(12)-H(12C)	109.5
C(18)-C(13)-C(14)	118.7(4)
C(18)-C(13)-P(1)	120.2(3)
C(14)-C(13)-P(1)	120.4(3)
C(13)-C(14)-C(15)	119.5(4)
C(13)-C(14)-H(14A)	120.3
C(15)-C(14)-H(14A)	120.3
C(16)-C(15)-C(14)	120.9(5)
C(16)-C(15)-H(15A)	119.6
C(14)-C(15)-H(15A)	119.6
C(15)-C(16)-C(17)	120.0(5)
C(15)-C(16)-H(16A)	120.0
C(17)-C(16)-H(16A)	120.0
C(16)-C(17)-C(18)	119.8(5)
C(16)-C(17)-H(17A)	120.1
C(18)-C(17)-H(17A)	120.1

C(13)-C(18)-C(17)	121.0(4)
C(13)-C(18)-H(18A)	119.5
C(17)-C(18)-H(18A)	119.5
C(20)-C(19)-C(24)	117.6(4)
C(20)-C(19)-P(1)	126.3(4)
C(24)-C(19)-P(1)	116.0(3)
C(19)-C(20)-C(21)	121.7(4)
C(19)-C(20)-H(20A)	119.2
C(21)-C(20)-H(20A)	119.2
C(22)-C(21)-C(20)	120.5(5)
C(22)-C(21)-H(21A)	119.7
C(20)-C(21)-H(21A)	119.7
C(23)-C(22)-C(21)	118.2(5)
C(23)-C(22)-H(22A)	120.9
C(21)-C(22)-H(22A)	120.9
C(22)-C(23)-C(24)	121.2(5)
C(22)-C(23)-H(23A)	119.4
C(24)-C(23)-H(23A)	119.4
C(23)-C(24)-C(19)	120.7(4)
C(23)-C(24)-H(24A)	119.7
C(19)-C(24)-H(24A)	119.7
C(26)-C(25)-C(30)	118.7(4)
C(26)-C(25)-P(2)	125.0(4)
C(30)-C(25)-P(2)	116.2(4)
C(25)-C(26)-C(27)	120.9(4)
C(25)-C(26)-H(26A)	119.6
C(27)-C(26)-H(26A)	119.6
C(28)-C(27)-C(26)	118.4(5)
C(28)-C(27)-H(27A)	120.8
C(26)-C(27)-H(27A)	120.8
C(29)-C(28)-C(27)	120.8(5)
C(29)-C(28)-H(28A)	119.6
C(27)-C(28)-H(28A)	119.6
C(28)-C(29)-C(30)	120.7(5)
C(28)-C(29)-H(29A)	119.7
C(30)-C(29)-H(29A)	119.7
C(29)-C(30)-C(25)	120.5(5)
C(29)-C(30)-H(30A)	119.7
C(25)-C(30)-H(30A)	119.7
C(32)-C(31)-C(36)	118.3(4)
C(32)-C(31)-P(2)	120.7(4)
C(36)-C(31)-P(2)	120.8(3)
C(31)-C(32)-C(33)	119.7(5)
C(31)-C(32)-H(32A)	120.1

C(33)-C(32)-H(32A)	120.1
C(34)-C(33)-C(32)	121.9(5)
C(34)-C(33)-H(33A)	119.0
C(32)-C(33)-H(33A)	119.0
C(35)-C(34)-C(33)	118.1(5)
C(35)-C(34)-H(34A)	120.9
C(33)-C(34)-H(34A)	120.9
C(34)-C(35)-C(36)	121.1(5)
C(34)-C(35)-H(35A)	119.4
C(36)-C(35)-H(35A)	119.4
C(31)-C(36)-C(35)	120.8(4)
C(31)-C(36)-H(36A)	119.6
C(35)-C(36)-H(36A)	119.6

Symmetry transformations used to generate equivalent atoms:

Table 4. Anisotropic displacement parameters ($Å^2 \times 10^3$) for **2-5**. The anisotropic displacement factor exponent takes the form: $-2\pi^2[h^2 a^{*2} U_{11} + ... + 2 h k a^* b^* U_{12}]$

	U_{11}	U_{22}	U_{33}	U_{23}	U_{13}	U_{12}
P(1)	42(1)	51(1)	39(1)	-7(1)	4(1)	3(1)
P(2)	47(1)	51(1)	39(1)	5(1)	12(1)	3(1)
O(1)	53(2)	52(2)	45(2)	0(2)	2(2)	16(2)
O(2)	91(3)	74(2)	41(2)	-24(2)	-7(2)	-4(2)
O(3)	85(3)	74(2)	58(2)	23(2)	21(2)	-5(2)
O(4)	48(2)	77(2)	62(2)	19(2)	14(2)	18(2)
O(5)	34(2)	67(2)	44(2)	-7(1)	-3(2)	17(2)
O(6)	47(2)	63(2)	49(2)	19(2)	4(2)	18(2)
N(1)	38(2)	45(2)	41(2)	2(2)	0(2)	-2(2)
N(2)	47(3)	32(2)	55(3)	-7(2)	7(2)	0(2)
N(3)	56(3)	39(2)	48(3)	5(2)	18(2)	4(2)
N(4)	51(3)	45(2)	44(2)	11(2)	0(2)	9(2)
C(1)	38(3)	38(3)	31(2)	-4(2)	1(2)	3(2)
C(2)	37(3)	42(3)	38(3)	5(2)	0(2)	-3(2)
C(3)	44(3)	40(3)	56(3)	4(3)	12(3)	4(3)
C(4)	36(3)	45(3)	36(3)	-5(2)	8(2)	-2(2)
C(5)	50(3)	26(3)	41(3)	-1(2)	13(3)	11(2)
C(6)	67(4)	30(3)	49(3)	3(2)	14(3)	2(3)
C(7)	42(3)	45(3)	42(3)	1(2)	13(3)	0(3)
C(8)	37(3)	37(3)	26(2)	3(2)	10(2)	11(2)
C(9)	68(4)	61(3)	42(3)	12(2)	-3(3)	8(3)
C(10)	71(4)	39(3)	77(3)	-14(2)	8(3)	-2(3)
C(11)	62(4)	64(3)	86(4)	7(3)	30(3)	-9(3)
C(12)	76(4)	71(3)	63(3)	25(3)	-14(3)	10(3)
C(13)	47(3)	44(3)	44(3)	-5(2)	11(3)	-6(2)
C(14)	53(4)	59(3)	70(4)	-13(3)	16(3)	4(3)
C(15)	62(4)	58(4)	109(5)	-37(3)	20(4)	-5(3)
C(16)	69(5)	60(4)	124(6)	-16(4)	13(4)	-18(3)
C(17)	75(4)	72(4)	79(4)	3(3)	11(3)	-19(3)
C(18)	65(4)	49(3)	64(3)	-9(3)	18(3)	-18(3)
C(19)	38(3)	51(3)	47(3)	-1(2)	8(3)	1(3)
C(20)	42(4)	154(5)	55(3)	35(3)	7(3)	8(4)
C(21)	41(4)	232(7)	76(4)	73(4)	12(3)	5(4)
C(22)	56(4)	152(5)	76(4)	27(4)	25(4)	-13(4)
C(23)	66(4)	94(4)	49(3)	11(3)	12(3)	-2(4)
C(24)	41(3)	98(4)	50(3)	-3(3)	7(3)	4(3)

C(25)	50(3)	52(3)	45(3)	-5(3)	15(3)	-4(3)
C(26)	61(4)	62(3)	56(3)	-5(3)	19(3)	1(3)
C(27)	74(4)	54(3)	100(5)	-11(3)	40(4)	1(3)
C(28)	112(6)	83(5)	59(4)	-25(4)	26(4)	-21(4)
C(29)	99(5)	91(5)	52(4)	-10(3)	4(4)	11(4)
C(30)	80(4)	83(4)	48(3)	-11(3)	11(3)	6(3)
C(31)	50(3)	47(3)	37(3)	5(2)	13(3)	1(3)
C(32)	66(4)	62(3)	53(3)	0(3)	17(3)	0(3)
C(33)	89(5)	60(4)	60(4)	-15(3)	-4(4)	-9(4)
C(34)	71(5)	51(4)	92(4)	-4(3)	5(4)	-9(3)
C(35)	64(4)	54(4)	96(4)	12(3)	31(4)	-5(3)
C(36)	67(4)	51(3)	63(3)	-2(3)	20(3)	-6(3)

Table 5. Hydrogen coordinates (x 10^4) and isotropic displacement parameters ($Å^2$x 10^3) for **2-5**.

	x	y	z	U(eq)
H(9A)	-3356	5582	83	87
H(9B)	-3545	6279	694	87
H(9C)	-4297	5437	566	87
H(10A)	-1269	2711	1764	94
H(10B)	-652	3082	1133	94
H(10C)	-1926	2838	926	94
H(11A)	-2104	3428	2938	103
H(11B)	-1676	3671	3798	103
H(11C)	-1683	2690	3535	103
H(12A)	2080	2206	4427	110
H(12B)	2796	3067	4479	110
H(12C)	2887	2367	3849	110
H(14A)	-988	7270	4125	72
H(15A)	-574	8717	3882	91
H(16A)	-78	9100	2752	102
H(17A)	-52	8061	1822	91
H(18A)	-453	6615	2051	70
H(20A)	-3428	5747	3174	101
H(21A)	-4627	5361	3974	139
H(22A)	-3937	5028	5240	112
H(23A)	-2045	5009	5655	83
H(24A)	-848	5319	4840	76
H(26A)	2831	3226	1606	71
H(27A)	3093	2212	667	88
H(28A)	1788	2155	-458	100
H(29A)	385	3166	-700	98
H(30A)	166	4195	199	84
H(32A)	1916	5618	3021	72
H(33A)	3449	6497	3429	86
H(34A)	4826	6670	2708	87
H(35A)	4645	5953	1563	83
H(36A)	3151	5037	1155	71

Table 6. Torsion angles [°] for **2-5**.

O(5)-P(1)-C(1)-C(4)	11.7(4)
C(13)-P(1)-C(1)-C(4)	133.5(3)
C(19)-P(1)-C(1)-C(4)	-108.6(4)
O(5)-P(1)-C(1)-C(2)	-164.9(3)
C(13)-P(1)-C(1)-C(2)	-43.1(4)
C(19)-P(1)-C(1)-C(2)	74.9(3)
C(3)-N(1)-C(2)-O(1)	-171.8(4)
C(9)-N(1)-C(2)-O(1)	7.0(5)
C(3)-N(1)-C(2)-C(1)	7.7(5)
C(9)-N(1)-C(2)-C(1)	-173.5(3)
C(4)-C(1)-C(2)-O(1)	173.8(4)
P(1)-C(1)-C(2)-O(1)	-9.6(6)
C(4)-C(1)-C(2)-N(1)	-5.7(5)
P(1)-C(1)-C(2)-N(1)	171.0(2)
C(2)-N(1)-C(3)-O(2)	177.9(4)
C(9)-N(1)-C(3)-O(2)	-0.9(6)
C(2)-N(1)-C(3)-N(2)	0.9(6)
C(9)-N(1)-C(3)-N(2)	-177.9(3)
C(4)-N(2)-C(3)-O(2)	170.9(4)
C(10)-N(2)-C(3)-O(2)	-5.1(6)
C(4)-N(2)-C(3)-N(1)	-12.1(5)
C(10)-N(2)-C(3)-N(1)	171.9(3)
C(2)-C(1)-C(4)-N(2)	-4.9(6)
P(1)-C(1)-C(4)-N(2)	178.6(3)
C(2)-C(1)-C(4)-C(5)	174.3(4)
P(1)-C(1)-C(4)-C(5)	-2.2(6)
C(3)-N(2)-C(4)-C(1)	14.6(6)
C(10)-N(2)-C(4)-C(1)	-169.7(4)
C(3)-N(2)-C(4)-C(5)	-164.7(4)
C(10)-N(2)-C(4)-C(5)	11.1(5)
C(6)-N(3)-C(5)-C(8)	8.3(6)
C(11)-N(3)-C(5)-C(8)	-177.3(4)
C(6)-N(3)-C(5)-C(4)	-171.5(4)
C(11)-N(3)-C(5)-C(4)	2.9(5)
C(1)-C(4)-C(5)-C(8)	-98.3(5)
N(2)-C(4)-C(5)-C(8)	80.9(5)
C(1)-C(4)-C(5)-N(3)	81.4(5)
N(2)-C(4)-C(5)-N(3)	-99.3(4)
C(7)-N(4)-C(6)-O(3)	-179.3(4)
C(12)-N(4)-C(6)-O(3)	1.6(6)
C(7)-N(4)-C(6)-N(3)	2.5(6)

C(12)-N(4)-C(6)-N(3)	-176.7(3)
C(5)-N(3)-C(6)-O(3)	174.6(4)
C(11)-N(3)-C(6)-O(3)	-0.2(6)
C(5)-N(3)-C(6)-N(4)	-7.1(6)
C(11)-N(3)-C(6)-N(4)	178.2(3)
C(6)-N(4)-C(7)-O(4)	-178.7(4)
C(12)-N(4)-C(7)-O(4)	0.5(6)
C(6)-N(4)-C(7)-C(8)	1.1(6)
C(12)-N(4)-C(7)-C(8)	-179.7(3)
N(3)-C(5)-C(8)-C(7)	-4.3(6)
C(4)-C(5)-C(8)-C(7)	175.5(3)
N(3)-C(5)-C(8)-P(2)	178.0(3)
C(4)-C(5)-C(8)-P(2)	-2.3(5)
O(4)-C(7)-C(8)-C(5)	179.5(4)
N(4)-C(7)-C(8)-C(5)	-0.2(5)
O(4)-C(7)-C(8)-P(2)	-2.6(6)
N(4)-C(7)-C(8)-P(2)	177.6(3)
O(6)-P(2)-C(8)-C(5)	11.5(4)
C(31)-P(2)-C(8)-C(5)	134.1(3)
C(25)-P(2)-C(8)-C(5)	-109.8(3)
O(6)-P(2)-C(8)-C(7)	-166.3(3)
C(31)-P(2)-C(8)-C(7)	-43.7(3)
C(25)-P(2)-C(8)-C(7)	72.4(3)
O(5)-P(1)-C(13)-C(18)	85.5(4)
C(19)-P(1)-C(13)-C(18)	-150.4(4)
C(1)-P(1)-C(13)-C(18)	-35.8(4)
O(5)-P(1)-C(13)-C(14)	-84.9(4)
C(19)-P(1)-C(13)-C(14)	39.2(4)
C(1)-P(1)-C(13)-C(14)	153.9(4)
C(18)-C(13)-C(14)-C(15)	2.8(7)
P(1)-C(13)-C(14)-C(15)	173.3(3)
C(13)-C(14)-C(15)-C(16)	-1.8(8)
C(14)-C(15)-C(16)-C(17)	0.9(9)
C(15)-C(16)-C(17)-C(18)	-1.0(8)
C(14)-C(13)-C(18)-C(17)	-3.0(7)
P(1)-C(13)-C(18)-C(17)	-173.5(3)
C(16)-C(17)-C(18)-C(13)	2.1(8)
O(5)-P(1)-C(19)-C(20)	-157.6(4)
C(13)-P(1)-C(19)-C(20)	77.9(5)
C(1)-P(1)-C(19)-C(20)	-37.5(5)
O(5)-P(1)-C(19)-C(24)	19.1(4)
C(13)-P(1)-C(19)-C(24)	-105.3(3)
C(1)-P(1)-C(19)-C(24)	139.3(3)
C(24)-C(19)-C(20)-C(21)	-4.4(8)

P(1)-C(19)-C(20)-C(21)	172.3(4)
C(19)-C(20)-C(21)-C(22)	4.1(9)
C(20)-C(21)-C(22)-C(23)	-1.6(9)
C(21)-C(22)-C(23)-C(24)	-0.3(9)
C(22)-C(23)-C(24)-C(19)	-0.2(8)
C(20)-C(19)-C(24)-C(23)	2.5(7)
P(1)-C(19)-C(24)-C(23)	-174.5(3)
O(6)-P(2)-C(25)-C(26)	177.9(4)
C(31)-P(2)-C(25)-C(26)	54.2(4)
C(8)-P(2)-C(25)-C(26)	-60.2(4)
O(6)-P(2)-C(25)-C(30)	-5.4(4)
C(31)-P(2)-C(25)-C(30)	-129.2(3)
C(8)-P(2)-C(25)-C(30)	116.4(3)
C(30)-C(25)-C(26)-C(27)	0.0(6)
P(2)-C(25)-C(26)-C(27)	176.6(3)
C(25)-C(26)-C(27)-C(28)	-2.4(7)
C(26)-C(27)-C(28)-C(29)	3.5(8)
C(27)-C(28)-C(29)-C(30)	-2.2(9)
C(28)-C(29)-C(30)-C(25)	-0.3(8)
C(26)-C(25)-C(30)-C(29)	1.3(7)
P(2)-C(25)-C(30)-C(29)	-175.5(4)
O(6)-P(2)-C(31)-C(32)	77.2(4)
C(25)-P(2)-C(31)-C(32)	-159.5(3)
C(8)-P(2)-C(31)-C(32)	-45.5(4)
O(6)-P(2)-C(31)-C(36)	-98.4(4)
C(25)-P(2)-C(31)-C(36)	24.9(4)
C(8)-P(2)-C(31)-C(36)	139.0(3)
C(36)-C(31)-C(32)-C(33)	-0.3(6)
P(2)-C(31)-C(32)-C(33)	-176.0(3)
C(31)-C(32)-C(33)-C(34)	0.6(7)
C(32)-C(33)-C(34)-C(35)	0.1(8)
C(33)-C(34)-C(35)-C(36)	-1.1(7)
C(32)-C(31)-C(36)-C(35)	-0.7(7)
P(2)-C(31)-C(36)-C(35)	175.0(3)
C(34)-C(35)-C(36)-C(31)	1.4(7)

Symmetry transformations used to generate equivalent atoms:

4. X-ray Diffraction Data for Compound (R)-2-7：

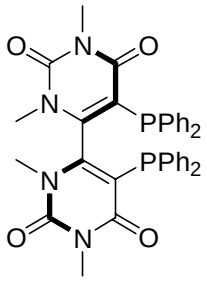

(R)-2-7

Table 1. Crystal data and structure refinement for **(R)-2-7**.

Identification code	(R)-2-7	
Empirical formula	C38 H34 Cl6 N4 O4 P2	
Formula weight	885.33	
Temperature	294(2) K	
Wavelength	0.71073 Å	
Crystal system	Monoclinic	
Space group	C2	
Unit cell dimensions	a = 22.527(5) Å	α= 90°.
	b = 8.2136(19) Å	β= 108.475(5)°.
	c = 11.826(3) Å	γ = 90°.
Volume	2075.4(8) Å^3	
Z	2	
Density (calculated)	1.417 Mg/m^3	
Absorption coefficient	0.535 mm^{-1}	
F(000)	908	
Crystal size	0.40 x 0.14 x 0.10 mm^3	
Theta range for data collection	3.04 to 27.52°.	
Index ranges	-23<=h<=29, -10<=k<=10, -15<=l<=10	
Reflections collected	7058	
Independent reflections	4565 [R(int) = 0.0264]	
Completeness to theta = 27.52°	99.1 %	
Absorption correction	Empirical	
Max. and min. transmission	0.9484 and 0.8144	
Refinement method	Full-matrix least-squares on F_2	
Data / restraints / parameters	4565 / 37 / 257	
Goodness-of-fit on F_2	1.036	
Final R indices [I>2sigma(I)]	R1 = 0.0661, wR2 = 0.1748	
R indices (all data)	R1 = 0.0908, wR2 = 0.1902	
Absolute structure parameter	-0.08(13)	
Largest diff. peak and hole	0.734 and -0.411 e.Å^{-3}	

Table 2. Atomic coordinates (x 10^4) and equivalent isotropic displacement parameters ($Å^2$x 10^3)
for **(R)-2-7**. U(eq) is defined as one third of the trace of the orthogonalized U_{ij} tensor.

	x	y	z	U(eq)
P(1)	4337(1)	1497(1)	8292(1)	40(1)
O(1)	3133(1)	2214(4)	9154(3)	50(1)
O(2)	4142(2)	5280(4)	12373(3)	61(1)
N(1)	3653(2)	3639(5)	10807(3)	42(1)
N(2)	4655(1)	4686(4)	11044(3)	36(1)
C(1)	4206(2)	2796(5)	9462(3)	34(1)
C(2)	3622(2)	2845(5)	9749(3)	37(1)
C(3)	4150(2)	4565(5)	11475(4)	41(1)
C(4)	4695(2)	3725(5)	10121(3)	32(1)
C(5)	3104(2)	3569(8)	11216(5)	69(2)
C(6)	5133(2)	5921(6)	11629(4)	48(1)
C(7)	3887(2)	-313(5)	8389(3)	40(1)
C(8)	3905(2)	-957(5)	9483(4)	54(1)
C(9)	3589(2)	-2365(5)	9556(5)	62(1)
C(10)	3281(2)	-3218(6)	8543(5)	68(2)
C(11)	3259(3)	-2632(6)	7452(5)	68(2)
C(12)	3564(2)	-1187(5)	7376(4)	56(1)
C(13)	3872(2)	2483(5)	6893(4)	46(1)
C(14)	3233(2)	2724(7)	6547(4)	62(1)
C(15)	2928(3)	3495(8)	5485(4)	88(2)
C(16)	3247(3)	4086(7)	4747(5)	82(2)
C(17)	3878(3)	3800(9)	5072(5)	92(2)
C(18)	4194(3)	3008(7)	6136(4)	73(2)
C(19)	3943(2)	-1317(9)	3286(4)	87(2)
Cl(1)	4430(2)	-156(6)	2730(4)	83(1)
Cl(2)	3159(1)	-1504(6)	2354(4)	91(1)
Cl(3)	4002(4)	-858(9)	4735(5)	162(3)
Cl(1')	4316(4)	279(9)	2868(8)	130(3)
Cl(2')	3184(4)	-836(18)	2743(11)	242(6)
Cl(3')	4152(4)	-1793(11)	4757(7)	160(3)

Table 3. Bond lengths [Å] and angles [°] for **(R)-2-7**.

P(1)-C(7)	1.822(4)
P(1)-C(13)	1.842(4)
P(1)-C(1)	1.844(4)
O(1)-C(2)	1.219(5)
O(2)-C(3)	1.219(5)
N(1)-C(3)	1.378(5)
N(1)-C(2)	1.393(5)
N(1)-C(5)	1.463(5)
N(2)-C(4)	1.373(5)
N(2)-C(3)	1.389(5)
N(2)-C(6)	1.482(5)
C(1)-C(4)	1.364(5)
C(1)-C(2)	1.458(5)
C(4)-C(4)#1	1.489(7)
C(5)-H(5A)	0.9600
C(5)-H(5B)	0.9600
C(5)-H(5C)	0.9600
C(6)-H(6A)	0.9600
C(6)-H(6B)	0.9600
C(6)-H(6C)	0.9600
C(7)-C(8)	1.387(5)
C(7)-C(12)	1.389(5)
C(8)-C(9)	1.375(5)
C(8)-H(8)	0.9300
C(9)-C(10)	1.372(6)
C(9)-H(9)	0.9300
C(10)-C(11)	1.362(6)
C(10)-H(10)	0.9300
C(11)-C(12)	1.389(5)
C(11)-H(11)	0.9300
C(12)-H(12)	0.9300
C(13)-C(14)	1.381(5)
C(13)-C(18)	1.386(5)
C(14)-C(15)	1.379(5)
C(14)-H(14)	0.9300
C(15)-C(16)	1.381(6)
C(15)-H(15)	0.9300
C(16)-C(17)	1.371(6)
C(16)-H(16)	0.9300
C(17)-C(18)	1.395(6)
C(17)-H(17)	0.9300

C(18)-H(18)	0.9300
C(19)-Cl(3)	1.719(5)
C(19)-Cl(1)	1.732(5)
C(19)-Cl(2)	1.768(5)
C(19)-H(19A)	0.9601
Cl(3')-H(19A)	1.7281

C(7)-P(1)-C(13)	104.27(17)
C(7)-P(1)-C(1)	101.57(17)
C(13)-P(1)-C(1)	103.86(18)
C(3)-N(1)-C(2)	124.9(3)
C(3)-N(1)-C(5)	116.8(4)
C(2)-N(1)-C(5)	118.2(4)
C(4)-N(2)-C(3)	121.2(3)
C(4)-N(2)-C(6)	122.9(3)
C(3)-N(2)-C(6)	115.8(3)
C(4)-C(1)-C(2)	118.5(3)
C(4)-C(1)-P(1)	117.4(3)
C(2)-C(1)-P(1)	124.1(3)
O(1)-C(2)-N(1)	119.7(3)
O(1)-C(2)-C(1)	124.8(4)
N(1)-C(2)-C(1)	115.5(3)
O(2)-C(3)-N(1)	122.1(4)
O(2)-C(3)-N(2)	121.7(4)
N(1)-C(3)-N(2)	116.2(3)
C(1)-C(4)-N(2)	122.0(3)
C(1)-C(4)-C(4)#1	121.2(3)
N(2)-C(4)-C(4)#1	116.7(3)
N(1)-C(5)-H(5A)	109.5
N(1)-C(5)-H(5B)	109.5
H(5A)-C(5)-H(5B)	109.5
N(1)-C(5)-H(5C)	109.5
H(5A)-C(5)-H(5C)	109.5
H(5B)-C(5)-H(5C)	109.5
N(2)-C(6)-H(6A)	109.5
N(2)-C(6)-H(6B)	109.5
H(6A)-C(6)-H(6B)	109.5
N(2)-C(6)-H(6C)	109.5
H(6A)-C(6)-H(6C)	109.5
H(6B)-C(6)-H(6C)	109.5
C(8)-C(7)-C(12)	117.4(4)
C(8)-C(7)-P(1)	121.2(3)
C(12)-C(7)-P(1)	121.1(3)
C(9)-C(8)-C(7)	121.1(4)

C(9)-C(8)-H(8)	119.4
C(7)-C(8)-H(8)	119.4
C(10)-C(9)-C(8)	120.2(5)
C(10)-C(9)-H(9)	119.9
C(8)-C(9)-H(9)	119.9
C(11)-C(10)-C(9)	120.2(5)
C(11)-C(10)-H(10)	119.9
C(9)-C(10)-H(10)	119.9
C(10)-C(11)-C(12)	119.5(5)
C(10)-C(11)-H(11)	120.2
C(12)-C(11)-H(11)	120.2
C(7)-C(12)-C(11)	121.4(4)
C(7)-C(12)-H(12)	119.3
C(11)-C(12)-H(12)	119.3
C(14)-C(13)-C(18)	118.2(4)
C(14)-C(13)-P(1)	124.9(3)
C(18)-C(13)-P(1)	116.9(3)
C(15)-C(14)-C(13)	120.4(5)
C(15)-C(14)-H(14)	119.8
C(13)-C(14)-H(14)	119.8
C(14)-C(15)-C(16)	121.9(6)
C(14)-C(15)-H(15)	119.0
C(16)-C(15)-H(15)	119.0
C(17)-C(16)-C(15)	117.5(6)
C(17)-C(16)-H(16)	121.2
C(15)-C(16)-H(16)	121.2
C(16)-C(17)-C(18)	121.4(6)
C(16)-C(17)-H(17)	119.3
C(18)-C(17)-H(17)	119.3
C(13)-C(18)-C(17)	120.4(5)
C(13)-C(18)-H(18)	119.8
C(17)-C(18)-H(18)	119.8
Cl(3)-C(19)-Cl(1)	113.6(4)
Cl(3)-C(19)-Cl(2)	112.7(4)
Cl(1)-C(19)-Cl(2)	116.0(4)
Cl(3)-C(19)-H(19A)	103.8
Cl(1)-C(19)-H(19A)	104.6
Cl(2)-C(19)-H(19A)	104.4

Symmetry transformations used to generate equivalent atoms:
#1 -x+1,y,-z+2

Table 4. Anisotropic displacement parameters ($Å^2 \times 10^3$) for **(R)-2-7**. The anisotropic displacement factor exponent takes the form: $-2\pi^2[h^2 a^{*2} U_{11} + ... + 2 h k a^* b^* U_{12}]$

	U_{11}	U_{22}	U_{33}	U_{23}	U_{13}	U_{12}
P(1)	37(1)	49(1)	35(1)	-5(1)	12(1)	-1(1)
O(1)	28(1)	66(2)	55(2)	-6(2)	11(1)	-8(1)
O(2)	72(2)	71(2)	54(2)	-19(2)	38(2)	-11(2)
N(1)	36(2)	48(2)	48(2)	-3(2)	23(2)	-4(2)
N(2)	32(2)	40(2)	40(2)	-5(2)	16(1)	-5(1)
C(1)	28(2)	41(2)	34(2)	0(2)	12(2)	3(2)
C(2)	35(2)	42(2)	37(2)	4(2)	15(2)	3(2)
C(3)	47(2)	44(2)	38(2)	1(2)	22(2)	-1(2)
C(4)	24(2)	41(2)	30(2)	5(2)	8(1)	2(2)
C(5)	56(3)	88(4)	83(4)	-18(3)	50(3)	-17(3)
C(6)	45(2)	49(2)	53(2)	-14(2)	18(2)	-8(2)
C(7)	36(2)	42(2)	42(2)	0(2)	12(2)	4(2)
C(8)	65(3)	55(3)	43(2)	3(2)	18(2)	12(2)
C(9)	58(3)	55(3)	80(4)	17(3)	32(3)	12(2)
C(10)	50(2)	43(3)	110(4)	10(3)	23(3)	8(2)
C(11)	62(3)	49(3)	79(4)	-1(3)	1(3)	-10(2)
C(12)	61(3)	55(3)	43(2)	0(2)	2(2)	-2(2)
C(13)	55(3)	47(2)	35(2)	-3(2)	11(2)	-7(2)
C(14)	63(3)	73(3)	45(3)	3(2)	13(2)	4(3)
C(15)	99(4)	92(4)	49(3)	-3(3)	-10(3)	27(4)
C(16)	126(6)	71(4)	43(3)	5(3)	17(3)	13(4)
C(17)	121(6)	102(5)	55(3)	20(4)	30(4)	-16(5)
C(18)	92(4)	79(4)	51(3)	9(3)	28(3)	-6(3)
C(19)	86(4)	96(5)	90(4)	-23(4)	41(4)	-17(4)
Cl(1)	82(2)	88(3)	95(3)	1(2)	52(2)	-15(2)
Cl(2)	40(1)	120(3)	114(3)	-24(2)	25(2)	2(2)
Cl(3)	279(8)	150	103(3)	-63(3)	124(4)	-72(5)

Table 5. Hydrogen coordinates (x 10^4) and isotropic displacement parameters ($Å^2$x 10^3) for **(R)-2-7**.

	x	y	z	U(eq)
H(5A)	2777	2965	10653	104
H(5B)	2961	4654	11285	104
H(5C)	3216	3042	11980	104
H(6A)	5293	5701	12468	73
H(6B)	4947	6984	11503	73
H(6C)	5469	5877	11294	73
H(8)	4134	-427	10180	65
H(9)	3585	-2741	10295	74
H(10)	3087	-4200	8600	82
H(11)	3041	-3196	6764	82
H(12)	3552	-796	6630	67
H(14)	3006	2365	7033	74
H(15)	2496	3621	5260	106
H(16)	3040	4656	4054	99
H(17)	4100	4142	4574	111
H(18)	4622	2831	6340	87
H(19A)	4109	-2401	3334	105

Table 6. Torsion angles [°] for **(R)-2-7**.

C(7)-P(1)-C(1)-C(4)	142.8(3)
C(13)-P(1)-C(1)-C(4)	-109.2(3)
C(7)-P(1)-C(1)-C(2)	-35.1(3)
C(13)-P(1)-C(1)-C(2)	73.0(3)
C(3)-N(1)-C(2)-O(1)	-171.5(4)
C(5)-N(1)-C(2)-O(1)	4.9(6)
C(3)-N(1)-C(2)-C(1)	10.5(6)
C(5)-N(1)-C(2)-C(1)	-173.0(4)
C(4)-C(1)-C(2)-O(1)	171.8(4)
P(1)-C(1)-C(2)-O(1)	-10.3(6)
C(4)-C(1)-C(2)-N(1)	-10.3(5)
P(1)-C(1)-C(2)-N(1)	167.5(3)
C(2)-N(1)-C(3)-O(2)	177.4(4)
C(5)-N(1)-C(3)-O(2)	0.9(7)
C(2)-N(1)-C(3)-N(2)	-0.5(6)
C(5)-N(1)-C(3)-N(2)	-176.9(4)
C(4)-N(2)-C(3)-O(2)	171.8(4)
C(6)-N(2)-C(3)-O(2)	-9.0(6)
C(4)-N(2)-C(3)-N(1)	-10.3(5)
C(6)-N(2)-C(3)-N(1)	168.8(4)
C(2)-C(1)-C(4)-N(2)	0.5(5)
P(1)-C(1)-C(4)-N(2)	-177.4(3)
C(2)-C(1)-C(4)-C(4)#1	179.7(3)
P(1)-C(1)-C(4)-C(4)#1	1.8(4)
C(3)-N(2)-C(4)-C(1)	10.4(5)
C(6)-N(2)-C(4)-C(1)	-168.7(4)
C(3)-N(2)-C(4)-C(4)#1	-168.9(3)
C(6)-N(2)-C(4)-C(4)#1	12.1(5)
C(13)-P(1)-C(7)-C(8)	-150.1(3)
C(1)-P(1)-C(7)-C(8)	-42.3(4)
C(13)-P(1)-C(7)-C(12)	36.2(4)
C(1)-P(1)-C(7)-C(12)	144.0(4)
C(12)-C(7)-C(8)-C(9)	-3.0(6)
P(1)-C(7)-C(8)-C(9)	-176.9(3)
C(7)-C(8)-C(9)-C(10)	4.1(7)
C(8)-C(9)-C(10)-C(11)	-3.4(7)
C(9)-C(10)-C(11)-C(12)	1.7(8)
C(8)-C(7)-C(12)-C(11)	1.3(7)
P(1)-C(7)-C(12)-C(11)	175.2(4)
C(10)-C(11)-C(12)-C(7)	-0.7(8)
C(7)-P(1)-C(13)-C(14)	46.0(5)

C(1)-P(1)-C(13)-C(14)	-60.1(4)
C(7)-P(1)-C(13)-C(18)	-133.7(4)
C(1)-P(1)-C(13)-C(18)	120.3(4)
C(18)-C(13)-C(14)-C(15)	-1.1(8)
P(1)-C(13)-C(14)-C(15)	179.2(4)
C(13)-C(14)-C(15)-C(16)	-1.6(9)
C(14)-C(15)-C(16)-C(17)	3.6(10)
C(15)-C(16)-C(17)-C(18)	-2.8(10)
C(14)-C(13)-C(18)-C(17)	1.8(8)
P(1)-C(13)-C(18)-C(17)	-178.5(5)
C(16)-C(17)-C(18)-C(13)	0.2(10)

Symmetry transformations used to generate equivalent atoms:
#1 -x+1,y,-z+2

5. X-ray Diffraction Data for Compound 4-6a

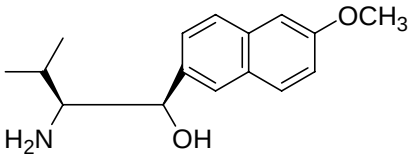

4-6a

Table 1. Crystal data and structure refinement for **4-6a**.

Identification code	4-6a	
Empirical formula	C16 H21 N O2	
Formula weight	259.34	
Temperature	294(2) K	
Wavelength	0.71073 Å	
Crystal system	Orthorhombic	
Space group	P2(1)2(1)2(1)	
Unit cell dimensions	a = 5.9607(19) Å	α= 90°.
	b = 9.066(3) Å	β= 90°.
	c = 26.848(9) Å	γ = 90°.
Volume	1450.9(8) Å^3	
Z	4	
Density (calculated)	1.187 Mg/m^3	
Absorption coefficient	0.078 mm^{-1}	
F(000)	560	
Crystal size	0.22 x 0.20 x 0.14 mm^3	
Theta range for data collection	2.71 to 27.60°.	
Index ranges	-7<=h<=7, -11<=k<=5, -34<=l<=34	
Reflections collected	9771	
Independent reflections	3340 [R(int) = 0.1888]	
Completeness to theta = 27.60°	99.2 %	
Absorption correction	EMPIRICAL	
Max. and min. transmission	0.9892 and 0.9831	
Refinement method	Full-matrix least-squares on F_2	
Data / restraints / parameters	3340 / 0 / 176	
Goodness-of-fit on F_2	0.740	
Final R indices [I>2sigma(I)]	R1 = 0.0612, wR2 = 0.1405	
R indices (all data)	R1 = 0.2456, wR2 = 0.1920	
Absolute structure parameter	-4(5)	
Extinction coefficient	0.089(4)	
Largest diff. peak and hole	0.231 and -0.265 e.Å^{-3}	

Table 2. Atomic coordinates (x 10^4) and equivalent isotropic displacement parameters ($Å^2$x 10^3)
for **4-6a**. U(eq) is defined as one third of the trace of the orthogonalized U_{ij} tensor.

	x	y	z	U(eq)
O(1)	5389(4)	5728(2)	5498(1)	84(1)
O(2)	7619(3)	403(2)	2867(1)	81(1)
N(1)	6701(4)	4254(2)	2420(1)	68(1)
C(1)	5885(5)	5129(3)	5040(1)	71(1)
C(2)	7995(5)	5625(3)	4843(1)	74(1)
C(3)	8758(5)	5115(3)	4394(1)	70(1)
C(4)	7461(5)	4103(3)	4117(1)	57(1)
C(5)	8163(5)	3538(3)	3651(1)	63(1)
C(6)	6912(5)	2576(3)	3368(1)	57(1)
C(7)	4814(5)	2133(3)	3568(1)	65(1)
C(8)	4071(5)	2631(3)	4018(1)	63(1)
C(9)	5328(5)	3632(3)	4309(1)	63(1)
C(10)	4583(5)	4137(3)	4781(1)	66(1)
C(11)	3336(5)	5222(4)	5724(1)	98(1)
C(12)	7757(4)	1984(3)	2880(1)	54(1)
C(13)	6496(4)	2634(3)	2429(1)	50(1)
C(14)	7241(4)	1959(3)	1934(1)	55(1)
C(15)	9764(5)	2206(4)	1831(1)	84(1)
C(16)	5859(5)	2534(4)	1488(1)	78(1)

Table 3. Bond lengths [Å] and angles [°] for **4-6a**.

O(1)-C(1)	1.376(3)
O(1)-C(11)	1.441(4)
O(2)-C(12)	1.436(3)
N(1)-C(13)	1.475(3)
C(1)-C(10)	1.376(4)
C(1)-C(2)	1.437(4)
C(2)-C(3)	1.370(4)
C(3)-C(4)	1.411(4)
C(4)-C(5)	1.414(4)
C(4)-C(9)	1.437(4)
C(5)-C(6)	1.376(4)
C(6)-C(7)	1.419(4)
C(6)-C(12)	1.503(3)
C(7)-C(8)	1.365(4)
C(8)-C(9)	1.412(4)
C(9)-C(10)	1.419(4)
C(12)-C(13)	1.543(3)
C(13)-C(14)	1.528(3)
C(14)-C(16)	1.545(4)
C(14)-C(15)	1.546(4)
C(1)-O(1)-C(11)	115.6(2)
O(1)-C(1)-C(10)	126.1(3)
O(1)-C(1)-C(2)	113.2(2)
C(10)-C(1)-C(2)	120.8(3)
C(3)-C(2)-C(1)	120.7(3)
C(2)-C(3)-C(4)	120.1(3)
C(3)-C(4)-C(5)	122.6(3)
C(3)-C(4)-C(9)	119.2(2)
C(5)-C(4)-C(9)	118.2(2)
C(6)-C(5)-C(4)	123.8(3)
C(5)-C(6)-C(7)	116.7(2)
C(5)-C(6)-C(12)	121.7(2)
C(7)-C(6)-C(12)	121.6(2)
C(8)-C(7)-C(6)	121.8(3)
C(7)-C(8)-C(9)	122.0(3)
C(8)-C(9)-C(10)	122.4(3)
C(8)-C(9)-C(4)	117.5(2)
C(10)-C(9)-C(4)	120.1(3)
C(1)-C(10)-C(9)	119.1(3)
O(2)-C(12)-C(6)	111.0(2)
O(2)-C(12)-C(13)	109.5(2)

C(6)-C(12)-C(13)	112.7(2)
N(1)-C(13)-C(14)	111.2(2)
N(1)-C(13)-C(12)	110.6(2)
C(14)-C(13)-C(12)	112.8(2)
C(13)-C(14)-C(16)	112.6(2)
C(13)-C(14)-C(15)	112.4(2)
C(16)-C(14)-C(15)	109.3(2)

Symmetry transformations used to generate equivalent atoms:

Table 4. Anisotropic displacement parameters ($Å^2 \times 10^3$) for **4-6a**. The anisotropic displacement factor exponent takes the form: $-2\pi^2[h^2 a^{*2} U_{11} + ... + 2 h k a^* b^* U_{12}]$

	U_{11}	U_{22}	U_{33}	U_{23}	U_{13}	U_{12}
O(1)	80(1)	100(2)	72(1)	-18(1)	5(1)	-12(1)
O(2)	97(2)	63(1)	82(1)	6(1)	0(1)	19(1)
N(1)	90(2)	52(1)	64(1)	5(1)	7(1)	12(1)
C(1)	78(2)	73(2)	62(2)	-6(2)	1(2)	-5(2)
C(2)	67(2)	86(2)	68(2)	-11(2)	-12(2)	-25(2)
C(3)	60(2)	80(2)	71(2)	1(2)	-6(2)	-24(2)
C(4)	59(2)	57(2)	56(2)	-2(1)	-4(2)	-8(2)
C(5)	51(2)	60(2)	78(2)	17(2)	-2(2)	-13(2)
C(6)	57(2)	52(2)	61(2)	14(2)	-8(1)	0(2)
C(7)	54(2)	59(2)	81(2)	-2(2)	3(2)	-10(2)
C(8)	51(2)	64(2)	73(2)	0(2)	0(2)	-11(2)
C(9)	58(2)	64(2)	67(2)	-1(2)	1(2)	-6(2)
C(10)	68(2)	65(2)	65(2)	6(2)	1(2)	-2(2)
C(11)	76(2)	118(3)	100(2)	-22(2)	20(2)	-6(2)
C(12)	57(2)	41(2)	62(2)	-3(2)	-3(2)	3(1)
C(13)	54(2)	41(2)	54(1)	1(1)	4(1)	3(2)
C(14)	46(2)	52(2)	67(2)	-9(1)	5(2)	-4(1)
C(15)	55(2)	105(3)	93(2)	-18(2)	13(2)	-10(2)
C(16)	68(2)	110(3)	56(2)	-2(2)	-3(2)	7(2)

Table 5. Hydrogen coordinates (x 10^4) and isotropic displacement parameters ($Å^2$x 10^3) for **4-6a**.

	x	y	z	U(eq)
H(2B)	8291	58	3107	121
H(1A)	7190	4692	2158	82
H(1B)	6331	4762	2678	82
H(2A)	8732	6565	5085	50
H(3A)	10132	5437	4271	84
H(5)	9318	3812	3547	27
H(7A)	3878	1196	3403	50
H(8A)	2695	2302	4138	75
H(10)	2245	3491	4919	193
H(11A)	3625	4280	5699	127(12)
H(11B)	3191	5541	6063	153
H(11C)	2040	5512	5535	153
H(12A)	9433	2209	2803	51
H(13A)	4549	2573	2483	50
H(14A)	6994	892	1956	66
H(15A)	9908	3142	1752	113(11)
H(15B)	10630	1972	2121	135
H(15C)	10240	1584	1561	135
H(16A)	6260	1840	1172	141(12)
H(16B)	4286	2484	1562	169
H(16C)	6250	3541	1420	169

Appendix IV

Published, to be published and conference papers

1. Chen, Gang, Wu, Jing; Guo, Rong-Wei, Kwok, Waihim, Chen, Guoshu; Yip, C. W.; Chan, Albert S. C. “Synthesis of A novel Chiral Bipyrimidine Diphosphine Ligand (C-Phos) and its Application in Asymmetric Allylic Alkylation”, in preparation.
2. Chen, Gang; Li, Xingshu; Zhou, Zhongyuan; Yip, Chiu-Wing and Chan, Albert S.C. “The Synthesis of Novel Chiral Ligands from Amino Acids and their Application in Asymmetric Catalysis”, in preparation.
3. Chen, Gang; Yip, C. W.; Chan, Albert S. C. “Ion exchanger promoted asymmetric hydrogenation of dehydronaproxen in water and the recycling of water-soluble catalysts”, *Abstracts of Papers*, 222nd ACS National Meeting, Chicago, IL, United States, August 26-30, 2001 (2001), ORGN-400.
4. Lu, Gui; Li, Xingshu; Chen, Gang; Chan, Wing Lai; Chan, Albert S. C. “Effective Activation of Chiral BINOL/Ti(OiPr)4 Catalyst with Phenolic Additives for the Enantioselective Alkynylation of Aldehydes.” *Tetrahedron: Asymmetry* (2003), 14(4), 449-452.
5. Wang, Ruihu; Xu, Lijin; Chen, Gang; Zhou, Zhongyuan; Hong, Maochun; Cao, Rong; Chan, Albert S. C. “(S)-2,2’-Bis(nitro-2-pyridyloxy)-1,1’-binaphthalene”, *Acta Chystallographica, Section E: Structure Reports Online* (2003), E59(6), o865-o867.

6. Chen, Gang; Wu, Jing; Kwok, Wai Him; Yip, Chiu-wing: Chan, Albert S.C. "Synthesis of a Bipyridyl C_2 Chiral Diphosphine Ligand (P-Phos) and its Application in Asymmetric Hydrogenation of β–ketoesters", *International Forum on Pharmaceutical Technology*, *Shenzhen, China*, April. 2002, 30.
7. Chen, Gang; Wu, Jing; Kwok, Wai Him; Yip, Chiu-wing; Chan, Albert S.C. "Synthesis of Novel N-containing C_2 Chiral Diphosphine Ligands and their Application in Asymmetric Hydrogenation of β-ketoesters", *the Ninth Symposium on Chemistry Postgraduate Research in Hong Kong*, 2002, O-16.
8. Chen, Gang; Yip, Chiu-wing; Chan, Albert S.C. "Ion exchanger immobilized water soluble asymmetric catalysts and their application in asymmetric hydrogenation", *the eighth Symposium on Chemistry Postgraduate Research in Hong Kong*, 2001.
9. Chen, Gang; Yip, Chiu-wing; Chan, Albert S.C. "Synthesis of sulfonated BINAP and Immobilization on silica gel based ion exchanger", *the seventh Symposium on Chemistry Postgraduate Research in Hong Kong*, 2000, O-20.